Summer 2017

High-volume recycled materials for sustainable transportation infrastructure

Seyedhamed Sadati

Department: Civil, Architectural and Environmental Engineering

HIGH-VOLUME RECYCLED MATERIALS FOR SUSTAINABLE TRANSPORTATION INFRASTRUCTURE

by

SEYEDHAMED SADATI

A DISSERTATION

Presented to the Faculty of the Graduate School of the

MISSOURI UNIVERSITY OF SCIENCE AND TECHNOLOGY

In Partial Fulfillment of the Requirements for the Degree

DOCTOR OF PHILOSOPHY

in

CIVIL ENGINEERING

2017

Approved
Kamal H. Khayat, Advisor
David Lange
Mohamed ElGawady
Hongyan Ma
V. A. Samaranayake

ABSTRACT

The objective of this study is to investigate the feasibility of using high performance concrete made with high-volume of recycled materials in transportation infrastructure. The main focus was to develop mixtures for rigid pavement construction. A variety of fine and coarse recycled concrete aggregates (RCA) were investigated. The feasibility of replacing 50% of Portland cement with industrial by-products and supplementary cementitious materials (SCMs) was also evaluated. Experimental program was conducted to quantify the effect of concrete mixture design and RCA characteristics on mechanical properties, drying shrinkage, cracking potential, and durability of concrete. The development of a database and analysis using artificial intelligence was considered to quantify the properties of concrete as a function of RCA characteristics. Results were validated during a field implementation project in Missouri. The project involved the design of the concrete mixtures, the sampling and testing of concrete at the job site, and in-situ monitoring of deformations of rigid pavement section under controlled traffic loading and environmental effect. Testing was also conducted on large-scale reinforced concrete beams cast with selected concrete mixtures to investigate the structural performance of such green materials. In general, satisfactory performance was achieved for the key properties of concrete for infrastructure applications, indicating that concrete with 50% SCM and over 50% coarse RCA can be considered for the production of sustainable and high performance concrete. The 120-day shrinkage of such concrete can be limited to 450 με, while meeting the design criteria for mechanical properties and durability and exhibiting no cracking under re-strained conditions up to 35 days.

ACKNOWLEDGMENTS

I would like to express my sincere gratitude for the advice, guidance, and support provided by my dear advisor, professor Kamal H. Khayat. What I have learned from him was far more than research and the art of engineering.

The insight, advice, and the support provided by my committee members, Dr. Lange, Dr. Samaranayake, Dr. ElGawady, and Dr. Ma is highly appreciated. I am also grateful for the support and contributions of Dr. Volz, Dr. Wunch, and Dr. Richardson.
This research could not have been done without the support provided by Mr. Stone, Mr. Ahlvers, Ms. Neely, and Mr. Trautman at Missouri Department of Transportation. The financial support provided by the National University Transportation Center (NUTC) and the RE-CAST University Transportation Center at Missouri S&T is highly appreciated.

I would like to appreciate the great support provided by my dear friends and colleagues at Missouri S&T, especially Dr. Hwang, Dr. Libre, Mr. Mehdipour, Mr. Valipour, Mr. Arezoumandi, Mr. Silva, Mr. Drury, Ms. Steele, and the rest of my colleagues at Center for Infrastructure Engineering Studies (CIES). None of these could have been accomplished without their help and contributions. It has been a great pleasure to work alongside these great colleagues in laboratory.

The support provided by the staff at CIES and civil engineering department is highly appreciated. Special thanks to Mrs. Spitzmiller and Mrs. Sherman for their support. I would also like to thank Mr. Assioun, Mr. Cox, Mr. Bullock, Mr. Swift, Mr. Lusher, and Mr. Abbott for helping me during my research.

This thesis could never be written without the unconditional love and support from my beloved parents. They have been my role models in life and supported me during all moments of difficulty. I also would like to thank my two dear brothers who have always helped and encouraged me.

And last but not least, I offer my deepest gratitude for the unconditional love, support, and dedication of my beloved wife, ***Samareh***, who has been my greatest support. I could never accomplish this without her. Being with her in this journey, made it possible to go through the impossible. I can never thank her enough for her understanding and support during the difficult moments of life.

TABLE OF CONTENTS

LIST OF ILLUSTRATIONS

Page

LIST OF TABLES

Page

1. INTRODUCTION

1.1. GENERAL

Interest for environmentally friendly concrete in transportation infrastructure has grown in recent years. Candidate technologies to improve the sustainability of pavement concrete include the use of supplementary cementitious materials (SCMs) as a replacement for Portland cement, the incorporation of recycled materials in concrete production, in particular recycled concrete aggregate (RCA), as well as the use of highly durable materials. Given the fact that fine and coarse aggregates occupy about 30% and 40% of the concrete volume in rigid pavement, respectively, partial replacement with recycled aggregate can be employed to reduce the use of natural resources. Sustainable solutions for the concrete industry should couple the durability of the material, the environmental impact on the structure, and the cost of the project (Kim 2013).

Considering the need to produce more than 2.5 billion tons of aggregate in the U.S. for the construction industry by 2020, an increase from 2 billion tons in 2004 (FHWA 2004), the incorporation of recycled concrete aggregate (RCA) to replace part of virgin aggregate can result in substantial reduction in the use of non-renewable natural resources and concrete waste in landfills. Construction and demolition (C&D) waste accounts for a considerable portion of solid wastes and generation of which has been increasing rapidly in the United States. Generation of C&D waste was estimated to be over 325 million tons in 2003 (EPA 2004). However, the fact sheets released by the Environmental Protection Agency (EPA) indicate generation of over 530 and 535 million tons of C&D waste in the United States (EPA 2015, 2016), with concrete constituting over 66.5% and 70% of the C&D waste in 2013 and 2014, respectively.

Historically, concrete from C&D waste has mostly been dealt with through disposal in landfills. However, due to the increasing rate of demolition, it is essential to effectively reuse demolition waste to conserve nonrenewable natural resources. Decrease in natural resources, increasing problems in waste management, ecological hazards, landfill limitations, and increase in distance between natural resources and consumption markets support the idea of using recycled wastes for new concrete production (Padmini et al., 2009). Furthermore, the reduction in the carbon footprint of the most commonly

used construction material, concrete, is a key factor to decrease the total greenhouse gas emissions produced by the construction industry (Mclntyre 2009).

The use of RCA to preserve natural resources and to reduce the amount of disposals in landfills has been growing in recent years. In spite of the environmental and potential economic merits, technical concerns may raise with the use of RCA in concrete production. The heterogeneous nature of RCA stemming from the adhered residual mortar, origin of the waste concrete source, recycling process, level of chemical contamination, etc. can lead to wide range of performance when RCA is incorporated. Given the variable characteristics of RCA when compared to virgin aggregate sources, there still exists a conservative approach that limits the use of RCA in concrete designated for transportation infrastructure (Surya 2013). Therefore, RCA is mostly being used in granular bases, embankments, sound barriers, fills, etc. (Kim 2013, Gabr 2012).

1.2. OBJECTIVE

Due to the economic and environmental merits of recycled materials, research has been undertaken to investigate the effect of RCA on the properties of concrete designated for pavement applications at Missouri University of Science and Technology in collaboration with the National University Transportation Center (NUTC) and Research on Concrete Applications for Sustainable Transportation (RE-CAST) University Transportation Center (UTC) at Missouri S&T and the Missouri Department of Transportation (MoDOT). The research involves mix design and field implementation of sustainable concrete materials made with high volumes of recycled materials for transportation infrastructure. The output of the research can endorse the development of guidelines for design of RCA concrete for future implementation of this technology in construction projects.

The main objective of this research is to evaluate the feasibility of using RCA for concrete production in rigid pavement applications. The experimental program was undertaken to investigate the performance of different concrete made with different amounts of RCA, water-to-cementitious materials ratios (w/cm), and supplementary cementitious materials to develop sustainable concrete designated for rigid pavement. Several sources of fine and coarse RCA were investigated in the laboratory. Concrete

mixtures were developed and investigated for key engineering properties, governing the design of rigid pavement systems, including mechanical properties, shrinkage, and durability.

1.3. OUTLINE

The scope of work that was implemented to achieve the objective of the research study is presented below:

Section 1: This section offers a brief introduction to the subject of the research and summarizes the significance of the work conducted throughout the dissertation.

Section 2: The purpose of this section is to conduct a literature review of past experience and previous research on RCA. RCA properties as well as the behavior of concrete containing RCA, including the fresh and hardened properties (e.g., workability, compressive strength, flexural strength, shrinkage), and durability (e.g., freeze-thaw resistance, permeability, scaling). Specifically, the literature review focuses on studies that investigated performance of rigid pavement made with partial or full replacement of RCA.

Section 3: The purpose of this section is to evaluate the properties of several candidate RCA sources for use in concrete production. Samples are taken from various sources at different time intervals. Key engineering properties, including the particle-size distribution, specific gravity, absorption rate, and abrasion resistance of the aggregates are evaluated. Optimizing a proper aggregate skeleton is another goal of this task.

Section 4: This section is focused on the optimization of eco-efficient binder systems for concrete production. Various types and replacement levels of supplementary cementitious materials (SCMs) are investigated. Several binary and ternary mixtures were investigated for mechanical properties, shrinkage, and durability of concrete equivalent mortar (CEM) designed based on MoDOT's rigid pavement mix design. A paper is submitted to the Journal of Construction and Building Materials based on the results presented this section.

Section 5: Several combinations of coarse and fine RCA are considered for producing concrete for rigid pavement applications. Key mechanical properties, including compressive strength, splitting tensile strength, flexural strength, and modulus of

elasticity (MOE) were evaluated for concrete made with different types and contents of fine and coarse RCA. A manuscript is prepared based on some of the results presented in this section.

Section 6: This section presents a summary of the work conducted on development of a theoretical model to quantify the effect of RCA on MOE. Given the fact that MOE is one of the main material characteristics that affect the design and performance of concrete pavements, characteristics and concrete mixture proportions were considered as input factors in a model based on Artificial Neural Network to determine the variations in MOE of concrete made with coarse RCA. A manuscript is prepared based on the results presented in this section.

Section 7: This section investigates the effect of RCA on drying shrinkage of concrete intended for transportation infrastructure. Several concrete mixtures were developed with different RCA types to evaluate the effect of mixture design parameters and RCA quality on drying shrinkage of concrete. A paper is submitted to the Journal of Materials in Civil Engineering based on the results presented this section.

Section 8: Given the higher rate of drying shrinkage along with the increase in stress relaxation due to the use of RCA, it is important to determine the extent of variations in cracking potential caused by shrinkage for concrete made with RCA. Effect of coarse RCA on cracking due to shrinkage under re-strained condition was investigated in this section. Different types of coarse RCA were used to cast ring-type specimens to monitor the time to cracking. A paper is submitted to the Journal of Materials and Structures based on the results presented this section.

Section 9: Effect of RCA on durability of concrete was investigated in this section. Various types and combinations of coarse and fine RCA were employed for developing concrete with different binder types. Durability against freeze and thaw cycles, resistance against scaling caused by de-icing salts, abrasion resistance, and sorptivity were the key parameters. A manuscript is prepared based on some of the results presented in this section.

Section 10: This section presents a summary of the results obtained from a demonstration project aiming at construction of rigid pavement using RCA. The work presented in this section summarizes the initial laboratory investigation, construction of pavement panels,

sampling, material properties, and long-term performance of concrete pavement made with RCA. A paper is published in Journal of Construction and Building Materials based on the results presented this section.

Section 11: A summary of the key findings is presented in this section. Recommendations are made and ideas are suggested for the future research.

Appendix A: The use of RCA in concrete for structural applications is of great interest for construction of reinforced concrete elements. Research was conducted in collaboration with Dr. Jeffery Volz and MoDOT to evaluate the effect of coarse RCA on shear strength of full-scale reinforced concrete beams designated for transportation infrastructure. A paper is published in Journal of Cleaner production based on the results presented this section.

Appendix B: Research was conducted in collaboration with Dr. Jeffery Volz and MoDOT to evaluate the effect of coarse RCA on bond strength of full-scale reinforced concrete beams designated for transportation infrastructure. The paper prepared based on the results obtained in this section is accepted for publication in ACI Materials Journal.

2. LITERATURE REVIEW

2.1. GENERAL

Based on the definition provided by the United Nations, sustainable development is development that meets the needs of the present without compromising the ability of future generations to meet their own needs (United Nations General Assembly 1987). The pavement industry is one of the fields where hard work is devoted to develop a focused meaning of sustainability in terms of design, materials, construction, and maintenance (Garber et al. 2011).

With the introduction of waste legislation in the form of regulations and directives in many places, a significant movement towards the sustainable management of construction and demolition (C&D) waste is becoming a legal requirement. In response, different sectors of the construction industry are undertaking various initiatives to minimize waste generation and improve the management of C&D waste to maximize economic and environmental benefits, generally by placing emphasis on increasing recycling for reuse (Limbachiya et al., 2007).

The construction industry in particular is a major consumer of materials and at the same time a major producer of waste (Padmini et al., 2009). According to Abbas et al. (2009), concrete accounts for up to 67% of construction and demolition waste, by mass. The amount of demolition waste dumped at landfill sites in the United Kingdom is said to be in excess of 20 million tons per year. The bulk of this material is concrete (50% to 55%) and masonry (30% to 40%) with only small percentages of other materials, such as metals, glass, and timber (Tam et al., 2007). In the Netherlands, about 14 million tons of building and demolishing waste per year is produced, of which about 8 million tons are recycled, mainly for unbound road base courses (Tam et al., 2007).

Production of C&D waste was estimated to be over 535 million tons in the United States, with concrete constituting over 70% of the C&D waste in 2014 (EPA 2004, 2015, 2016). Historically, waste concrete is deposited in landfills. However, environmental impact, raising issues with depletion of natural sources, more restrictive land use policies for landfills, and potential savings in construction cost in some markets, support the idea of seeking alternative use of C&D waste. One of the main scenarios is to use recycled

concrete aggregate (RCA) as a partial replacement of virgin aggregate in concrete construction, in particular for concrete pavement (Gonzalez and Young 2004; NCHRP 2013). However, given the potentially marginal quality of RCA compared to that of virgin aggregate, the incorporation of RCA can impact the performance of such pavement materials.

Based on a survey conducted by Federal Highway Administration (FHWA 2004), an example of reduction in landfill disposals, noted that construction of a mile of one lane rigid pavement with thickness of 10 in. will require about 2000 yd^3 of concrete that corresponds to incorporation of 3000 tons of aggregate. Recycling of such a section on the other hand can produce 4000 tons of RCA. Moreover, saving the energy required for mining and extraction of aggregate and hauling can add extra value to the recycling practice and reduce greenhouse gas emissions.

Considering the need to produce more than 2.5 billion tons of aggregate in the U.S. for the construction industry by 2020 (FHWA 2004), the incorporation of RCA as a substitute for virgin aggregate can play an important role towards sustainable development. The Construction and Demolition Recycling Association (CDRA 2012) estimates that recycling concrete in the U.S. was limited to 140 million tons annually in 2012. Approximately 73% of concrete waste in the U.S. is used in road base and backfill as demonstrated in Figure 2.1. However, a small portion (6.5%) of RCA is incorporated as a replacement of virgin aggregate in new concrete production.

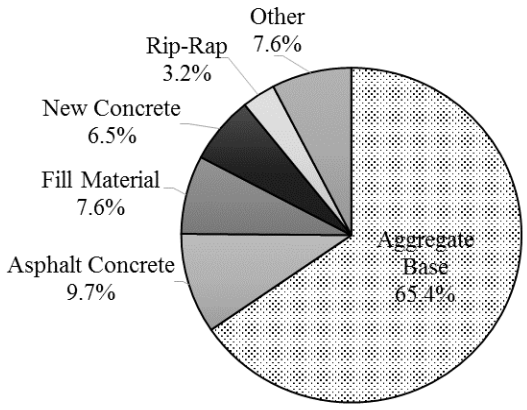

Figure 2.1 Break down of RCA use in the U.S. (Van Dam et al., 2015; Hansen and Copeland. 2013)

2.2. USE OF RECYCLED CONCRETE AGGREGATE IN CONCRETE PRODUCTION

2.2.1. Background. RCA can be obtained by crushing Portland cement concrete from various sources, including pavements and buildings. However, the Federal Highway Administration (FHWA 2004), limits the definition of RCA to processed concrete by-products obtained from old Portland cement concrete pavements, bridge structures/decks, sidewalks, curbs, and gutters in which steel is removed from the old concrete. Based on the definition provided by FHWA (2004), RCA is a granular material manufactured by removing, crushing, and processing hydraulic-cement concrete pavement for reuse with a hydraulic cementing medium to produce fresh paving concrete. The aggregate retained on the #4 sieve is called coarse aggregate and the material passing through the #4 sieve is called fine aggregate.

The main idea supporting such definition is to provide RCA from high quality state approved old concrete (NCHRP, 2013). State projects historically use high-quality aggregate sources with consistent quality accepted by the state agencies. RCA produced from processing state approved high-quality and durable old concrete may be useful in producing concrete for other state applications. On the other hand, the RCA obtained from construction and demolition waste may be useful in base and/or fill applications.

The Construction Material Recycling Association (2009) indicates that RCA can be used to:

- Provide high-quality material in some highway applications
- Provide aggregate acceptable by ASTM and AASHTO standards
- Produce concrete and asphalt products
- Provide improved base and subbase materials
- Reduce haul and material costs
- Reduce landfill waste streams
- Minimize environmental impacts

Depending on the considerations of the project, the use of RCA can save money, save time, and reduce the environmental impact of pavement application. The use of RCA can potentially shorten project delivery as a result of expedited construction schedules due to reduced haul times. The potential for increased material transportation

savings is even greater when there is no locally available aggregate (Garber et al., 2011). According to a survey published by FHWA in 2004, 41 states recycled concrete for use as aggregate in new construction. At least 45 states are recycling concrete as aggregate in 2016, as shown in Figure 2.2. Thirty eight of these states allow the use of RCA in base applications, as shown in Figure 2.3. Of these states, however, only 11 were using RCA in new Portland cement concrete production, as shown in Figure 2.4.

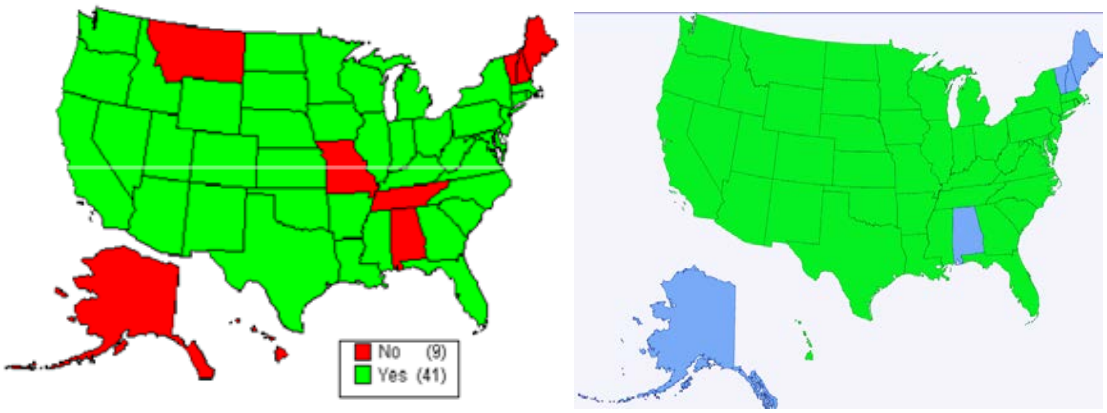

Figure 2.2 States recycling concrete as aggregate (left, FHWA 2004) and (right, NCHRP 2013 and Snyder and Cavalline, 2016)

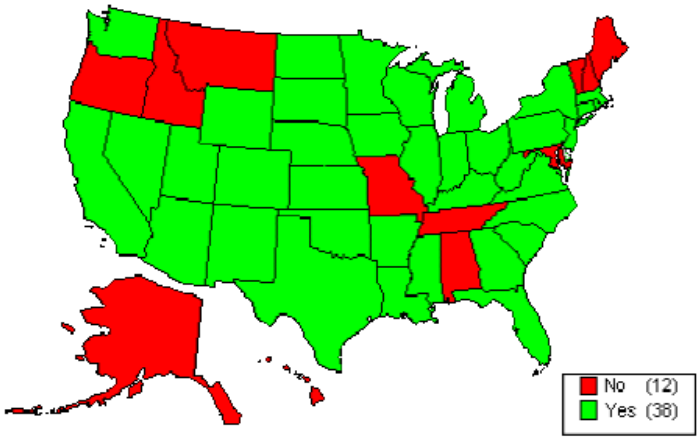

Figure 2.3 States recycling concrete as aggregate base (FHWA 2004)

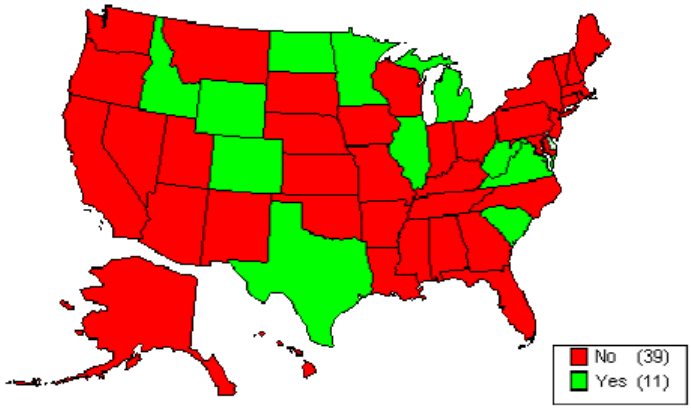

Figure 2.4 States recycling concrete as aggregate for new concrete production (FHWA 2004)

2.2.2. RCA Production. Given the fact that RCA is produced from demolished concrete elements including structural members and pavement sections, etc. one or a combination of the following methods is required for concrete removal suitable for RCA production (ACI 555-01):

- Using hand tools
- Hand-operated power tools
- Vehicle-mounted equipment
- Explosive blasting
- Drills and saws
- Non-explosive demolition agents
- Mechanical splitters
- Demolition of concrete structures by heat
- Hydro-demolition (water-jet blasting)

Considering the fact that recycling old pavement is one of the widely accepted sources of RCA production for rigid pavement applications, the American Concrete Pavement Association (ACPA 2008) provided guidance for recycling rigid pavement into RCA. The process starts with removal of potential contaminates such as hot mixed asphalt (HMA) shoulders, patches, or crack sealants. ACPA recommends limiting the contaminants to less than 10%. However, this number may vary depending on different agency regulations. For example, Minnesota allows no more than 3% asphalt binder by

weight of aggregate, whereas in California there was no limit on reclaimed asphalt pavement (RAP) in RCA (ACPA 2008). In Australia, as much as 20% HMA by-products were allowed when lower quality RCA was produced. Removal of motor oils and other surface contaminants should be considered. These surface contaminants were reported as limited to the upper few millimeters of the pavement surface (ACPA 2008). Pre-crushing preparation needs to consider the maximum feed size needed for the crusher and how much steel, wood, dirt, and other contaminates need to be removed before crushing (CMRA 2009).

Depending on the use of the RCA, crushing concrete for RCA production usually continues with crushing using jaw or impact crushers. As reported by ACPA (2008), primary jaw crushers typically produce 4 to 8 in. minus crushed materials that could be used as fill. Impact crushers use a spinning rotor with bars or hammers that throw the concrete into solid objects (plate or plates) and produced 2 in. minus recycled materials that could be further reduced in size in primary, secondary, or tertiary crushers.

The type of the crusher employed for production of RCA can affect RCA reclamation efficiency, defined as the percentage of coarse RCA produced during the crushing process. Results of a survey conducted by Snyder and Cavalline (2016) indicate that the reclamation efficiency can vary from 44% to 87% depending on the processing procedure and the type of virgin aggregate used in parent concrete. Table 2.1 offers a summary of the results.

Table 2.1 Effect of crushing procedure and virgin aggregate type on reclamation efficiency adapted from Snyder and Cavalline (2016)

Process	Reclamation Efficiency		
	RCA Type		
	Limestone	Gravel	Granite
Jaw-Jaw-Roller	71	73	87
Jaw-Cone	73	80	76
Impact-Impact	44	63	53

Crushing, sizing, and removal of contaminates of the old concrete could be accomplished using portable, mobile, or stationary recycling plants (CMRA 2009). Mobile plants are truck-mounted and can move from site to site. Portable plants consist of a crusher and a feeder (loader or backhoe) employed for producing the required RCA specification properties. Portable crushers are usually mounted on rubber tired chassis, towed to the site, and moved around with loaders or tugs. Mobile crushers have their own track-mounted drive system. Stationary crushers on the other hand are permanently fixed to the ground and the material is being trucked to the site. In the case of reinforced steel sections, the old slab should be sufficiently broken to ensure separation from the reinforcing and dowel bars and the old concrete could be lifted out of the pavement and the steel mesh, rebar, and dowel bars removed. Any metals left in the concrete can be removed with magnets placed over the feeder belt into the secondary crusher. Air blowing through the crushed concrete can be employed to remove any lightweight contaminants and dust. Table 2.2 summarizes the RCA production data obtained through a survey conducted in the United States (NCHRP 2013).

2.2.3. Engineering Properties of RCA. RCA is typically regarded as a double phase material which consists of the original virgin aggregate and the adhered residual mortar. The RCA-made concrete will have more constituents: the new mortar and the new virgin coarse aggregates. Thus, there are two types of interfacial transition zones (ITZs) in RCA-made concrete mixtures: the old ITZ between the original virgin coarse aggregate and the adhered mortar and the ITZ between the new mortar and the RCA (Figure 2.5).

As a result of high amounts of adhered mortar content in recycled aggregates, RCA can have higher water absorption, lower specific gravity, and higher porosity compared to natural aggregate (Kou et al., 2012). Both fine and coarse RCA particles are believed to have rough surface texture compared to virgin aggregate due to the crushing process. Some technical problems, including weak ITZ between cement paste and aggregate, porosity and traverse cracks within demolition concrete, high level of sulfate and chloride contents, impurity, and high variations in quality, render the use of RCA more challenging. Table 2.3 provides a breakdown of the typical properties of RCA provided by FHWA (2004).

Table 2.2 RCA production data in the United States (NCHRP 2013)

Million tons per year	No. of plants		States or regions served
	Fixed	Mobile	
2.75	1	9	Ohio, W. Va., Pa., the Southeast
2.5	1	5	California and Arizona
2.2	20	0	Arizona, California, Illinois, New Mexico, Virginia
2.1	1	8	Southeastern U.S.
1.9	3	3	Georgia
1.83	2	8	Western U.S.
1.73	0	6	Southern California
1.45	0	4	Minnesota and the Dakotas
1.43	3	0	Texas
1.28	3	3	Texas and Louisiana
1.09	9	0	Texas
1.07	3	2	Nevada, Arizona, Utah, California
0.83	4	1	California
0.82	0	4	California
0.8	2	0	Massachusetts, New Hampshire, Rhode Island
0.66	1	1	California
0.6	0	4	S. Carolina, N. Carolina, Ga., Va., Fla., Ala., Miss.
0.59	1	5	Iowa, Minnesota, Nebraska, Missouri, S. Dakota
0.58	4	2	New Jersey
0.5	0	3	New Jersey, New York, Delaware, Pennsylvania
Total	58	68	

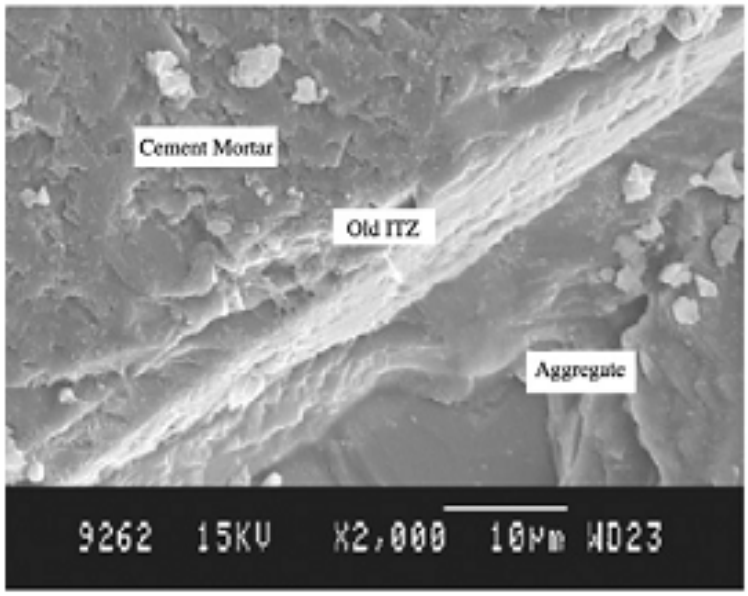

Figure 2.5 Scanning electron microscope (SEM) of old ITZ in RCA particle (Xiao et al., 2012)

Table 2.3 Typical physical properties of RCA (FHWA 2004)

Property	Fine RCA	Coarse RCA
Specific gravity	2.0 to 2.3	2.2 to 2.5
Absorption	4% to 8%	2% to 6%
Loss Angeles abrasion loss	-	20 to 45
California bearing ratio (CBR)	94% to 148%	

It is usually believed that adhered mortar is the main cause of the lower properties of RCA compared to virgin aggregates. For a clear understanding of the recycled aggregate and to predict its possible effects on concrete, the constituents of these composite particles must be identified separately (Nagataki et al., 2000). It has also been suggested that the quality of RCA increases with a decrease in residual mortar content attached to the virgin aggregate particles. Adjustments to crushing methods used for RCA production can help minimizing the mortar content. However, too much crushing might compromise the integrity of the original aggregate and may not be cost effective (Garber et al., 2011).

The more recent systematic studies dealing with use of RCA has resulted in development of standards, recommendations, and selection criteria in some Asian and European countries, as well as the United States (ACI 555-01, AASHTO MP16). Such technical documents are mainly classifying the RCA based on some of the key engineering properties of the recycled aggregate sources. These properties are generally divided into two main categories, including the physical properties of the aggregate particles and the chemical contaminations available in recycled aggregate sources. As an example, the standard developed by the American Association of State Highway and Transportation Officials (AASHTO MP16) recommends using RCA with less than 50% mass loss due to Los Angeles abrasion test, containing less than 1.5% materials finer than 75 µm, chloride ion contents no more than 0.6 lb/yd^3 of weight of concrete, and less than 12% mass loss due to soundness test using sodium sulfate solution. RILEM specification also sets limitations on water absorption rate, specific gravity, deleterious materials content, the amount of materials finer than 63 µm, and water soluble sulfate content to classify RCA into three main quality levels (RILEM TC121). Unit weight, water absorption, and deleterious materials content are usually used as criteria for selecting RCA for different applications. A summary of classification criteria for RCA used in different countries is presented in Table 2.4. Data presented in this table is a summary of the review results provided by McNeil and Kang (2013) and Duan et al. (2017).

Considerable research is also devoted to developing guidelines for the use of RCA in concrete production. For instance, Silva et al., (2014) conducted a comprehensive study to correlate the initial properties of the recycled aggregate sources, including RCA, construction and demolition waste, etc. to performance of concrete cast with various amounts of RCA. Authors summarized the key properties of the various recycled aggregate sources with the normal distributions presented in Figure 2.6. Based on the analytical investigation conducted by the authors, the mean values of the investigated properties for fine and coarse RCA sources are summarized in Table 2.5.

Table 2.4 RCA classification criteria in different standards

Country	Standard	Aggregate type	SG (kg/m^3)	Absorption (%)	Composition (%)*				Replacement ratio (%)	Application filed	Allowable class
					NA	OC	m	δ			
Germany	(DIN 4226-100) (DIN 2006)	Type 1	≥ 2000	≤ 10	0	≥90	≤10	≤1.2	20	Interior element	C30/37
		Type 2	≥ 2000	≤ 15	0	≥70	≤30	≤1.5	35	Interior element	C25/30
		Type 3	≥ 1800	≤ 20	0	≤20	≥80	≤1.5	n.a.	Non-structural	n.a.
		Type 4	≥ 1500	n.a.	n.a.	n.a.	n.a.	n.a.	n.a.	n.a.	n.a.
Hong Kong	WBTC 2002	Type II	≥ 2000	≤ 10	0	≤100	-	≤1	100	Non-structural	20 MPa
			≥ 2000	≤ 10	0	≤100	-	≤1	20	Structural	35 MPa
Japan	(JIS A 5021, 5022, and 5023) (JIS 2011, 2012a, b)	Coarse- H	≥ 2500	≤ 3	0	≤100	0	≤2	100	All elements	~ Virgin agg.
		Fine- H	≥ 2500	≤ 3.5	n.a.	n.a.	n.a.	n.a.	n.a.	n.a.	n.a.
		Coarse- M	≥ 2300	≤ 5	0	≤100	0	≤2	100	Piles, etc.	n.a.
		Fine- M	≥ 2200	≤ 7	n.a.	n.a.	n.a.	n.a.	n.a.	n.a.	n.a.
		Coarse- L	NA	≤ 7	0	≤100	0	NA	100	Temporary use	n.a.
		Fine- L	NA	≤ 13	n.a.	n.a.	n.a.	n.a.	n.a.	n.a.	n.a.
RILEM		MRA	≥ 2200	≤ 7	0	n.a.	≥65	≤1	100	Non-structural	18 MPa
		Type 1	≥ 1500	≤ 20	0	0	≤100	≤5	100	Non-structural	C16/20
		Type 2	≥ 2000	≤ 10	0	≤100	0	≤1	100	Non-structural	C50/60
		Type 3	≥ 2500	≤ 3	≥80	≤20	≤10	≤1	100	Structural	~ Virgin agg.
The Netherlands	NEN 5905	RCA	≥ 2000	n.a.	0	≥95	≤5	≤1	100	Structural	C40/50
		RCA	≥ 2000	n.a.	0	≥95	≤5	≤1	≥20	Structural	C50/60
		RCA	≥ 2000	n.a.	0	≥95	≤5	≤1	≤20	Structural	~ Virgin agg.
		RMA	≥ 2000	n.a.	0	n.a.	≥65	≤1	100	n.a.	C20/50

Table 2.4 RCA classification criteria in different standards (cont.)

Portugal	LNEC E471	ARB 1	≥ 2200	≤ 7	0	≥90	≤10	0.2	25	Structural	C40/50
		ARB 2	≥ 2200	≤ 7	0	≥70	≤30	0.5	20		C35/45
		ARC	≥ 2000	≤ 7	0	≥90	n.a.	2	n.a.		n.a.
		ARB	n.a.	n.a.	0	≥90	≤10	0.5	100		n.a.
		ARM	n.a.	n.a.	50	≥40	≤10	1	100		n.a.
		ARA	n.a.	n.a.	0	≤40	≥60	1	100		n.a.
		RCA- A	n.a.	≤7	0	≥95	≤10	3	100		15 MPa
		MA- A	n.a.	≤12	0	<90	≥10	3	100		NA
Denmark	DS 2426	GP 1	≥ 2200	NA	0	≥95	NA	NA	100	Passive environment	n.a.
		GP 2	≥ 1800	NA	0	≥95	NA	NA	100		n.a.
Switzerland	SIA 2030	BC	n.a.	n.a.	0	100	n.a.	≤3	100	RC concrete, pre-stressed conc. with additional testing	C30/37
		BNC	n.a.	n.a.	0	100	n.a.	n.a.	100	Non-structural	n.a.
Russia			n.a.	n.a.	0	100	n.a.	n.a.	100	Non-structural	15 MPa
			n.a.	n.a.	0	100	n.a.	n.a.	50	Non-structural	20 MPa
China	DG/TJ07-008	Type I	≥ 2400	≤7	0	≥95	≤5	≤1	n.a.	n.a.	n.a.
		Type II	≥ 2200	≤10	0	≥90	≤10	≤1	n.a.	n.a.	n.a.
Australia	(AS1141.6.2) (AS1996)	Class 1A	≥ 2100	≤ 6	n.a.	n.a.	n.a.	n.a.	n.a.	n.a.	n.a.
		Class 1B	≥ 1800	≤ 8	n.a.	n.a.	n.a.	n.a.	n.a.	n.a.	n.a.
Korea	(KS F 2573) (KS 2002)	Coarse	≥ 2500	≤ 3	n.a.	n.a.	n.a.	n.a.	n.a.	n.a.	n.a.
		Fine	≥ 2200	≤ 5	n.a.	n.a.	n.a.	n.a.	n.a.	n.a.	n.a.
Spain	(EHE 2000)	-	≥ 2000	≤ 5	n.a.	n.a.	n.a.	n.a.	n.a.	n.a.	n.a.

*NA, OC, m, and δ are natural aggregate, old concrete, old masonry, and impurities, respectively

** n.a. indicates that no limits were available

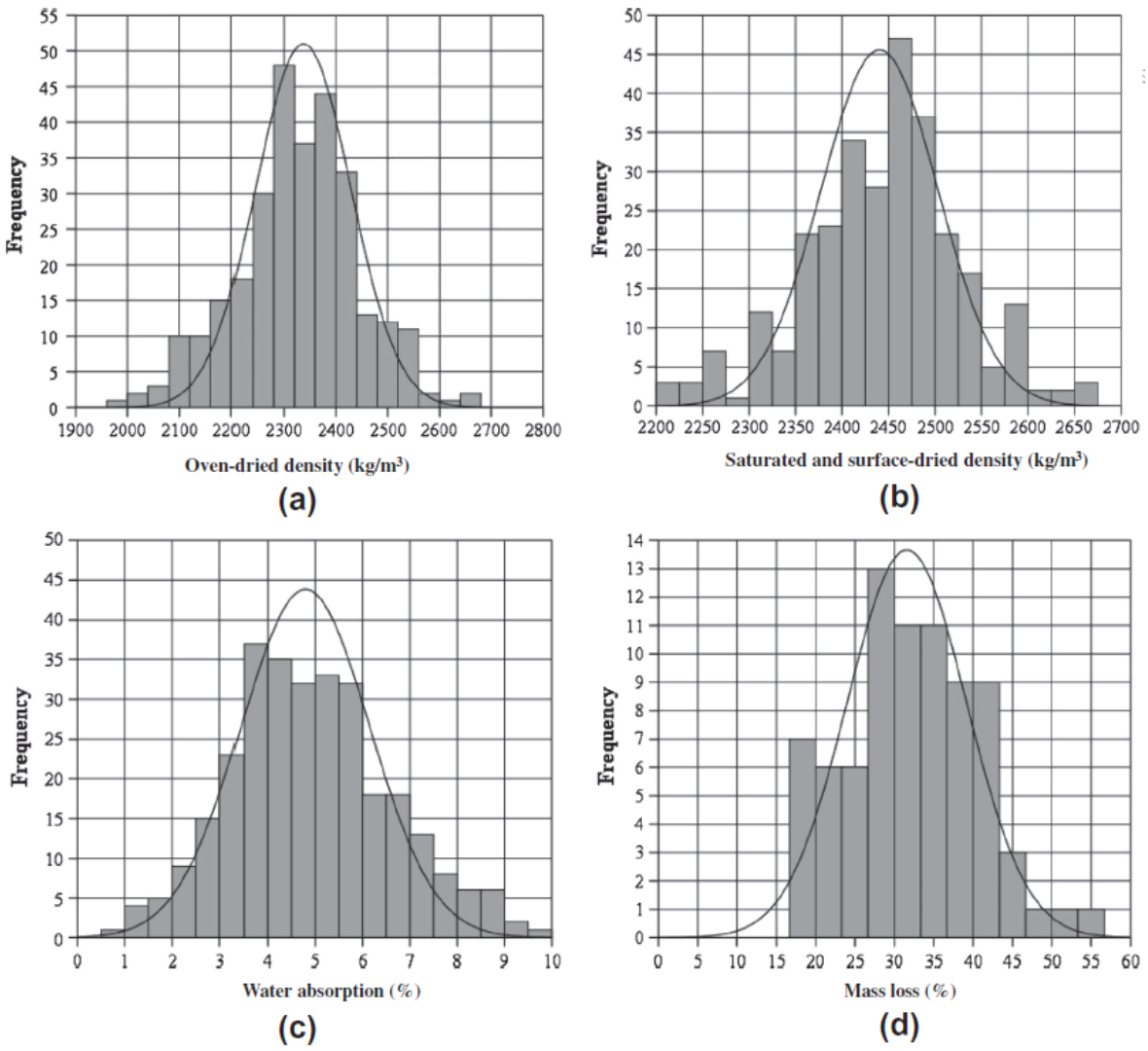

Figure 2.6 Normal distribution of the (a) oven dried density, (b) saturated surface dried density (c) water absorption, and (d) Loss Angeles mass loss of coarse RCA (Silva et al., 2014)

Table 2.5 Mean engineering properties of the coarse and fine RCA sources studied by Silva et al. (2014)

Property	Coarse RCA	Fine RCA
Specific gravity	2442	2300
Absorption rate (%)	4.9	9.5
LA abrasion (%)	32.5	-

The authors (Silva et al. 2014) have also established a correlation between the oven-dry density and absorption rate of the investigated recycled aggregate sources as presented in Figure 2.7.

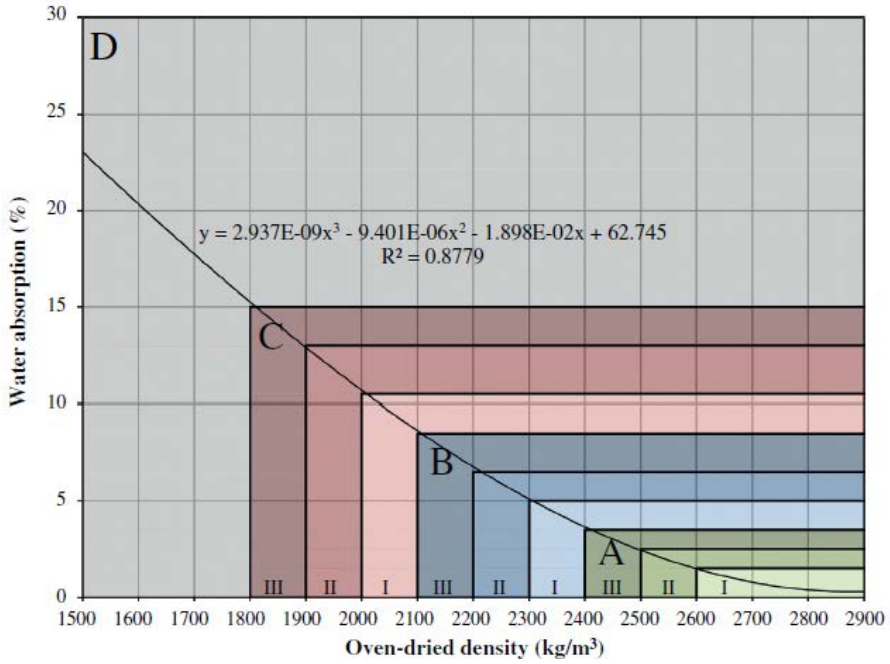

Figure 2.7 Correlation between oven dried density and absorption rate of recycled aggregate (Silva et al., 2014)

Quality of the aggregates is ranked based on the density and absorption rate in this method. Results of the analytical study conducted by the authors indicated that there is 81.3% probability of having RCA sources fitting in group A, 11.7% chance to have RCA from group B, 5.0% chance to have RCA from group C, and 0.6% chance to have RCA from group D of this identification system. In general, observations are in line with the bulk of literature and available standards that deal with RCA quality by means of absorption rate and specific gravity.

2.3. PROPERTIES OF CONCRETE MADE WITH RCA

2.3.1. General. In general, the quality of RCA-made concrete is related to the properties of the original waste concrete, the new composition, the mixing approach, and the deterioration conditions of the recycled aggregates. Initial investigations on the use of

recycled aggregate usually focused on incorporating recycled aggregate and its influence on mechanical and durability properties of the recycled aggregate concrete (RAC). It was an adopted concept that although the use of recycled aggregate may be viable, a decrease in the performance of the RAC should be regarded as a normal outcome which can be mitigated through various approaches such as increasing cement content in the mixture etc. (Bagragi et al., 1990).

Table 2.6 provides a summary of the influence of RCA on some key properties of Portland cement concrete obtained from a survey by the National Cooperative Highway Research Program (NCHRP 2013).

2.3.2. Fresh Properties.

2.3.2.1 Unit weight. As a result of high amounts of adhered mortar existing in RCA particles, the density of RCA is usually lower than that of virgin aggregates which in turn decreases the unit weight of concrete containing RCA (Xiao et al., 2012).

2.3.2.2 Workability. Surface texture of the RCA particles have significant effect on workability. Domingo et al., (2009) reported that a greater presence of recycled aggregates decreases the workability of the concrete, which may be related to the shape, texture, and absorption characteristics of the recycled aggregate. This necessitates the use of saturated recycled aggregate or a greater amount of superplasticizer to maintain workability.

2.3.3. Mechanical Properties.

2.3.3.1 Compressive strength. The use of RCA can have significant effect on compressive strength of concrete. This is mainly due to the presence of micro-cracks, damaged ITZ, availability of deleterious materials, and the inferior properties of the residual mortar phase of the RCA particles. However, this effect can be negligible for replacement levels up to 30% (Xiao et al., 2012). Nixon (1978) found that the compressive strength of concrete made with RCA replacement is somewhat lower compared to that of control mixtures without any RCA. Hansen (1986) concluded that the compressive strength of RCA-made concrete is largely controlled by a combination of the w/cm of the original concrete from which the RCA is produced and that of the RAC when other factors are essentially identical. Exteberia et al. (2007) reported up to 25%

decrease in compressive strength due to full RCA replacement in concrete mixtures proportioned with water-to-cement ratio (w/c) of 0.50 and 325 kg/m^3 of Portland cement.

Gonzalez-Taboada et al. (2016) investigated the effect of water absorption (Figure 2.8) and specific gravity (Figure 2.9) of coarse RCA on compressive strength of concrete prepared with water-to-cement ratio (w/c) of 0.40 to 0.70. Results indicated reduction in compressive strength as a function of increase in water absorption and reduction in oven-dry specific gravity of RCA.

Table 2.6 Influence of RCA on properties of concrete (NCHRP, 2013)

Property	Expected changes in properties	
	Coarse RCA only	Coarse and fine RCA
Specific gravity	0 to 10% lower	5% to 15% lower
Compressive strength	0 to 24% lower	15% to 40% lower
Tensile strength	0 to 10% lower	10% to 20% lower
Strength variability	Slightly greater	Slightly greater
Modulus of elasticity	10% to 33% lower	25% to 40% lower
Creep	30% to 60% higher	30% to 60% higher
Drying shrinkage	20% to 50% higher	70% to 100% higher
Permeability	0 to 500% higher	0 to 500% higher
Coefficient of thermal expansion	0 to 30% higher	0 to 30% higher
Corrosion rate	May be faster	May be faster
Freeze/thaw durability	Dependent on air void system	Dependent on air void system
Sulfate resistance	Dependent on mixture	Dependent on mixture

Several methodologies are proposed in the literature for predicting the compressive strength of concrete incorporating RCA. Duan et al. (2013) developed a model based on artificial neural network (ANN) to predict the compressive strength as a function of RCA characteristics, RCA replacement ratio, and concrete mix design. The authors employed a total numbers of 146 test results from literature were incorporated for training the system, as well as 22 test results for testing the performance of the system.

Actual test results ranged from 33.7 to 66.8 MPa for different mixtures and the prediction error ranged from 1.4% to 16.2%, with a coefficient of correlation of R=0.99, which approved the accuracy of the developed model.

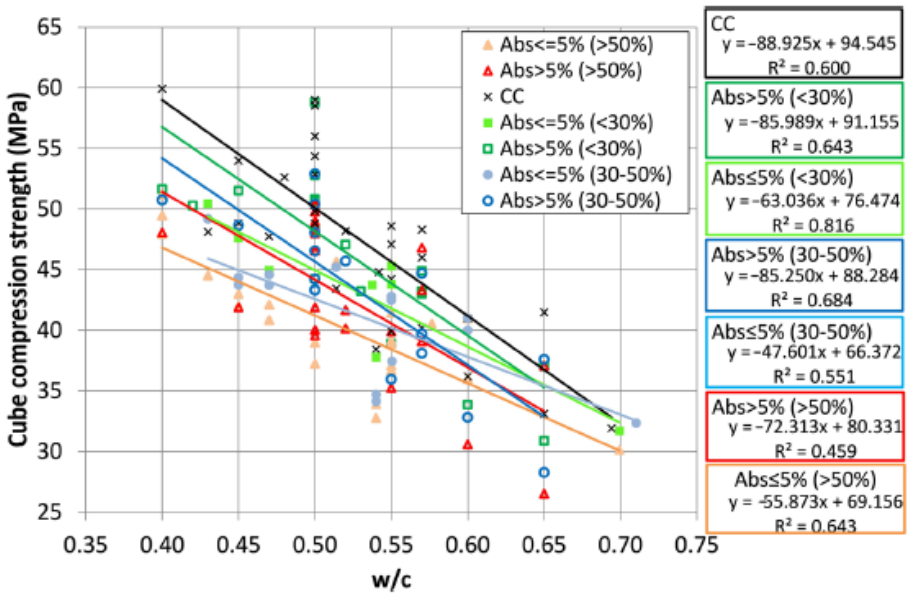

Figure 2.8 Effect of coarse RCA content and water absorption on compressive strength (Gonzalez-Taboada et al. 2016)

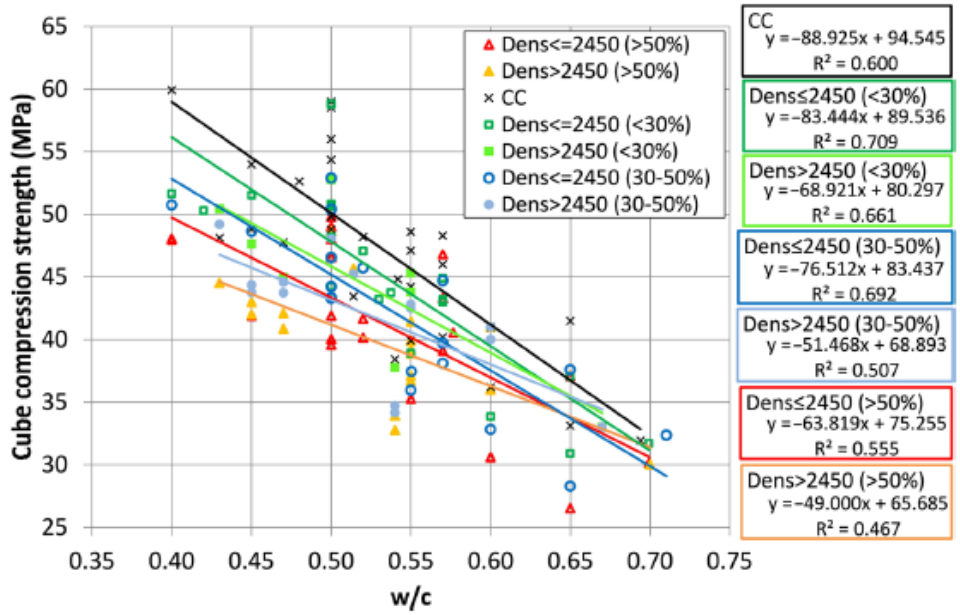

Figure 2.9 Effect of coarse RCA content and specific gravity on compressive strength (Gonzalez-Taboada et al. 2016)

2.3.3.2 Splitting tensile strength. As in the case of compressive strength, RCA replacement mostly results in a decrease in splitting tensile strength of concrete. Ravindrarajah et al., (1985) reported that the splitting tensile strength of concrete was consistently 10% lower than that of conventional concrete without RCA. Tabsh and Abdelfatah (2009) reported that about 25% to 30% drop in the tensile strength was observed in concrete made with RCA. Kou et al. (2012) observed that regardless of the type of the recycled aggregate used, the splitting tensile strength of the specimens decreased with an increase in RCA replacement ratio before the age of 28 days. However, for some types of the RCAs used, an increase in the splitting tensile strength at the age of 90 days is observed. Sagoe et al., (2001) reported that there is no significant difference between the splitting tensile strength of the reference and the recycled aggregate concrete specimens. Limbachiya (2012) and Yong and Teo (2009) reported that while replacing up to 50% of coarse aggregate with RCA, there was no difference in splitting tensile and flexural strengths between the RAC and the reference, but at full replacement (100%) results were improved for RCA due to better interlocking.

2.3.3.3 Flexural strength. The RCA replacement does not have significant negative effects on flexural strength of concrete. Xiao and Li (2005), Hu (2007), and Cheng (2005) have reported that up to 100% RCA replacement in concrete mixtures of w/cm varying from 0.43 to 0.57 only has marginal effects on the flexural strength of concrete. Ravindrarajah and Tam (1985) also reported that increasing the RCA content does not have a significant effect on flexural strength. Topçu and Sengel (2004) reported that the flexural strength is decreasing due to the increase in RCA replacement level.

2.3.3.4 Fracture energy. Studying the fracture properties of concrete can provide realistic measures of load carrying capacity of materials in a structural system. Bordelon et al. (2009) studied the 7-d fracture behavior of concrete containing 50% and 100% coarse RCA, reinforced with 0 to 2% synthetic fibers. Authors reported similar fracture properties for the reference concrete and the one cast with 50% coarse RCA. However, a decrease in fracture properties was observed as a result of 100% RCA replacement. Results of the reference virgin aggregate concrete and those of the mixture with 50% RCA were 53% higher than that of the 100% RCA mixture. Authors reported that incorporation of 2% of synthetic fibers was helpful in enhancing the fracture performance

of the investigated mixtures, even in comparison with that of the reference concrete with no fibers and without any RCA. No significant difference in fracture properties of the fiber reinforced concrete was observed regardless of the variation in RCA content from 0 to 100%. Brand et al. (2014) investigated the fracture behavior of single lift and two lift full scale pavement slabs measuring 6 ft× 6 ft × 6 in. cast with 100% coarse RCA. Two lift slabs were cast with a 4.0 in. bottom layer of 100% RCA topped with a 2.0 in. layer of virgin aggregate concrete. Single layer slabs were cast with virgin aggregate and 100% coarse RCA. Authors reported higher average maximum tensile strength at failure for the RCA-made slabs in comparison with the virgin aggregate slab. For the case of full depth RCA replacement, the average maximum tensile strength was 1250 psi, in comparison to 1180 psi for the virgin aggregate slab and 1415 psi for the two lift slabs cast with virgin aggregate on top of 100% RCA. Beams measuring 3.1 × 5.9 × 28 in. were incorporated for the measurement of fracture energy of the reference and 100% RCA beams. Authors reported higher peak load for virgin aggregate concrete (3.57 vs. 3.18 kN). However, the total fracture energy of the RCA-made beams was higher than that of the reference concrete (84.5 vs. 73.8 N/m).

Volz et al. (2014) investigated the fracture energy of concrete mixtures proportioned with 0, 50%, and 100% coarse RCA replacement. Concrete mixtures were proportioned with 0.40 w/c and 535 lb/yd^3 of Type I cement. Authors reported a decrease in fracture energy as a function of an increase in RCA content. It was observed that the average fracture energy reduced from 0.80 lb/in. in the case of the reference concrete to 0.75 and 0.59 lb/in. at 50% and 100% RCA replacements, respectively.

2.3.3.5 Modulus of elasticity. Data published in the literature indicate that among all types of mechanical properties, MOE is one the characteristics that can be highly sensitive to RCA incorporation. Availability of residual mortar in RCA particles reduces the overall stiffness of the coarse aggregate skeleton and increases the absolute volume of mortar in hardened state. This reduces the rigidity of the concrete, resulting in lower MOE compared to the mixtures cast with virgin aggregate. Moreover, given the sensitivity of MOE, existence of micro-cracks and defected interfacial transition zone (ITZ), typical of RCA particles, can affect the MOE significantly (Mehta). Results of a

survey conducted by the National Cooperative Highway Research Program (NCHRP 2013) reveal that using coarse RCA can result in up to 35% reduction in MOE.

Kcnaack and Kurama (2014) investigated the effect of coarse RCA on properties of concrete mixtures proportioned with 0.40 water-to-cement ratio (w/c) and 341 kg/m^3 of Portland cement. The authors reported decrease in 28-day MOE from 33.5 to 29.4 and 22.6 GPa as a result of 50% and 100% coarse RCA incorporation, corresponding to 12 % and 33% MOE reduction, respectively. Fonseca et al. (2011) used 20%, 50%, and 100% coarse RCA in concrete mixtures proportioned with 446 kg/m^3 of Portland cement and 0.43 w/c. The authors reported reduction in MOE from 43.5 to 35.5, 38.0, and 33.5 GPa, due to 20%, 50%, and 100% RCA replacement, corresponding to 23% lower MOE with 100% coarse RCA. Vieira et al. (2011) investigated the effect of up to 100% RCA incorporation in concrete prepared with 445 kg/m^3 Portland cement and 0.43 w/c. The authors reported up to 24% reduction in 28-day MOE, with values of 43.7, 36.7, 40.4, and 33.2 GPa for the Reference, 20%, 50%, and 100% RCA mixtures, respectively.

Historically, MOE is considered as a function of compressive strength and such properties as unit weight, or type of aggregate used in concrete. European standard (Eurocode 2) considers MOE as a function of compressive strength, with estimated values for each strength category presented in tabular format. Japanese standard (JSCE 07) uses a tabular format to present estimations for MOE as a function of compressive strength. However, two main categories are considered by JSCE (07): (1) normal aggregate concrete; (2) light weight aggregate concrete.

Building design code of the American Concrete Institute (ACI 318-14) considers two equations for estimating the MOE as a function of compressive strength: (1) Equation (2-1) for light weight concrete with density of 1440 to 2560 kg/m^3; (2) equation (2-2) for normal weight concrete as follows:

$$E_c = \left(0.043\sqrt{f_c'}\right)(W_c)^{1.5} \quad (2\text{-}1)$$

$$E_c = 4700\sqrt{f_c'} \quad (2\text{-}2)$$

where W_c is the density of concrete (kg/m^3) and f_c' is the compressive strength (MPa).

Similar approach is used by the Canadian standard (CSA 2004) that considers MOE for light weight concrete with density of 1500-2500 kg/m^3, and concrete with normal density as presented in Equations (2-3) and (2-4), respectively.

$$E_c = \left(3300\sqrt{f'_c} + 6900\right)\left(\frac{\gamma_c}{2500}\right)^{1.5} \quad (2\text{-}3)$$

$$E_c = 4500\sqrt{f'_c} \quad (2\text{-}4)$$

where γ_c is the density of concrete (kg/m^3) and f'_c is the compressive strength (MPa).

CEB code (CEB-FIB 1990) proposes the use of compressive strength and aggregate type for prediction of MOE as shown in Equation (2-5). The model is developed based on data obtained from concrete made with quartzitic coarse aggregate and correction factors were suggested for other aggregate types.

$$E_{ci} = \alpha_E \times E_{C0}[(f_{ck} + \Delta f)f_{cm0}]^{1/3} \quad (2\text{-}5)$$

where E_{ci} is the 28-day modulus of elasticity (MPa), Δf is considered as 8 MPa, f_{cm0} is considered as 10 MPa, f_{ck} is characteristic compressive strength (MPa), E_{c0} is 2.15×10^4 MPa, and α_E is a correction factor, with values of 1.2, 1.0, 0.9, and 0.7 for basalt aggregate, quartzitic aggregate, limestone aggregate, and sandstone, respectively.

Such models cannot represent the MOE in mixtures cast with recycled aggregate accurately (Behnood et al. 2015). Given the importance of the issue, considerable effort was devoted to quantify the effect of RCA on MOE. Such methodologies are either based on experimental data obtained from laboratory investigation, or based on literature survey. A summary of such models is provided below. However, considering the limited number of data points used for development of such prediction tools, and given the variable nature of the RCA sources, there still exists the need to expand the available analytical models.

Ravindrarajah and Tam (1985):

$$E_c = 4.63\, f_{cy}^{0.50} \quad (2\text{-}6)$$

Ravindrarajah and Tam (1985):

$$E_c = 7.77\, f_{cu}^{0.33} \tag{2-7}$$

Dhir et al. (1999):

$$E_c = 0.37 f_c + 13.1 \tag{2-8}$$

Dillmann (1998):

$$E_c = 0.0.63443 f_{cu} + 3.0576 \tag{2-9}$$

Mellmann (1999):

$$E_c = 0.378 f_c + 8.242 \tag{2-10}$$

Kakizaki et al (1988):

$$E_c = 190\ (\rho/2300)^{1.5} \sqrt{\frac{f_{cu}}{2000}} \tag{2-11}$$

Zilch and Roos (2001):

$$E_c = 9.1\ (f_{cu} + 8)^{1/3} \times (\rho/2400)^2 \tag{2-12}$$

Corinaldesi (2010):

$$E_c = 0.909 f_{cu} + 8.738 \tag{2-13}$$

Corinaldesi (2010):

$$E_c = 18.8 \sqrt[3]{\frac{0.83 f_{cu}}{10}} \tag{2-14}$$

Xiao et al. (2006):

$$E_c = \frac{100}{\left(2.8 + \frac{40.1}{f_{cu}}\right)} \tag{2-15}$$

where E_c is the MOE in GPa, f_c values are in MPa, and ρ is concrete density in kg/m^3.

2.3.4. Shrinkage.

2.3.4.1 Drying shrinkage. Drying shrinkage is one of the main challenges that burden the widespread use of RCA in transportation infrastructure. The porosity of the adhered mortar, along with higher amounts of fines and dust available in RCA sources, increases the water absorption rate of the RCA compared to virgin aggregate. Results of a survey (Silva et al. 2014) reveals the fact that coarse RCA sources typically exhibit absorption rates of 2% to 6%, compared to values of usually less than 2% for virgin aggregates. Such an increase in absorption, along with the decreased restraining capacity due to the lower rigidity of the RCA particles contribute in higher shrinkage of the hardened concrete (Sagoe et al. 2001, Xiao et al. 2012).

Several studies have considered the effect of RCA on drying shrinkage. Corinaldesi (2010) investigated the effect of 50% coarse RCA replacement on shrinkage of concrete cast with 350 kg/m^3 of Portland cement and water-to-cement ratio (w/c) of 0.40. An increase in 28- and 56-day drying shrinkage from 260 and 340 με to 310 and 500 με was reported, when 50% RCA was used, which corresponded to 19% and 47% increase. Cui et al. (2014) investigated the effect of 100% coarse RCA replacement on drying shrinkage of concrete prepared with 400 kg/m^3 of Portland cement and w/c of 0.35. The authors reported an increase in 28-, 56-, and 91-day shrinkage from 310 to 470, 450 to 660, and 410 to 700 με, corresponding to 52%, 47%, and 37% increase, respectively. Gonzalez and Etxeberria (2016) investigated shrinkage in concrete proportioned with 380 kg/m^3 of cement and w/c of 0.29. Coarse RCA from three different sources was incorporated at replacement rates of 20%, 50%, and 100%. LA abrasion of 24.0% to 25.2%, and absorption rates of 3.74%, 4.90%, and 5.91% was reported for the RCA. The authors reported 90-day shrinkage value of 300 με for the Reference concrete, compared to 320, 400, and 400 με for 20%, 50%, and 100% RCA with absorption of 3.74%. Such values were 410, 430, and 480 με, and 380, 480, and 720 με for concrete made with 20%, 50%, and 100% RCA with absorption rate of 4.90% and 5.91%, respectively (Gonzalez and Etxeberria 2016).

Kou et al., (2007), Kou and Poon (2012), Hansen and Boegh (1985), Fathifazl et al., (2011), Nassar and Soroushian (2012), and Gomez (2002) studied the shrinkage behavior of the RCA-made concrete and reported that the drying shrinkage increases with

the increase in RCA content. However, this increase is negligible up to 20% replacement ratio (Kou et al., 2007). Domingo-Cabo et al., (2009) found that the RAC with a RCA replacement level of 20% exhibited a similar shrinkage to the conventional concrete at early age. For a period of 6 months, the shrinkage in RAC was only 4% higher. In the case of a RCA replacement level of 50%, the shrinkage was 12% greater than that of the conventional concrete after 6 months. Moreover, Sagoe et al., (2001) reported that drying shrinkage of RAC was about 25% higher than that of conventional concrete. Kou et al., (2012) reported that drying shrinkage of RAC increases as the RCA replacement ratio increases. They also observed that recycled aggregates with lower water absorption capacities result in lower shrinkage rates. Kim and Bentz (2008) investigated the drying shrinkage in concrete mixtures made with RCA. They reported that the RCA can provide internal curing in concrete, which is useful in reducing drying shrinkage. Similar results were reported by Hu et al., (2013) who reported that incorporating fine RCA is useful in decreasing the drying shrinkage through internal curing.

A wide spread in effect of RCA on drying shrinkage can be detected from data available in the literature. Such variations can be attributed to both the RCA characteristics and concrete mixture proportions. For an example, Silva et al. (2015) conducted a survey that revealed that the use of 100% coarse RCA can lead to as little as 10% to as high as 100% increase in drying shrinkage compared to similar concrete without any RCA. Based on the survey results and regardless of the mixture proportioning of the concrete, the authors recommended considering an average increase of 20%, 40%, and 80% in drying shrinkage of concrete made with 20%, 50%, and 100% RCA, respectively. Similar trends were reported by the Task Force of the Standing committee of Concrete of Spain (Vazquez et al. 2004) where no significant change in drying shrinkage can be expected in concrete containing up to 20% coarse RCA. Correction factors are recommended to compensate for the incorporation of 100% RCA, as summarized in Table 2.7. Results of a survey conducted by (NCHRP 2013) also imply that up to 50% increase in drying shrinkage can be expected when coarse RCA is used in concrete designated for pavement construction.

Table 2.7 Shrinkage correction factors suggested by Vazquez et al. (2004) adapted from (Silva et al. 2015)

Source	Correction factor for drying shrinkage	
	20% Coarse RCA	100% Coarse RCA
Belgium	1.00	1.50
RILEM	1.00	1.50
The Netherlands	1.00	1.35-1.50

2.3.4.2 Cracking due to re-strained shrinkage. Limited studies are available on the impact of RCA on restrained shrinkage. Adams et al. (2016) investigated the cracking potential of concrete made with RCA. The mixtures were proportioned with 394 kg/m^3 of Portland cement and water-to-cement ratio (w/c) of 0.40. A laboratory produced RCA and a RCA from commercial source were incorporated at 25% and 100% replacements, by mass. The laboratory RCA had a parent concrete made with rounded gravel, and the commercial RCA was obtained from recycling airfield concrete cast with crushed aggregate. The authors reported no significant difference between the drying shrinkage of the mixtures made with and without RCA; spread of 50 to 100 με was obtained after 100 days of drying. The 28-day MOE ranged from 27 GPa for the mixture with 100% commercial RCA to 33 GPa for the Reference concrete with crushed aggregate. Times to cracking under restrained ring test (ASTM C1581, 2016) were 5.4 and 9.3 days for the Reference mixtures incorporating rounded and crushed virgin aggregates, respectively, and 7.9 and 10.8 days for mixtures cast with 25% and 100% commercial RCA, and approximately 7.5 days for laboratory produced RCA.

Jeong (2011) used ring specimens to evaluate the restrained shrinkage cracking potential of concrete made with 100% coarse RCA. The mixtures were prepared using a single source of RCA, 525 kg/m3 of binder and 0.42 w/cm. Initial moisture status of the RCA was 0, 74%, or 100% of the SSD condition. No cracking was observed for the investigated concrete by the time of test termination at 100 days. The minimum and the maximum 28-day values of strain in steel rings of 70 and 100 με were reported for the Reference and the 100% dry RCA mixtures, respectively. Similar performance was reported for mixtures proportioned with fully saturated RCA and RCA with 74% moisture content (Jeong 2011). The strain in the steel ring ranged between 115 με in the

case of the mixture with 100% dry RCA to 130 με for the mixtures with moisture content of 74% or 100%. Further investigation using dog bone specimens revealed cracking before 7 days. Mixture with 100% saturated RCA cracked at 5.5 days, compared to 6.7 days for the rest of the specimens (Jeong 2011).

2.3.5. Durability.

2.3.5.1 Chloride ion permeability. Andreu and Miren (2014) investigated the electrical resistivity and RCP of concrete proportioned with 0.29 w/cm and 380 kg/m3 of Portland cement (OPC). The authors reported decrease in 28-day electrical resistivity from 26.8 to 25, 20.1, and 9.5 KΩ.cm corresponding to increase in 28-day RCP values from 880 to 1050, 1200, and 2070 Coulomb with the use of 20%, 50%, and 100% coarse RCA. Kou et al. (2011) investigated the effect of RCA as a full replacement for virgin coarse aggregate on durability of concrete prepared with 390 kg/m3 of binder and 0.5 w/cm. Increase in 90-day RCP from 3250 and 2200 to 4000 and 3800 Coulomb was reported with the use of RCA in mixtures made with 100% OPC or binary cement with 55% GGBS, respectively. Duan and Poon (2014) investigated the relation between the water absorption of RCA and RCP results for full coarse RCA replacement. The investigated mixtures were prepared with 485 kg/m3 of OPC and 0.34 w/c. The authors reported increase in total passed charge from 2050 to 2350, 2850, and 3850 Coulomb when RCA with water absorption of 3.24%, 6.61%, and 7.1% was used, respectively. Similar trends were reported by Kou et al. (2012) who examined concrete prepared with 410 kg/m3 of OPC and 0.55 w/c for chloride ion permeability at 90 days. Greater RCP values were observed with higher water absorption of RCA. Increase in RCP from 4200 to 5300, 6100, and 7600 Coulomb was observed when 20%, 50%, and 100% RCA with water absorption of 6.2% was incorporated. Such results were 4650, 5400, and 6150 Coulomb when virgin coarse aggregate was replaced with 20%, 50%, and 100% RCA with water absorption of 3.77%.

Sim and Park (2011) observed that in the case of concrete made with coarse RCA and partial replacement of fine recycled aggregates, there is no significant difference between the total charges passing through the specimens (electrical conductivity) with up to 100% fine recycled aggregate replacement. However, as the curing time increases, the incorporation of a greater volume of fine recycled aggregate can lead to a decrease in

conductivity. By increasing the curing period and incorporating proper types and contents of supplementary cementitious materials (SCMs), the chloride-ion permeability could be controlled (Sim and Park, 2011).

2.3.5.2 Freeze/thaw resistance. Several studies have considered the effect of RCA on resistance of concrete to freeze and thaw cycles and exposure to scaling caused by de-icing salts. Zaharieva et al (2004) investigated the frost durability of concrete made with 100% coarse and fine RCA, 400 kg/m^3 of Portland cement (OPC), and free water-to-cement ratio (w/c) of 0.27 to 0.37. The authors reported durability factor over 82% for all investigated mixtures regardless of the degree of saturation of the RCA. However, the highest durability factor of 100% was reported for the reference concrete cast without any RCA. Yildirim et al. (2015) investigated the effect of up to 100% coarse RCA with 0, 50%, and 100% saturation level on freeze/thaw resistance of concrete proportioned with 400 kg/m^3 of cement and w/c of 0.5 to 0.7. No significant effect due to the use of RCA was observed, with 2.4%-7.1% and 4.3%-13.2% loss in mass and vibration frequency, respectively, after 300 cycles of freeze and thaw. Gokce et al. (2004) incorporated 100% RCA obtained from either a source of air entrained concrete or a concrete without any air entrainment to develop mixtures with w/c of 0.55. Up to 13% improvement in durability factor after 500 test cycles was reported with the use of RCA from an air-entrained source, regardless of the adhered mortar content and absorption rate of the RCA. This was believed to be due to pressure dissipation in porous structure of the aggregates with use of RCA from an air entrained source. However, severe drop in durability factor to values lower than 60% after 200 cycles was reported when non-air entrained RCA or a combination of the two types of RCA were used as coarse aggregate. Such an observation was proved to be due to cracking of the non-porous residual mortar phase of the RCA, along with crack propagation in the old interfacial transition zone (ITZ), which was quantified through image analysis. In the case of the mixtures made with non-air entrained RCA, the authors reported that even the reduction in w/cm from 0.55 to 0.30, and the incorporation of binary cements with 10% silica fume or 10% meta kaolin could not guaranty frost durability and values of durability factor lower than 60% were obtained after 300 test cycles for such modified mixtures. Liu et al. (2016) also reported increase in crack density due to freeze and thaw action in adhered mortar phase of RCA

obtained from non-air entrained sources. Such cracking behavior was believed to be the reason for reduced durability factor (80% vs. 95%) of mixtures cast with non-air entrained RCA while compared to that of the mixtures made with RCA obtained from air entrained concrete. Medina (2013), Richardson (2011), Ajdukiewicz (2002), and Limbachyia (2000) have investigated the frost durability of the RCA-made concrete mixtures and reported that given the similar strength grade, there is no significant difference in freeze/thaw resistance of the RCA-made and conventional concrete. On the other hand, Xiao et al. (2012) reported that concrete made with RCA is more susceptible to damage due to the freeze/thaw cycles.

In summary, and based on the data available in the literature, it may be concluded that the pore structure of the RCA can play an important role in frost durability of new concrete. Concrete made with RCA obtained from crushing air entrained concrete can exhibit proper resistance against frost action. The use of RCA from non-air entrained origin on the other hand, can have negative impacts on resistance against frost action. Speare and Ben-Othman (2000) have reported that there is no difference between the de-icing salt scaling performance of RCA-made concrete and that of the virgin aggregate mixtures. Movassaghi (2006) also studied the de-icing salt scaling resistance of concrete made with RCA and reported that the scaling resistance increases with an increase in the age of the RCA source.

2.3.5.3 Carbonation depth. Carbonation depth is proven to increase with the increase in the RCA content in concrete (Abbas et al., 2009). The mortar phase attached to the virgin aggregate available in RCA particles provide permeable paths through the RCA-made concrete. This increases the depth to which carbon dioxide can reach.

2.3.5.4 Absorption. Absorption of RCA concrete is usually reported to be higher than that of virgin aggregate concrete. This is mainly due to the attached porous mortar content of the RCA particles that can provide more water reservoirs, thus maintaining higher relative humidity inside the pore solution (Volz et al., 2014).

2.4. USE OF RCA IN RIGID PAVEMENT CONSTRUCTION

Most of the application of RCA in the U.S. involves the use of RCA as aggregate in base and subbase layers (FHWA 2004). Other applications include cement-treated

base, backfill, embankment, stabilization, erosion control (riprap), and landscaping (ACPA 2009). According to a survey conducted by Garber et al., (2011), the use of RCA in new concrete production is rather advanced in European and East Asian countries. For example, in Finland, 10% of all RCA applications are bound applications implying new concrete mixtures or cement-treated bases (Englesen et al., 2005). In Austria, RCA is used for producing the bottom layer in two-lift concrete pavement applications. In Australia, RCA is allowed for use in new concrete production for curbs and sidewalks.

Use of RCA in construction of rigid pavements started in early 1970's. Most of these pavements have performed well. However, several states in U.S. stopped using RCA in pavement construction due to poor performance of some cases (Cuttell et al. 1997), which was associated with: (1) higher shrinkage and thermal deformations of RCA concrete, resulting in distress in mid-panel cracks of jointed reinforced concrete pavement (JRCP); (2) inferior load transfer along with faulting in non-doweled sections due to reduced aggregate interlock; (3) durability issues including delayed D-cracking due to use of RCA obtained from crushing of old concrete proportioned with aggregate that are highly susceptible to frost damage (Wade et al. 1997).

Cuttel et al. (1997) investigated the use of RCA for construction of single layer concrete pavements in the 1970s and 1980s in Connecticut (one section), Kansas (one section), Minnesota (four sections), Wisconsin (two sections) and Wyoming (one section). Jointed plain concrete pavements (JPCP), continuously reinforced concrete pavements (CRCP), and jointed reinforced concrete pavements (JRCPs) were investigated. Joint spacing ranged from 3.7 to 12 m, and slab thicknesses varied between 200 and 280 mm. The water-to-cementitious materials ratio (w/cm) of the incorporated mixtures ranged from 0.38 to 0.47. Based on the core sample results, authors reported comparable compressive strength and splitting tensile strength values for the control and RCA sections. The modulus of elasticity results proved to be up to 18% lower than that of the control concrete. Up to 23% increase in coefficient of thermal expansion (CTE) was observed for the RCA-made sections. In addition, investigated sections had similar responses to falling weight deflection test. However, inferior load transfer efficiency in the case of RCA sections was observed (Cuttel et al. 1997). The investigation was followed by a second survey in 2006 by Gress et al. (2009) on same sections (20- to 22-

years old at the time of survey). Based on the field measurements and inspections, the authors reported increase in transverse cracking and transverse joint spalling, increase in length of deteriorated transverse cracks, and decrease (up to 0.8 points out of 5.0) in present serviceability rating (PSR) of the pavement made with RCA.

Salas et al., (2010) used up to 100% RCA for producing concrete for rigid pavement applications as a part of O'Hare Airports modernization project using the two stage mixing approach developed by Tam et al. (2005). Similar or higher compressive strength compared to the virgin aggregate mixtures, similar shrinkage to the virgin aggregate mixtures at early ages, reduced bleeding and segregation, and similar concrete workability was reported as a result of using RCA in concrete production. Choi and Won (2009) studied the performance of a CRCP highway section made totally with fine and coarse RCA located in Houston, TX. Based on the results by testing core samples, it was observed that the average compressive strength decreased due to use of RCA. The modulus of elasticity of the RCA concrete was lower than that of the virgin aggregate mixture. It is interesting to note that the coefficient of thermal expansion of the RCA concrete was similar to the virgin aggregate mixtures. The rapid chloride-ion permeability results of the RCA concrete were surprisingly lower than that of the virgin aggregate concrete and rated as "Very low" based on the ASTM C1202 (2012). The sulfate content of the RCA-made and the virgin aggregate mixtures were found to be similar. It was also reported that the RCA sections had overall good performance after more than 10 years of service life with no structural distress taking place. The transverse crack distributions were also found to be similar to that of the virgin limestone mixtures (Choi and Won, 2009).

2.5. REMARKS

In general, it can be concluded that given the variable properties of RCA particles compared to the virgin aggregate sources, the mechanical properties and durability of concrete made with RCA may be lower than conventional concrete without any RCA. However, the degree of variation in results depends on the concrete composition and source of RCA. Laboratory investigation is required for the selection of RCA for use in construction projects. Furthermore, a comprehensive test matrix is required to investigate

the properties of concrete mixtures made with RCA for such applications as sustainable pavement applications. Based on the results published in the literature, the following conclusions can be made:

- Reduction in specific gravity and workability can be expected with the use of RCA in concrete production.
- Key physical properties, including the oven-dry specific gravity, water absorption, LA abrasion, and availability of deleterious materials, and degree of ionic contamination (chloride ions, sulfates, etc.) should be considered in categorizing the RCA depending the applications.
- Reduction in mechanical properties, including compressive strength, splitting tensile strength, flexural strength, and MOE can be expected with the use of RCA. Both the RCA content and quality affect such properties.
- Drying shrinkage can be affected by the use of RCA significantly. A greater content of RCA with lower quality can result in higher shrinkage.
- Durability against freeze and thaw cycles can be affected by the use of RCA from non-air entrained and low quality RCA. Carbonation, electrical resistivity, chloride ion permeability can be affected by the use of RCA with high water absorption and/or contaminated with chloride ions.

2.6. RESEARCH NEED

A review on the existing literature on use of RCA in transportation infrastructure demonstrates the need to quantify the effect of using high-volume RCA on properties of pavement concrete. Of great interest was the use of at least 50% recycled materials in construction of single-layer rigid pavement and the use of more than 50% recycled materials in two-lift rigid pavement systems.

Laboratory investigation and analysis of database using artificial intelligence was employed to quantify the effect of high-volume RCA on key engineering properties of concrete. Mechanical properties, drying shrinkage, cracking potential, and durability of concrete designated for rigid pavement construction were investigated. Effect of RCA on such properties was quantified within the extent of the investigated experimental domain.

3. AGGREGATE PROPERTIES

3.1. GENERAL

The present section provides a summary of the laboratory investigation on recycled aggregate sources for use in concrete production. Several fine and coarse RCA sources procured from different recycling centers in the state of Missouri, Kansas, and Illinois were examined for key engineering properties. Moreover, a source of coarse RCA was produced and tested in the laboratory. Three different types of virgin coarse aggregate and a source of river-bed sand were also examined in the laboratory for key physical properties. In total, three different types of virgin coarse aggregate, the river-bed sand, two selected types of fine RCA, and seven selected types of coarse RCA were employed for concrete production.

3.2. LABORATORY PRODUCED RCA

The parent concrete used for the production of RCA in laboratory was a mixture used by the Missouri department of Transportation (MoDOT) as a Class B concrete. Such concrete has a design compressive strength of 31 MPa, typically used for interior structural elements and substructures. Table 3.1 offers a summary of the proportions of the concrete used for developing the RCA. The parent concrete was proportioned with 317 kg/m^3 of type I/II Portland cement and water-to-cement ratio (w/c) of 0.45. A source of state approved crushed dolomite coarse aggregate (DOL2) and siliceous river-bed sand were incorporated for developing the concrete. High range water reducing admixture (HRWRA) and air-entraining agent (AEA) were used to reach proper initial slump and secure 6%±1% air content in fresh concrete.

Table 3.1 Mixture proportions of the concrete used for RCA production in laboratory

Cement (kg/m^3)	Water	w/c	Coarse (kg/m^3)	Sand
317	143	0.45	1089	772

The concrete was delivered by a local ready mix plant. Non-reinforced concrete beams were cast in the laboratory as shown in Figure 3.1. Cylindrical specimens were also cast in the laboratory for monitoring the strength development during the curing time. The beams and the companion cylindrical specimens were covered with wet burlap and plastic sheets for 24 hours after casting. The beams were then demolded and stored in laboratory at room temperature for 28 days, and transported to an aggregate quarry by the end of the curing period. In total, 15.3 m^3 of concrete was delivered in five different steps, each time casting five beam elements using about 3 m^3 of concrete. An average air content in fresh state of 9% was obtained for the parent concrete. The concrete exhibited an average compressive strength of 37.0 MPa at the time of crushing.

Figure 3.1 Concrete beams cast using the parent concrete for RCA production in laboratory

A mobile crusher with both primary and secondary steel jaw crusher was used at the quarry. The concrete was crushed and sieved to produce coarse RCA with nominal maximum size of 19 mm, as shown in Figure 3.2. Key engineering properties of the produced RCA were determined in the laboratory.

Figure 3.2 Laboratory produced coarse RCA

3.3. RCA FROM RECYCLING CENTERS

In total, 19 different types of fine and coarse RCA produced in eight recycling centers in the states of Missouri, Illinois, and Kansas were examined in the laboratory. The initial laboratory investigation included testing the fine and aggregate sources for key physical properties, including the particle-size distribution, dry rodded unit weight, specific gravity, water absorption, and the Los Angeles (LA) abrasion resistance. Table 3.2 summarizes the properties of the investigated RCA sources. Figure 3.3 presents the particle-size distribution of the RCA sources. One source of fine RCA and three coarse RCA sources were rejected during the initial investigations. This was due to the availability of excessive amounts of fines and contaminations in the rejected coarse RCA, and/or due to mono-sized gradation of the aggregates. No information was available regarding the properties of the parent concrete used for developing the commercially produced RCA.

The residual mortar content available in RCA particles is the main source of variations in properties of RCA while compared to the virgin aggregate. The residual mortar is generally more porous than the old virgin aggregate phase of the RCA particles. Therefore, the availability of a higher content of the porous and low quality residual mortar can result in inferior properties of RCA. Bulk of technical literature on RCA implies that the variations in quality of RCA due to the presence of residual mortar can be best reflected in the water absorption and oven-dry specific gravity of fine and coarse RCA, and in the mass loss due to LA abrasion for the coarse RCA. (Silva et al. 2014;

Butler et al. 2013; ASHTO 2015; Mc Neil and Kang 2012). Therefore, the aforementioned characteristics were considered for selection of the RCA. Two types of fine RCA, six types of commercially produced coarse RCA, and the laboratory produced coarse RCA were finally used for further investigations and development of concrete mixtures in the laboratory.

The chemical contaminations available in the RCA particles, availability of impurities and deleterious materials, including bituminous materials, steel, organic substances, masonry, etc. can also impact the engineering properties of the RCA. Therefore, it the deleterious materials content of the selected coarse RCA was determined. Samples measuring at least 4000 g were taken from each coarse RCA source. The aggregates were washed using tap water and dried in oven set at 110±5 ºC until constant mass. The impurities were handpicked from each aggregate source and weighed. The deleterious materials content was then reported as the percentage of the initial mass of the aggregate sample.

The aggregate soundness test introduced by ASTM C88 was modified as proposed by Abbas et al. (2007) to determine the resistance of coarse RCA materials against freeze-thaw cycles. The test method involved: (1) obtaining a representative sample of different size portions of RCA as suggested by Abbas et al. (2007); (2) washing the aggregate with tap water, drying in oven set at 110±5 ºC until constant mass; (3) immersing the aggregates in saturated solution of Sodium Sulfate; (4) exposure of the samples to seven daily cycles of freezing and thawing with temperature range similar to requirements of ASTM C 672 (2012) test on de-icing salt scaling; (5) washing the aggregate using tap water, drying in oven set at 110±5 ºC until constant mass, and sieving on 4.75 mm mesh by the end of the freeze-thaw cycles; (6) calculating the percentage mass loss for each size fraction and determining overall mass loss for each aggregate type based on aggregate particle size distribution. Table 3.3 summarizes the results obtained for selected RCA types.

Table 3.2 Physical properties of the investigated RCA sources

Aggregate		Source	Specific gravity	Dry rodded unit weight (kg/m^3)	Absorption (%)	Los Angles abrasion (%)
Fine aggregate	RCA 1	Lambert Airport, MO*	2.41	-	6.80	-
	RCA 2	Lambert Airport, MO*	2.11	-	7.33	-
	RCA 3	Gen2 Rocs, MO	2.10	-	9.29	-
	RCA 4	Bridgetone, MO	1.90	-	14.19	-
	RCA 5	Surmier Recycling, IL	2.05	-	10.47	-
	RCA 6	KHC, KS	Rejected in visual inspection			
Coarse aggregate	RCA 1	Laboratory produced*	2.35	1437	4.56	41
	RCA 2	Lambert Airport, MO*	2.38	1458	4.2	33
	RCA 3	Lambert Airport, MO*	2.35	1445	4.46	33
	RCA 4	Gen2 Rocs, MO	2.32	1416	4.99	35
	RCA 5	Bridgetone, MO	2.15	1362	8.17	43
	RCA 6	Metro Fill, MO*	2.25	1397	5.75	39
	RCA 7	Bridgetone, MO*	2.17	1336	7.58	44
	RCA 8	Bridgetone, MO*	2.21	1357	7.13	53
	RCA 9	Surmier Recycling, IL	2.21	1379	6.66	43
	RCA 10	Kaw Valley, KS*	2.24	1384	6.05	38
	RCA 11	KHC, KS	Rejected in visual inspection			
	RCA 12	Surmier Recycling, IL	Rejected in visual inspection			
	RCA 13	Eco Recycling , MO	Rejected in visual inspection			

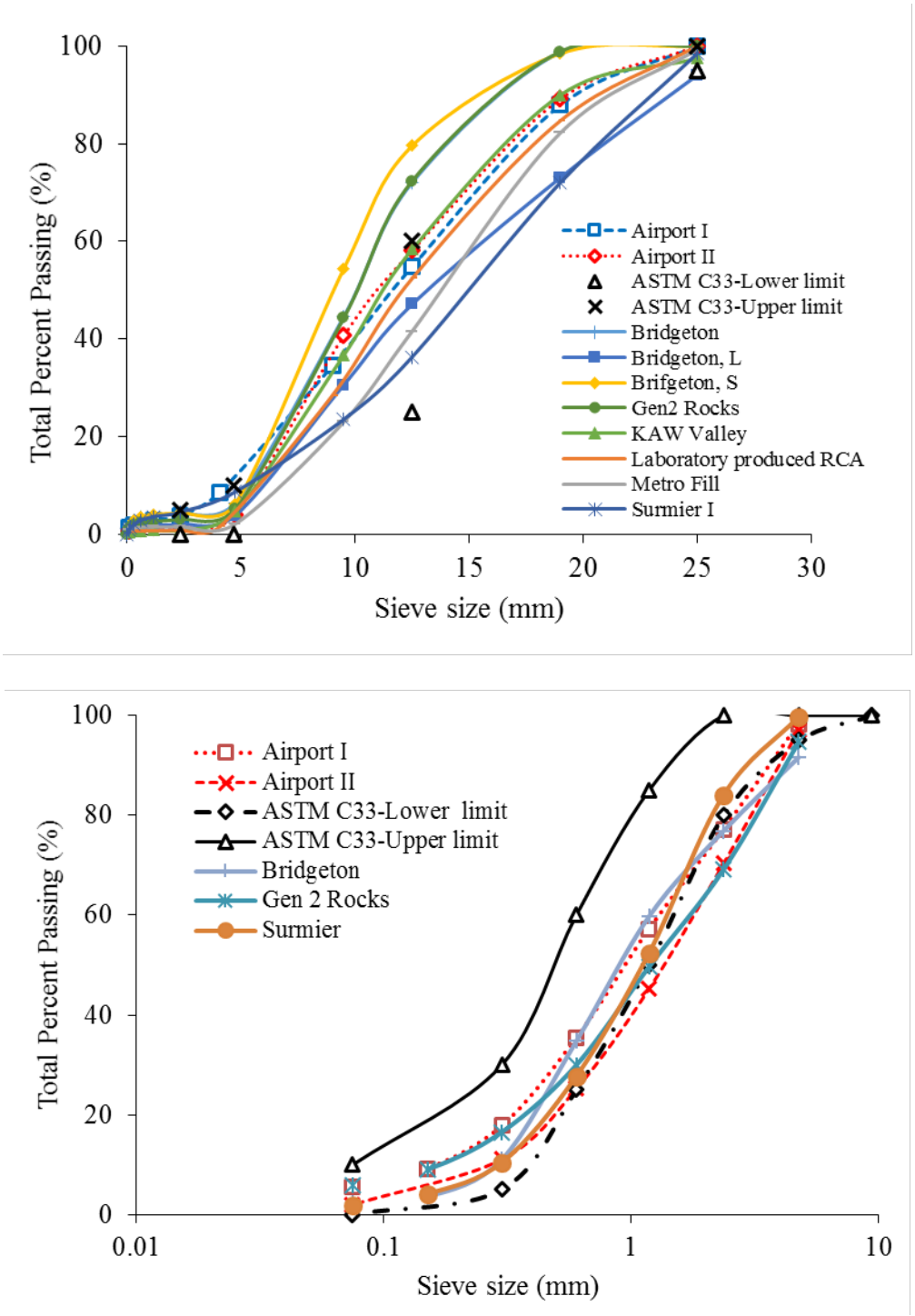

Figure 3.3 Particle-size distribution of various coarse RCA sources (top) and fine RCA sources (bottom)

Table 3.3 Deleterious materials content and soundness of coarse RCA

Aggregate	Source	Deleterious materials (% mass)	Soundness mass loss (%)	NMAS (mm)
RCA 1	Laboratory produced	0.3	21	19
RCA 2,3	Lambert Airport, MO	4.0	19	19
RCA 6	Metro Fill, MO	4.5	36	19
RCA 7	Bridgetone, MO	1.3	23	19
RCA 8	Bridgetone, MO	1.9	40	12.5
RCA 10	Kaw Valley, KS	2.2	17	19

Table 3.4 summarizes the key engineering properties of the virgin aggregate sources incorporated in the study. One source of well-graded siliceous river-bed sand with fineness modulus of 2.47 was used as the natural fine aggregate. Two types of crushed dolomite and a source of crushed limestone were also used.

Table 3.4 Physical properties of the virgin aggregate

Aggregate	Source	Specific gravity	Dry rodded unit weight (kg/m^3)	Absorption (%)	Los Angles abrasion (%)
Sand	River-bed sand, MO	2.63	-	0.40	-
Coarse 1	Crushed dolomite, MO	2.73	1632	0.80	28
Coarse 2	Crushed dolomite, MO	2.72	1597	0.98	43
Coarse 3	Crushed limestone, MO	2.64	1602	0.50	24

3.4. EFFECT OF RCA ON PACKING DENSITY OF AGGREGATE COMBINATION

Availability of a higher void content between the aggregate particles will require more paste to fill the void between larger particles. Therefore, it is important to optimize the aggregate combinations to ensure reducing the void volume, i.e. the required paste content. This can be done in terms of selecting proper combinations of fine and coarse

aggregates in concrete production. One selected source of fine RCA and one selected source of coarse RCA were incorporated to determine the packing density of various aggregate combinations using different replacement levels of fine and/or coarse RCA. Natural river sand and ta source of crushed dolomite (coarse 1) were incorporated as the virgin coarse aggregate. Several combinations of aggregates produced with fine-to-coarse ratios ranging from 0 to 100% were produced in the laboratory and tested for packing density. Fine RCA content ranged from 0 to 50% (by vol.) and the coarse RCA content ranged from 0 to 100%. Table 3.5 summarizes the investigated test matrix.

The gyratory compactor shown in Figure 3.4 was employed to determine the packing density of the aggregate combinations. Several trial runs were conducted to optimize the proper pressure to make sure aggregates will not crush under loading and the particle-size distribution of the aggregates will not change. This was more important in the case of the coarse RCA particles. Finally, a pressure of 0.7 bar (10 psi) was selected for running the tests. Each test was replicated at least two times.

Table 3.5 Test matrix for investigating the packing density of aggregate combinations

Fine-to-Aggregate ratio	0-100% (vol.)
Coarse aggregate	Dolomite, Coarse RCA
Fine aggregate	Sand, Fine RCA
Coarse RCA content	0-100%
Fine RCA content	0-50%

Table 3.6 summarizes the different fine and coarse RCA replacement levels considered for determination of the packing density. It should be noted that the fine-to-aggregate ratio ranged from 0 to 100% (by vol.) in all cases and the following ratios of fine-to-aggregate were investigated for all scenarios: 0, 0.2, 0.3, 0.35, 0.4, 0.45, 0.5, 0.55, 0.6, 0.65, and 1.0.

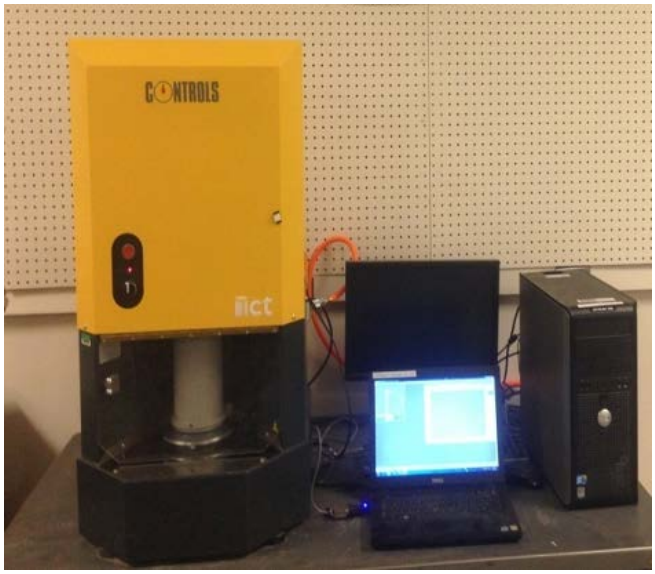

Figure 3.4 Gyratory compactor employed for determining the packing density of aggregate combinations

Table 3.6 RCA replacement levels for each of the investigated categories

	Fine RCA (% vol.)	Coarse RCA (% vol.)
Group I	0, 20	0, 30, 50
Group II	30, 40, 50	50, 60, 70
Group III	50	50, 70, 100

Figure 3.5 presents some of the results obtained for variations in packing density as a function of fine-to-coarse aggregate ratio. It was observed that the packing density of the investigated combinations varied from 0.59 to 0.79. However, regardless of the RCA replacement level, for the range of fine-to-aggregate ratio of 0.4 to 0.5, the packing density was mostly ranging from 0.75 to 0.77. Therefore, a fine-to-aggregate ratio of 0.42 was selected for concrete production. This ratio was validated in the laboratory to evaluate the workability and segregation of concrete.

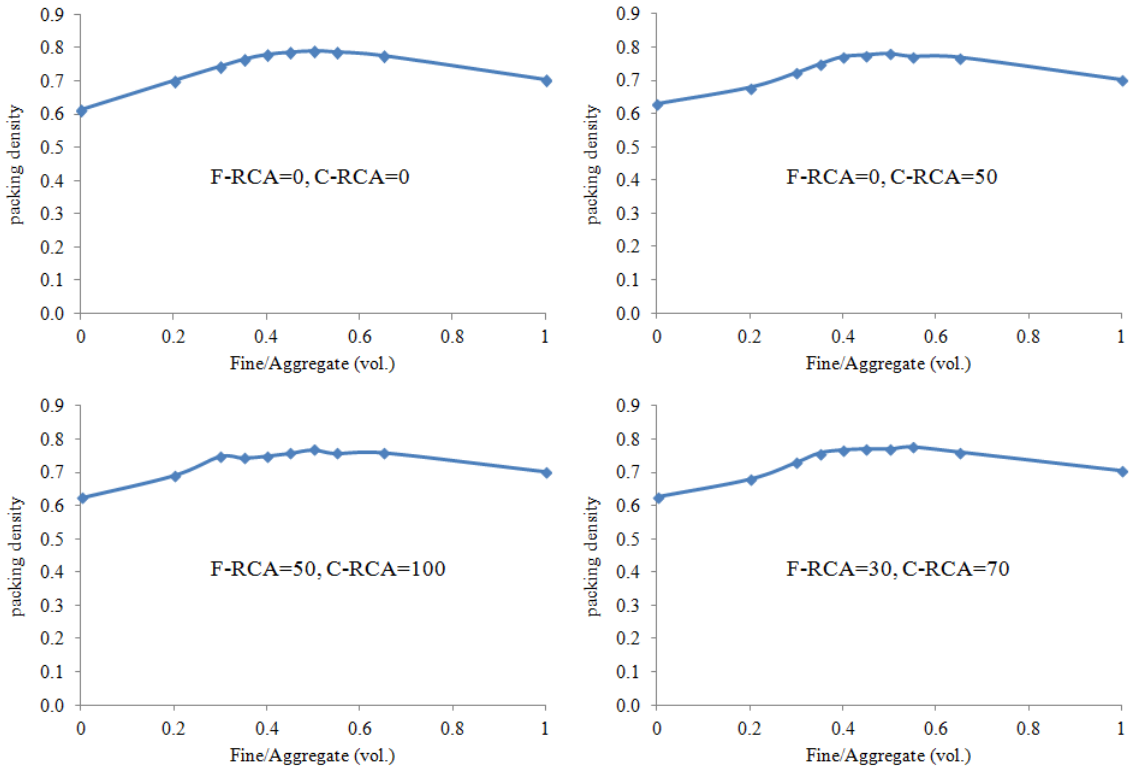

Figure 3.5 Variations in packing density as a function of fine-to-aggregate ratio

3.5. REMARKS

- Properties of various fine and coarse RCA sources were investigated. Particle-size distribution, and key engineering properties including abrasion resistance, absorption, and specific gravity were among the investigated parameters.
- Two types of fine RCA and seven types of coarse RCA were considered for concrete production in rest of the study. Deleterious materials content was determined for the selected coarse RCA types. Aggregate soundness test was also conducted for the selected coarse RCA.
- The fine-to-aggregate ratio of 0.42, corresponding to 42% fine and 58% coarse aggregate (by vol.) was selected for concrete production.

4. OPTIMIZATION OF ECO-EFFICIENT BINDER FOR INFRASTRUCTURE CONSTRUCTION

4.1. RESEARCH SIGNIFICANCE

Enhancing the engineering properties, along with potential reductions in cost, have urged the incorporation of supplementary cementitious materials (SCMs) in concrete production. In addition, mitigating the environmental impacts associated with cement production acts as another major motivate for the incorporation of cement replacements. With an approximate rate of 0.6 to 0.7 ton of CO_2 per ton of cement, production of Portland cement accounts for about 8% of worldwide CO_2 emission (Carrasco et al. 2016, Olivier et al. 2015). SCMs are typically by-products of industrial and/or agricultural activities with mechanisms of influence that depend on the chemical composition and physical properties of the SCM. Fly ash (Class C or F), ground granulated blast furnace slag (GGBS), silica fume (SF), metakaolin, zeolite, and rice husk ash are the most widely used types of SCMs. In the case of such SCMs as GGBS, the presence of anhydrous calcium silicate phases can contribute to hydraulic reaction in alkaline environment. On the other hand, such SCMs as fly ash and SF with high concentration of amorphous silica and aluminate phases can lead to pozzolanic reactions by means of converting part of the calcium hydroxide (CH) to calcium silicate hydrate (C-S-H), i.e. pozzolanic activity (Tashima et al. 2016).

GGBS, FA-C, and FA-F are some of the most commonly used types of SCMs. A great amount of data is available in the literature that deal with the effect of these SCMs on fresh and hardened properties of concrete and cementitious systems. Ground glass fiber (GGF) is a relatively new type of SCM, obtained from recycling waste glass fibers, with potential applications in concrete production (Hemmings 2005). Glass fibers are typically produced with a specific type of glass that secures high electrical resistivity, which is known as E-Glass (Rashidian and Rangaraju 2017). The raw material incorporated in production of glass fiber is an amorphous vitreous calcium aluminio-silicate (VCAS) powder. Production of VCAS involves heating a blend of ground silica, lime, and alumina compounds to a molten state, followed by solidifying by quench cooling, and grinding to a fine white colored powder (Hossain et al. 2008).

Given the uniform physical and chemical properties, and considering the aluminate-silica rich composition, incorporation of GGF as a cement replacement was suggested by (Hemmings 2005). Incorporation of GGF along with an alkaline solution of sodium hydroxide was proposed for development of alkali activated cements in a series of studies by Tashima et al. (2012, 2013a, 2013b). Limited studies have focused on use of GGF as a cement replacement in concrete production. Neithalath et al. (2009) investigated the use of up to 15% GGF as a cement replacement in the production of binary cement paste with water-to-cementitious materials ratio (w/cm) of 0.42. Based on the data obtained from thermo-gravimetric analysis (TGA) followed by monitoring the variations in calcium hydroxide concentration, the authors reported that GGF had no hydraulic qualities. However, the pozzolanic activity observed for up to 15% substitution of such GGF was reported to be higher than that of Class F fly ash and lower than that of SF. Hossain et al. (2008) also investigated the effects of 6%, 9%, and 15% GGF cement replacement in concrete mixtures made with w/cm of 0.4 and 0.5. The authors reported that the incorporation of 15% GGF resulted in an increase in slump from 75 to 200 mm in mixtures proportioned with 0.50 w/cm and no water reducing admixture (WRA). No significant difference in plastic shrinkage and cracking potential was reported for such concrete made with up to 15% GGF replacement. The authors reported a decrease in sorptivity from 0.80 to 0.62 $kg/m^2/h^{0.5}$ due to the use of 15% GGF replacement in concrete proportioned with 0.40 w/cm. The diffusion coefficient was also reduced from 3.31×10^{-5} to 1.55×10^{-5} m^2/h. Rashidian and Rangaraju (2017) incorporated up to 30% GGF in production of concrete with 0.40 w/cm and 355 kg/m^3 of cementitious materials. The authors reported reduction in 56-day compressive strength from 55.0 MPa in the case of the Reference mixture to 51.0, 47.0, and 52.5 MPa due to 10%, 20%, and 30% GGF replacement, respectively. The authors also reported that the incorporation of GGF was helpful in mitigating the expansion of mortar bars exposed to alkali silica reaction (ASR) test environment. The 28-day mortar expansion values were reduced from 1.2% in the case of the Reference mixture, to 0.25%, 0.2%, and 0.1% due to 10%, 20%, and 30% GGF incorporation, respectively (Rashidian and Rangaraju (2017).

The research presented in this section investigates the properties of concrete equivalent mortar (CEM) mixtures proportioned with high volume SCM of up to 70%

incorporated in binary and ternary systems. The testing program involved the evaluation of the effect of binder composition on properties of CEM made with 0.40 w/cm. The investigated properties included rheological properties, heat of hydration, strength development and pozzolanic activity, shrinkage, and electrical resistivity.

4.2. EXPERIMENTAL PROGRAM

4.2.1. Concrete Equivalent Mortar Mixture Design. Originated from the multi-scale theory (Ferraris et al., 2001, and Mahaut et al., 2008), the concept of CEM is based on representing coarse aggregate by using an additional mass of sand to secure the same total surface area. As stated by Hernandez et al. (2013), adopting the following criteria is necessary to design CEM: (1) use of the same type and content of cementitious materials, (2) use of the same water-to-cementitious materials ratio (w/cm), (3) same mixing procedure and mixture proportion, and (4) the replacement of coarse aggregate with extra sand with equal specific area.

The reference concrete used for the design of CEM corresponded to the mixture employed by the Missouri Department of Transportation (MoDOT) for rigid pavement construction. This mixture is typically proportioned with 323 kg/m^3 of binder and w/cm of 0.4. Table 4.1 summarizes the mixture proportions of the reference concrete and corresponding CEM.

Table 4.1 Mixture composition of base concrete mixture and corresponding CEM mixture (kg/m^3)

	Cementitious materials	w/cm	Water content	Sand	Coarse aggregate	Coarse-Equivalent sand content
Concrete	323	0.40	129	750	1121	-
CEM	587	0.40	235	1350	-	181

4.2.2. Materials and Mixing Procedure. Mixtures were proportioned with Type I/II Portland cement (OPC), GGF, FA-C, FA-F, and GGBS. The chemical composition and physical properties of the binder materials are summarized in Table 4.2. Scanning electron microscopy (SEM) was performed on these materials as shown in Figure 4.1. A siliceous river sand, and a lignosulfonate based water reducing admixture (WRA) with a solid content of 37% and specific gravity of 1.2 were used. The fineness modulus, specific gravity and absorption rate of the sand were 2.47, 2.63 and 0.4%, respectively.

In total, 32 CEM mixtures were investigated. Table 4.3 summarizes the types and replacement rates (by mass) of the investigated SCM. A mortar cast with 100% OPC was considered as the Reference mixture. The test matrix included binary systems with 10%, 20%, 30%, 40%, and 50% of GGF, as well as 50% of FA-C, FA-F, or GGBS. Ternary blends with 50% to 70% SCM replacement were also investigated. Table 4.4 summarizes the compositions of the mixtures.

A Hobart mixer with 10-liter capacity was used. The mixing procedure consisted of: (1) mixing the dry sand at low speed for 1 min; (2) adding half of the water and mixing for 1 min; (3) addition of cementitious materials and mixing for 0.5 min at low speed; (4) incorporating the WRA diluted with the rest of the water and mixing at high speed for 2.5 min; after two minutes of rest, mixing was resumed for 3 min at high speed.

Table 4.2 Chemical composition and physical properties of cement and SCMs

Property	OPC	FA-F	FA-C	GGBS	GGF
SiO_2, %	19.8	49.4	36.1	36.8	50-55
Al_2O_3, %	4.5	20.2	23.7	9.2	15-20
Fe_2O_3, %	3.2	15.0	4.9	0.76	<1
CaO, %	64.2	6.8	27.9	37.1	20-25
MgO, %	2.7	1.1	4.9	9.5	<1
SO_3, %	3.4	2.12	2.5	0.06	<0.1
Na_2O eq., %	–	–	–	0.34	<1
Blaine surface area, m^2/kg	410	455	490	590	600
Specific gravity	3.14	2.45	2.71	2.86	2.6
LOI, %	1.5	0.95	0.5	–	<0.5

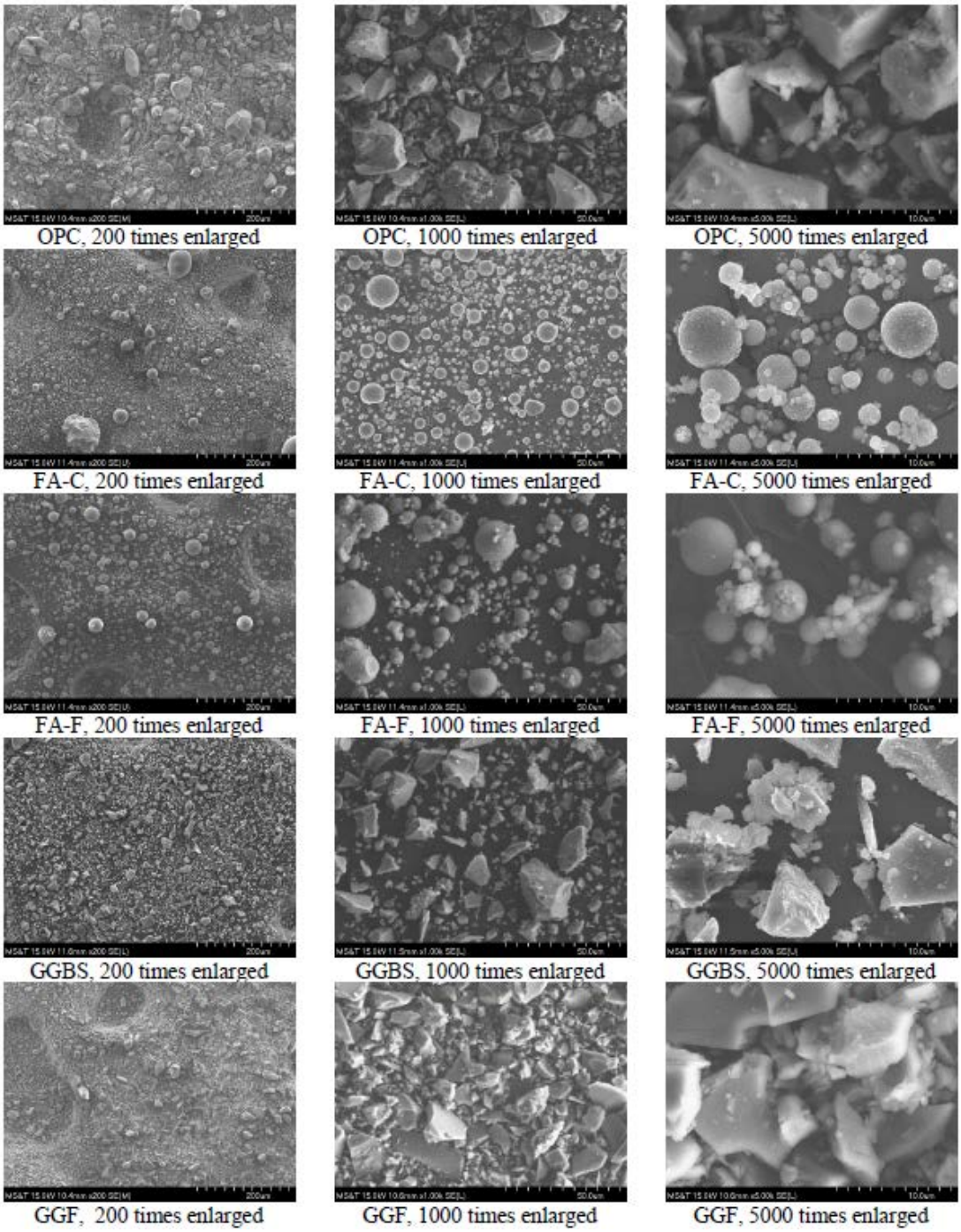

Figure 4.1 Scanning electron microscopy on powder samples

Table 4.3 Cementitious materials replacement levels (% mass)

Mixture	OPC	FA-C	FA-F	GGBS	GGF
Reference	100	-	-	-	-
Binary	30-90	50	50	50-70	10-50
Ternary	30-50	0-50	0-50	0-50	0-50

Table 4.4 Mixture compositions of evaluated CEM mixtures

	Mixture	OPC	FA-C	FA-F	GGBS	GGF	water	w/cm	WRA (l/m^3)	Mini slump
		Kg/m^3								
	Ref.	587	-	-	-	-	235	0.40	2.53	130
Binary systems	C50	293	293	-	-	-	235	0.40	2.02	135
	F50	293	-	293	-	-	235	0.40	0.60	140
	GGF10	528	-	-	-	59	235	0.40	2.53	130
	GGF20	470	-	-	-	117	235	0.40	2.58	125
	GGF30	411	-	-	-	176	235	0.40	2.35	120
	GGF40	352	-	-	-	235	235	0.40	2.58	120
	GGF50	293	-	-	-	293	235	0.40	2.16	125
	SL50	293	-	-	293	-	235	0.40	2.02	125
	SL70	176	-	-	411	-	235	0.40	2.08	125
Ternary systems	GGF15C35	293	205	-	-	88	235	0.40	1.40	135
	GGF25C25	293	147	-	-	147	235	0.40	1.40	130
	GGF15F35	293	-	205	-	88	235	0.40	1.40	150
	GGF25F25	293	-	147	-	147	235	0.40	1.40	145
	GGF15SL3	293	-	-	205	88	235	0.40	1.65	140
	GGF25SL2	293	-	-	147	147	235	0.40	1.65	135
	SL10C50	235	293	-	59	-	235	0.40	1.20	135
	SL15C35	293	205	-	88	-	235	0.40	1.30	145
	SL20C50	176	293	-	117	-	235	0.40	1.16	135
	SL25C25	293	147	-	147	-	235	0.40	1.75	140
	SL30C35	205	205	-	176	-	235	0.40	1.73	145
	SL40C15	264	88	-	235	-	235	0.40	1.89	145
	SL45C25	176	147	-	264	-	235	0.40	1.85	135
	SL50C15	205	88	-	293	-	235	0.40	1.50	130
	SL10F50	235	-	293	59	-	235	0.40	0.92	145
	SL15F35	293	-	205	88	-	235	0.40	1.75	160
	SL20F50	176	-	293	117	-	235	0.40	0.46	135
	SL25F25	293	-	147	147	-	235	0.40	1.66	145
	SL30F35	205	-	205	176	-	235	0.40	1.39	140
	SL35F25	235	-	147	205	-	235	0.40	1.59	150
	SL45F25	176	-	147	264	-	235	0.40	1.85	125
	SL55F15	176	-	88	323	-	235	0.40	1.87	125

4.2.3. Test Methods. Immediately after mixing, a sample of fresh mortar was extracted to evaluate the mini slump value using a conical mold with height and base diameter of 50 and 100 mm, respectively. The cone was filled in two layers, and each layer was tamped 20 times. The cone was then raised, and two diameters of the mortar were measured in orthogonal directions after the cease of the spread. The mini slump value corresponds to the average of the two readings. Fresh mortar samples were taken to monitor the heat of hydration using iso-thermal calorimetry at 20ºC. Calorimetry data were logged up to 72 hours.

Fresh mortar samples were used to determine rheological properties using a coaxial cylinder type rheometer. The mortar sample was allowed to rest initially for 5 min inside the rheometer before the first measurement of static yield stress (t_5). Three additional measurements of static yield stress were conducted, each time allowing the sample to rest for 15 min between two successive measurements. A low shear rate of 0.04 rps was used for the shear growth measurement. The increase in applied torque was monitored until the maximum point (T_i) was obtained, as illustrated in Figure 4.2.

The static yield stress was then determined based on the geometry of the rheometer vane, container, and maximum torque as follows:

$$\tau = \frac{T_i}{2\pi R_i^2 h} \tag{4-1}$$

where T_i is the maximum torque (N.m), R_i is the radius of the internal cylinder, i.e. rheometer vane (m), and *h* is the average height of mortar in contact with the rheometer vane (m).

Following the completion of the first measurement of static yield stress (t_5), the mortar sample was pre-sheared for 30 s at 0.35 rps. The yield stress and plastic viscosity were then determined using a descending rotational velocity of 0.35 to 0.025 rps during 10 measurement steps. Each step took place over 4 seconds and consisted of 50 readings. All steps were inspected on the torque-time graph to eliminate the unstable data points. Moreover, the first 10 points of each step were excluded from analysis to ensure reporting the average torque of each step based on stabilized readings. The time corresponding to the first dynamic rheological properties is denoted as t_8. The same

procedure was performed at the end of last measurement of static yield stress that corresponded to 65 min of age (t_{65}).

Results were incorporated to produce the torque-rotational velocity graph, as depicted in Figure 4.2. A linear function was fitted through the experimental data to obtain the Bingham parameters. The Reiner-Riwlin equations were then employed to determine the values of yield stress and plastic viscosity, as presented in Equations (4-2) and (4-3) (Reiner 1949).

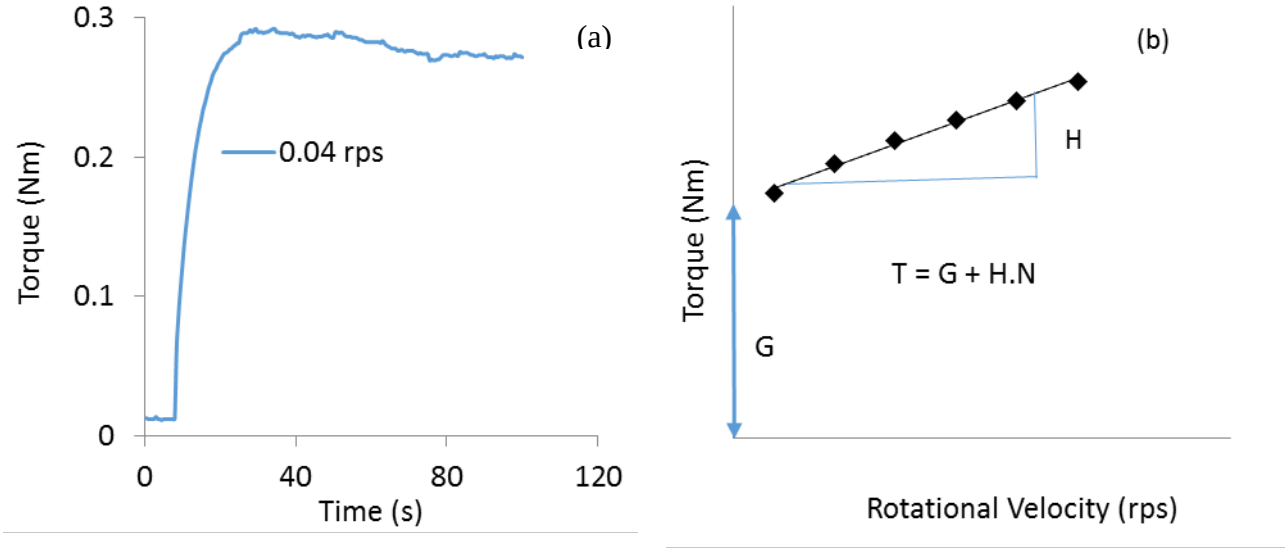

Figure 4.2 Monitoring the structural build-up for static yield stress (a) and Bingham model for analyzing the rheological properties (b)

$$\tau_0 = \frac{\left(\frac{1}{R_i^2} - \frac{1}{R_o^2}\right)}{4\pi h \ln\left(\frac{R_o}{R_i}\right)} G \qquad (4\text{-}2)$$

$$\mu = \frac{\left(\frac{1}{R_i^2} - \frac{1}{R_o^2}\right)}{8\pi^2 h} H \qquad (4\text{-}3)$$

where R_o and R_i are the outside and inside radii, respectively, of the co-axial cylinders (m), *h* is the height of mortar in contact with the rheometer vane (m), and *G* and *H* are the intercept and slope of the linear fit in torque-rotational velocity graph.

For the determination of compressive strength, 50-mm cubes were employed in accordance with ASTM C109 (2016). The samples were demolded after 24 hours and cured in lime-saturated water at 21±1°C until the time of testing. Three samples were tested for each of the reported compressive strength values.

Shrinkage was monitored using 25×25×285 mm prisms according to ASTM C157 (2014). Samples were cured in lime-saturated water for seven days before curing at 23±1°C and 50%±3% relative humidity. Shrinkage data were recorded from the first day of drying up to three months of age.

Bulk electrical resistivity was determined using 100×200 mm cylindrical specimens according to ASTM C1760 (2012). The specimens were cured in lime-saturated water and tested until the age of 91 days.

4.3. RESULTS AND DISCUSSION

4.3.1. Rheological Properties. Figure 4.3 presents the variations in yield stress for the Reference CEM made with 100% OPC and binary mixtures. The Reference mixture exhibited the yield stress values of 170 and 295 Pa for the first (t_8) and second measurement time (t_{65}). Increasing the GGF content reduced yield stress. This could be due to the fact that the glassy surface of GGF particles adsorb less water in comparison with cement particles, making it possible for the extra water to act as lubricant in the system and reduce yield stress. For the initial measurement (t_8), increasing the GGF content from 0 to 50% reduced the yield stress from 170 to 110 Pa. For the second step of measurements (t_{65}), increasing the GGF content from 0 to 50% reduced the yield stress from 295 to 150 Pa.

Increase in yield stress was observed as a function of time regardless of the GGF content. However, the GGF incorporation reduced the degree of sensitivity to time. Results obtained for testing the Reference sample at two dynamic measurement steps showed that the yield stress increased from 170 to 295 Pa, corresponding to a 75%

increase. The rate of increase for sample made with 50% GGF was 36%, with an increase in stress value from 110 to 150 Pa.

Reduction in yield stress at first measurement time (t_8) was observed where 50% SCM was incorporated in binary mixtures. The yield stress was reduced from 170 Pa in the case of the Reference mortar to 160, 150, 140, and 110 Pa for the samples made with 50% of FA-F, FA-C, GGBS, and GGF, respectively. Similar trends were observed for the second measurement time (t_{65}), except for the C50 mixture. Yield stress of the Reference mixture was 295 Pa at this time. Incorporation of 50% of FA-F, GGBS, and GGF reduced the yield stress to 260, 220, and 150 Pa. However, the yield stress of the C50 sample was increased to 325 Pa. The rate of increase in yield stress as a function of time was 2.2, 0.7, 3.1, 1.8, and 1.4 Pa/min for the Reference, GGF50, C50, F50, and SL50 mixtures, respectively.

Similar trends were reported by Khayat et al. (2008) who investigated the rheological properties of grouts prepared with w/cm of 0.4 and incorporating 0.8% by cement weight of high range water reducing admixture (HRWRA). The authors reported an increase in yield stress from approximately 11 to 13.0, 15, and 17 Pa due to 10%, 20%, and 30% FA-F replacements were used, respectively. Authors also reported decrease in yield stress from 11 to 10 Pa as a result of 40% GGBS replacement in similar grouts. Jau and Yang (2010) on the other hand reported increase in yield stress from 3.8 to 4.3 and 8.3 Pa, due to 40% and 60% FA-F incorporation in SCC mixtures with 500 kg/m^3 of binder and 0.38 w/cm.

Variations in plastic viscosity of the Reference and the binary mixtures are presented in Figure 4.4. It was observed that increasing the GGF replacement increases the plastic viscosity. This can be due to the increased inter-particle friction caused by the angular shape of the GGF particles. Increase in time was also influential and led to an increase in viscosity. For the first measurement time (t_8), increasing the GGF content from 0 to 50% increased the plastic viscosity from 5.5 to 11.0 Pa.s. Similar trend was observed for the second measurement time (t_{65}), with an increase in plastic viscosity from 7.0 to 12.9 Pa.s.

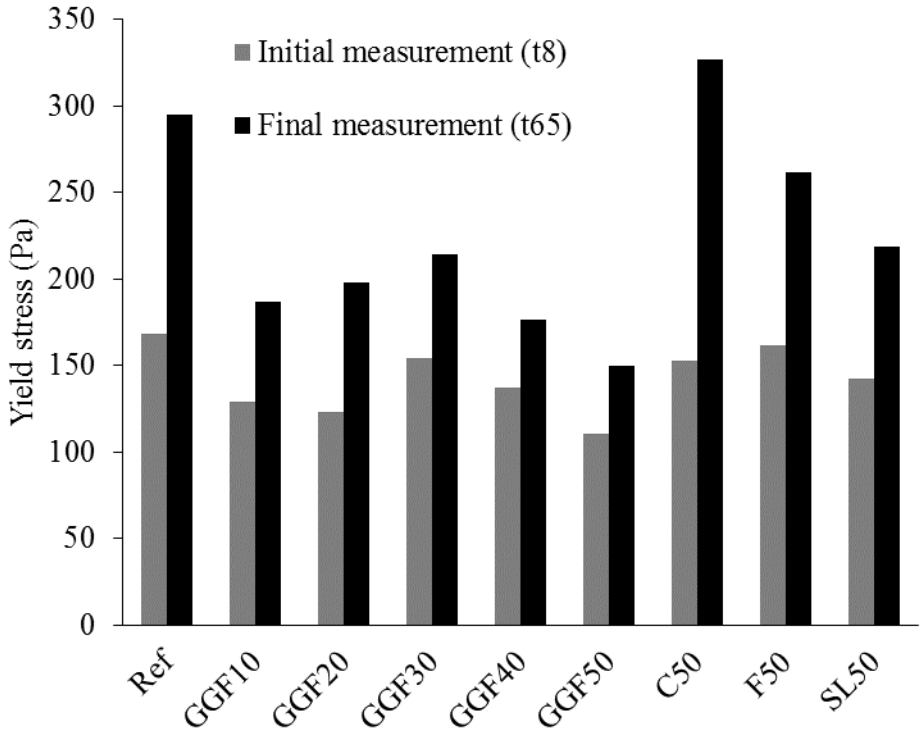

Figure 4.3 Variations in yield stress of the Reference and binary mixtures

For both measurement times, the viscosity of the GGF50 mixture was comparable to that of the SL50. Such an observation may be expected given the similar particle shapes and fineness of these two powders. The rate of increase in plastic viscosity was 0.026, 0.032, 0.043, 0.035, and 0.06 Pa.s/min for the Reference, GGF50, C50, F50, and SL50 mixtures, respectively.

Similar trends were reported by Khayat et al. (2008) who reported increase in plastic viscosity from 177 to 415 mPa.s due to 30% Class F fly ash incorporation in grouts proportioned with w/cm of 0.4 and 0.8% HRWRA. Authors also reported that the incorporation of 40% GGBS in such grouts resulted in an increase in plastic viscosity from 177 to 283 mPa.s. Gesoglu et al. (2009) also reported increase in V-funnel time, i.e. viscosity of SCC mixtures proportioned with 0.44 w/cm and up to 60% GGBS replacement. The authors reported that the increase in GGBS content from 0 to 40% and 60% enhanced the V-funnel time from 3.2 to 14.0 and 12.0 s, respectively. The authors also reported an increased in V-funnel time from 3.2 to 6.0 and 4.0 s, due to 40% and

60% FA-F incorporation, which indicates an increase in viscosity of the mixtures Gesoglu et al. (2009).

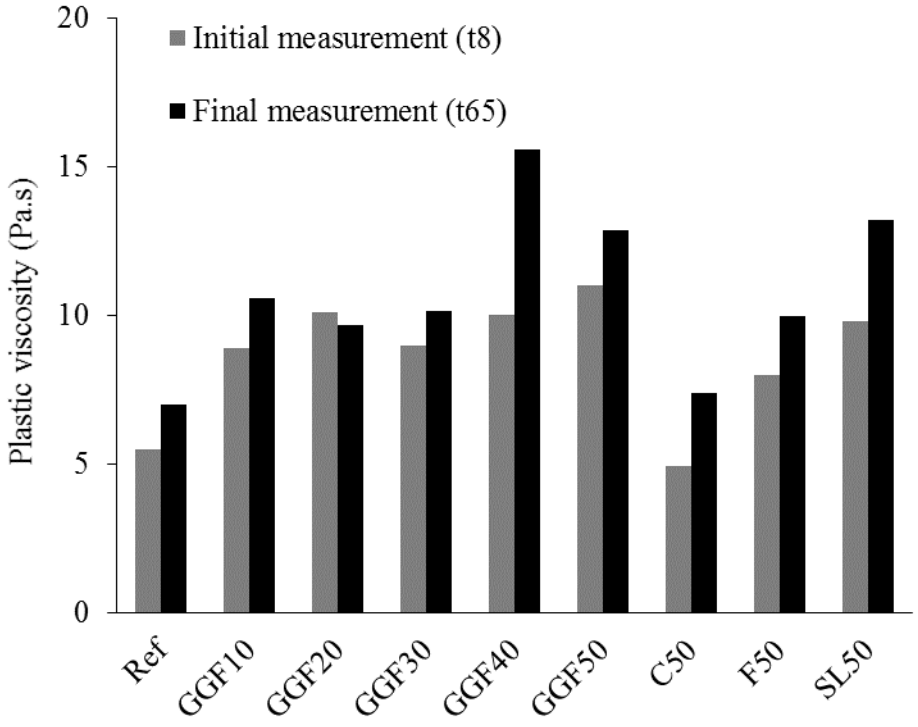

Figure 4.4 Variations in plastic viscosity of the Reference and binary mixtures

Figure 4.5 illustrates the variations in static yield stress as a function of time for the Reference and the binary mixtures. A linear time-dependent increasing trend was observed for all mixtures. It was generally observed that incorporation of GGF and GGBS tend to reduce the rate of increase in static yield stress. The incorporation of 50% GGF and 50%GGBS reduced the static yield stress by 64% and 59% at t_{62}, respectively. Use of 50% Class C or Class F fly ash on the other hand, increased the static yield stress by 30% and 18% at t_{62}, respectively. The maximum and the minimum rates of increase in static yield stress, i.e. thixotropic behavior, were observed for the C50 and GGF50 mixtures with 10.1 and 0.8 Pa/min. This rate was 7.1, 7.7, and 1.1 Pa/min for the Reference, F50, and SL50 mixtures, respectively.

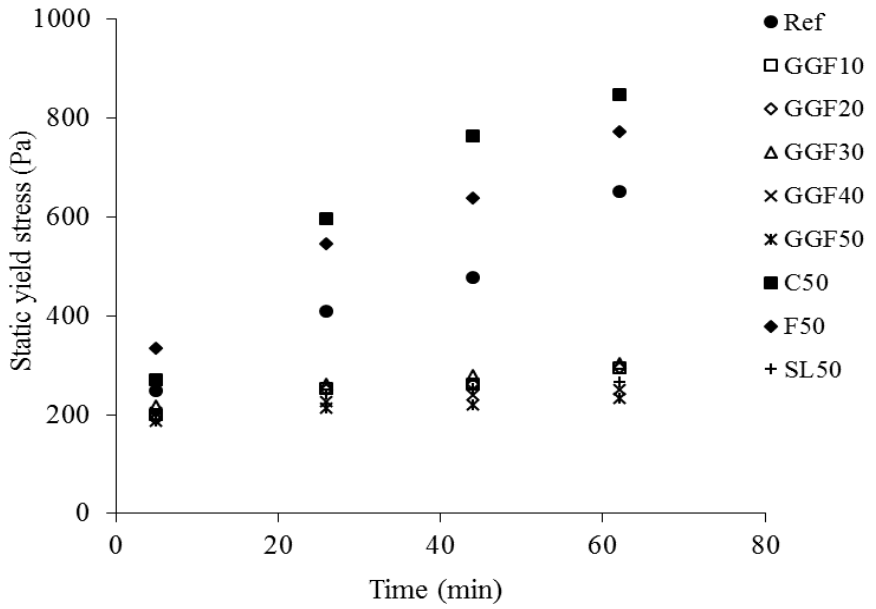

Figure 4.5 Variations in static yield stress of the Reference and binary mixtures

A potential increase in packing density of the system can be the reason for reduced torque values for mixtures incorporating GGBS and GGF (Ahari et al. 2015). Similar results were reported by Ahari et al. (2015) who investigated the thixotropic behavior of binary self-consolidating concrete (SCC) mixtures cast with w/cm of 0.44, 0.50, and 0.56. The authors reported increase in thixotropic behavior when 36% FA-C or FA-F replacement, while structural breakdown area of such mixtures was reduced when 18% GGBS was incorporated. In the case of mixtures cast with w/cm of 0.44, breakdown area was increased by 110% and 40% due to the use of 36% FA-C and FA-F, respectively. About 10% decrease in breakdown area was reported due to 18% GGBS incorporation.

4.3.2. Heat of Hydration. The rate of heat evolution and the cumulative heat of hydration normalized to the dry mass of cementitious materials, were determined as illustrated in Figure 4.6. The area underneath the heat evolution graph and the final value of the accumulative heat were determined as measure of the total heat release over time. A summary of the results obtained for investigated binary and ternary mixtures is presented in Figure 4.7.

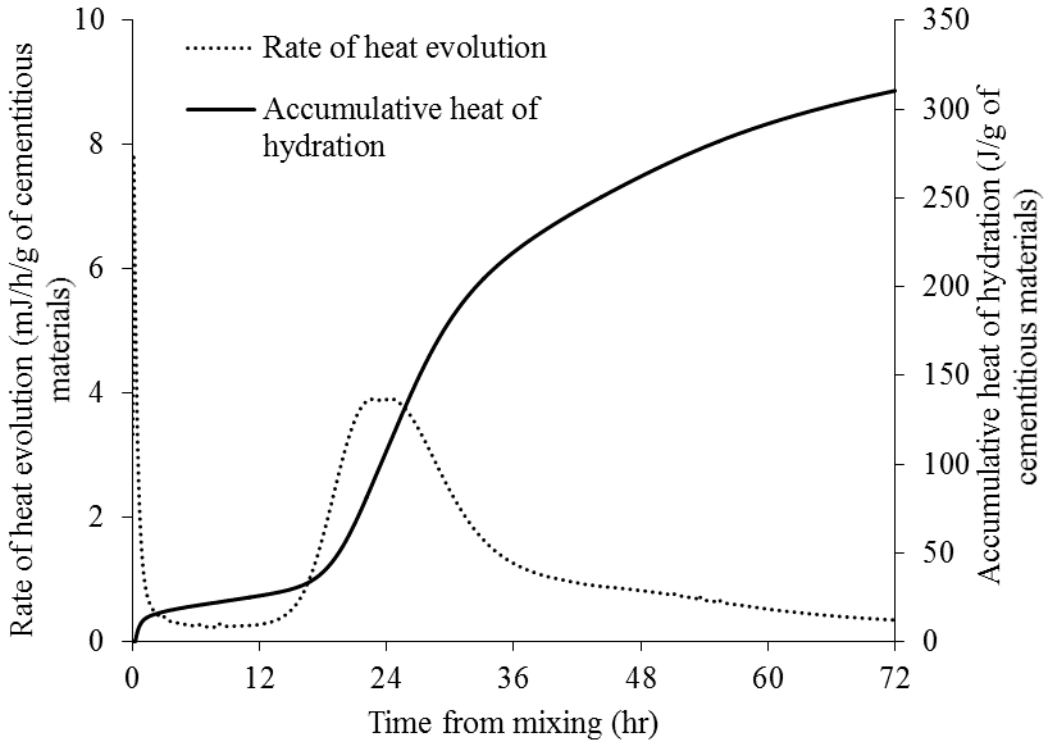

Figure 4.6 Calorimetry measurement of the Reference mixture (100% OPC)

It was generally observed that for all SCM types and combinations, the normalized total heat and the normalized cumulative heat of hydration after 72 hours were lower than that of the Reference sample. For the binary mixtures with 50% SCM, replacing cement with up to 50% GGF reduced the total released heat of hydration from 12.7 to 3.6 kJ.h per gram of cementitious materials. The normalized total heat of hydration was 7.3, 9.3, and 6.5 KJ.h/g for the case of the C50, F50, and SL50 mixtures, respectively. Replacing cement with GGF reduced the accumulative heat of hydration significantly. The normalized cumulative hydration heat of the Reference sample after 72 hours was 310 J/g compared to 240, 210, 200, 170, and 140 J/g for GGF10, GGF20, GGF30, GGF40, and GGF50 mixtures, respectively. In the case of the rest of binary mixtures cast with 50% SCM, the final normalized values were 205, 190, and 170 J/g for F50, C50, and SL50 mixtures, respectively.

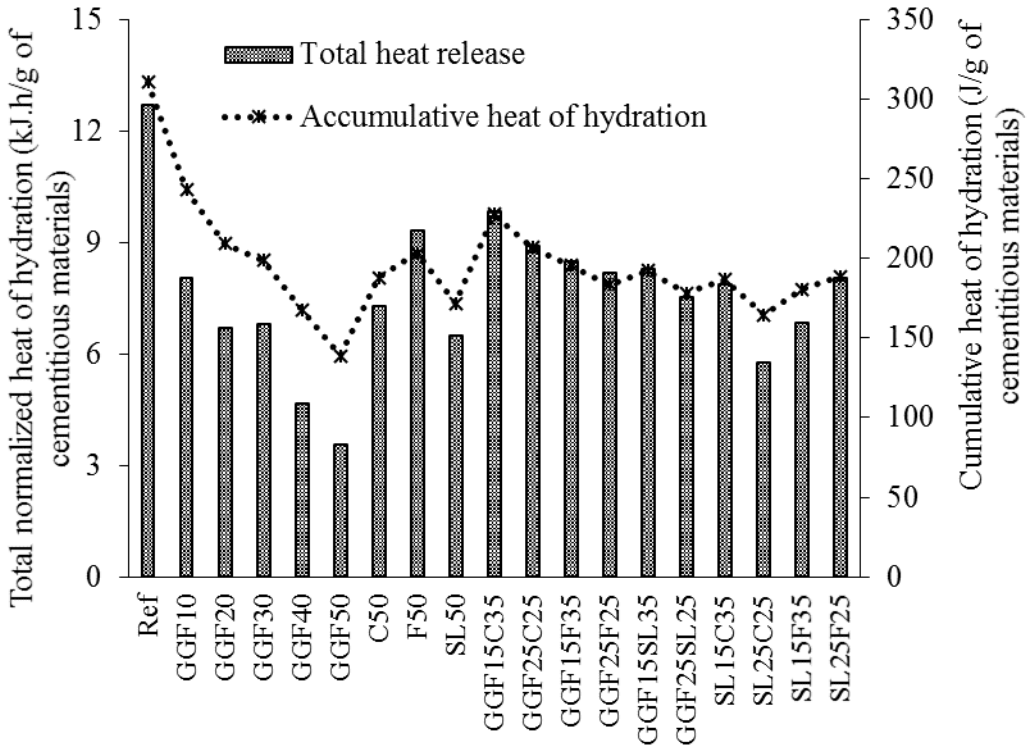

Figure 4.7 Heat of hydration during 72 hours for investigated mixtures

4.3.3. Compressive Strength. Table 4.5 presents the compressive strength results measured at 7, 28, 56, and 91 days for investigated CEM mixtures. The reference mixture made with 100% OPC developed compressive strength of 27.3 and 34.1 MPa at 7 and 91 days, respectively. For the CEM made with binary or ternary blends of GGBS, FA-F, and FA-C, the minimum 7-day compressive strength of 16.4 MPa was observed for the mixture made with 20% GGBS and 50% FA-C. The maximum 7-day compressive strength of 38.8 MPa was obtained for CEM made with 15% GGBS and 35% FA-C. This mixture also exhibited the maximum 91-day compressive strength of 61.5 MPa, while the minimum 91-day compressive strength of 32.6 MPa was attributed to the mixture with 15% GGBS and 35% FA-F.

The use of high-volume GGBS in binary mixtures reduced the early age strength development. Reduction in 7-day compressive strength from 27.3 to 22.5 and 19.9 MPa was observed for mixtures with 50% and 70% GGBS, respectively. Improvement in long-term compressive strength was observed for these mixtures, where the mixture made with

70% GGBS exhibited similar 91-day compressive strength to that of mixture with 100% OPC; about 34 MPa. An improvement of 4.5 MPa, corresponding to 13% increase in 91-day compressive strength was observed for CEM made with 50% GGBS compared to the reference mixture. The use of 50% FA-C increased both the 7- and 91-day compressive strength, with values of 30.9 and 44.1 MPa, corresponding to 13% and 30% increase, respectively, compared to the reference mixture. Trends were similar for CEM made with 50% FA-F. The 7- and 91-day compressive strength values were 13% and 51% higher than those of the reference mixture, respectively.

Figure 4.8 presents the variation in compressive strength of mixtures made with different amounts of GGF in binary and ternary systems. Comparing the results obtained for binary mixtures incorporating 10% to 50% GGF, regardless of the age of testing, compressive strength decreased with the increase in GGF content. However, the rate of such decrease was higher at earlier ages. The incorporation of up to 50% GGF reduced the 7-day compressive strength from 27.3 to 8.8 MPa due to cement dilution. However, considerable improvements were observed at later ages. The compressive strength of the Reference mixture ranged from 27.3 MPa at 7 days to 34.1 MPa at 91 days, corresponding to 20% spread, with a marginal increase of 2 MPa between 28 and 91 days. In the case of the samples prepared with 10%, 20%, 30%, 40%, and 50% of GGF replacement, the increase in compressive strength from 7 to 91 days was 60%, 70%, 100%, 160%, and 210%, respectively. This is principally due to the pozzolanic effect of the GGF (Idir et al. 2011).

Hossain et al. (2005) also reported that the incorporation of up to 15% GGF with mean particle size of 3 μm in concrete cast with 0.4 and 0.5 w/cm increased the 56-day compressive strength by a limited value of 15%.

In the case of the ternary systems made with GGF, the GGF15F35 and GGF25F25 mixtures developed 91-day compressive strength of 34.3 and 37.6 MPa, while the GGF15C35 and GGF25C25 mixtures exhibited strength values of 47.7 and 49.3 MPa, respectively. Based on the 91-day measurements, the combinations of the GGF/FA-C developed the highest compressive strength, followed by the GGF/GGBS, and GGF/FA-F combinations, with up to 45%, 28%, and 10% increase in 91-day compressive strength compared to the Reference mixture. Regarding the relative effects of GGBS and

GGF in ternary mixtures with fly ash, the GGBS/FA-F mixtures developed higher strength (on average 14%) compared to the GGF/FA-F mixtures.

Table 4.5 Compressive strength results

	Mixture	7-d	28-d	56-d	91-d
	Ref.	27.3	33.3	32.6	34.1
Binary systems	C50	30.9	38.9	41.2	44.1
	F50	21.0	28.9	36.3	45.9
	GGF10	19.1	24.3	26.5	28.1
	GGF20	17.1	25.2	25.5	29.2
	GGF30	15.8	19.8	27.2	30.9
	GGF40	10.2	17.1	23.2	26.3
	GGF50	8.8	20.3	26.2	27.7
	SL50	22.5	36.3	35.5	38.6
	SL70	19.9	29.4	29.8	34.4
Ternary systems	GGF15C35	24.9	39.1	42.2	47.7
	GGF25C25	22.8	31.7	40.9	49.3
	GGF15F35	16.9	24.7	33.9	34.3
	GGF25F25	15.4	25.9	28.7	37.6
	GGF15SL35	23.0	31.9	38.6	44.2
	GGF25SL25	22.2	24.9	39.6	43.8
	SL10C50	25.8	34.6	43.3	57.1
	SL15C35	38.3	38.6	51.4	61.5
	SL20C50	16.4	24.8	28.8	43.8
	SL25C25	21.3	46.7	48.0	49.8
	SL30C35	20.5	26.0	35.4	54.2
	SL40C15	28.5	41.4	45.5	47.3
	SL45C25	25.0	40.5	45.0	48.0
	SL50C15	23.5	40.9	45.1	51.2
	SL10F50	18.1	33.1	34.1	41.2
	SL15F35	16.8	30.5	29.3	32.6
	SL20F50	17.3	32.0	36.0	42.4
	SL25F25	19.8	32.0	35.5	37.1
	SL30F35	24.2	37.5	41.2	47.4
	SL35F25	22.5	33.5	33.6	38.8
	SL45F25	31.2	43.0	50.6	51.6
	SL55F15	17.1	35.5	34.2	39.3

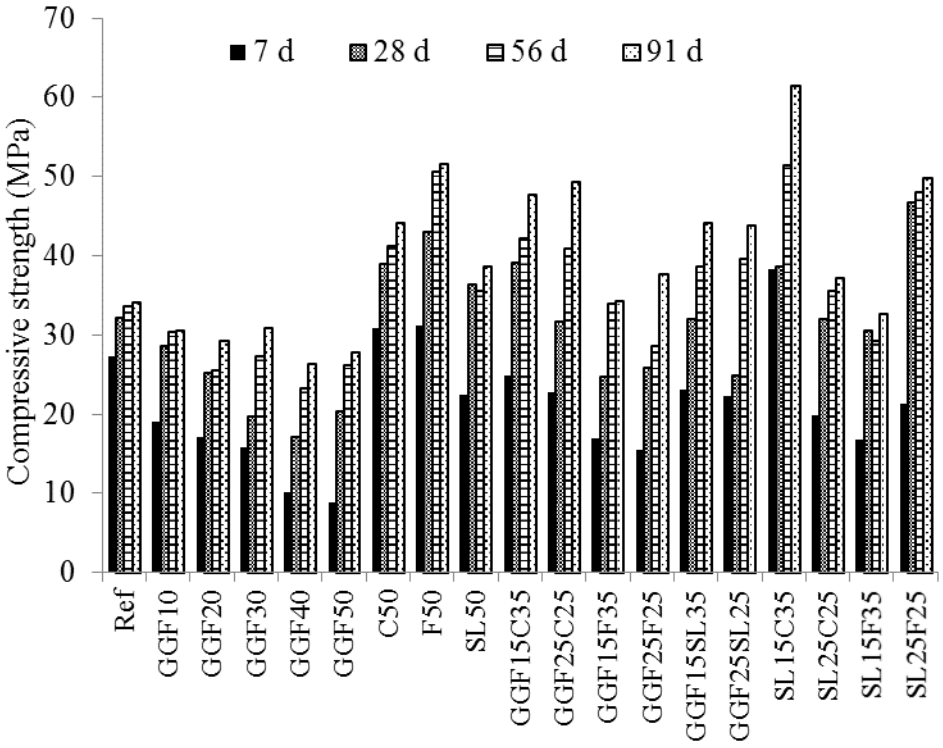

Figure 4.8 Cube compressive strength

Bolomey's law introduced in Equation (4-4) was employed to investigate the pozzolanic activity of selected SCM types and combinations, as recommended by Idir et al. (2011), Khokhar et al. (2010), and Khelifi et al. (2013).

$$\sigma = K_b\left(\frac{C + \chi_b A}{W + V} - 0.5\right) \tag{4-4}$$

where σ is the compressive strength of the mortar sample, C is the mass of the portland cement, W is the mass of water, A is the mass of the SCM, and V is the volume of the air voids (considered as 10% here), K_b is the constant of Bolomey, i.e. a coefficient that takes into account the characteristics of cement and aggregate, and X_b is the coefficient of pozzolanic activity of the SCM.

The values of K_b were initially determined by fitting the data obtained from testing the Reference specimens, cast without any SCM for each testing age. The value of X_b was then calculated by fitting the equation to the compressive strength values

measured for each of the SCM types and combinations, replacement level, and testing age.

Figure 4.9 presents the variations in strength activity index for each of the binary mixtures, along with the inert lines for each corresponding replacement level, as recommended by Idir et al. (2011) and Afshinnia and Rangaraju (2015). It was observed that for all GGF substitution rates, the strength activity index was lower than the inert line until 28 days of age. This reveals the fact that the pozzolanic activity of the GGF and its positive effect on strength development was negligible before 28 days. Moreover, the strength activity index of less than 1.0 for binary mixtures of GGF suggest that the pozzolanic reaction was not sufficient to compensate for the cement dilution effect. Results were contrary to the observations of Neithalath et al. (2009) who reported strength activity index of 1.15, 1.12, and 1.17 at 14, 28, and 56 days for mixtures with15% GGF content with median particle size of 8 µm.

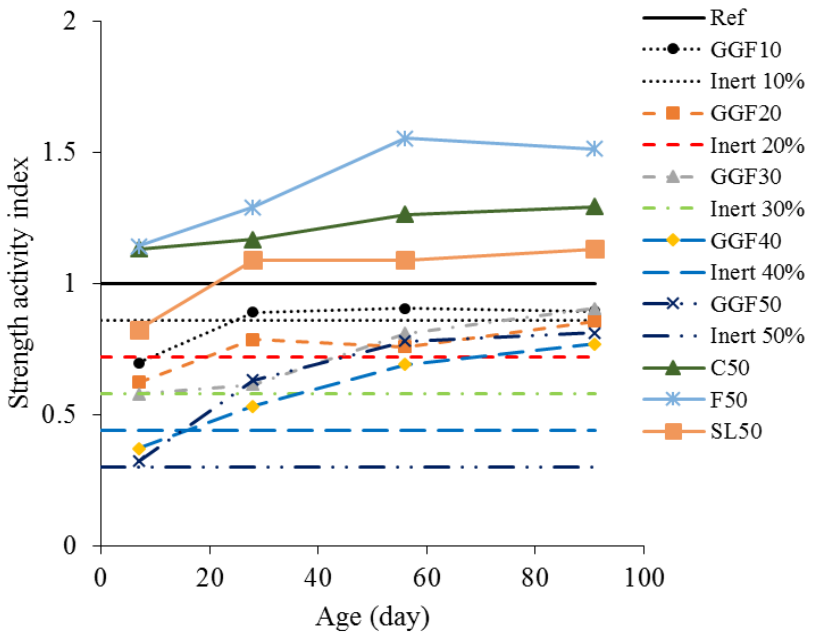

Figure 4.9 Strength activity index of binary mixtures compared to the corresponding inert lines

In the case of the SL50, C50, and F50 mixtures, the strength activity index was higher than 1.0 for all investigated ages, except for the 7-day strength of the SL50 mixture. In addition, the strength activity index of the SL50, F50, and C50 mixtures were higher than the inert line of 50%. In other words, the pozzolanic activity of these SCM types started before 7 days, which is contrary to that of the GGF.

Figure 4.10 illustrates the variations in coefficient of pozzolanic activity for different GGF replacement levels. Results indicate that the X_b value was not constant and increased with time and GGF content. Similar trends were observed by Tashima et al. (2016) who reported an increase in cementing efficiency factor from 0.51 to 0.82 for increase in GGF content from 10% to 30%.

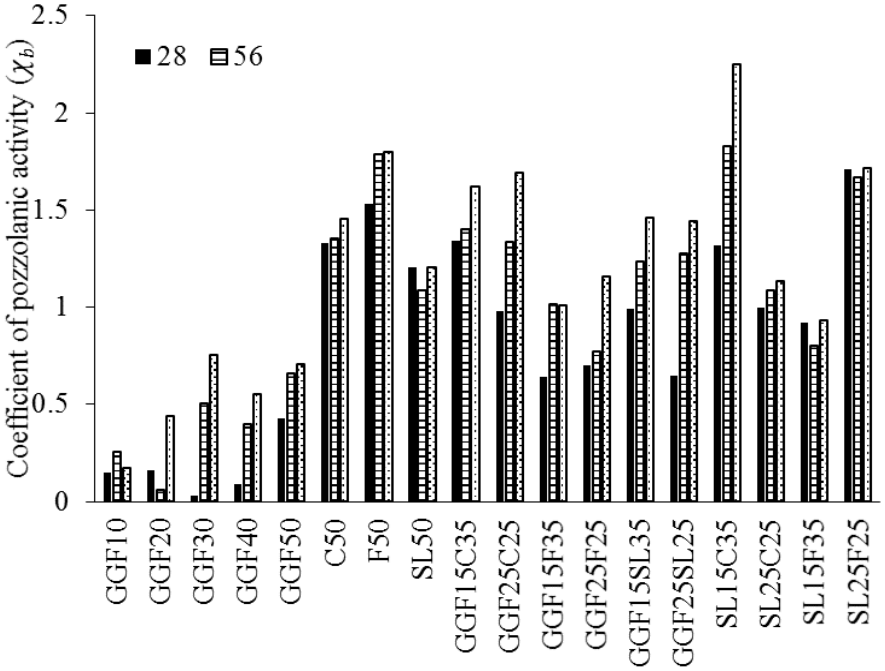

Figure 4.10 Values of coefficient of activity (χ_b)

In the case of the binary mixtures cast with 50% SCM, the minimum value of X_b was obtained for the GGF (0.43) compared to 1.33, 1.53, and 1.20 for FA-C, FA-F, and GGBS, respectively. These results were in agreement with calorimetry measurements, where the highest and the lowest total values of heat release were observed for the F50 and GGF50 mixtures, respectively. Trends were similar at 91 days, where the X_b was

ranging from 0.71 to 1.80 for GGF and FA-F, respectively. Similar to the results presented in Figure 4.9, it was observed that the values obtained for X_b at different ages are not the same and an increasing trend was noticed as a function of time. This could be attributed to the fact that pozzolanic reactions typically advance with time and higher rate of pozzolanic activity is expected at later ages.

4.3.4. Drying Shrinkage. Table 4.6 summarizes the drying shrinkage results. The Reference mixture made with 100% OPC exhibited the highest shrinkage values of 850 and 1030 με at 7 and 120 days, respectively. The lowest 7-day shrinkage of 370 με was obtained for the mixture prepared with 20% GGBS and 50% FA-C. This was followed by the CEM made with 10% GGBS and 50% FA-C, with 7-day shrinkage of 395 με.

The minimum 120-day shrinkage of 500 με was observed for the mixture with 20% GGBS and 50% FA-C. The use of 50% FA-C, 50% FA-F, and 50% GGBS reduced the 7-day shrinkage from 850 to 540, 600, and 550 με, respectively. These mixtures exhibited 120-day shrinkage of 690, 845, and 820 με, respectively. Based on the data presented in Table 1 it can be concluded that the ternary systems with GGBS and FA-C exhibited lower drying shrinkage compared to corresponding mixtures prepared with GGBS and FA-F. For instance, the mixture made with 25% GGBS and 25% FA-C exhibited 120-day drying shrinkage of 780 με. Such value was 910 με for the mixture made with 25% GGBS and 25% FA-F.

Figure 4.11 offers a summary of the drying shrinkage of mixtures made with different amounts of GGF in binary and ternary systems. In general, it was observed that shrinkage is reducing as a result of increase in GGF content. The mixture proportioned with 10% GGF exhibited 710 με of shrinkage at 7 days, while reached the 120-day value of 1010 με. The incorporation of 50% GGF reduced the 7- and 120-day shrinkage values to 600 and 875 με, respectively. The 120-day shrinkage values of the ternary mixtures incorporating 15% or 25% GGF was limited to 900 με. For the ternary mixtures incorporating GGF, the lowest 120-day shrinkage of 760 με was observed for the GGF15F35 mixture. This was followed by the GGF15SL35, GGF25C25 and GGF25F25 mixtures with 800, 840, and 840 με at 120 days. In general both SL and GGF had

comparable performance on reducing the shrinkage of the ternary mixtures with 50% SCM replacement, regardless of the fly ash type.

Table 4.6 Summary of drying shrinkage results (με)

	Mixture	7-d	56-d	91-d	120-d
	Ref.	850	1020	1020	1030
Binary systems	C50	540	670	680	690
	F50	600	790	820	845
	GGF10	770	970	1010	1010
	GGF20	710	920	940	940
	GGF30	660	820	890	890
	GGF40	600	750	840	840
	GGF50	600	810	875	875
	SL50	550	805	810	820
	SL70	450	870	920	940
Ternary systems	GGF15C35	440	870	890	895
	GGF25C25	490	805	830	840
	GGF15F35	465	740	760	760
	GGF25F25	520	815	830	840
	GGF15SL35	380	790	800	800
	GGF25SL25	460	870	890	900
	SL10C50	395	530	550	565
	SL15C35	400	690	690	700
	SL20C50	370	460	500	500
	SL25C25	540	770	780	780
	SL30C35	500	560	580	580
	SL40C15	620	760	775	780
	SL45C25	600	795	840	815
	SL50C15	570	836	870	885
	SL10F50	570	800	880	900
	SL15F35	550	840	830	855
	SL20F50	550	850	940	950
	SL25F25	605	855	870	910
	SL30F35	510	690	800	830
	SL35F25	790	810	870	880
	SL45F25	560	784	840	850
	SL55F15	560	920	940	940

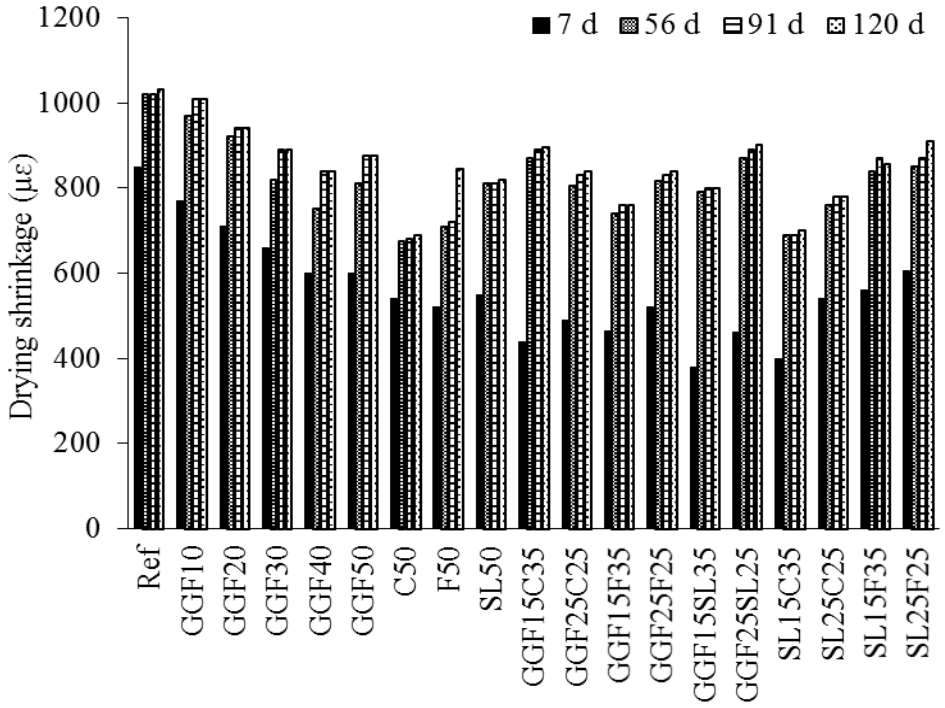

Figure 4.11 Drying shrinkage results (με)

4.3.5. Electrical Resistivity. Table 4.7 summarizes the bulk electrical resistivity measurements. The reference mixture made with 100% OPC exhibited 91-day electrical resistivity of 9.9 KΩ.cm. The incorporation of FA-C in binary system was not effective in enhancing the electrical resistivity. However, significant improvement in resistivity was observed due to the use of FA-F or GGBS. The use of 50% FA-C, 50% FA-F, and 50% GGBS resulted in 91-day resistivity of 5.8, 25.2, and 29.5 KΩ.cm, respectively. The use of ternary system with GGBS and FA-C was effective in enhancing the electrical resistivity, except for the mixtures made with 50% FA-C. The mixture made with 10% GGBS and 50% FA-C, and the one with 20% GGBS and 50% FA-C exhibited 91-day results of 8.7 and 5.5 KΩ.cm. The rest of such ternary mixtures developed electrical resistivity ranging from 11.7 to 30.1 KΩ.cm and 91 days. The use of GGBS and FA-F in ternary mixtures enhanced the electrical resistivity significantly. The 91-day resistivity of such mixtures ranged from 36.7 to 68.2 KΩ.cm.

Table 4.7 Electrical resistivity measurements (KΩ.cm)

	Mixture	28-d	56-d	91-d
	Ref.	7.6	9.7	9.9
Binary systems	C50	2.6	4.9	5.8
	F50	5.5	9.8	25.2
	GGF10	9.0	12.6	17.4
	GGF20	15.3	27.2	39.3
	GGF30	20.6	50.2	67.8
	GGF40	24.3	63.9	86.6
	GGF50	21.9	60.8	88.0
	SL50	24.1	26.7	29.5
	SL70	39.6	48.6	63.2
Ternary systems	GGF15C35	10.8	18.9	24.9
	GGF25C25	13.2	30.6	39.4
	GGF15F35	13.5	31.8	38.2
	GGF25F25	21.6	46.4	52.2
	GGF15SL35	43.0	53.8	54.6
	GGF25SL25	38.5	60.7	60.4
	SL10C50	2.2	3.9	8.7
	SL15C35	4.5	NA	14.2
	SL20C50	3.7	3.4	5.5
	SL25C25	8.8	11.7	18.3
	SL30C35	3.7	5.6	11.7
	SL40C15	16.2	22.1	32.4
	SL45C25	14.1	20.9	30.1
	SL50C15	11.4	20	NA
	SL10F50	9.3	15	37.6
	SL15F35	18.7	25.6	41.4
	SL20F50	14.9	24.1	53.7
	SL25F25	21.1	27.8	36.7
	SL30F35	23.3	35	54.9
	SL35F25	16	24.8	40.7
	SL45F25	33.2	50.6	67.7
	SL55F15	43.4	51.8	68.2

Figure 4.12 illustrates the bulk electrical resistivity measurements that increased as function of GGF content. In the case of the 28-day measurements, a bulk electrical resistivity of 7.6 kΩcm was obtained for the Reference mixture in comparison with 24.3

and 21.9 kΩcm for GGF40 and GGF50 specimens. At 91 days, the resistivity of the Reference mixture was 9.9 kΩcm in comparison with 86.6 and 88.0 kΩcm for GGF40 and GGF50 ones. Similar trends were observed by Hossain et al. (2005) who investigated the rapid chloride ion permeability (RCP) of concrete mixtures made with 0.40 w/cm. The authors reported that increasing the GGF from 0 to 15% reduced the 28-day RCP from 4500 to 1500 Coulomb. The incorporation of GGF in ternary mixtures was also effective in enhancing the resistivity, with best performance observed for combination of GGF and GGBS, followed by GGF and FA-F, and GGF and FA-C.

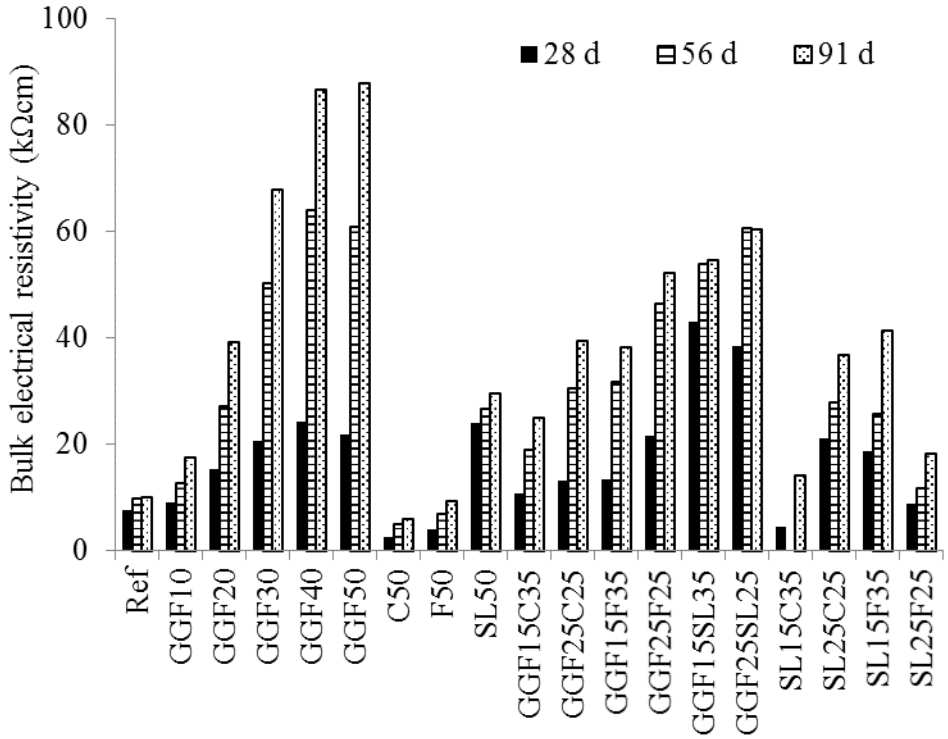

Figure 4.12 Electrical resistivity measurements (kΩcm)

4.3.6. Cost and CO_2 Emission. Given the fact that this research aims at developing sustainable concrete for transportation infrastructure, it was necessary to take into consideration the cost of candidate binders, as well as the CO_2 emission associated with each binder type. Various sources were considered to determine the cost of different binder compositions incorporating OPC, GGBS, FA-C, and FA-F. Various sources within

the literature were also considered for estimating the CO_2 emissions. Recommendations provided by Buhler (2011) were considered for determining the emissions. Table 4.8 is a summary of the unit cost and emission rates considered for determining the cost per ton of different binder compositions. Using the unit values for cost and emission as presented in this table, the cost and carbon footprint were determined as a linear function of cementitious materials amount:

$$Binder\ cost\ (\$/ton) = 100 \times OPC + 45 \times FA\text{-}C + 68 \times FA\text{-}F + 91 \times GGBS \quad (4\text{-}5)$$

$$CO_2\ emission\ (kg/ton\ of\ binder) = 960 \times OPC + 93 \times Fly\ Ash + 155 \times GGBS \quad (4\text{-}6)$$

Table 4.8 Unit cost and carbon footprint of cement and cementitious materials

	OPC	FA-C	FA-F	GGBS
Cost ($/ton)	100	45	68	91
Emission rate (kg/ton)	960	93	93	155

4.4. MULTI-CRITERIA OPTIMIZATION

An optimized binder composition needs to meet several requirements, including proper mechanical properties, i.e. compressive strength, reduced shrinkage, lower carbon footprint, and minimum possible cost. Multi-criteria decision making is therefore necessary to select such an optimized binder composition. Weight factors were selected as summarized in Table 4.9. The weight factors ranged from 0 to 5, indicating the least and the most important factors, respectively.

Table 4.9 Importance weights considered in binder type optimization

Factor	Compressive strength	Shrinkage	Cost	CO_2 emission
Weight factor	3	5	5	3

Responses included in optimization were 91-d compressive strength, 7-d and 120-d shrinkage, cost, and emission. Experimental data were ranked from highest to least performance. Results were then normalized from 0 to 100, indicating the lowest and the best performances, respectively. Weight factors were then applied to the normalized data. Closed loop star graphs were developed to compare the overall performance of each of the binder compositions. Figure 4.13 is a sample of developed star graphs. The area of each star corresponding to each binder composition was determined. Figure 4.14 offers a summary of the obtained area obtained for CEM prepared with binary and ternary combinations of GGBS, FA-C, FA-F as main candidates for further investigation through the report.

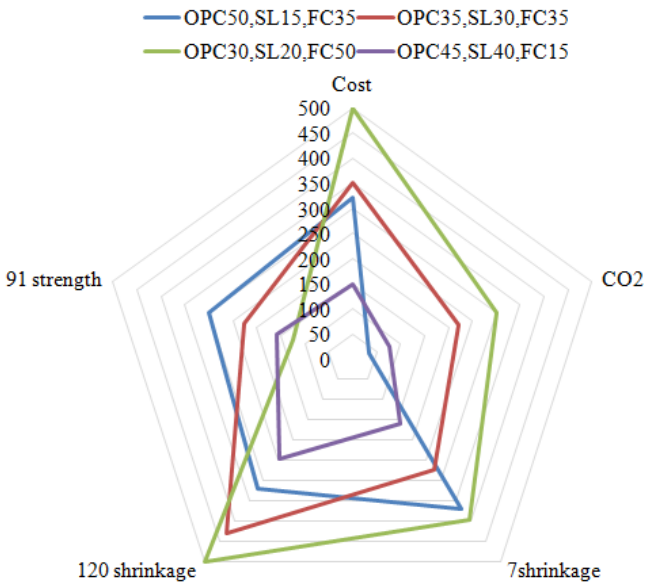

Figure 4.13 Typical star graph incorporated for ranking the performance of binders

Given the importance of 1-day compressive strength of concrete for pavement construction, and considering the fact that SCM replacement levels needed to be within acceptable ranges for field practice, it was decided to select binder compositions with no more than 50% SCM replacement. Therefore, a ternary blend produced with 50% OPC,

35% FA-C, and 15% GGBS was finally selected as the optimized candidate for further investigation in the concrete phase.

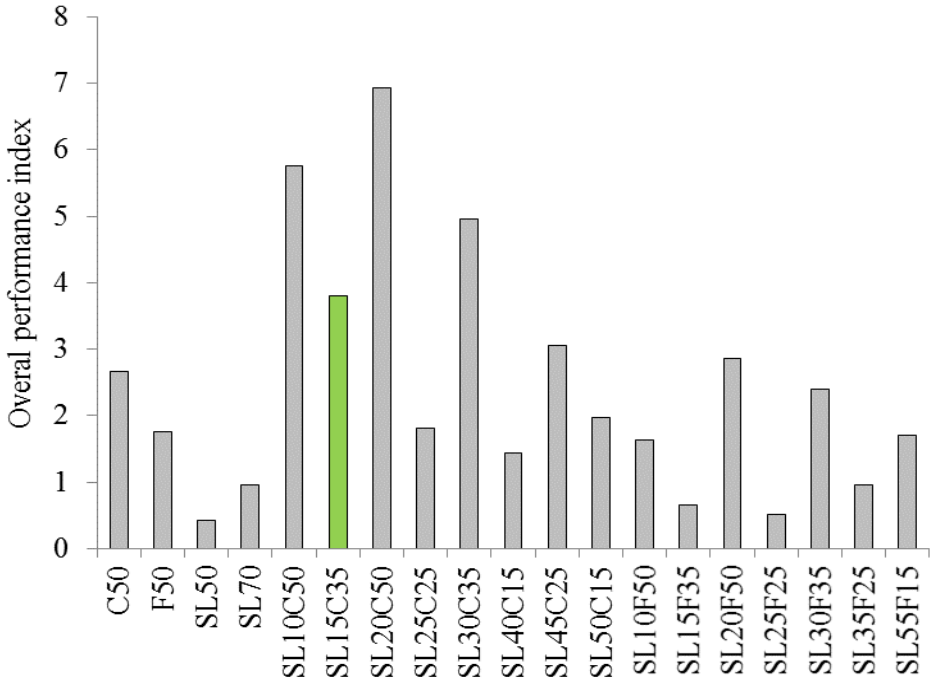

Figure 4.14 Ranking the overall performance of candidate binders

Considering the overall performance of the mixtures cast with GGF, it was decided to limit the use of GGF to 15% in concrete production. Given the acceptable performance, a ternary blend of 50% OPC, 35% FA-C, and 15% GP was also added to the test matrix of the concrete phase.

4.5. REMARKS

This section offers a summary of the experimental work and analysis conducted to determine the key engineering properties of concrete equivalent mortar prepared with various sustainable cementitious blends. The Reference mixture corresponded to a mortar with 100% OPC. Different binary and ternary combinations of OPC, FA-C, GGBS, FA-F, and GGF were investigated. The test matrix included binary systems with 10% to 50% GGF, 50% FA-C, 50% FA-F, 50% GGBS, and 70% GGBS. Ternary systems with 15%

or 25% GGF with either 35% or 25% of FA-F, FA-C, or GGBS were considered. Additional ternary blends of GGBS with either FA-C or FA-F with 50% to 70% SCM replacement were also studied. Rheological properties, heat of hydration, strength development, shrinkage, and electrical resistivity were investigated in laboratory. Multi-criteria decision making approach was employed to rank the performance of the candidate binders. Based on the results obtained in this investigation, the following conclusions are warranted:

- The use of up to 50% GGF in binary mixtures reduced the rate of structure build-up at rest from 7.1 to 0.8 Pa/min, and the yield stress was reduced from 170 to 110 Pa at 8-min measurement and 295 to 150 Pa for 62-min. The plastic viscosity was increased by up to 100% when using 50% GGF substitution compared to the Reference mixture. The plastic viscosity was increased from 5.5 to 11.0 Pa.s at 8-min measurement and 7.0 to 12.9 Pa.s for 65-min.
- The use of SCMs reduced the rate of hydration with both the accumulative heat of hydration and total released heat reduced after 72 hours. Incorporating 50% GGF reduced the total normalized released heat from 12.7 to 3.6 kJ.hr/g of binder, while the accumulative heat of hydration was reduced from 310 to 140 J/g.
- The increase in the coefficient of pozzolanic activity was observed as a function of age and SCM replacement. Mortar mixture cast with 50% GGF exhibited the minimum 91-day coefficient of pozzolanic activity of 0.71, compared to 1.80, 1.46, and 1.21 for the F50, C50, and SL50 mixtures, respectively.
- The use of high volume SCM a replacement rates of over 50% reduced the early age strength development. However, the long-term compressive strength values were mostly higher than that of the mixture made with 100% OPC (34.1 MPa), with maximum value of 61.5 MPa. The use of 15% and 25% GGF in ternary blends was effective in enhancing the compressive strength. The best performances were observed in the case of the GGF/FA-C mixtures, followed by the GGF/GGBS, and GGF/FA-F, with up to 45%, 28%, and 10% increase in 91-day compressive strength compared to the Reference mixture.
- Both the early age and long-term shrinkage values reduced with the use of SCMs. The maximum 7- and 120-day shrinkage values of 850 and 1030 με were

observed for the mixture made with 100% OPC. Reduction in 120-day shrinkage to values as low as 500 με was observed with high-volume SCM incorporation, with replacement rates of up to 70%.

- The use of FA-F, GGBS, and GGF was effective in enhancing the electrical resistivity of the investigated binder systems. Bulk electrical resistivity was increased from about 10 to 88 kΩcm due to 50% GGF replacement. For the investigated ternary mixtures cast with 15% or 25% GGF, the 91-day bulk electrical resistivity values ranged from 25 to 60 KΩcm, in comparison with 10 KΩcm for the Reference mixture.
- Multi criteria decision making was conducted to rank the overall performance of binary and ternary mixtures prepared with various amounts of GGBS, FA-C, and FA-F. Given the technical considerations, cost, emissions, and considering the performance of the investigated mixtures, it was decided to use a ternary blend of 50% OPC, 15% GGBS, and 35% FA-C as a candidate binder for concrete production. The CEM made with this binder exhibited 91-day compressive strength of 61.5 MPa and 120-day drying shrinkage of 700 με, and electrical resistivity of 14.2 KΩ.cm.
- Considering the overall performance of the mixtures cast with GGF, it was decided to limit the use of GGF to 15% in concrete production. Given the acceptable performance, a ternary blend of 50% OPC, 35% FA-C, and 15% GP was also added to the test matrix of the concrete phase. The CEM made with this binder exhibited 91-day compressive strength of 47.7 MPa and 120-day drying shrinkage of 900 με, and electrical resistivity of 24.9 KΩ.cm.

5. EFFECT OF RCA ON MECHANICAL PROPERTIES OF CONCRETE FOR PAVEMENT CONSTRUCTION

5.1. RESEARCH SIGNIFICANCE

This section presents the results of the experimental work conducted to evaluate the performance of concrete mixtures proportioned with different types and contents of fine and coarse RCA. The goal was to investigate the effect of RCA on key mechanical properties of concrete made with RCA for rigid pavement application.

Concrete with normal compressive strength is typically used for rigid pavement construction. As stated earlier, the incorporation of RCA as a replacement for virgin aggregate affects the mechanical properties of concrete, including the compressive strength. Therefore, it is required to investigate the effect of both RCA characteristics and content on compressive strength of concrete.

Flexural strength of concrete is another concrete property that can affect the design of rigid pavement. For a given thickness of pavement, the stress ratio defined as the ratio of the maximum tensile stress to material's flexural strength, affects the number of traffic loading cycles required for fatigue life of the pavement.

Modulus of elasticity (MOE) is considered as one of the key mechanical properties that govern the design and serviceability of rigid pavements, which can be significantly affected by the use of RCA. Variations in MOE influence the stress and deflection due to traffic loading, deformation due to environmental effects, and optimum pavement panel length. Therefore, it is necessary to quantify the effect of RCA on MOE of concrete designated for rigid pavement construction.

Compressive strength, splitting tensile strength, MOE, and flexural strength of concrete made with w/cm of 0.37 and 0.40 prepared with binary or ternary cement were investigated. The binary system was adopted from the concrete mixture design used by the Missouri Department of Transportation (MoDOT) for rigid pavement construction. The ternary cement was selected based on the data presented in previous sections.

5.2. EXPERIMENTAL PROGRAM

An experimental program was undertaken to investigate the performance of RCA concrete mixtures for pavement applications. Class PCCP concrete used by MoDOT was employed as the reference concrete. This concrete was prepared with 323 kg/m^3 of cementitious materials, 25% Class C fly ash, w/cm of 0.40, sand-to-aggregate ratio (S/A) of 0.42, and without any RCA.

5.2.1. Materials. The cementitious materials used for the development of the investigated concrete included a Type I/II Portland cement (OPC), Class C fly ash (FA-C), ground granulated blast furnace slag (GGBS), and ground glass fiber (GGF). The mixtures were proportioned with either a binary or a ternary cement. The binary cement was composed of 75% (by mass) OPC and 25% FA-C. The ternary systems included a binder with 35% FA-C+15% GGBS (by mass), and a system with 35% FA-C+15% GGF (by mass). Crushed dolomite or crushed limestone coarse aggregate with nominal maximum size of 19 mm were incorporated as the virgin coarse aggregate in proportioning the concrete mixtures. Coarse RCA procured from seven different sources, including six types from commercial recycling centers and one type of a laboratory produced RCA, were considered. Table 5.1 summarizes the aggregate properties. A lignum-based water reducing admixture (WRA) with specific gravity of 1.2 and 40% solid content, and an air-entraining admixture (AEA) were incorporated.

5.2.2. Concrete Mixture Proportions. In total, 53 concrete mixtures were produced with w/cm ranging from 0.37 to 0.42. The investigated mixtures were proportioned using the DOL1 or LIM as virgin coarse aggregate. The AEA was used to secure 6%±1% air and the WRA was incorporated to attain required initial slump values. Three different groups of concrete were developed and tested in the laboratory. A summary of the mixture properties is presented below:

Group I: concrete mixtures were produced with different replacement ratios (% vol.) of the fine RCA1 and coarse RCA1. All mixtures were produced with DOL1 as virgin coarse aggregate. Binary cement with 25% FA-C was used for developing the reference concrete. Two additional mixtures were prepared without any RCA, using the ternary system with 15% GGBS and 35% FA-C, with 0.37 and 0.40 w/cm. The rest of the mixtures were proportioned with the same ternary cement, except for one mixture that

was produced with a ternary system of 35% FA-C and 15% GGF. This concrete incorporated 30% (by vol.) coarse RCA1 and 0.37 w/cm.

Table 5.2 summarizes the mixture proportions and fresh properties of the concrete investigated in Group I. A coding system was adapted to label the concrete mixtures, which indicates the RCA type and content, the binder type, and the w/cm. For instance, the “RCA2-50-B-40” mixture refers to the concrete containing 50% (by vol.) of “RCA2”, binary cement (B), and 0.40 w/cm.

Group II: crushed limestone was used as the virgin coarse aggregate. The reference concrete was prepared with 0.40 w/cm, binary cement with 25% FA-C, and without any RCA. The mixture were produced with coarse RCA2 fixed at 30% (by vol.). The fine RCA2 was used as a replacement for river sand in replacement rate of 0 to 20% (by vol.). The w/cm ranged from 0.37 to 0.42, and FA-C content varied from 25% to 40%. Table 5.3 summarizes the mixture proportions and fresh properties of the concrete investigated in Group II. A coding system was adapted to label the concrete mixtures, which indicates the Class C fly ash content, fine RCA2 content, and the w/cm. For instance, the “C35-F15-37” mixture refers to the concrete containing 35% (by mass) of fly ash, 15% (by vol.) fine RCA2, and 0.37 w/cm.

Group III: Crushed dolomite (DOL1) was used as the virgin coarse aggregate. The mixtures were prepared with binary cement and 0.40 w/cm, or with ternary cement and 0.37 w/cm. The binary system included 25% (by mass) FA-C, while the ternary system composed of 35% FA-C and 15% GGBS. Six different sources of coarse RCA were use at 30%, 50%, and 100% replacement rates. No fine RCA was used for producing the concrete of Group III. Table 5.4 summarizes the mixture proportions and fresh properties of the investigated mixtures. The concrete labeling system is similar to that used for mixtures in Group I.

Table 5.1 Virgin aggregate and RCA properties

Aggregate	Source	Specific gravity	Absorption (%)	Los Angles abrasion (%)	NMAS (mm)
Sand	River-bed sand	2.63	0.40	-	4
Fine RCA1	Residual concrete, airfield	2.11	7.33	-	4
Fine RCA2	Residual concrete, airfield	2.41	6.80	-	4
Virgin coarse 1	Dolomite (DOL1)	2.73	0.80	28	19
Virgin coarse 2	Limestone (LIM)	2.64	0.50	24	19
RCA1	Residual concrete, airfield	2.35	4.46	33	19
RCA2	Residual concrete, airfield	2.38	4.20	33	19
RCA3	Laboratory produced RCA	2.35	4.56	41	19
RCA4	Commercial recycling, Missouri	2.25	5.75	39	19
RCA5	Commercial recycling, Kansas	2.24	6.05	38	19
RCA6	Commercial recycling, Missouri	2.17	7.58	44	19
RCA7	Commercial recycling, Missouri	2.21	7.13	53	12.5

Table 5.2 Mixture proportions and fresh properties of the concrete investigated in Group I

Mix.	Binder (kg/m^3)	OPC	GGBS	FA-C	w/cm	Water	DOL	C-RCA1	Sand	F-RCA1	C-RCA1	F-RCA1	Air (%)	Slump (mm)
		(% mass)				(kg/m^3)					(% vol.)			
DOL1-B-40	323	75	-	25	0.40	129	112	0	782	0	0	0	6.2	85
DOL1-T-37	323	50	15	35	0.37	120	113	0	793	0	0	0	7.2	65
DOL1-T-40	323	50	15	35	0.40	129	112	0	782	0	0	0	5.0	85
RCA1-30-T-37	323	50	15	35	0.37	120	795	293	793	0	30	0	6.8	85
RCA1-30-T-40	323	50	15	35	0.40	129	784	290	782	0	30	0	5.0	75
RCA1-30-T-37-15F	323	50	15	35	0.37	120	795	293	674	96	30	15	5.0	85
RCA1-30-T-40-15F	323	50	15	35	0.40	129	784	290	665	94	30	15	5.0	40
RCA1-40-T-40-15F	323	50	15	35	0.40	129	672	386	665	94	40	15	5.9	65
RCA1-50-T-37	323	50	15	35	0.37	120	568	489	793	0	50	0	7.0	85
RCA1-50-T-40	323	50	15	35	0.40	129	560	482	782	0	50	0	5.4	50
RCA1-50-T-37-15F	323	50	15	35	0.37	120	568	489	674	96	50	15	6.8	85
RCA1-50-T-40-15F	323	50	15	35	0.40	129	560	482	665	94	50	15	5.6	65
RCA1-50-T-40-30F	323	50	15	35	0.40	129	560	482	548	188	50	30	5.0	85
RCA1-50-T-40-40F	323	50	15	35	0.40	129	560	482	469	250	50	40	5.0	50
RCA1-60-T-40-30F	323	50	15	35	0.40	129	448	578	548	188	60	30	5.0	50
RCA1-70-T-37	323	50	15	35	0.37	120	341	685	793	0	70	0	5.5	75
RCA1-70-T-40	323	50	15	35	0.40	129	336	675	782	0	70	0	6.9	85
RCA1-70-T-40-15F	323	50	15	35	0.40	129	336	675	665	94	70	15	5.4	50
RCA1-70-T-40-30F	323	50	15	35	0.40	129	336	675	548	188	70	30	5.2	25
RCA1-30-GGF15-37	323	50	-*	35	0.37	120	795	293	793	0	30	0	5.5	75

*This mixtures was prepared with 15% GGF instead of GGBS for ternary binder

Table 5.3 Mixture proportions and fresh properties of the concrete investigated in Group II

Mix.	Binder (kg/m^3)	OPC	FA-C	w/cm	Water	LIM	C-RCA2	Sand	F-RCA2	C-RCA2	F-RCA2	Air	Slump
		(% wt.)								(% wt.)		(%)	(mm)
LIM-B-40	323	75	25	0.40	129	1121	0	745	0	0	0	5.5	65
C35-F0-40	323	65	35	0.40	129	785	303	745	0	30	0	5.2	90
C35-F15-37	323	65	35	0.37	120	785	303	633	102	30	15	5.5	50
C40-F20-37	323	60	40	0.37	120	785	303	596	136	30	20	5.3	50
C35-F10-42	323	65	35	0.42	136	785	303	670	68	30	10	5.3	65
C25-F15-40	323	75	25	0.40	129	785	303	633	102	30	15	5.2	50
C25-F10-37	323	75	25	0.37	120	785	303	670	68	30	10	6.0	40
C25-F0-40	323	75	25	0.40	129	785	303	745	0	30	0	5.9	40

Table 5.4 Mixture proportions and fresh properties of the concrete investigated in Group III

Mix.	Binder (kg/m^3)	OPC	GGBS	FA-C	w/cm	Water	DOL	C-RCA	Sand	RCA	Air	Slump
		(% mass)				(kg/m^3)				(% vol.)	(%)	(mm)
RCA1-50-B-40	323	75	0	25	0.40	129	560	482	782	50	7.2	115
RCA1-100-B-40	323	75	0	25	0.40	129	0	965	782	100	5.0	100
RCA3-30-B-40	323	75	0	25	0.40	129	784	289	782	30	6.3	65
RCA3-50-B-40	323	75	0	25	0.40	129	560	482	782	50	5.8	70
RCA4-30-B-40	323	75	0	25	0.40	129	784	277	782	30	6.1	55
RCA4-50-B-40	323	75	0	25	0.40	129	560	462	782	50	5.2	65
RCA4-100-B-40	323	75	0	25	0.40	129	0	923	782	100	5.0	115
RCA5-30-B-40	323	75	0	25	0.40	129	784	276	782	30	5.5	50
RCA5-50-B-40	323	75	0	25	0.40	129	560	460	782	50	5.1	65
RCA5-100-B-40	323	75	0	25	0.40	129	0	920	782	100	6.0	100
RCA6-30-B-40	323	75	0	25	0.40	129	784	268	782	30	5.8	45
RCA6-50-B-40	323	75	0	25	0.40	129	560	446	782	50	6.0	80
RCA7-30-B-40	323	75	0	25	0.40	129	784	272	782	30	5.9	65
RCA7-50-B-40	323	75	0	25	0.40	129	560	453	782	50	6.8	75
RCA7-100-B-40	323	75	0	25	0.40	129	0	907	782	100	7.0	135
RCA3-30-T-37	323	50	15	35	0.37	120	795	292	793	30	6.0	60
RCA3-50-T-37	323	50	15	35	0.37	120	568	488	793	50	6.8	65
RCA4-30-T-37	323	50	15	35	0.37	120	795	279	793	30	6.2	55
RCA4-50-T-37	323	50	15	35	0.37	120	568	466	793	50	5.4	70
RCA5-30-T-37	323	50	15	35	0.37	120	795	279	793	30	5.5	35
RCA5-50-T-37	323	50	15	35	0.37	120	568	466	793	50	5.6	35
RCA6-30-T-37	323	50	15	35	0.37	120	795	271	793	30	5.8	45
RCA6-50-T-37	323	50	15	35	0.37	120	568	451	793	50	5.2	50
RCA7-30-T-37	323	50	15	35	0.37	120	795	272	793	30	5.4	55
RCA7-50-T-37	323	50	15	35	0.37	120	568	460	793	50	6.0	50

5.2.3. Specimen Preparation and Testing. A drum mixer with 110-l capacity was used for preparing the concrete. The batching sequence consisted of: (1) mixing the aggregates and one third of the water at low speed for 3 min to ensure homogenized distribution and saturation of the particles; (2) AEA diluted in one third of the mixing water was added and agitation continued at high speed for 1 min; (3) introducing the cementitious materials and mixing for 1 min at high speed; (4) WRA was diluted in rest of the water and added to the batch and mixed for 2 min at high speed. After 2 min of rest, mixing was resumed for 3 min at high speed. Slump and air content in fresh state were determined according to ASTM C143 (2015) and ASTM C231 (2014), respectively.

A vibrating table was used to secure proper consolidation of the concrete. The specimens were covered with wet burlap and plastic sheets up to 24 hours after casting. The specimens were then cured in lime-saturated of 21±2 ºC up to the time of testing. A grinder machine was used for the preparation of the cylindrical specimens used for the determination of compressive strength and MOE.

For the determination of compressive strength, 100×200 mm cylindrical specimens were employed in accordance with ASTM C39 (2001). Three samples were tested for compressive strength values. Similar samples were used for testing the splitting tensile strength in accordance with ASTM C469 (2010). The flexural strength was measured on 75×75×400 mm or 150×150×500 mm beams in accordance with ASTM C78 (2010). Two specimens were tested for each mixture at each testing age. A four-point bending setup was used for testing the flexural strength. A schematic of the test setup is presented in Figure 5.1. The load is applied on the concrete beam, and the failure load (P) is recorded. The flexural strength is then calculated using the following equation:

$$R = \frac{Pl}{bh^2} \tag{5-1}$$

where R= modulus of rupture (MPa), P = the ultimate load (N), l = span length, $_b$ = average beam width at fracture (mm), and h= average beam height at fracture (mm).

Cylindrical specimens measuring 100×200 mm were used for determining the modulus of elasticity, according to ASTM C469. Figure 5.2 shows the test setup used for measuring the modulus of elasticity.

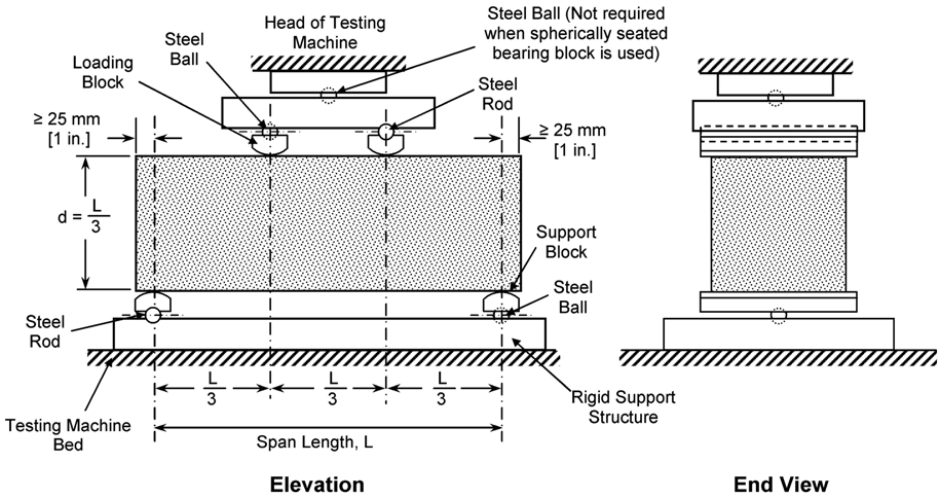

Figure 5.1 Simply supported beam for determining the flexural strength (ASTM C78)

Figure 5.2 Modulus of elasticity test setup

The loading cycles were repeated three times for each sample. The vertical strain of the specimen corresponding to each stress level was measured using a LVDT system. The results were then used for determining the modulus of elasticity based on the following equation:

$$E = \frac{S_2 - S_1}{\varepsilon_2 - 0.000050} \quad (5\text{-}2)$$

where E= chord modulus of elasticity (GPa), S_2= stress corresponding to 40% of the ultimate load capacity, S_1= stress corresponding to a longitudinal strain of 0.000050, and ε_2= longitudinal strain caused by the stress S_2.

5.3. RESULTS AND DISCUSSION

5.3.1. Compressive Strength.

5.3.1.1 Effect of mixture parameters and fine RCA. Table 5.5 summarizes the compressive strength results obtained for the first group of investigated concrete, with various contents of coarse RCA1 and fine RCA1. The maximum 1-day compressive strength of 15 MPa was observed in the case of the MoDOT reference mixture with 75% OPC and 25% FA-C. The rest of the mixtures prepared with ternary cement with 50% SCM exhibited 1-day compressive strength ranging from 6.0 to 12.5 MPa.

All investigated mixtures met the minimum compressive strength requirement of 28 MPa at 28 days. The maximum 28-day compressive strength of 49 MPa was observed for the samples proportioned with ternary blend of 15% GGF + 35% FA-C and for the RCA1-30-T-37-15F mixture with w/cm of 0.37. The minimum 28-day strength of 31.4 MPa was observed in the case of the mixture proportioned with 50% coarse RCA1, 40% fine RCA1, and w/cm of 0.40. An increase in compressive strength as a function of extended curing period was observed for all specimens. The maximum 91-day strength of 61.0 MPa was in the case of the RCA1-30-GGF15-37 mixture, proportioned with 30% coarse RCA1 and w/cm of 0.37, and incorporating a ternary system of 15% GGF and 35% FA-C. Results highlight the encouraging performance of the RCA-made mixtures proportioned with the optimized binder composition and reduced w/cm.

Based on the data obtained for concrete made with 50% or 70% coarse RCA1, 0.40 w/cm, and different fine RCA1 contents of 0 to 40%, a reduction in compressive strength due to the use of fine RCA1 was observed. For the first group of such mixtures prepared with 50% RCA1, the increase in fine RCA1 from 0 to 40% reduced the 28-day compressive strength from 40.5 to 31.4 MPa, corresponding to up to 22% reduction. Such

values ranged from 48.0 to 41.5 MPa at 91 days, corresponding to 14% reduction in 91-day compressive strength due to 40% fine RCA1 replacement.

Table 5.5 Compressive strength results of concrete made with different contents of coarse RCA1 and fine RCA1 (Group I) (MPa)

Mixture	1 day	7 days	28 days	56 days	91 days
DOL1-B-40	15.0	32.0	38.5	42.0	46.5
DOL1-T-37	10.0	32.9	50.0	54.3	58.6
DOL1-T-40	8.5	28.0	41.5	49.5	50.5
RCA1-30-T-37	12.5	34.0	44.0	55.0	59.5
RCA1-30-T-40	8.5	26.0	40.0	46.5	45.5
RCA1-30-T-37-15F	11.5	39.0	49.0	57.0	56.0
RCA1-30-T-40-15F	7.0	24.5	37.0	40.0	45.8
RCA1-40-T-40-15F	6.5	20.5	31.5	38.0	40.5
RCA1-50-T-37	7.5	36.0	47.0	52.5	54.5
RCA1-50-T-40	8.5	29.5	40.5	46.5	48.0
RCA1-50-T-37-15F	6.0	30.0	41.5	43.0	49.0
RCA1-50-T-40-15F	8.0	23.5	38.5	42.5	41.0
RCA1-50-T-40-30F	7.0	23.0	32.0	39.5	43.5
RCA1-50-T-40-40F	7.0	23.0	31.4	34.5	41.5
RCA1-60-T-40-30F	8.0	25.5	37.1	39.5	43.0
RCA1-70-T-37	6.0	30.0	46.5	51.5	53.0
RCA1-70-T-40	7.5	24.0	36.5	40.5	44.5
RCA1-70-T-40-15F	6.6	21.5	35.0	37.5	44.5
RCA1-70-T-40-30F	8.5	27.0	37.0	41.0	43.0
RCA1-30-GGF15-37	6.5	37.0	49.0	56.0	61.0

For the concrete prepared with 70% coarse RCA1, the reduction in 28- and 91-day compressive strength due to 30% fine RCA1 incorporation was negligible. One justification for this observation can be the higher air content of the concrete made with 70% coarse RCA1 and without any fine RCA1 (7.0%) compared to lower air contents of

5.4% and 5.2% for corresponding mixtures prepared with 15% and 30% fine RCA1, respectively.

In the case of the concrete made with 0.37 w/cm and 30% or 50% coarse RCA2, the use of 15% fine RCA1 also reduced the compressive strength results. The use of 15% fine RCA reduced the 91-day compressive strength of the concrete with 30% coarse RCA from 59.5 to 56.0 MPa, corresponding to 6% reduction. Such a reduction (due to the use of 15% fine RCA) was 10% (from 54.5 to 49.0 MPa) in concrete incorporating 50% coarse RCA2. In general and based on the data presented in Table 5.5, it can be concluded that the use of fine RCA can reduce the compressive strength significantly. However, the use of proper binder composition and the reduction in w/cm can be considered as effective means for compensating for the negative impacts of the fine RCA on compressive strength.

Similar results were observed in the case of mixtures prepared with different combinations of fine RCA, w/cm, and FA-C replacement, presented in Table 5.6. The reference concrete made with limestone coarse aggregate, 0.40 w/cm, 25% FA-C, and without any RCA, exhibited the 28- and 91-day compressive strength of 43.5 and 51.8 MPa, respectively.

Table 5.6 Compressive strength results of concrete made with different contents of coarse RCA2 and fine RCA2 (Group II) (MPa)

Age	LIM-B-40	C35-F0-40	C35-F15-37	C40-F20-37	C35-F10-42	C25-F15-40	C25-F10-37	C25-F0-40
1 d	19.8	20.2	18.7	17.3	19.8	22.2	21.3	18.7
7 d	35.4	35.6	35.5	37.9	33.1	37.6	34.0	34.1
28 d	43.5	52.1	53.6	48.5	42.7	49.5	48.8	42.1
56 d	48.1	53.2	54.8	55.7	49.5	52.4	50.0	46.6
91 d	51.8	56.7	53.2	54.3	50.9	50.3	52.2	48.0

The use of 30% coarse RCA2 reduced the 28- and 91-day compressive strength to 42.1 and 48.0 MPa, corresponding to 3% and 7% reduction, respectively. The adjustments in mixture design parameters, including the reduction in w/cm to 0.37 and the use of 35% or 40% FA-C were effective in enhancing the compressive strength. Results presented in

Table 1 indicate 91-day compressive strength ranging from 50.3 to 56.7 MPa in mixtures made with 30% coarse RCA1, and up to 20% fine RCA2.

5.3.1.2 Effect of coarse RCA content. Figure 5.3 presents the variations in compressive strength of mixtures made with 0 to 70% coarse RCA1. The investigated mixtures were prepared with ternary cement (15% GGBS+35% FA-C), with 0.37 and 0.40 w/cm. In general, decrease in compressive strength was observed with the use of RCA. Rate of such reduction was 12% for both 28- and 91-day measurements of concrete with 0.40 w/cm at 70% RCA1 replacement. Reduction in compressive strength of 7% and 10% was observed for the 28- and 91-day results of concrete with 0.37 w/cm at 70% RCA1 replacement.

Figure 5.4 presents the effect of 30% and 50% coarse RCA obtained from various sources on compressive strength of concrete prepared with ternary cement (15% GGBS+35% FA-C) and 0.37 w/cm, investigated in Group III. In general, a tendency to reduction in compressive strength was observed due to the RCA incorporation. Similar trends were obtained with the use of 30%, 50%, and 100% of coarse RCA from different sources in concrete prepared with 0.40 w/cm and binary cement with 25% FA-C.

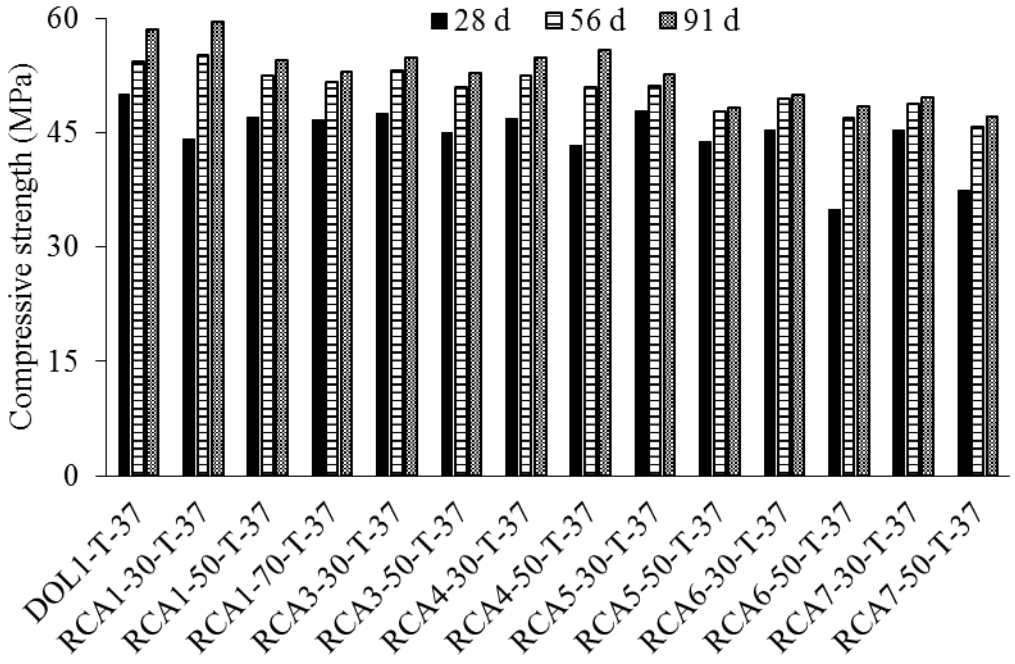

Figure 5.3 Effect of RCA type on compressive strength of concrete prepared with ternary cement and 0.37 w/cm (Group III)

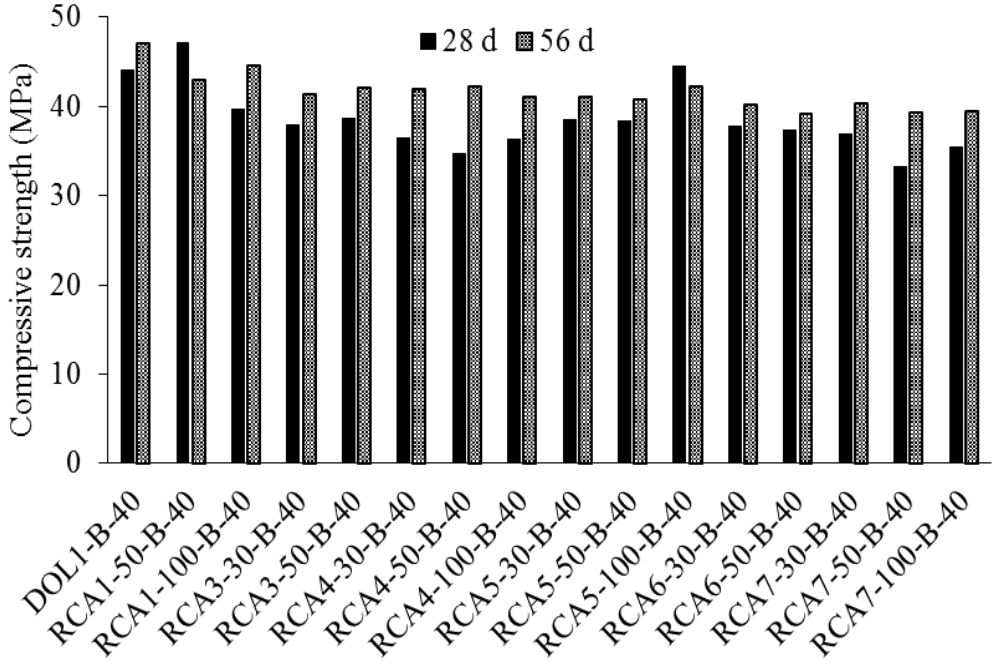

Figure 5.4 Effect of RCA type on compressive strength of concrete prepared with binary cement and 0.40 w/cm (Group III)

5.3.1.3 Effect of coarse RCA properties. Results presented in previous sections indicate that a considerable spread in compressive strength can be observed for a given RCA content, thus indicating that the compressive strength is affected by the properties of RCA. Different properties of coarse aggregate, including aggregate shape, surface texture, maximum size, etc. can affect the mechanical properties of concrete. However, given the fact that all investigated coarse aggregate sources were crushed and had rough surface textures, and considering the limitations in quantifying such factors on mechanical properties, the main characteristics for coarse RCA (Silva et al. 2014) including water absorption, Los Angeles (LA) abrasion resistance, and oven-dry specific gravity were employed for further analysis. It should be noted that these physical properties (water absorption, specific gravity, and mass loss due to LA abrasion), are employed by the standards, recommendations, and guidelines to define RCA quality (Butler et al. 2013; ASHTO 2015; Mc Neil and Kang 2012).

The residual mortar phase available in RCA particles is the main source of difference in properties of RCA compared to virgin aggregate (Silva et al., 2014). A

higher content of residual mortar is normally expected to cause greater impact on engineering properties of RCA, i.e. lower specific gravity, higher absorption rate, and higher mass loss due to LA abrasion. An aggregate skeleton formed by the combination of virgin and recycled aggregate is therefore expected to exhibit relatively higher water absorption, greater LA abrasion, and lower specific gravity, compared to virgin aggregate. This is in agreement with data reported by Omary et al. (2016) that describe the properties of an aggregate blend as a linear combination of the properties of the blend constituents. Such a concept can be incorporated to calculate the properties of the aggregate combination as a function of the relative mass/volume of the fractions found in the composition. The following equations were used to determine the oven-dry specific gravity, water absorption, and mass loss due to LA abrasion of a given combination of coarse aggregate, respectively, as suggested by Omary et al. (2016).

$$Coarse_{SG} = [(Mass_{RCA} \times RCA_{SG}) + (Mass_{NC} \times NC_{SG})]/(Mass_{Rca} + Mass_{NC}) \quad (5\text{-}3)$$

$$Coarse_{Abs} = [(Mass_{RCA} \times RCA_{Abs}) + (Mass_{NC} \times NC_{Abs})]/(Mass_{Rca} + Mass_{NC}) \quad (5\text{-}4)$$

$$Coarse_{LA} = [(Mass_{RCA} \times RCA_{LA}) + (Mass_{NC} \times NC_{LA})]/(Mass_{Rca} + Mass_{NC}) \quad (5\text{-}5)$$

where $Mass_{RCA}$ is the RCA content (kg/m^3), $Mass_{NC}$ is the virgin coarse aggregate content (kg/m^3), RCA_{SG} is the oven-dry specific gravity of RCA, NC_{SG} is the oven-dry specific gravity of the virgin coarse aggregate, RCA_{Abs} is the water absorption of the RCA (%), NC_{Abs} is the virgin coarse aggregate absorption rate (%), RCA_{LA} is the mass loss due to LA abrasion of RCA (%), NC_{LA} is the mass loss due to LA abrasion of the virgin coarse aggregate (%), and $Coarse_{SG}$, $Coarse_{Ab,}$ and $Coarse_{LA}$ are the oven-dry specific gravity, water absorption rate (%), and LA abrasion (%) of the coarse aggregate combination, respectively.

Data obtained from testing concrete with different types and contents of coarse RCA were incorporated to establish correlations between the combined aggregate physical properties and compressive strength at different testing ages. Two main scenarios were investigated: (1) concrete prepared with 323 kg/m^3 of binary cement (25%

FA-C) and 0.40 w/cm; (2) concrete made with 323 kg/m^3 of ternary cement (15% GGBS+35% FA-C) and 0.37 w/cm.

Figure 5.5 presents the correlation between the LA abrasion of the combined coarse aggregate and compressive strength results obtained for the investigated concrete. Reduction in compressive strength was observed with an increase in LA abrasion value of the coarse aggregate combination. In other words, result indicate that a higher coarse RCA content, and/or the use of RCA with lower quality result in reductions in compressive strength of concrete. Values of R^2 ranged from 0.60 to 0.70 for the 28-day and 91-day results of the ternary mixtures. The slopes of the trend lines were higher in the case of the mixtures prepared with ternary cement and 0.37 w/cm, indicating that the rate of reduction in compressive strength is more sensitive to the increase in RCA content and/or the use of RCA of lower quality.

Figure 5.6 presents the correlation between the water absorption of the combined coarse aggregate and compressive strength results. Reduction in compressive strength was observed as a function of higher absorption rate of the combined coarse aggregate. Values of R^2 obtained for the linear correlation between the compressive results and the combined water absorption ranged between 0.53 and 0.66 for the ternary mixtures. Higher spread was obtained for the binary mixtures, making it difficult to develop trend lines. However, it can be stated that stronger correlations were obtained for the concrete made with ternary cement and 0.37 w/cm, while compared to the ones prepared with binary cement and 0.40 w/cm.

Figure 5.7 presents the correlations between the oven dry specific gravity of coarse aggregate combination and compressive strength at different ages. As expected, compressive strength was increased as a function of increase in specific gravity of combined coarse aggregate. In general, stronger correlations were observed for the ternary mixtures compared to the binary concrete for corresponding ages. Moreover, the trend lines for the ternary mixtures had higher slopes than the binary ones, suggesting that the increase in RCA content and/or use of lower RCA quality can have a more pronounced effect on rate of variations in compressive strength.

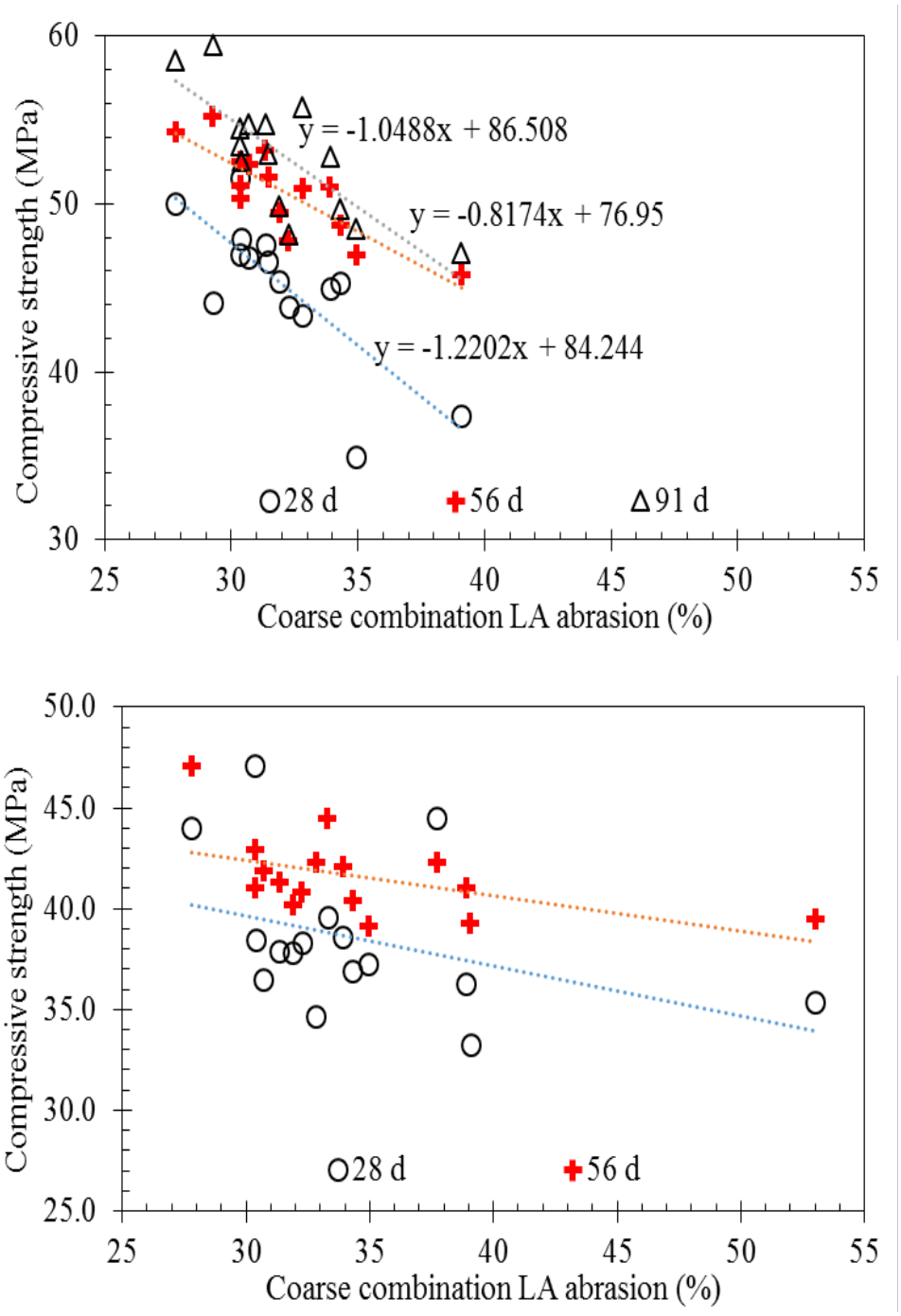

Figure 5.5 Effect of combined coarse aggregate LA abrasion on compressive strength; Top: ternary mixtures, Bot.: binary mixtures

In general, it was observed that the variations in LA abrasion and water absorption of the combined coarse aggregate can be considered as proper means of estimating the effect of coarse RCA on compressive strength of concrete. No significant

trends could be attributed to the rate of the variations in results, i.e. the slope of the trend lines, as a function of the testing age.

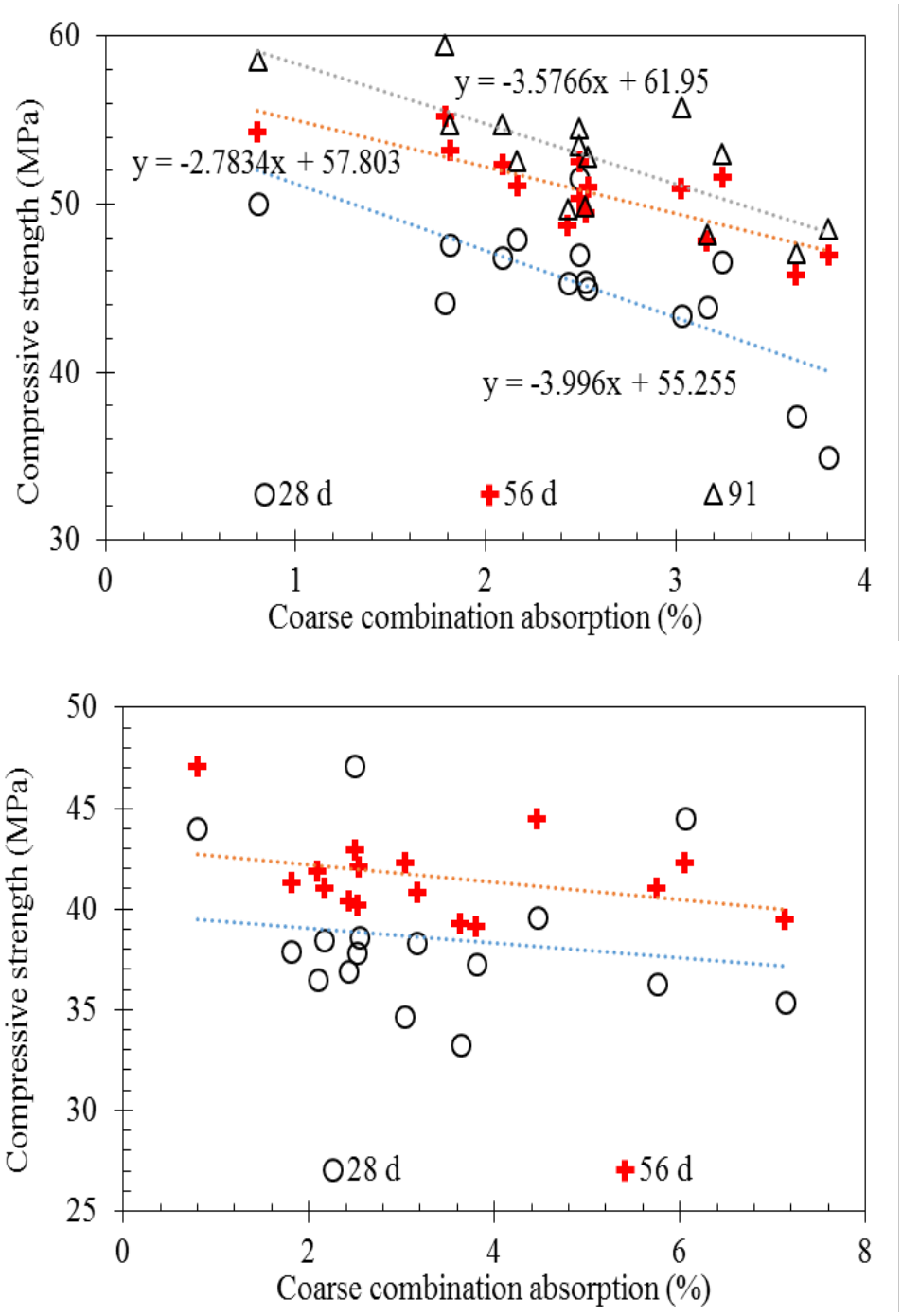

Figure 5.6 Effect of combined coarse aggregate water absorption on compressive strength; Top: ternary mixtures, Bot.: binary mixtures

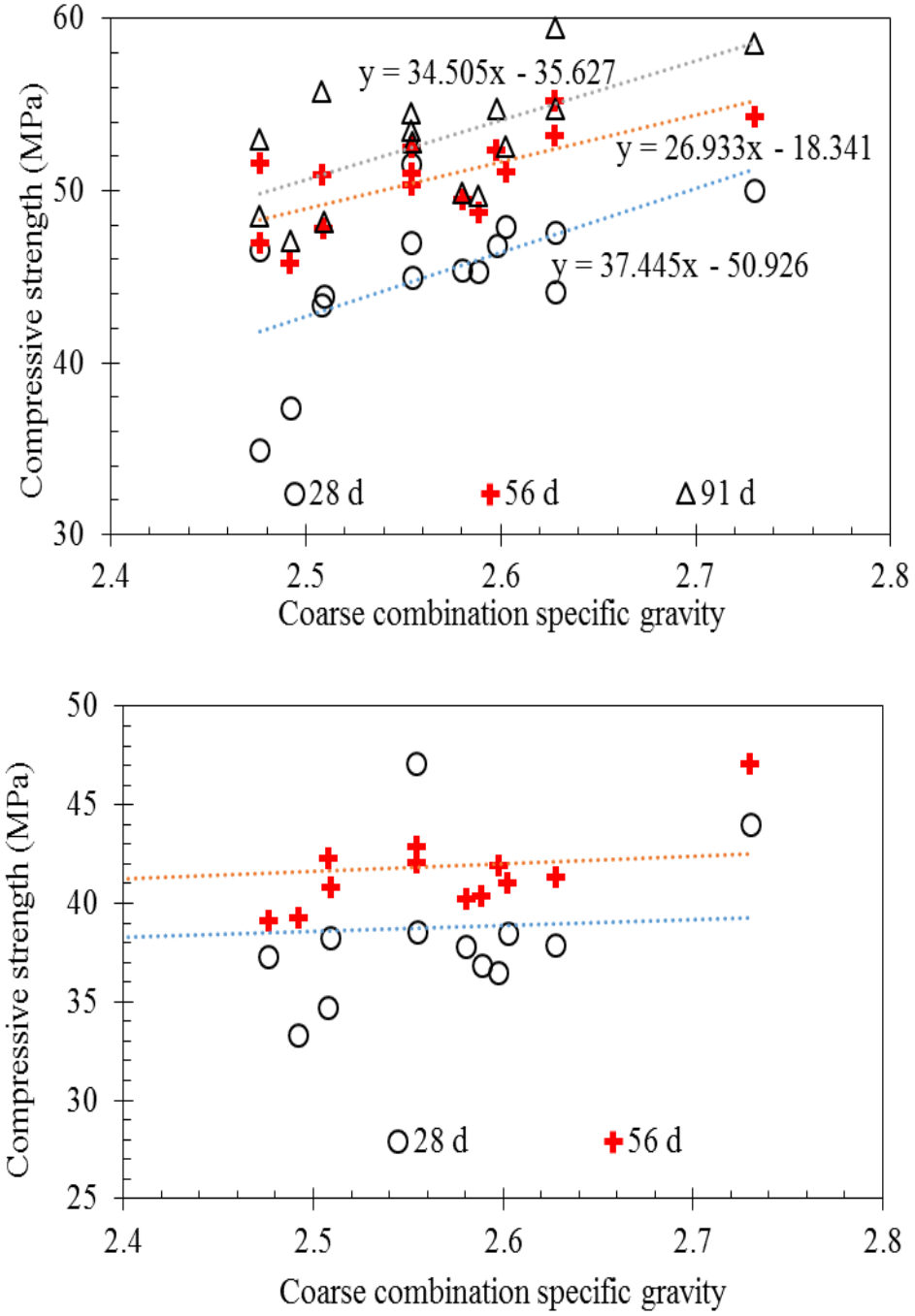

Figure 5.7 Effect of combined coarse aggregate specific gravity on compressive strength; Top: ternary mixtures, Bot.: binary mixtures

It was also concluded that the effect of RCA on mechanical properties can be better reflected in the case of concrete prepared with higher quality paste, i.e. ternary cement and reduced w/cm. in other words, the sensitivity to the use of RCA is increasing

with the quality of concrete. However, the use of high-quality binder systems and the reduction in w/cm can compensate for reduction in compressive strength due to the use of RCA. It should be noted that the evaluation of the coupled effect of the investigated factors (LA abrasion, absorption, and specific gravity) did not present any significant correlations.

Given the limits of the experimental domain are met, the results obtained in this section can be incorporated to estimate the compressive strength of concrete made with coarse RCA. For instance, contour diagrams were generated based on the 91-day results of concrete made with ternary cement and 0.37 w/cm. A hypothetical scenario was investigated for concrete made with 0.37 w/cm, ternary cement, and DOL1 coarse aggregate (LA abrasion: 28%, Absorption: 0.8%, and specific gravity: 2.73). Contour graphs were developed to illustrate the effect of RCA content (% mass) and RCA characteristics on 91-day compressive strength.

Figure 5.8 presents the effect of RCA content and LA abrasion on 91-day compressive strength of concrete made with 0.37 w/cm and ternary cement. Results indicate reduction in compressive strength with the use of higher RCA content and the use of RCA with higher LA abrasion mass loss. The use of 50% coarse RCA with LA abrasion of 35% and 45% can result in approximate compressive strength of 53.0 and 49.0 MPa, respectively, compared to values of higher than 55.0 MPa for concrete made without any RCA.

Figure 5.9 presents the effect of RCA content and water absorption on 91-day compressive strength of concrete made with 0.37 w/cm and ternary cement. Results indicate reduction in compressive strength with the use of higher RCA content and the use of RCA with higher water absorption. The use of 50% coarse RCA with water absorption of 3% and 6% can result in approximate compressive strength of 56.0 and 50.0 MPa, respectively, compared to values of about 57.5 MPa for concrete made without any RCA.

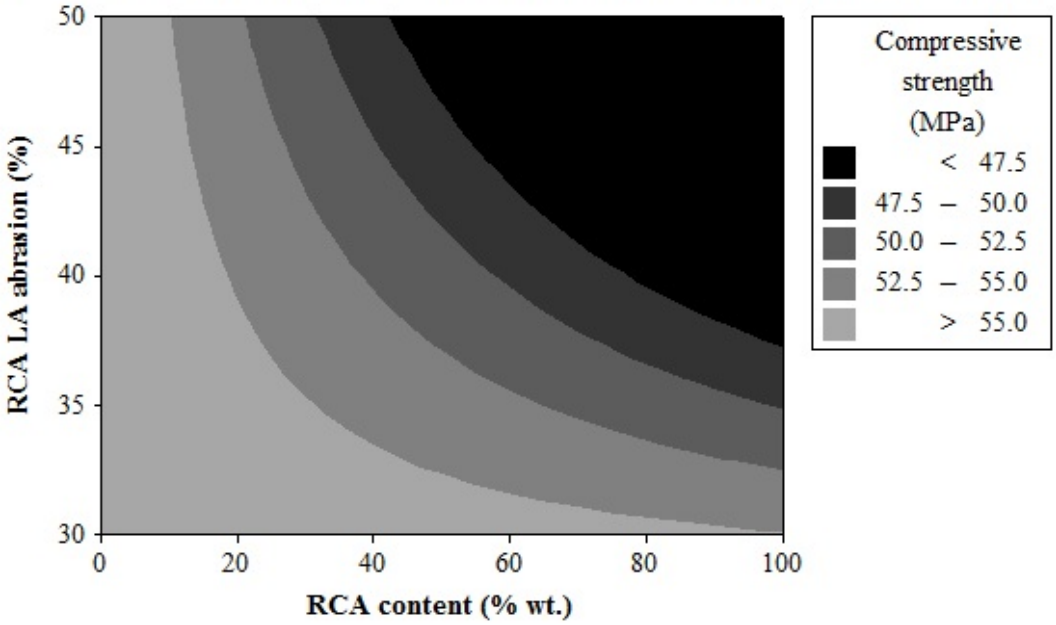

Figure 5.8 Effect of coarse RCA content and LA abrasion on 91-day compressive strength of concrete made with 0.37 w/cm and ternary cement

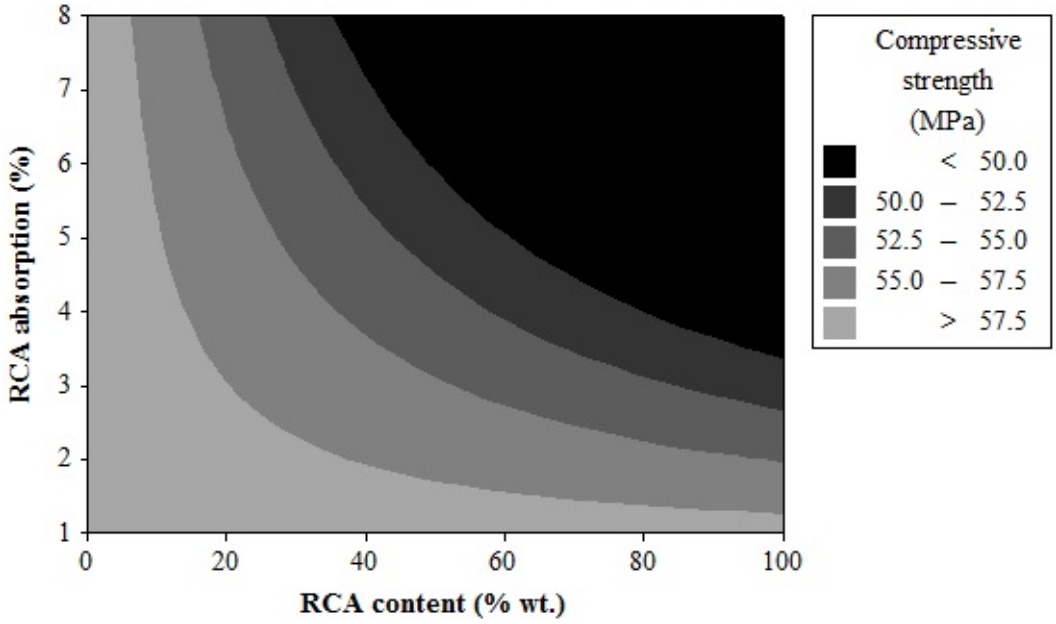

Figure 5.9 Effect of coarse RCA content and water absorption on 91-day compressive strength of concrete made with 0.37 w/cm and ternary cement

Figure 5.10 presents the effect of RCA content and oven-dry specific gravity on 91-day compressive strength of concrete made with 0.37 w/cm and ternary cement. Results indicate reduction in compressive strength with the use of higher RCA content and the use of RCA with lower specific gravity. The use of 50% coarse RCA with oven-dry specific gravity of 2.20 and 2.50 can result in approximate compressive strength of 50.0 and 55.0 MPa, respectively, compared to values of about 57.5 MPa for concrete made without any RCA.

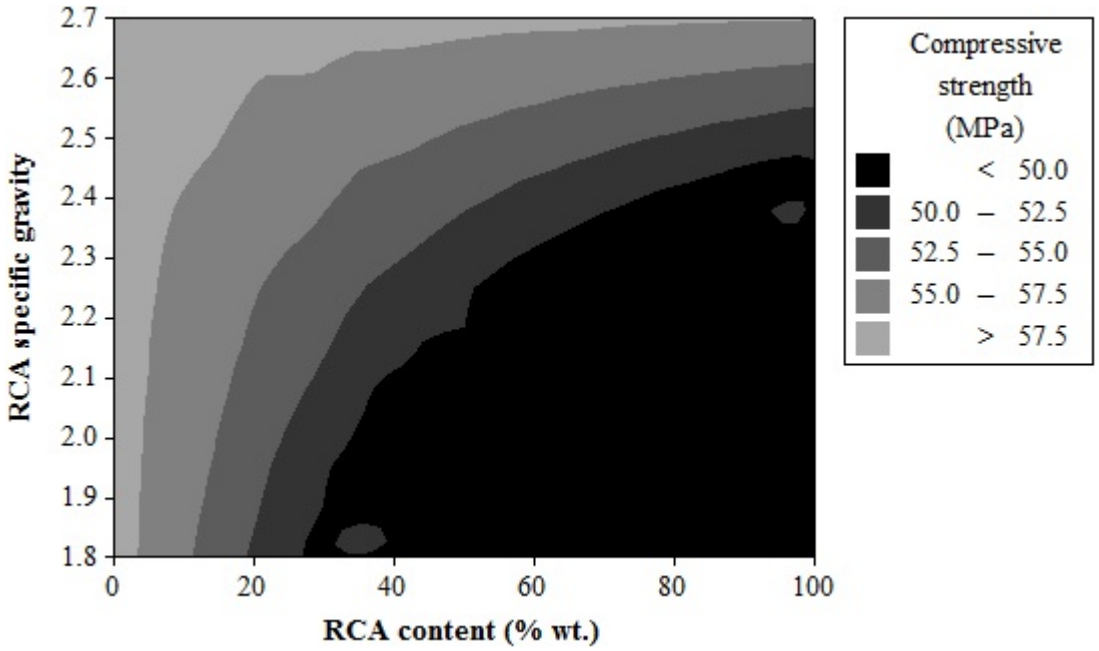

Figure 5.10 Effect of coarse RCA content and oven-dry specific gravity on 91-day compressive strength of concrete made with 0.37 w/cm and ternary cement

5.3.2. Splitting Tensile Strength.

5.3.2.1 Effect of mixture parameters and fine RCA. The splitting tensile strength results of concrete investigated in Group I are summarized in Table 5.7. The reference concrete prepared with binary cement, 0.40 w/cm, and 100% dolomitic aggregate exhibited 7-day splitting tensile strength of 2.34 MPa. The use of ternary cement in concrete made with 0.40 w/cm slightly reduced the 7-day splitting tensile strength to 2.21 MPa. The maximum 7-day splitting tensile strength of 2.79 MPa was observed in the case of the mixture prepared with ternary cement, 0.37 w/cm and without

any RCA. The incorporation of the fine RCA1 did not have a significant effect on splitting tensile strength of the mixtures prepared with 50% or 70% coarse RCA, 0.40 w/cm, and ternary cement. For instance, the 56-day splitting tensile strength results of the concrete made with 50% coarse RCA1 and 0, 15%, 30%, and 40% fine RCA1 were 2.55, 2.76, 2.90, 2.52 MPa, respectively. In general, results presented in Table 1 indicate that the reduction in w/cm from 0.40 to 0.37 was effective in enhancing the splitting tensile strength of concrete prepared with fine and/or coarse RCA.

Table 5.7 Splitting tensile strength results of concrete made with different contents of coarse RCA1 and fine RCA1 (Group I) (MPa)

Mixture	7 days	28 days	56 days
DOL1-B-40	2.34	3.17	3.45
DOL1-T-37	2.79	4.27	4.32
DOL1-T-40	2.21	2.76	3.21
RCA1-30-T-37	1.69	3.34	3.34
RCA1-30-T-40	2.45	2.55	3.45
RCA1-30-T-37-15F	2.10	3.00	3.14
RCA1-30-T-40-15F	2.07	2.65	3.34
RCA1-40-T-40-15F	2.21	2.45	3.10
RCA1-50-T-37	2.45	2.96	2.90
RCA1-50-T-40	2.21	2.90	2.55
RCA1-50-T-37-15F	1.90	2.79	2.90
RCA1-50-T-40-15F	2.07	2.69	2.76
RCA1-50-T-40-30F	1.97	3.10	2.90
RCA1-50-T-40-40F	1.86	2.21	2.52
RCA1-60-T-40-30F	2.00	2.41	2.31
RCA1-70-T-37	1.86	3.00	3.00
RCA1-70-T-40	1.34	2.10	2.62
RCA1-70-T-40-15F	1.55	2.90	2.69
RCA1-70-T-40-30F	1.76	2.90	2.86
RCA1-30-GGF15-37	2.45	2.69	3.03

Splitting tensile strength results obtained from testing the concrete mixtures investigated in Group II also indicate comparable performance of investigated mixtures with that of the reference concrete prepared with 100% limestone coarse aggregate and river sand (Table 5.8). The reference concrete with 0.40 w/cm, 25% FA-C, and without any RCA, exhibited 28- and 56-day splitting tensile strength of 3.50 and 3.85 MPa, respectively. The use of 30% coarse RCA2 slightly reduced the 28- and 56-day splitting tensile strength to 3.25 and 3.60 MPa, respectively. Incorporation of 15% fine RCA in this mixture reduced the 56-day splitting tensile strength from 3.60 to 3.50 MPa. The reduction in w/cm to 0.37 was effective in enhancing the splitting tensile strength. The maximum 56-day splitting tensile strength of 4.05 MPa was observed for the concrete made with 40% FA-C, 20% fine RCA, and 0.37 w/cm.

Table 5.8 Splitting tensile strength results of concrete made with different contents of coarse RCA2 and fine RCA2 (Group II) (MPa)

Age	LIM-B-40	C35-F0-40	C35-F15-37	C40-F20-37	C35-F10-42	C25-F15-40	C25-F10-37	C25-F0-40
7 d	2.65	2.80	2.70	2.75	2.80	2.50	3.15	2.70
28 d	3.50	3.30	3.60	3.50	3.70	3.60	3.45	3.25
56 d	3.85	3.85	3.40	4.05	3.30	3.50	3.50	3.60

5.3.2.2 Effect of coarse RCA content. Figure 5.11 presents the variations in splitting tensile strength of concrete made with up to 70% coarse RCA1, prepared with ternary cement and 0.37 and 0.40 w/c. In general, a tendency to decrease in splitting tensile strength can be detected for concrete with higher coarse RCA content. For instance, the use of 70% coarse RCA1 reduced the 56-day tensile strength from 3.21 to 2.62 and from 4.32 to 3.00, corresponding to 18% and 31% reduction for concrete with 0.40 and 0.37 w/cm, respectively.

Similar trends were obtained for the mixtures prepared with up to 100% coarse RCA from different sources investigated in Group III. Results indicated decreasing trend for splitting tensile strength as a function of coarse RCA incorporation. Results presented

in Figure 5.12 indicate up to 33% reduction in 56-day splitting tensile strength of concrete made with 0.37 w/cm and ternary cement. Splitting tensile strength results obtained for concrete made with 0.40 w/cm and binary cement are presented in Figure 5.13. Trend were similar to the previous observations, where up to 20% reduction in 56-day tensile strength was observed due to the use of 100% coarse RCA in such concrete.

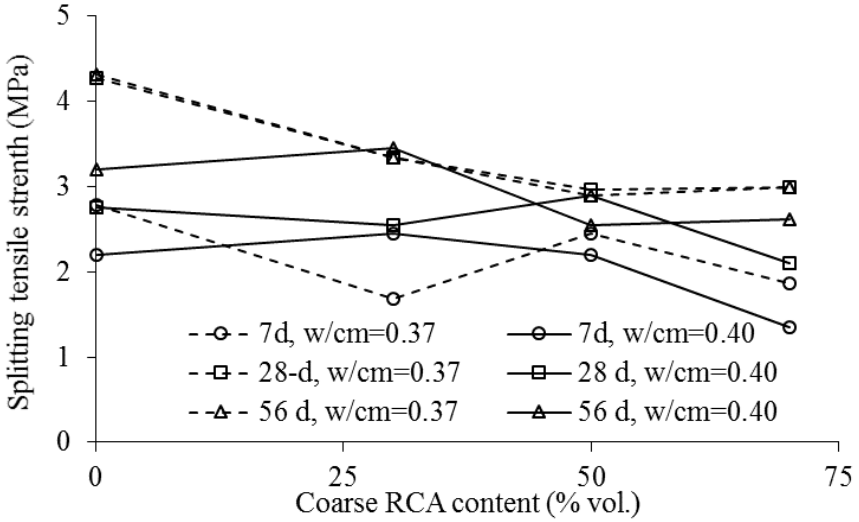

Figure 5.11 Effect of coarse RCA2 content on splitting tensile strength

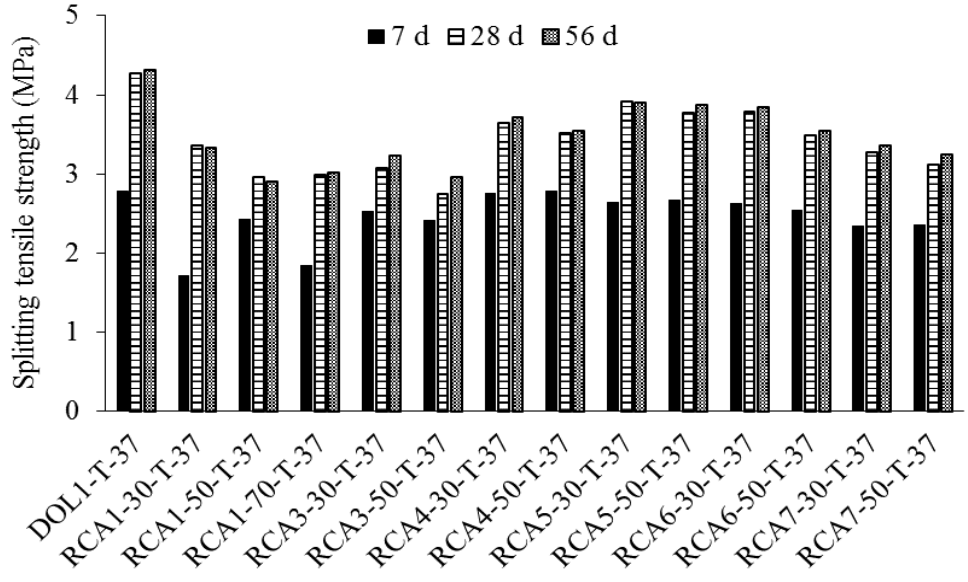

Figure 5.12 Effect of coarse RCA on splitting tensile strength of concrete made with ternary cement and 0.37 w/cm

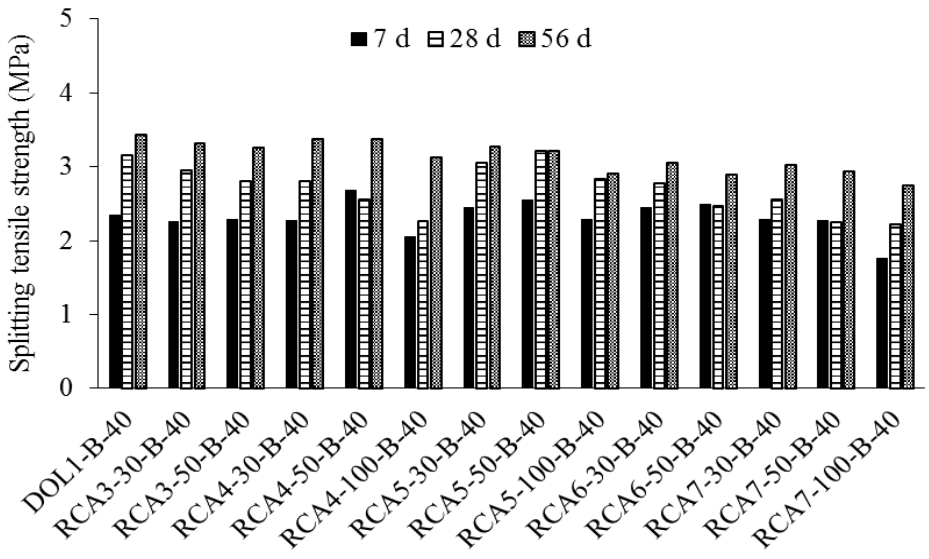

Figure 5.13 Effect of coarse RCA on splitting tensile strength of concrete made with binary cement and 0.40 w/cm

5.3.2.3 Effect of coarse RCA properties. Data obtained from testing concrete with different types and contents of coarse RCA were incorporated to establish correlations between the combined aggregate physical properties and splitting tensile strength at different testing ages. Two main scenarios were investigated: (1) concrete prepared with 323 kg/m^3 of binary cement (25% FA-C) and 0.40 w/cm; (2) concrete made with 323 kg/m^3 of ternary cement (15% GGBS+35% FA-C) and 0.37 w/cm.

Figure 5.14 presents the correlation between the water absorption of the combined coarse aggregate and splitting tensile strength results. Reduction in splitting tensile strength was observed as a function of higher absorption rate of the combined coarse aggregate. Values of R^2 obtained for the linear correlation between the compressive results and the combined water absorption ranged between 0.34 and 0.59 for the mixtures prepared with binary cement. Higher spread was obtained for the ternary mixtures, making it difficult to develop trend lines. However, it can be stated that stronger correlations were obtained for the concrete made with binary cement and 0.40 w/cm, while compared to the ones prepared with ternary cement and 0.37 w/cm.

Figure 5.15 presents the correlations between the oven dry specific gravity of coarse aggregate combination and slitting tensile strength at different ages. As expected,

tensile strength was enhanced as a function of increase in specific gravity of combined coarse aggregate.

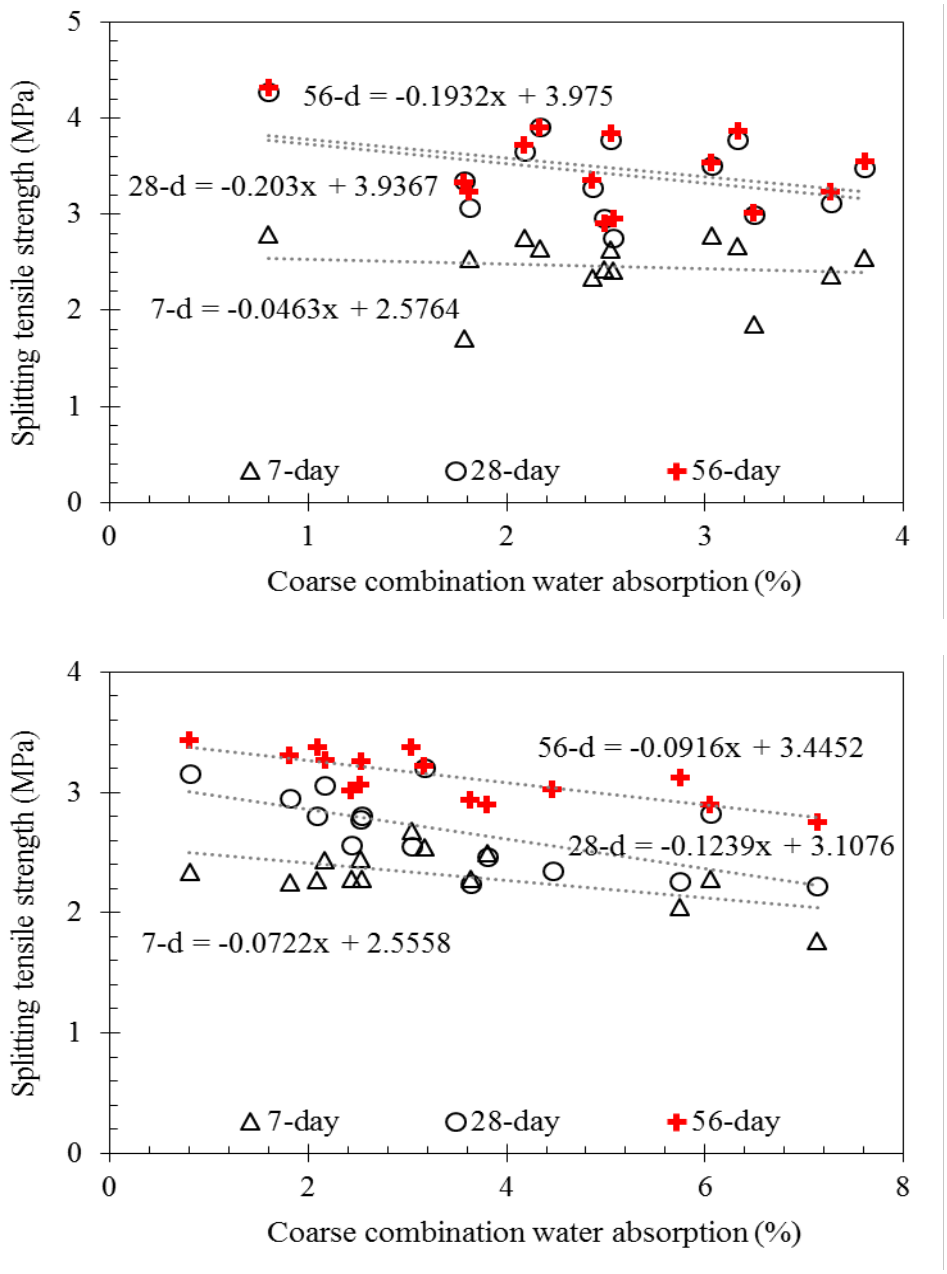

Figure 5.14 Effect of combined coarse aggregate water absorption on splitting tensile strength; Top: ternary mixtures, Bot.: binary mixtures

Similar to the previous observations, stronger correlations were observed for the binary mixtures compared to the concrete made with ternary cement for all corresponding

ages. The trend lines for the ternary mixtures had higher slopes than the binary ones, suggesting that the concrete prepared with ternary cement can be more sensitive to the increase in RCA content and/or use of RCA with lower quality.

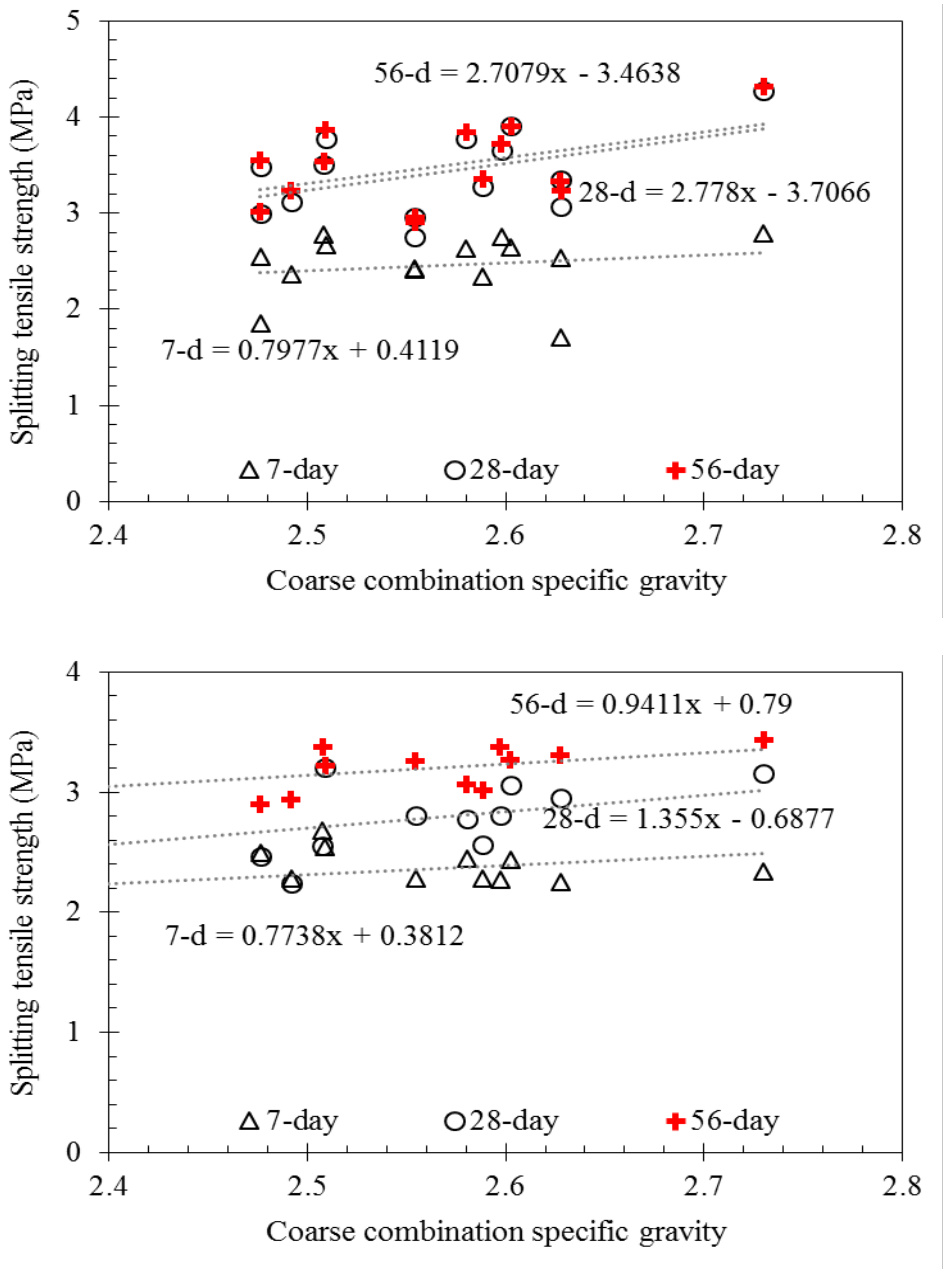

Figure 5.15 Effect of combined coarse aggregate specific gravity on splitting tensile strength; Top: ternary mixtures, Bot.: binary mixtures

Figure 5.16 presents the correlation between the LA abrasion of the combined coarse aggregate and splitting tensile strength results obtained for the investigated concrete. Reduction in tesile strength was observed with an increase in LA abrasion value of the coarse aggregate combination. In other words, result indicate that a higher coarse RCA content, and/or the use of RCA with lower quality result in reductions in compressive strength of concrete.

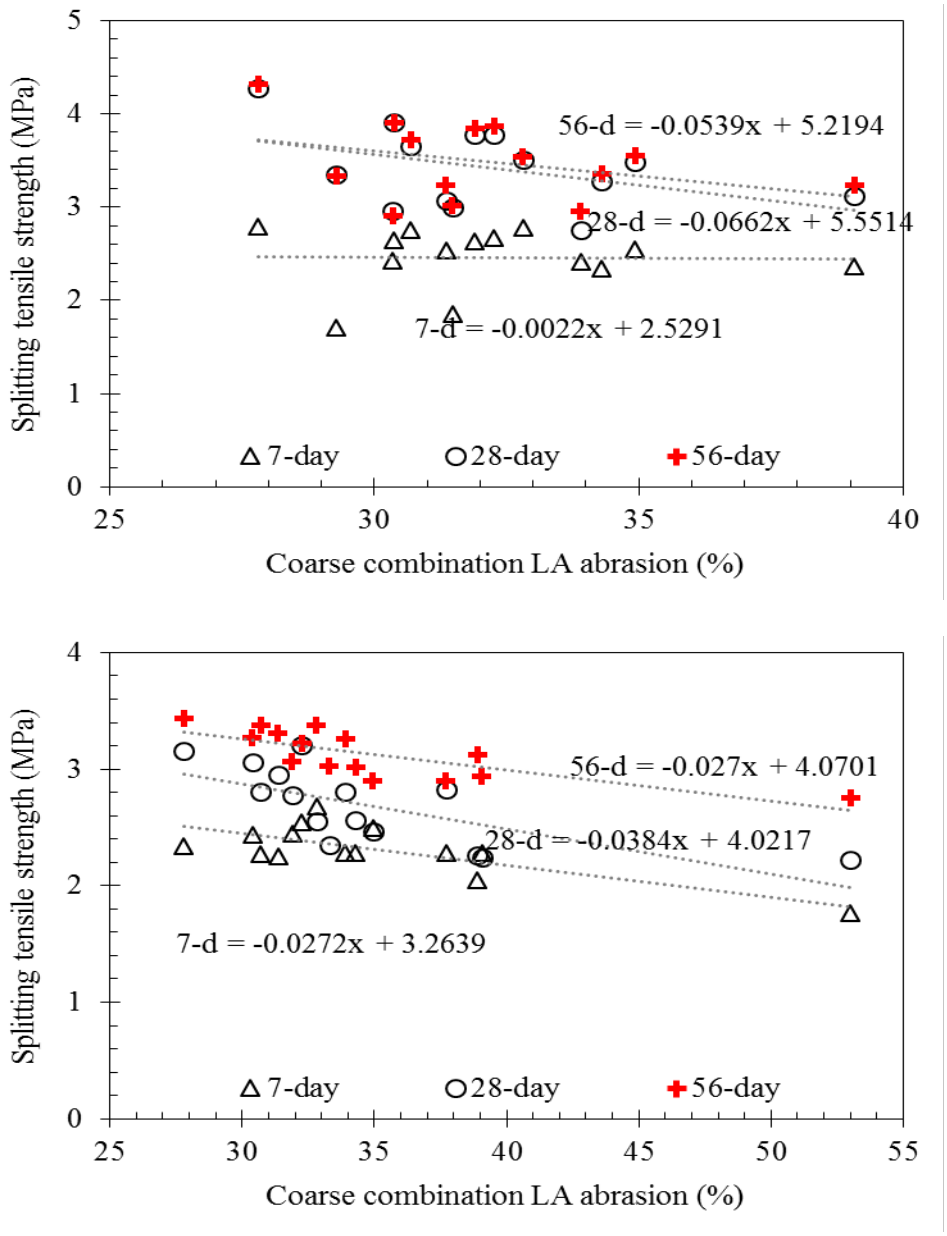

Figure 5.16 Effect of combined coarse aggregate LA abrasion on splitting tensile strength; Top: ternary mixtures, Bot.: binary mixtures

Values of R^2 ranged from 0.47 to 0.59 for different testing ages of the mixtures prepared with binary cement. The slopes of the trend lines were higher in the case of the mixtures prepared with ternary cement and 0.37 w/cm, indicating that the rate of reduction in compressive strength is more sensitive to the increase in RCA content and/or the use of RCA of lower quality.

In general, it was observed that the variations in LA abrasion and water absorption of the combined coarse aggregate can be considered as proper means of estimating the effect of coarse RCA on splitting strength of concrete. No significant trends could be attributed to the rate of the variations in results, i.e. the slope of the trend lines, as a function of the testing age. It should be noted that the evaluation of the coupled effect of the investigated factors (LA abrasion, absorption, and specific gravity) did not present any significant correlations.

Similar to the previous results, and given the limits of the experimental domain are met, the results obtained in this section can be incorporated to estimate the splitting tensile strength of concrete made with coarse RCA. For instance, contour diagrams were generated based on the 28-day results of concrete made with binary cement and 0.40 w/cm. A hypothetical scenario was investigated for concrete made with DOL1 coarse aggregate (LA abrasion: 28%, Absorption: 0.8%, and specific gravity: 2.73). Contour graphs were developed to illustrate the effect of RCA content (% mass) and RCA characteristics on 28-day flexural strength.

Figure 5.17 presents the effect of RCA content and LA abrasion on 56-day splitting tensile strength of such concrete, made with 0.40 w/cm and binary cement. Results indicate reduction in tensile strength with the use of higher RCA content and the use of RCA with higher LA abrasion mass loss. The use of 50% coarse RCA with LA abrasion of 40% and 50% can result in approximate splitting tensile strength of 3.15 and 3.0 MPa, respectively, compared to values of higher than 3.3 MPa for concrete made without any RCA.

Figure 5.18 presents the effect of RCA content and water absorption on 91-day splitting tensile strength of concrete made with 0.40 w/cm and binary cement. Results indicate reduction in tensile strength with the use of higher RCA content and the use of RCA with higher water absorption. The use of 50% coarse RCA with water absorption of

3% and 7% can result in approximate splitting tensile strength of 3.25 and 3.1 MPa, respectively, compared to values of about 3.3 MPa for concrete made without any RCA.

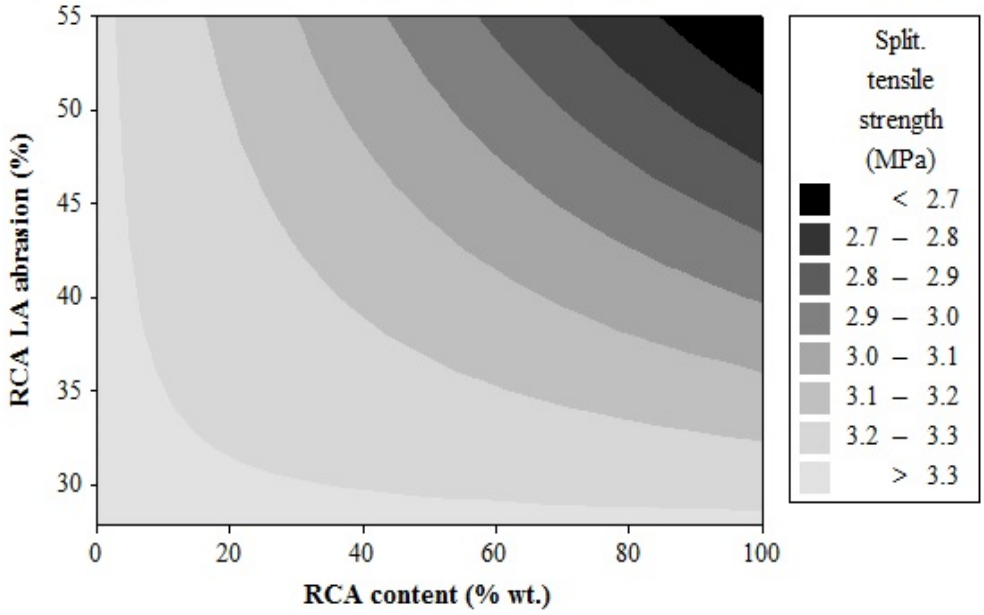

Figure 5.17 Effect of coarse RCA content and LA abrasion on 56-day splitting tensile strength of concrete made with 0.40 w/cm and binary cement

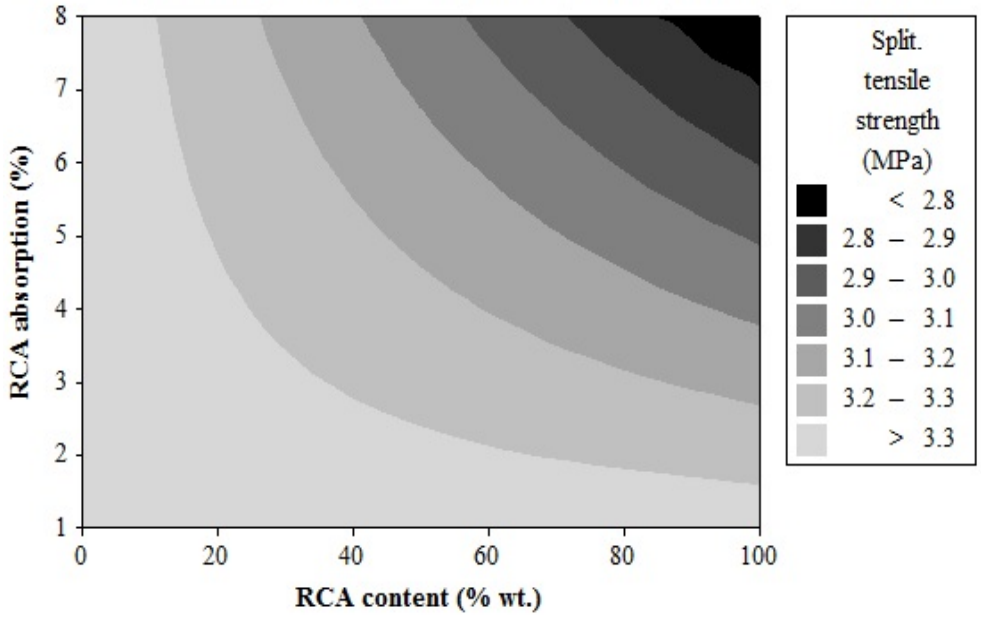

Figure 5.18 Effect of coarse RCA content and water absorption on 56-day splitting tensile strength of concrete made with 0.40 w/cm and binary cement

Figure 5.19 presents the effect of RCA content and oven-dry specific gravity on 56-day splitting tensile strength of concrete made with 0.40 w/cm and binary cement. Results indicate reduction in tensile strength with the use of higher RCA content and the use of RCA with lower specific gravity. The use of 50% coarse RCA with oven-dry specific gravity of 1.80 and 2.40 can result in approximate compressive strength of 2.95 and 3.2 MPa, respectively, compared to values of higher than 3.3 MPa for concrete made without any RCA.

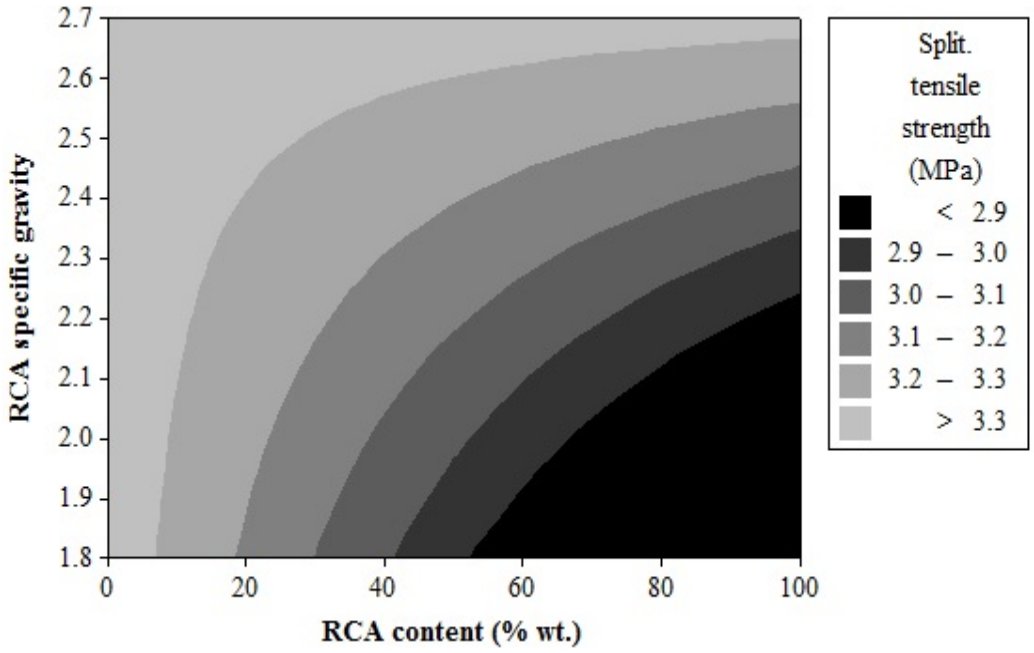

Figure 5.19 Effect of coarse RCA content and specific gravity on 56-day splitting tensile strength of concrete made with 0.40 w/cm and binary cement

5.3.3. Flexural Strength.

5.3.3.1 Effect of mixture parameters and fine RCA. Table 5.9 summarizes the flexural strength results obtained for concrete investigated in Group I, prepared with different amounts of coarse RCA1 and fine RCA1. Reduction in 28-day flexural strength from 5.22 to 4.48 MPa was observed with the use of ternary cement in concrete prepared with 0.40 w/cm and without any RCA. This is believed to be due to the high amount of SCM replacement in the ternary binder which resulted in initial drops in strength at early age measurements. With the increase in curing period to 56 days, the flexural strength of

the samples cast with optimized binder increased to 5.27 MPa in comparison to 5.61 MPa for the MoDOT reference mixture prepared with binary cement. No significant difference in flexural strength of the MoDOT reference specimen was observed with increasing the curing period from 28 to 56 days. Reducing the w/cm from 0.37 to 0.40 in concrete made with ternary cement and 100% virgin aggregate was effective in enhancing the flexural strength for both 28 and 56-day measurements. The highest values of flexural strength, 6.32 and 6.65 MPa at 28 and 56 days, respectively, were observed for the concrete made with 0.37 w/cm and ternary cement.

All mixtures exhibited flexural strength of higher than 4.0 MPa at 28 days, except for the RCA1-70-T-40-15F mixture (3.76 MPa). It was generally observed that the use of fine RCA tends to reduce the flexural strength. For instance, in the case of the mixture prepared with 50% coarse RCA2, 0.40 w/cm, and ternary binder, the use of 15%, 30%, and 40% fine RCA resulted in reduction in 56-day flexural strength from 5.27 to 5.03, 4.96, and 4.38 MPa, respectively. The reduction in w/cm from 0.40 to 0.37 was effective in controlling the negative impact of fine RCA of flexural strength for concrete made with 30% or 50% coarse RCA2 and ternary cement. No reduction in flexural strength due to 15% fine RCA incorporation was observed for such mixtures.

In general, it was observed that the reduction in w/cm and the use of ternary cement were effective in developing concrete with proper flexural strength in spite of the use of RCA. However, the reduction in flexural strength due to the use of fine RCA can cause concerns regarding the performance of such concrete for rigid pavement construction.

Similar results were obtained for concrete investigated in Group II, made with different mounts of fine RCA1 and up to 30% coarse RCA 1, presented in Table 5.10. Even though the use of fine and/or coarse RCA tends to reduce the flexural strength, the reduction in w/cm and the use of 35% or 40% FA-C were effective in securing proper flexural strength. For instance, the concrete made with 30% coarse RCA1, 10% fine RCA1, 25% FA-C, and 0.37 w/cm exhibited 56-day flexural strength of 5.85 MPa compared to 5.50 MPa for the reference concrete made without any RCA. The use of 35% FA-C and 0.37 w/cm also resulted in 56-day flexural strength of 5.55 MPa which

was similar to that of the reference concrete prepared with 0.40 w/cm, 25% FA-C, and without any RCA.

Table 5.9 Flexural strength results of concrete made with different contents of coarse RCA1 and fine RCA1 (Group I) (MPa)

Mixture	28 days	56 days
DOL1-B-40	5.22	5.61
DOL1-T-37	6.32	6.65
DOL1-T-40	4.48	5.27
RCA1-30-T-37	5.58	5.38
RCA1-30-T-40	4.83	4.93
RCA1-30-T-37-15F	5.14	5.24
RCA1-30-T-40-15F	4.52	4.34
RCA1-40-T-40-15F	4.17	4.90
RCA1-50-T-37	5.03	5.17
RCA1-50-T-40	4.93	5.27
RCA1-50-T-37-15F	4.93	5.10
RCA1-50-T-40-15F	4.14	5.03
RCA1-50-T-40-30F	4.31	4.96
RCA1-50-T-40-40F	4.65	4.38
RCA1-60-T-40-30F	4.65	4.21
RCA1-70-T-37	5.00	5.21
RCA1-70-T-40	4.41	4.76
RCA1-70-T-40-15F	3.76	4.00
RCA1-70-T-40-30F	4.72	5.00
RCA1-30-GGF15-37	5.17	6.31

Table 5.10 Flexural strength results of concrete made with different contents of coarse RCA2 and fine RCA2 (Group II) (MPa)

Age	LIM-B-40	C35-F0-40	C35-F15-37	C40-F20-37	C35-F10-42	C25-F15-40	C25-F10-37	C25-F0-40
28 d	4.50	4.20	5.55	4.60	4.15	4.70	5.90	4.40
56 d	5.50	4.65	5.55	5.00	4.40	4.85	5.85	5.20

5.3.3.2 Effect of coarse RCA content. Results suggest the fact that the greater coarse RCA content can result in reduced flexural strength. The use of 70% coarse RCA1 in concrete made with 0.40 w/cm and ternary cement reduced the flexural strength from 5.22 to 4.41 MPa and from 5.61 to 4.76 MPa at 28 and 56 days, respectively. This corresponds to about 15% reduction in flexural strength due to 70% coarse RCA 1 incorporation. Trends were similar for the concrete made with 0.37 w/cm and ternary cement. The use of 70% coarse RCA1 in such mixtures reduced the 56-day flexural strength from 6.65 to 5.21 MPa, corresponding to 22% reduction.

Figure 5.20 presents the variations in flexural strength of concrete made with 30% and 50% coarse RCA from different sources on flexural strength of concrete made with ternary cement and 0.37 w/cm, investigated in Group III. A decreasing trend in flexural strength can be observed as a function of RCA incorporation. Similar results were obtained for concrete made with 0 to 100% of coarse RCA from different sources, proportioned with binary cement and 0.40 w/cm, as presented in Figure 5.21. The use of 50% coarse RCA in mixtures made with ternary cement and 0.37 w/cm resulted to up to 22% reduction in 56-day flexural strength. In the case of the mixtures made with binary cement and 0.40 w/cm, the use of 50% and 100% coarse RCA reduced the 56-day flexural strength by up to 23%.

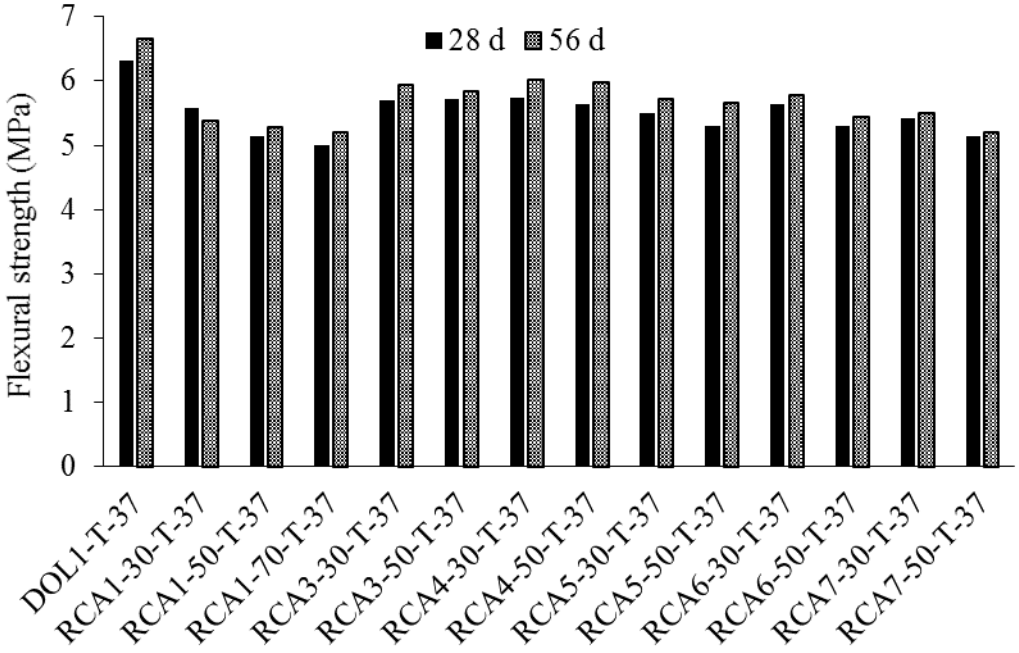

Figure 5.20 Effect of coarse RCA on flexural strength of concrete made with ternary cement and 0.37 w/cm

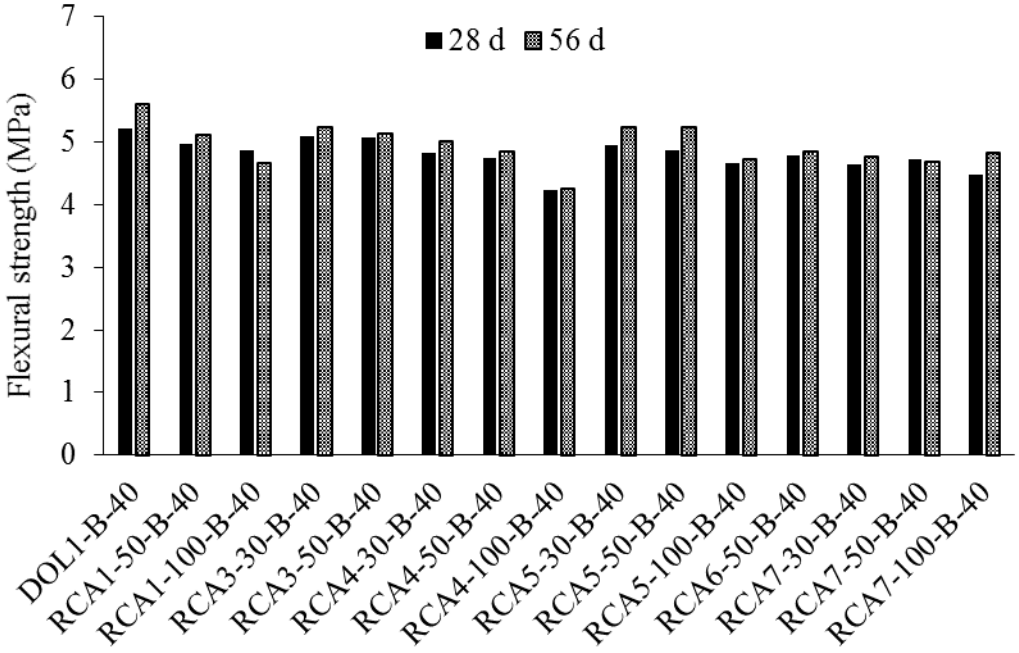

Figure 5.21 Effect of coarse RCA on flexural strength of concrete made with binary cement and 0.40 w/cm

5.3.3.3 Effect of coarse RCA properties. Data obtained from testing concrete with different types and contents of coarse RCA were incorporated to establish correlations between the combined aggregate physical properties and flexural strength at different testing ages. Two main scenarios were investigated: (1) concrete prepared with 323 kg/m^3 of binary cement (25% FA-C) and 0.40 w/cm; (2) concrete made with 323 kg/m^3 of ternary cement (15% GGBS+35% FA-C) and 0.37 w/cm.

Figure 5.22 presents the correlation between the water absorption of the combined coarse aggregate and flexural strength results. Reduction in flexural strength was observed as a result of higher absorption rate of the combined coarse aggregate. In other words, results indicate that the use of greater RCA content, and/or the use of RCA with lower quality (i.e. higher absorption) result in reductions in flexural strength. The higher slope of the trend lines obtained for the concrete made with ternary cement, indicate the increase in sensitivity of the results to RCA incorporation while compared to the mixtures made with binary cement.

Figure 5.23 presents the correlations between the flexural strength and oven dry specific gravity of the combined coarse aggregate. It was observed that the increase in specific gravity of the combined coarse aggregate affects the flexural strength, significantly. Similar to previous observations, and comparing the slope of the trend lines, it was noticed that the concrete prepared with higher paste quality (i.e. lower w/cm and ternary cement) was more sensitive to use of RCA.

Figure 5.24 presents the correlation between the LA abrasion of the combined coarse aggregate and flexural strength results obtained for the investigated concrete. Reduction in flexural strength was observed with an increase in LA abrasion value of the coarse aggregate combination. Values of R^2 ranged from 0.60 to 0.70 for the 28-day and 91-day results of the ternary mixtures. Similar to previous observations, slopes of the trend lines were higher in the case of the mixtures prepared with ternary cement and 0.37 w/cm, indicating that the increase in RCA content and/or the use of RCA of lower quality can have a stronger impact on flexural strength of concrete with higher quality.

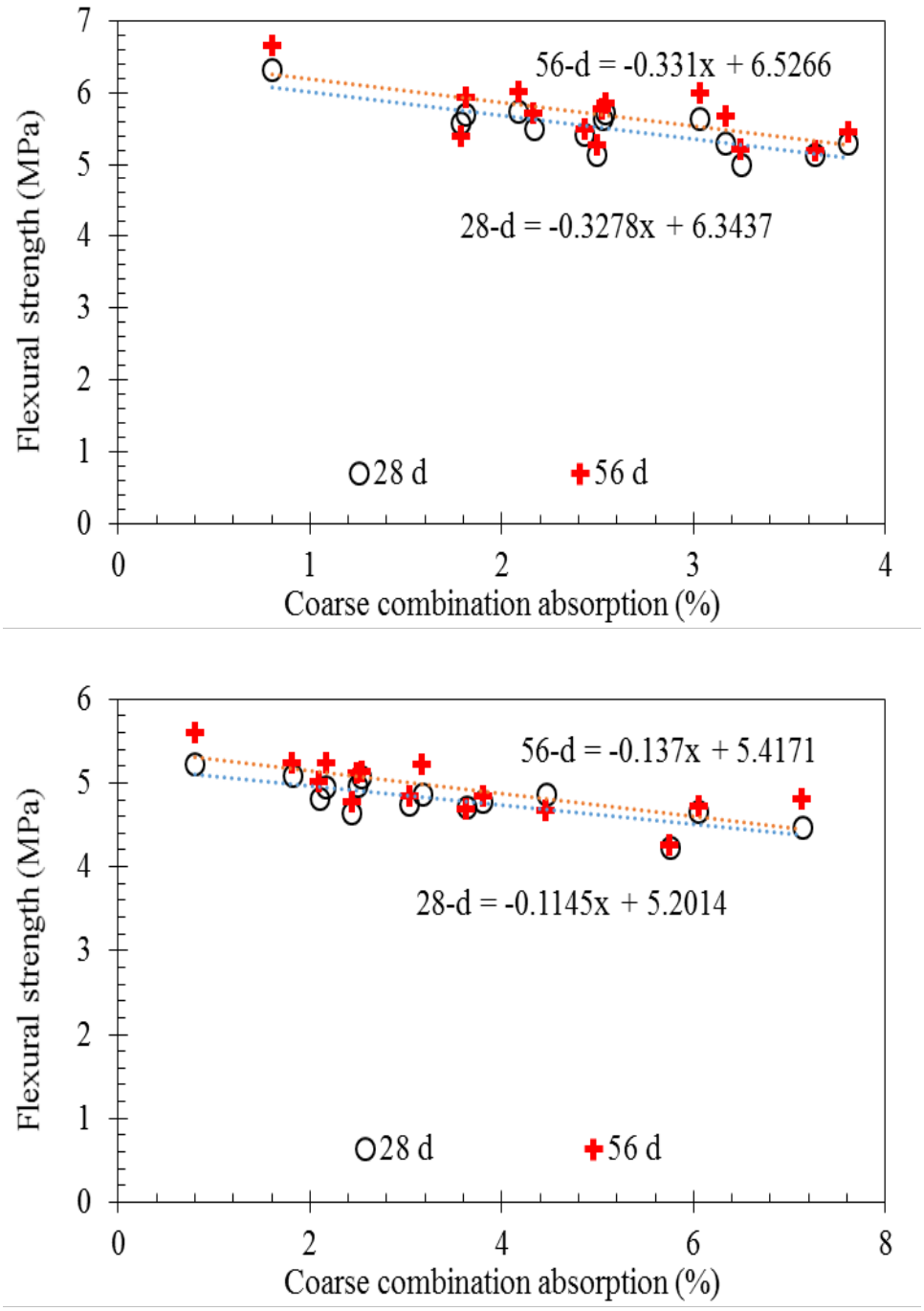

Figure 5.22 Effect of combined coarse aggregate water absorption on flexural strength; Top: ternary mixtures, Bot.: binary mixtures

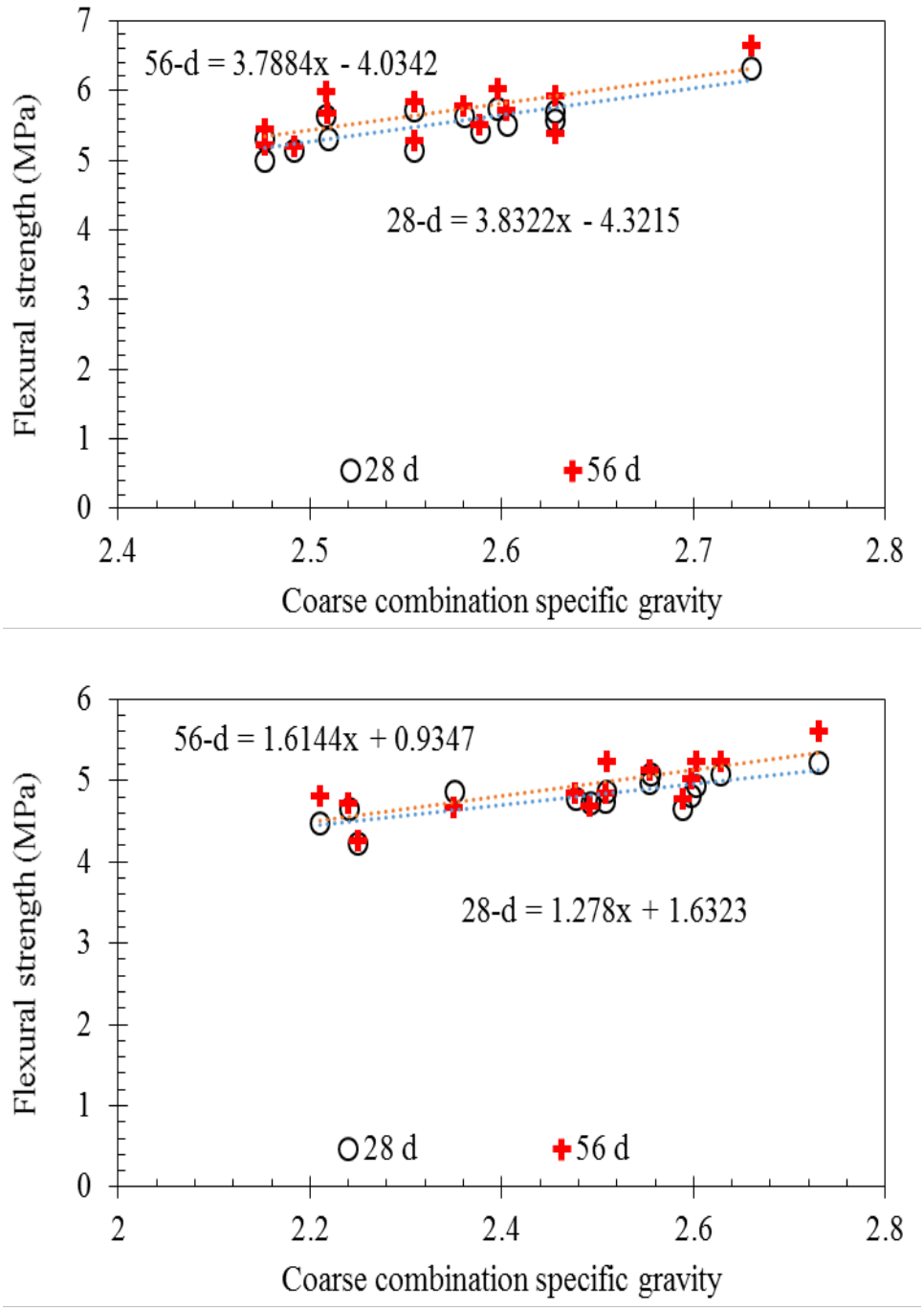

Figure 5.23 Effect of combined coarse aggregate specific gravity on flexural strength; Top: ternary mixtures, Bot.: binary mixtures

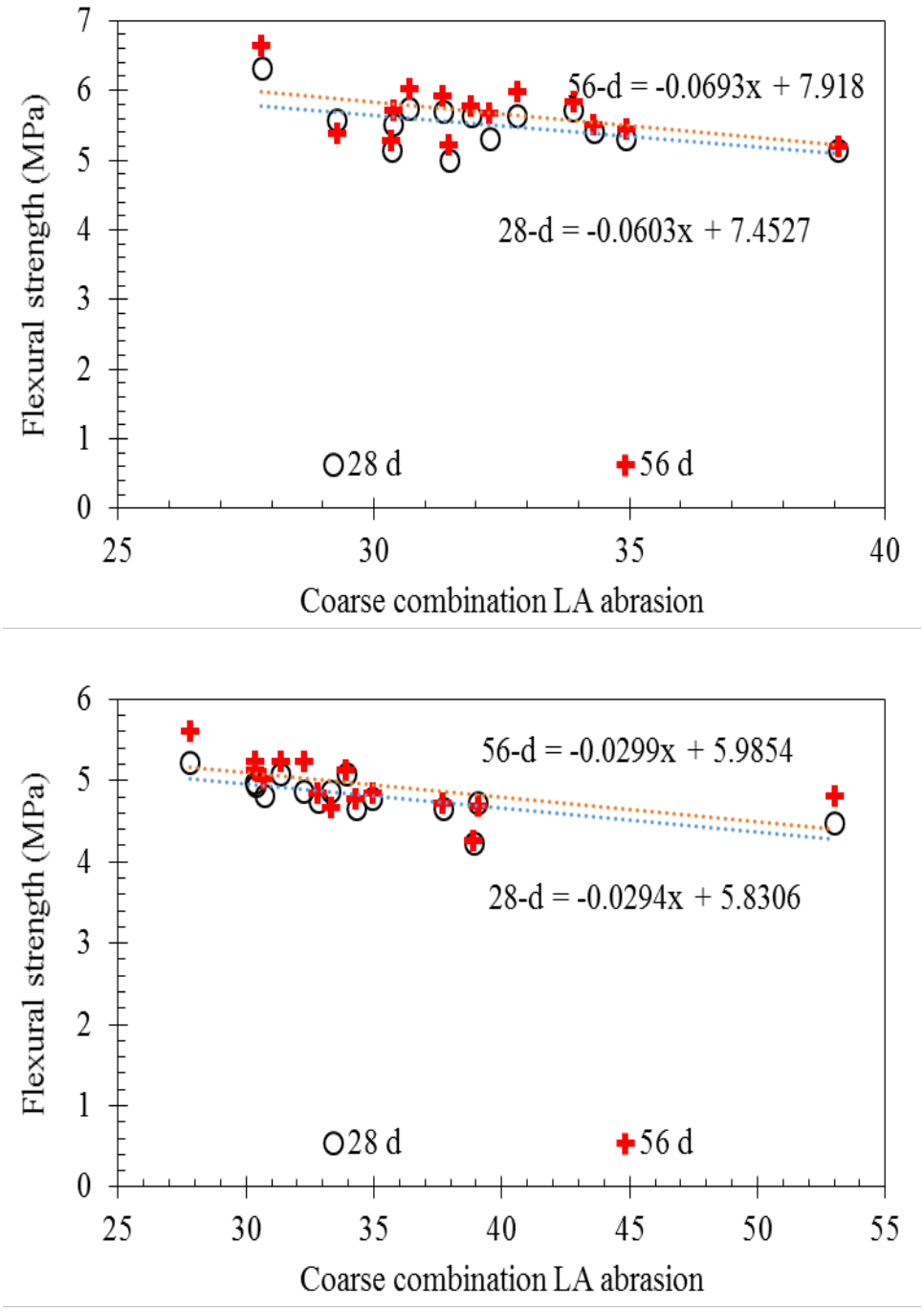

Figure 5.24 Effect of combined coarse aggregate LA abrasion on flexural strength; Top: ternary mixtures, Bot.: binary mixtures

In general, it was observed that the variations in water absorption and specific gravity of the combined coarse aggregate can be considered as proper means of estimating the effect of coarse RCA on flexural strength of concrete. Slight increase in

slope of the trend lines was observed as a result of testing age. It was also concluded that the effect of RCA on flexural strength was more highlighted in the case of concrete prepared with higher quality paste, i.e. ternary cement and reduced w/cm. In other words, the sensitivity to the use of RCA is increasing with the quality of concrete. However, the use of high-quality binder systems and the reduction in w/cm can compensate for reduction in flexural strength due to the use of RCA.

Similar to the previous results, and given the limits of the experimental domain are met, the results obtained in this section can be incorporated to estimate the flexural strength of concrete made with coarse RCA. For instance, contour diagrams were generated based on the 28-day results of concrete made with binary cement and 0.40 w/cm. A hypothetical scenario was investigated for concrete made with DOL1 coarse aggregate (LA abrasion: 28%, Absorption: 0.8%, and specific gravity: 2.73). Contour graphs were developed to illustrate the effect of RCA content (% mass) and RCA characteristics on 28-day flexural strength.

Figure 5.25 presents the effect of RCA content and LA abrasion on 28-day flexural strength of such concrete, made with 0.40 w/cm and binary cement. Results indicate reduction in flexural strength with the use of higher RCA content and the use of RCA with higher LA abrasion mass loss. The use of 50% coarse RCA with LA abrasion of 40% and 50% can result in approximate flexural strength of 4.85 and 4.70 MPa, respectively, compared to values of higher than 5.0 MPa for concrete made without any RCA.

Figure 5.26 presents the effect of RCA content and water absorption on 28-day flexural strength of concrete made with 0.40 w/cm and binary cement. Results indicate reduction in flexural strength with the use of higher RCA content and the use of RCA with higher water absorption. The use of 50% coarse RCA with water absorption of 4% and 7% can result in approximate flexural strength of 4.95 and 4.80 MPa, respectively, compared to values of about 5.10 MPa for concrete made without any RCA.

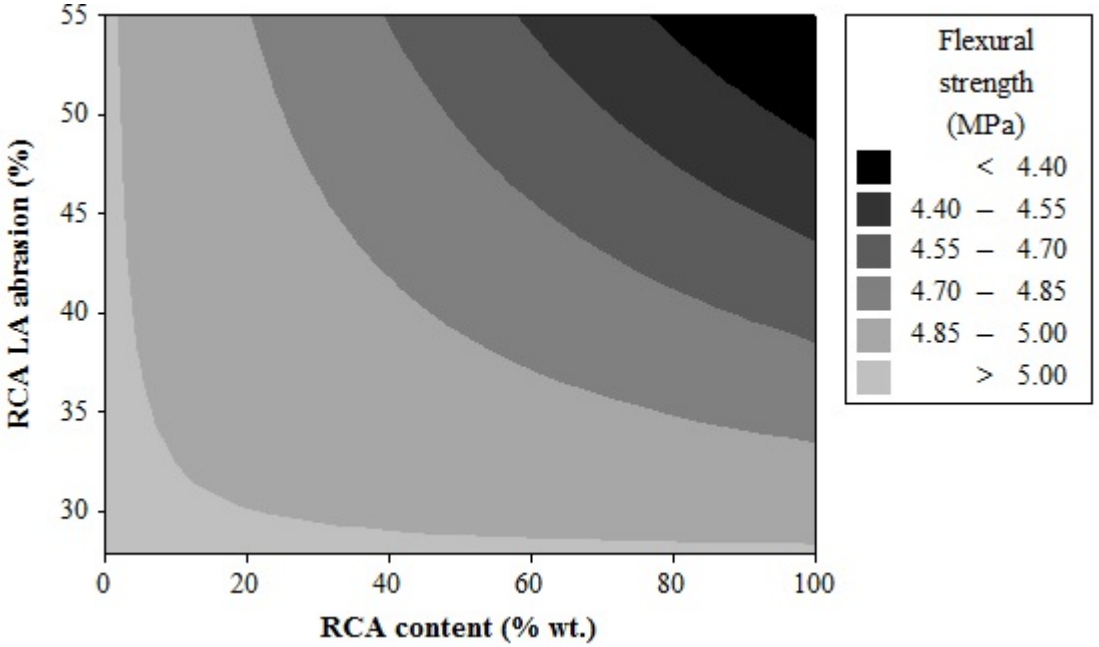

Figure 5.25 Effect of coarse RCA content and LA abrasion on 28-day flexural strength of concrete made with 0.40 w/cm and binary cement

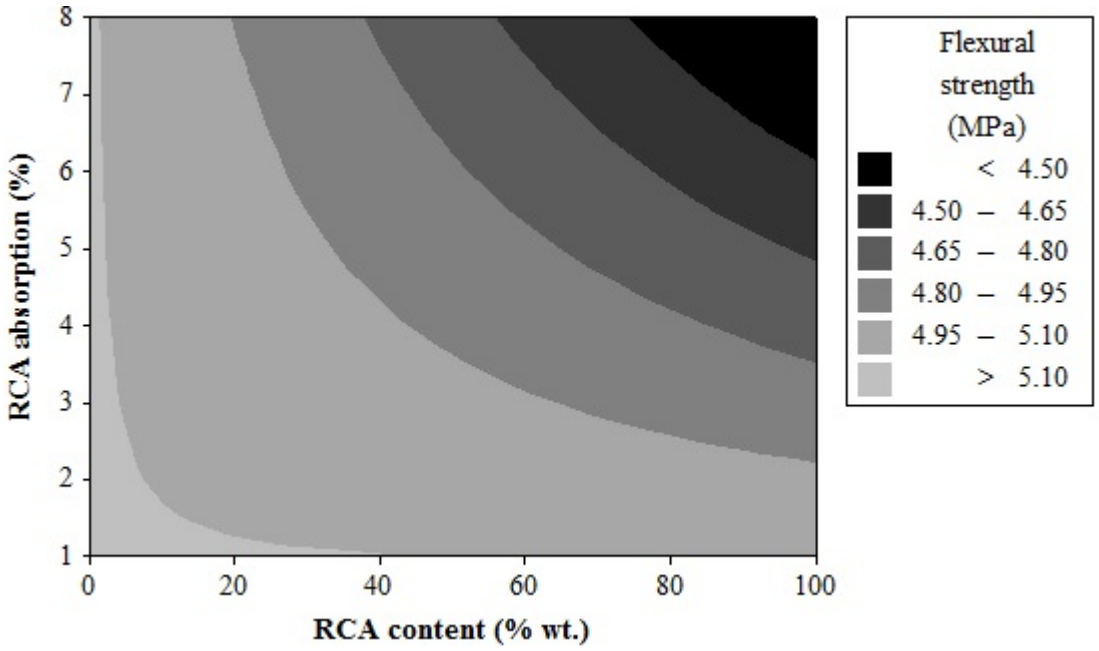

Figure 5.26 Effect of coarse RCA content and water absorption on 28-day flexural strength of concrete made with 0.40 w/cm and binary cement

Figure 5.27 presents the effect of RCA content and oven-dry specific gravity on 28-day flexural strength of concrete made with 0.40 w/cm and binary cement. Results indicate reduction in flexural strength with the use of higher RCA content and the use of RCA with lower specific gravity. The use of 50% coarse RCA with oven-dry specific gravity of 1.80 and 2.45 can result in approximate flexural strength of 4.50 and 5.10 MPa, respectively, compared to values of about 5.25 MPa for concrete made without any RCA.

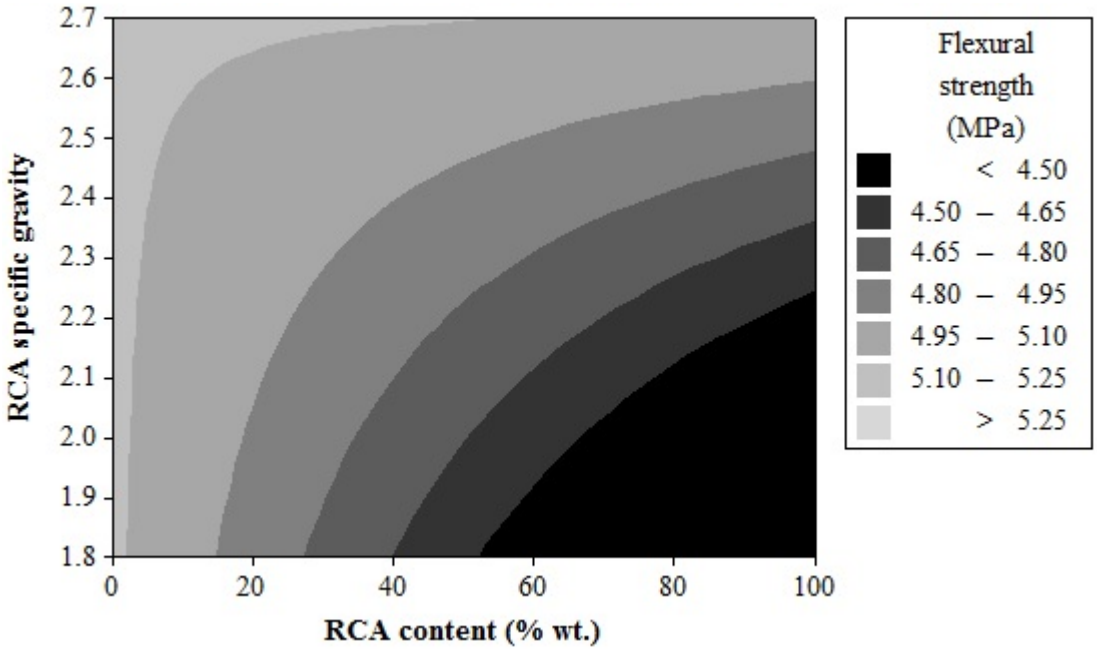

Figure 5.27 Effect of coarse RCA content and oven-dry specific gravity on 28-day flexural strength of concrete made with 0.40 w/cm and binary cement

5.3.4. Modulus of Elasticity.

5.3.4.1 Effect of fine RCA and mixture parameters. Table 5.11 includes a summary of the static modulus of elasticity (Young's modulus) results obtained for concrete prepared with different combinations of fine RCA1 and coarse RCA1 investigated in Group I. A slight reduction in 28-d MOE from 42.7 to 40.3 GPa was observed due to the use of the ternary cement with 50% SCM in concrete prepared with 0.40 w/cm and without any RCA. However, the 56-day MOE of concrete made with ternary cement was 8% higher than that of the reference concrete prepared with binary

system (44.2 vs. 40.8 GPa). The highest of MOE of 42.9 and 46.4 GPa, were observed for the mixture prepared with 0.37 w/cm, 30% coarse RCA1, and ternary cement including 15% GGF and 35% FA-C. This was followed by the result obtained for the concrete prepared with 0.37 w/cm, ternary cement with 15% GGBS and 35% FA-C, and without any RCA.

Table 5.11 Modulus of elasticity results of concrete made with different contents of coarse RCA1 and fine RCA1 (Group I) (GPa)

Mixture	28 days	56 days
DOL1-B-40	42.7	40.8
DOL1-T-37	42.9	44.3
DOL1-T-40	40.3	44.2
RCA1-30-T-37	42.2	42.7
RCA1-30-T-40	37.2	38.4
RCA1-30-T-37-15F	41.0	46.5
RCA1-30-T-40-15F	35.1	34.0
RCA1-40-T-40-15F	30.5	32.9
RCA1-50-T-37	37.9	40.3
RCA1-50-T-40	35.9	37.3
RCA1-50-T-37-15F	36.2	37.6
RCA1-50-T-40-15F	33.8	35.6
RCA1-50-T-40-30F	28.4	33.9
RCA1-50-T-40-40F	28.4	33.0
RCA1-60-T-40-30F	31.4	33.9
RCA1-70-T-37	37.7	37.9
RCA1-70-T-40	32.9	33.8
RCA1-70-T-40-15F	29.0	32.6
RCA1-70-T-40-30F	31.8	34.1
RCA1-30-GGF15-37	42.9	46.4

Significant reduction in MOE was observed for the rest of the mixtures that were produced with fine and/or coarse RCA1, regardless of the testing age. The use of fine RCA1 in concrete prepared with 50% and 70% coarse RCA1, proportioned with 0.40 w/cm, and ternary system (15% GGBS+35% FA-C) highlight the influence of fine RCA incorporation on MOE. For the concrete prepared with 50% coarse RCA1, the use of 15%, 30%, and 40% fine RCA1 reduced the 56-day MOE from 37.3 to 35.6, 33.9, and 33.0 GPa, corresponding to 5%, 9%, and 12% reduction, respectively.

Reduction in w/cm from 0.40 to 0.37 was effective in partial mitigating of the effect of RCA on MOE. For instance, and in the case of the concrete prepared with 50% coarse RCA1 and 15% fine RCA1, the reduction in w/cm from 0.40 to 0.37 resulted in an increase in 28-day MOE from 33.8 to 36.2 GPa, corresponding to 7% increase.

Results obtained for mixtures prepared with different amounts of fine RCA 2 and coarse RCA2 investigated in Group II also indicate reduction in MOE due to RCA incorporation (Table 5.12). For instance, results indicate reduction in 56-day MOE from 5.5 to 5.2 GPa due to 30% coarse RCA2 replacement in concrete made with 0.40 w/cm, binary cement with 25% FA-C, and limestone coarse aggregate. However, the use of reduced w/cm of 0.37, and adjustments in incorporation of FA-C could enhance the performance of concrete.

Table 5.12 Modulus of elasticity results of concrete made with different contents of coarse RCA2 and fine RCA2

Age	LIM-B-40	C35-F0-40	C35-F15-37	C40-F20-37	C35-F10-42	C25-F15-40	C25-F10-37	C25-F0-40
28 d	4.50	4.20	5.55	4.60	4.15	4.70	5.90	4.40
56 d	5.50	4.65	5.55	5.00	4.40	4.85	5.85	5.20

5.3.4.2 Effect of coarse RCA content. Figure 5.28 presents the variations in MOE of mixtures made with 0 to 70% coarse RCA1. The investigated mixtures were prepared with ternary cement (15% GGBS+35% FA-C), with 0.37 and 0.40 w/cm. In general, decrease in MOE was observed as a function of RCA content. Rate of such reduction was 18% and 24% for 28- and 56-day measurements of concrete with 0.40 w/cm

at 70% RCA1 replacement. Reduction in MOE of 12% and 14% was observed for the 28- and 56-day results of concrete with 0.37 w/cm at 70% RCA1 replacement.

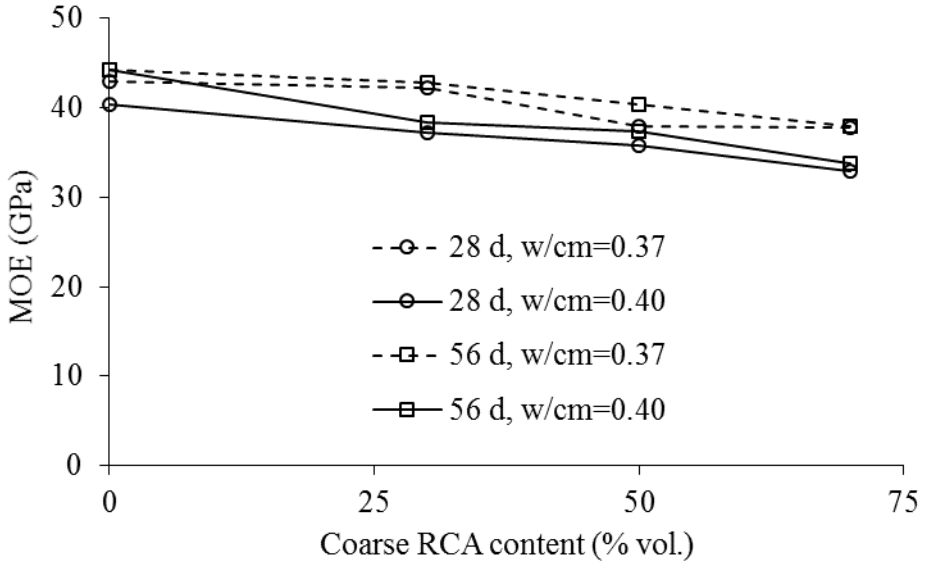

Figure 5.28 Effect of coarse RCA content on MOE

Figure 5.29 presents the variations in MOE of concrete made with ternary cement and 0.37 w/cm as a result of coarse RCA incorporation. Six different types of coarse RCA were incorporated at different replacement rates of 30%, 50% and 70%. Results indicated reduction in MOE as a function of increase in RCA content, regardless of the source. Similar trends were obtained for the mixtures prepared with binary cement and 0.40 w/cm.

The incorporation of up to 100% coarse RCA in such mixtures also reduced the MOE significantly, as presented in Figure 5.30. The highest values of MOE presented in this figure were attributed to the reference concrete produced without any RCA. However, up to 24% reduction in 56-day MOE was observed when 100% coarse RCA was used for replacement of the coarse aggregate.

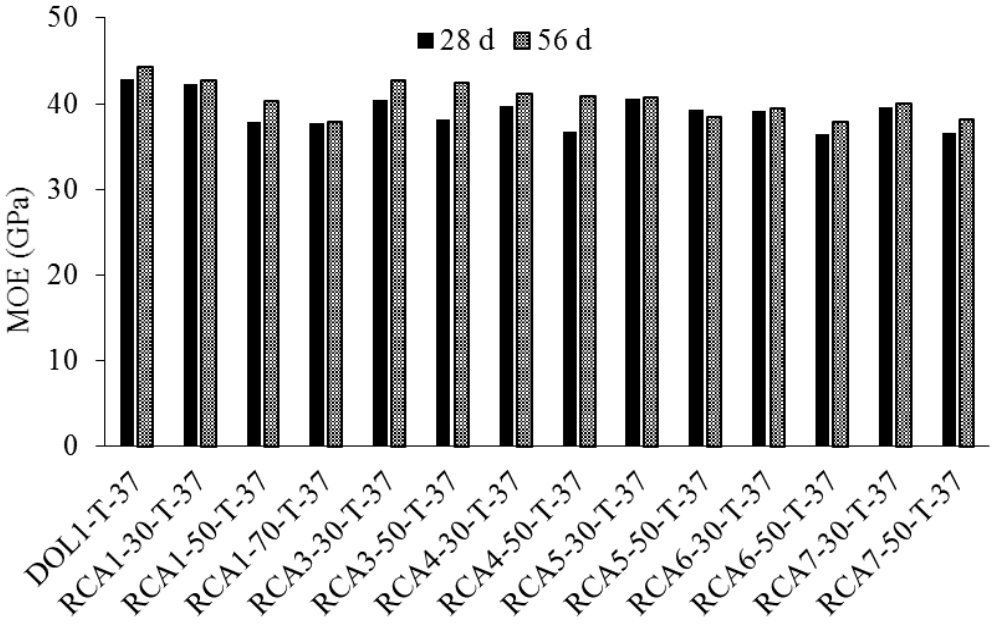

Figure 5.29 Effect of RCA type on MOE of concrete prepared with ternary cement and 0.37 w/cm

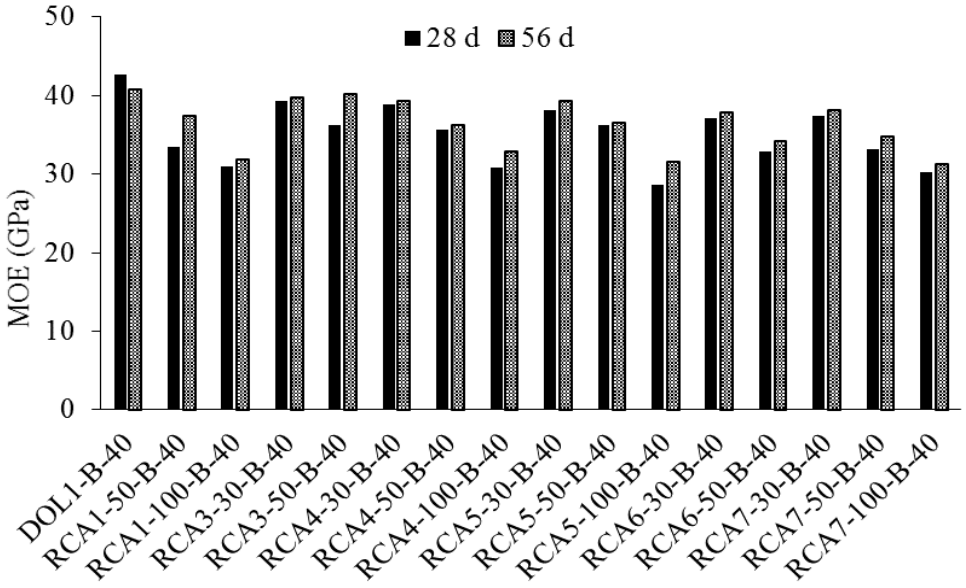

Figure 5.30 Effect of RCA type on MOE of concrete prepared with binary cement and 0.40 w/cm

5.3.4.3 Effect of coarse RCA properties. Data obtained from testing concrete with different types and contents of coarse RCA were incorporated to establish correlations between the combined aggregate physical properties and MOE at 28 and 56 days. Two main scenarios were investigated: (1) concrete prepared with 323 kg/m^3 of binary cement (25% FA-C) and 0.40 w/cm; (2) concrete made with 323 kg/m^3 of ternary cement (15% GGBS+35% FA-C) and 0.37 w/cm.

Figure 5.31 presents the correlation between the water absorption of the combined coarse aggregate and MOE at 28 and 56 days. Reduction in MOE was observed as a result of higher absorption rate of the combined coarse aggregate. Values of R^2 obtained for the linear correlation between the MOE results and the combined water absorption were 0.74 and 0.78 for the 28-day and 56-day measurements of the mixtures made with ternary cement, respectively. Such values were 0.85 and 0.88 for the mixtures prepared with binary cement and 0.40 w/cm. The slope of the trend lines were comparable for 28- and 56-day results of the investigated mixtures, indicating negligible interaction between the measurement time and the RCA incorporation. The MOE values of the concrete made with ternary cement and 0.37 w/cm were generally higher than those of the mixtures made with binary cement and 0.40 w/cm. However, the higher slopes of the trend lines obtained for the ternary mixtures reveal the fact that these mixtures were more sensitive to RCA incorporation.

Figure 5.32 presents the correlation between the oven-dry specific gravity of coarse aggregate combination and MOE at 28 and 56 days. As expected, increase in MOE was observed as a function of increase in specific gravity of combined coarse aggregate. The coefficient of determination (R^2) values of the linear correlations obtained between the MOE results and the combined specific gravity, were 0.78 and 0.73 for the 28-day and 56-day measurements of the mixtures made with ternary cement, respectively. Such values were 0.88 and 0.89 for the mixtures prepared with binary cement and 0.40 w/cm. The trend lines for the ternary mixtures had higher slopes than the ones made with binary cement and 0.40 w/cm, suggesting that the increase in RCA content and/or use of lower RCA quality can have a more pronounced effect on MOE in mixtures with higher quality.

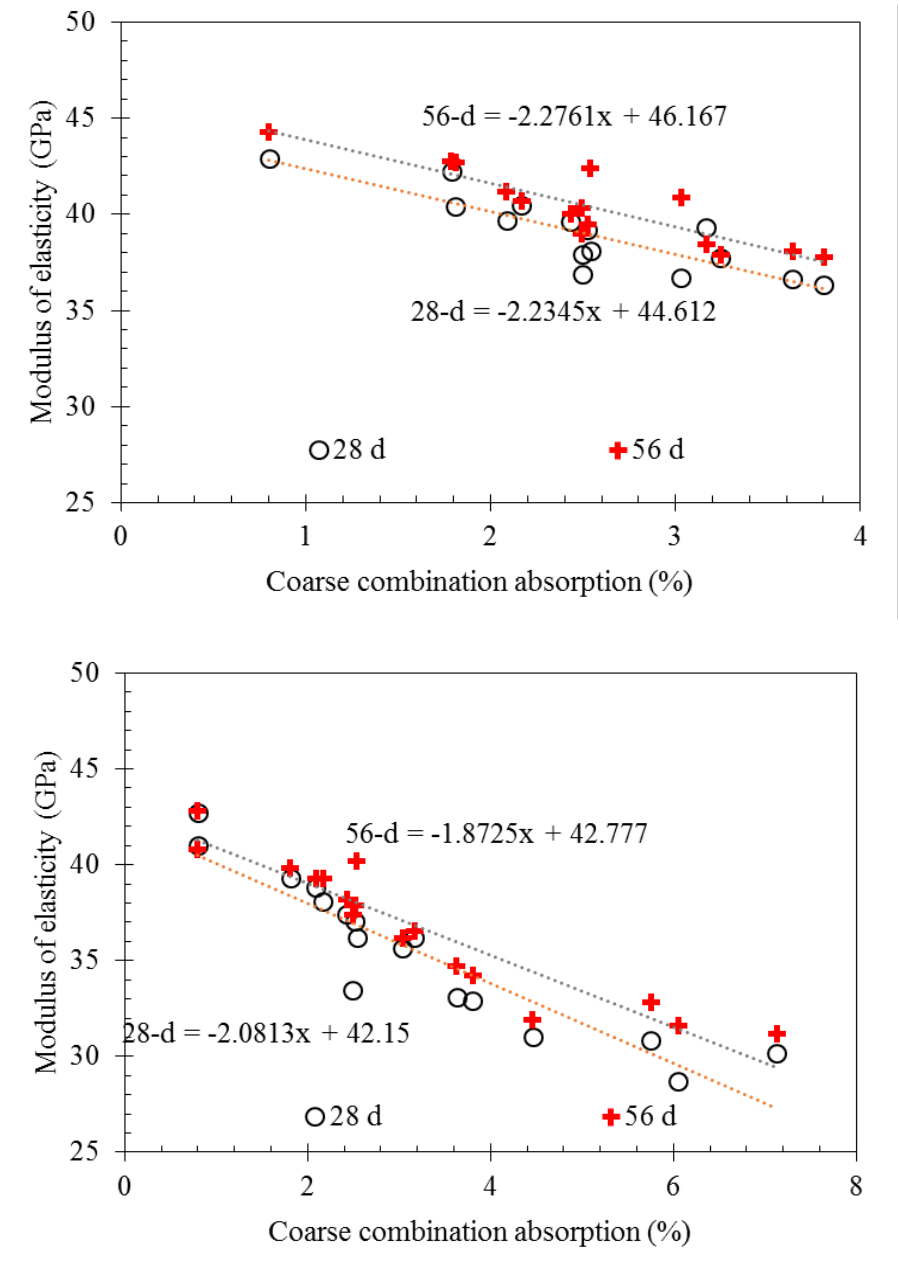

Figure 5.31 Effect of combined coarse aggregate water absorption on MOE; Top: ternary mixtures, Bot.: binary mixtures

Figure 5.33 presents the correlation between the LA abrasion of the combined coarse aggregate and MOE at 28 and 56 days. MOE was reduced with an increase in LA abrasion of the coarse aggregate combination. Values of R^2 obtained for the linear correlation between the MOE results and the combined LA abrasion were 0.32 and 0.42 for the 28-day and 56-day measurements of the mixtures made with ternary cement,

respectively. Such values were 0.50 and 0.55 for the mixtures prepared with binary cement and 0.40 w/cm. In general it was observed that the water absorption and the oven dry specific gravity were better predictors for estimation of MOE.

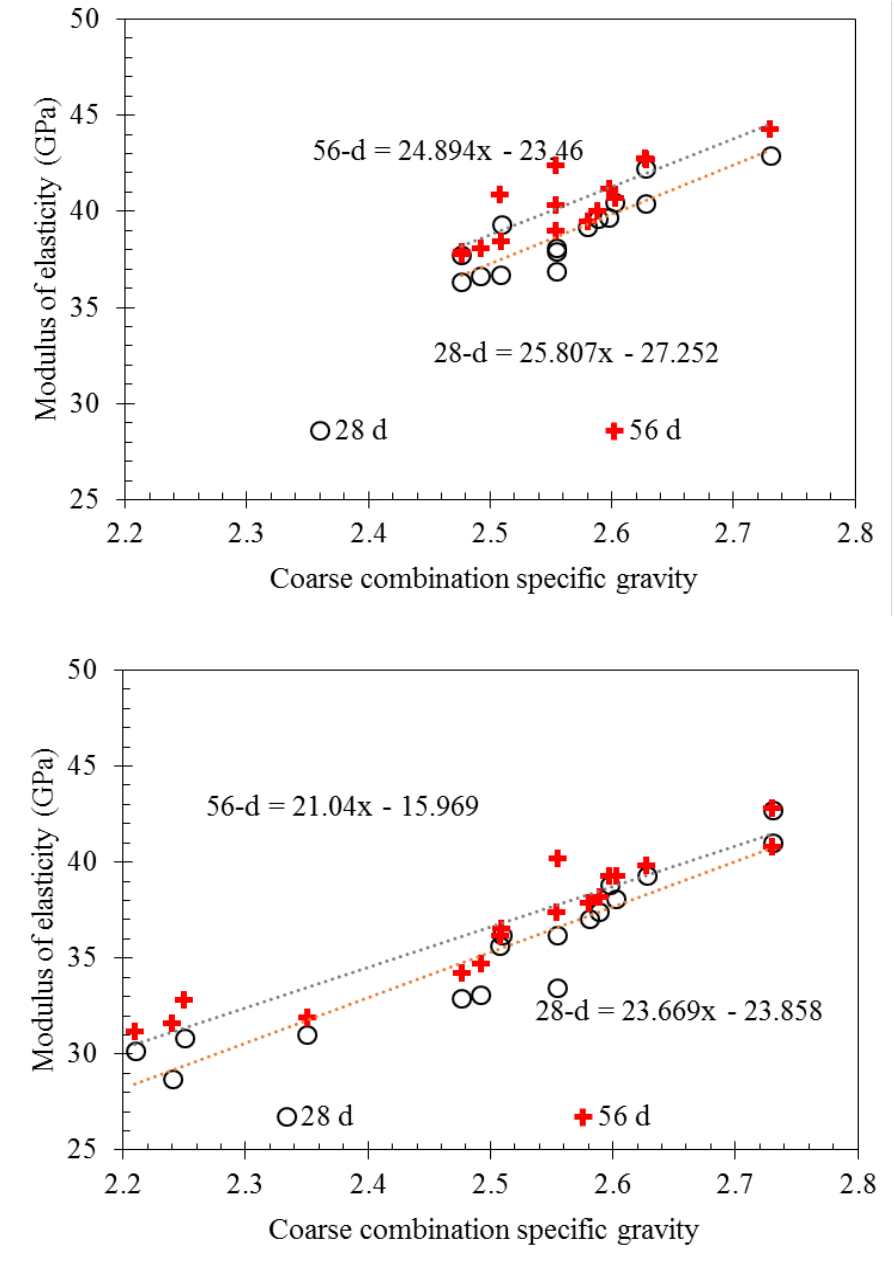

Figure 5.32 Effect of combined coarse aggregate specific gravity on MOE; Top: ternary mixtures, Bot.: binary mixtures

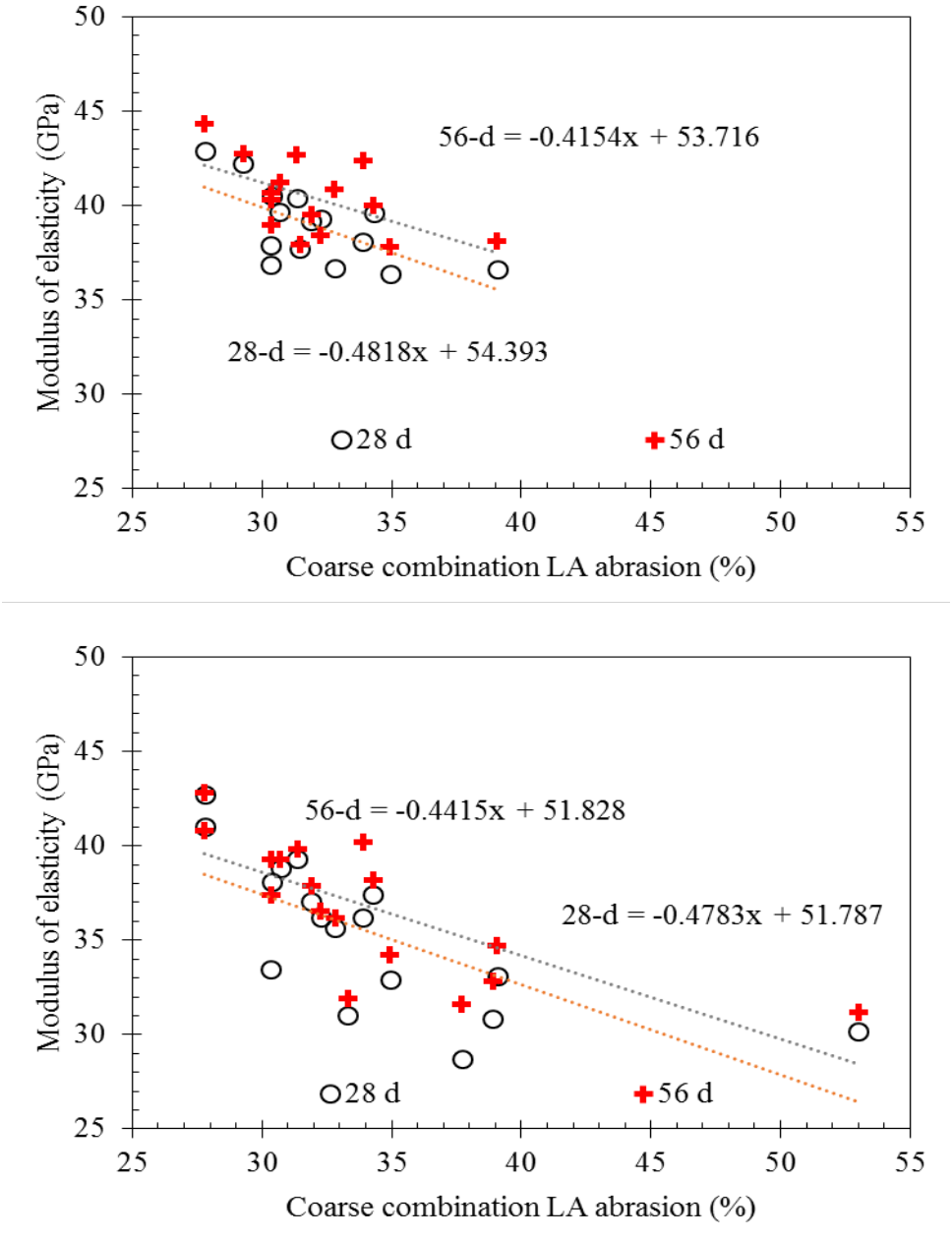

Figure 5.33 Effect of combined coarse aggregate LA abrasion on MOE; Top: ternary mixtures, Bot.: binary mixtures

Given the limits of the experimental domain are met, the results obtained in this section can be incorporated to estimate the MOE of concrete made with coarse RCA. For instance, contour diagrams were generated based on the 28-day results of concrete made with binary cement and 0.40 w/cm. A hypothetical scenario was investigated for concrete made with DOL1 coarse aggregate (LA abrasion: 28%, Absorption: 0.8%, and specific

gravity: 2.73). Contour graphs were developed to illustrate the effect of RCA content (% mass) and RCA characteristics on 28-day MOE.

Figure 5.34 presents the effect of RCA content and LA abrasion on 28-day MOE of such concrete, made with 0.40 w/cm and binary cement. Results indicate significant reduction in MOE with the use of higher RCA content and the use of RCA with higher LA abrasion mass loss. The use of 50% coarse RCA with LA abrasion of 35% and 50% can result in approximate MOE of 37.0 and 31.5 GPa, respectively, compared to values of higher than 38.0 GPa for concrete made without any RCA.

Figure 5.35 presents the effect of RCA content and water absorption on 28-day MOE of concrete made with 0.40 w/cm and binary cement. Results indicate reduction in MOE with the use of higher RCA content and the use of RCA with higher water absorption. The use of 50% coarse RCA with water absorption of 3% and 7% can result in approximate MOE of 38.5 and 34.0 GPa, respectively, compared to values of about 40.0 GPa for concrete made without any RCA.

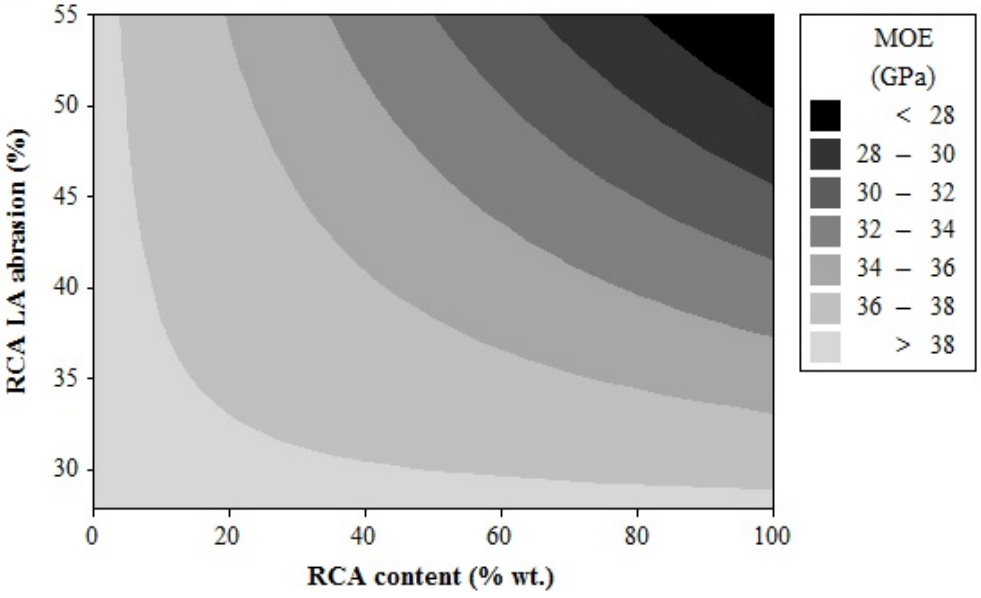

Figure 5.34 Effect of coarse RCA content and LA abrasion on 28-day MOE of concrete made with 0.40 w/cm and binary cement

Figure 5.36 presents the effect of RCA content and oven-dry specific gravity on 28-day MOE of concrete made with 0.40 w/cm and binary cement. Results indicate

reduction in MOE with the use of higher RCA content and the use of RCA with lower specific gravity. The use of 50% coarse RCA with oven-dry specific gravity of 1.80 and 2.40 can result in approximate MOE of 38.0 and 30.0 GPa, respectively, compared to values of about 40.0 GPa for concrete made without any RCA.

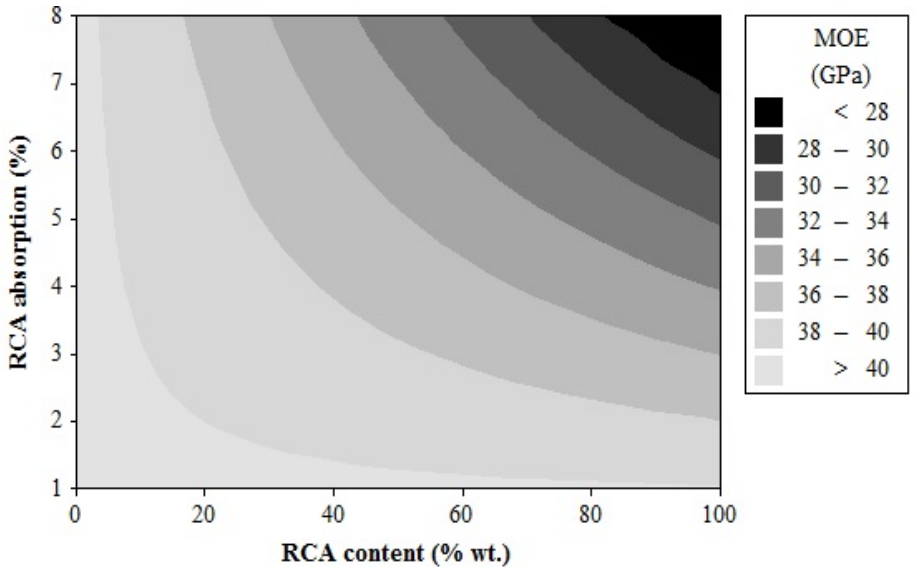

Figure 5.35 Effect of coarse RCA content and water absorption on 28-day MOE of concrete made with 0.40 w/cm and binary cement

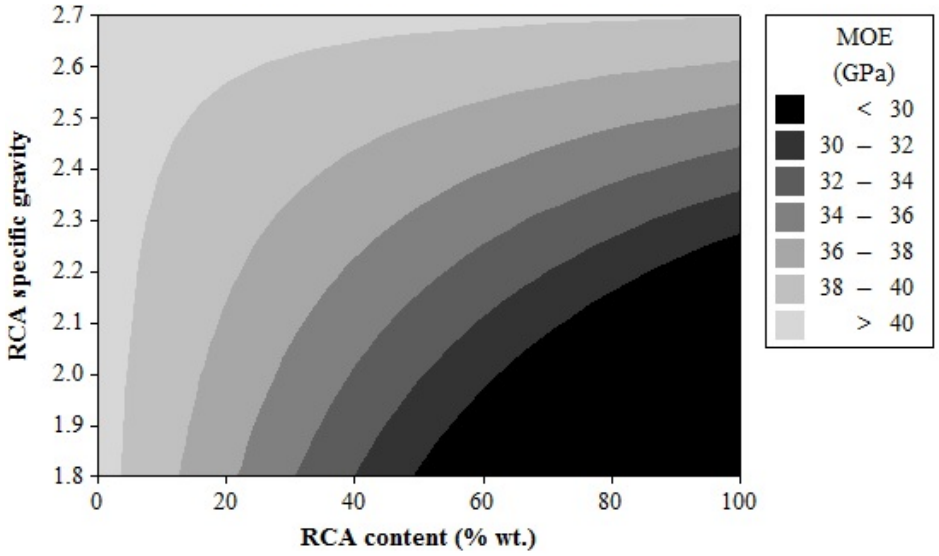

Figure 5.36 Effect of coarse RCA content and oven-dry specific gravity on 28-day MOE of concrete made with 0.40 w/cm and binary cement

5.4. REMARKS

The present section investigates the effect of fine and coarse RCA incorporation on mechanical properties of concrete designated for rigid pavement construction. Two types of fine RCA and seven different types of coarse RCA were employed for development of concrete mixtures. Two different types of crushed virgin aggregate were incorporated along with a natural river sand. The investigated mixtures were proportioned with binary or ternary binder systems. Compressive strength, splitting tensile strength, flexural strength, and modulus of elasticity was investigated at different ages. Based on the obtained data the following conclusions can be warranted:

- The use of fine RCA results in reduction in mechanical properties. Up to 17% reduction in 56-day flexural strength (from 5.27 to 4.38 MPa) and up to 12% reduction in 56-day MOE (from 37.3 to 33.0 GPa)was observed as a result of 40% fine RCA incorporation in concrete made with 0.40 w/cm and ternary cement with 15% GGBS and 35% FA-C.
- The modifications in concrete mix design, i.e. the reduction in w/cm to values as low as 0.37 and the use of proper binder composition were effective in enhancing the performance of concrete made with fine RCA.
- The incorporation of coarse RCA reduced the mechanical properties of the investigated mixtures. Up to 24% reduction in 56-day MOE was observed when 100% coarse RCA was used for replacement of the coarse aggregate in concrete made with binary cement and 0.40 w/cm. The use of 50% coarse RCA in mixtures made with ternary cement and 0.37 w/cm resulted to up to 22% reduction in 56-day flexural strength. In the case of the mixtures made with binary cement and 0.40 w/cm, the use of 50% and 100% coarse RCA reduced the 56-day flexural strength by up to 23%.
- Physical properties of the combined coarse aggregate, calculated as a function of mass fractions of the coarse virgin aggregate and coarse RCA can be incorporated to estimate the variations in mechanical properties. In spite of the generally improved mechanical properties, the concrete prepared with lower w/cm (0.37) and ternary cement was more sensitive to the incorporation of RCA. Contour diagrams were developed to estimate the variations in key mechanical properties

of the concrete as a result of coarse RCA incorporation for investigated pavement concrete scenarios.

- In general, it was observed that the variations in LA abrasion and water absorption of the combined coarse aggregate can be considered as proper means of estimating the effect of coarse RCA on compressive strength and splitting tensile strength of concrete. The water absorption and the oven dry specific gravity were better predictors for estimation of flexural strength and MOE.

6. USING ARTIFICIAL INTELLIGENCE TO PREDICT MODULUS OF ELASTICITY OF RECYCLED AGGREGATE CONCRETE

6.1. RESEARCH SIGNIFICANCE

The construction of residential and commercial buildings, along with highways, bridges, and other types of infrastructures has been increasing from the beginning of the past century, especially in areas of high population density. These facilities need to be repaired or replaced with the passing of time by the end of service life, or in situations where the original design no longer satisfies the needs due to the growth in population and/or traffic, etc. This results in two major concerns: (1) a growing demand for construction aggregates, raising questions about the depletion of non-renewable natural aggregates; (2) an increase in the amount of construction and demolition (C&D) waste.

The environmental impacts, raising issues with depletion of virgin aggregate sources, more restrictive landfill policies, and potential savings in construction cost, mainly associated with reduced hauling distances, support the idea of seeking alternative uses for C&D waste. One of the main ideas is to recycled the waste concrete and use recycled concrete aggregate (RCA) as a partial/full replacement of virgin aggregate used in concrete construction (NCHRP 2013).

Questions regarding the performance of concrete incorporating RCA may raise given the potentially marginal quality of the RCA compared to that of the virgin aggregate sources. Data published in the literature indicate that among all types of mechanical properties, MOE is one the characteristics that can be highly sensitive to RCA incorporation. Availability of residual mortar in RCA particles reduces the overall stiffness of the coarse aggregate skeleton and increases the absolute volume of mortar in hardened state. This reduces the rigidity of the concrete, resulting in lower MOE compared to the mixtures cast with virgin aggregate. Moreover, given the sensitivity of MOE, existence of micro-cracks and defected interfacial transition zone (ITZ), typical of RCA particles, can affect the MOE significantly (Monteiro 2006). Results of a survey conducted by the National Cooperative Highway Research Program (NCHRP 2013) reveal that using coarse RCA can result in up to 35% reduction in MOE.

This section presents a model developed based on artificial neural networks to quantify the effect of coarse RCA on concrete MOE. A wide range of mixture design parameters, including the binder content and type, water content, virgin aggregate properties and content, and RCA content and characteristics were considered as input factors. The extent of variation of MOE due to RCA incorporation was used as the output. A database was developed and analyzed to establish a predictive model. Given the wide range of investigated features, the developed model can be employed to estimate the effect of RCA on MOE of concrete designated for a variety of applications, including concrete for transportation infrastructure.

6.2. RESEARCH METHODOLOGY

The proposed research was composed of three main phases. The first phase of the research involved development and screening of a database of published literature on MOE. The second phase was to generate laboratory data for validation and/or testing the model. The third phase involved development and testing of the model based on artificial neural networks.

6.2.1. Development and Analysis of Database. The database consisted of 484 data series obtained from 52 research articles from literature. The 28-day compressive strength of the investigated concrete mixtures ranged from a minimum of 15.4 to a maximum of 108.5 MPa. The minimum and the maximum values of MOE were 10 and 10 GPa, respectively. Each dataset included a summary of the concrete mixture design, virgin aggregate content and properties, and RCA content and characteristics. The investigated input factors are elaborated below.

Binder: binder content (kg/m^3); binder type which was considered as a categorical factor of 1 or 2. Input value of 1 was attributed to the concrete with plain Portland cement while binder type 2 was representing concrete mixtures with supplementary cementitious materials.

Water: water-to-binder ratio (w/b), water-to-cement ratio (w/c), and water content (kg/m^3).

Fine aggregate: fine aggregate content (kg/m^3).

Virgin coarse aggregate: virgin coarse aggregate content (kg/m^3), virgin coarse aggregate water absorption (%), virgin coarse aggregate oven-dry specific gravity, and virgin coarse aggregate LA abrasion value (%).

Coarse RCA: coarse RCA content (kg/m^3), coarse RCA water absorption (%),coarse RCA oven-dry specific gravity, coarse RCA LA abrasion value (%), and coarse RCA replacement ratio (% mass).

Total coarse aggregate: total coarse aggregate content (kg/m^3), combined coarse aggregate water absorption (%), combined coarse aggregate oven-dry specific gravity, and combined coarse aggregate LA abrasion value (%). The combined coarse aggregate properties were calculated as a linear combination of the properties and relative mass of the blend constituents, as proposed by Omary et al. (2016). The following equations were used to determine the oven-dry specific gravity, water absorption, and mass loss due to LA abrasion of a given combination of coarse aggregate, respectively, as suggested by Omary et al. (2016).

$$Coarse_{SG} = [(Mass_{RCA} \times RCA_{SG}) + (Mass_{NC} \times NC_{SG})]/(Mass_{Rca} + Mass_{NC}) \quad (6\text{-}1)$$

$$Coarse_{Abs} = [(Mass_{RCA} \times RCA_{Abs}) + (Mass_{NC} \times NC_{Abs})]/(Mass_{Rca} + Mass_{NC}) \quad (6\text{-}2)$$

$$Coarse_{LA} = [(Mass_{RCA} \times RCA_{LA}) + (Mass_{NC} \times NC_{LA})]/(Mass_{Rca} + Mass_{NC}) \quad (6\text{-}3)$$

where $Mass_{RCA}$ is the RCA content (kg/m^3), $Mass_{NC}$ is the virgin coarse aggregate content (kg/m^3), RCA_{SG} is the oven-dry specific gravity of RCA, NC_{SG} is the oven-dry specific gravity of the virgin coarse aggregate, RCA_{Abs} is the water absorption of the RCA (%), NC_{Abs} is the virgin coarse aggregate absorption rate (%), RCA_{LA} is the mass loss due to LA abrasion of RCA (%), NC_{LA} is the mass loss due to LA abrasion of the virgin coarse aggregate (%), and $Coarse_{SG}$, $Coarse_{Abs}$, and $Coarse_{LA}$ are the oven-dry specific gravity, water absorption rate (%), and LA abrasion (%) of the coarse aggregate combination, respectively.

Table 6.1 offers a summary of the input features, along with the corresponding minimum and maximum values. Four different arrangements of input factors were explored to ensure most generalized and robust predictions with lowest chance of overfitting the data. The investigated input scenarios are elaborated below.

6.2.1.1 Scenario I. The input factors included 13 independent types of data summarizing the key mixture design details, virgin aggregate properties, and RCA characteristics. The aggregate-related properties considered in the first scenario included the aggregate content (kg/m^3), oven-dry specific gravity, and water absorption (%) for both the virgin and RCA materials. The LA abrasion value was not included in the first scenario. This was due to the fact that not all the investigated sources from literature reported the LA abrasion values of the RCA. Table 1 presents the factors included in scenario 1.

6.2.1.2 Scenario II. A total number of 18 input factors were investigated for the second scenario. The input parameters included the 13 independent properties (elaborated in scenario I) and an additional set of 5 dependent parameters. The aggregate-related properties considered in the first scenario included the aggregate content (kg/m^3), oven-dry specific gravity, and water absorption (%) for both the virgin and RCA materials. Again, LA abrasion was not included in the analysis. The additional dependent variables were the total water content in the mixture, total coarse aggregate content (kg/m^3), RCA replacement ratio (% mass), combined coarse aggregate water absorption (%), and combined coarse aggregate oven-dry specific gravity.

6.2.1.3 Scenario III. A total number of 15 independent input parameters were considered for the third scenario. The 13 factors elaborated in scenario I were incorporated along with the LA abrasion values of the virgin coarse aggregate and the RCA materials. As stated earlier, not all the investigated references were reporting the LA values of the aggregates. Therefore, a literature survey was conducted, in addition to laboratory investigation, to establish correlations between the LA abrasion and two key RCA properties, including water absorption and specific gravity as suggested by González-Taboada et al. (2016). Figure 6.1 presents the correlations between the LA abrasion and water absorption developed by González-Taboada et al. (2016) and further updated by the authors obtained from over 100 different RCA types. Strong relationship was observed, with R^2 values of 0.75 for the relationship between LA abrasion and water absorption. The correlation established in Figure 6.1 was employed to estimate the LA abrasion in the case of the missing data points of the database.

Table 6.1 ANN model input and output features

		Feature	Database		Scenario			
			Min.	Max.	I	II	III	IV
Input Parameters	1	Binder content (kg/m^3)	210	609	*	*	*	*
	2	Binder type	1: OPC	2: SCM	*	*	*	*
	3	Virgin coarse content (kg/m^3)	0	1950	*	*	*	*
	4	Coarse RCA content (kg/m^3)	0	1800	*	*	*	*
	5	water/binder (w/b)	0.25	0.87	*	*	*	*
	6	water/cement (w/c)	0.29	1.22	*	*	*	*
	7	Fine content (kg/m^3)	465.00	1301	*	*	*	*
	8	Coarse aggregate absorption (%)	0.20	6.10	*	*	*	*
	9	C-RCA absorption (%)	1.93	18.91	*	*	*	*
	10	Coarse specific gravity, OD	2483	2880	*	*	*	*
	11	C-RCA specific gravity, OD	1800	2602	*	*	*	*
	12	Coarse aggregate NMAS (mm)	8	32	*	*	*	*
	13	Coarse RCA NMAS (mm)	8	32	*	*	*	*
	14	Coarse aggregate LA abrasion (%)	14	43			*	*
	15	C-RCA LA abrasion (%)	14	82			*	*
	16	water content (kg/m^3)	108	234		*		*
	17	Total coarse aggregate content (kg/m^3)	640	1950		*		*
	18	Coarse combination absorption (%)	0	16		*		*
	19	Coarse combination specific gravity, OD	1800	2880		*		*
	20	Coarse combination LA abrasion (%)	14	51				*
	21	Coarse RCA replacement ratio	0	1		*		*
Output		Relative MOE ($\boldsymbol{R_{MOE}}$)	0.44	1.37				

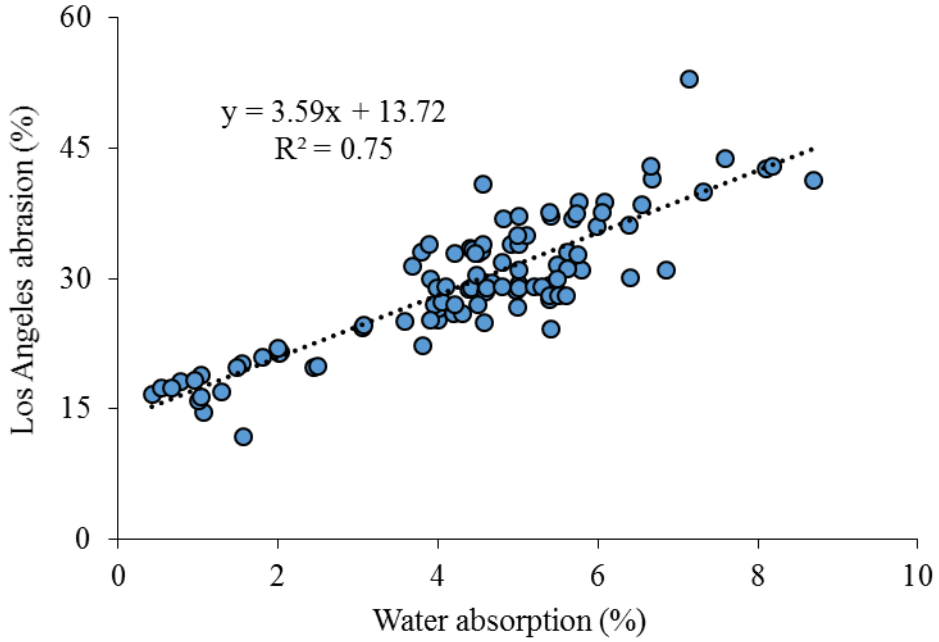

Figure 6.1 Correlation between LA abrasion and water absorption

6.2.1.4 Scenario IV. A total number of 21 input parameters were included in the study. The investigated parameters included all the mixture properties and aggregate characteristics presented earlier.

6.2.1.5 Output. The output of the study was the relative variation in MOE, as defined in Equation (6-4). Considering the relative MOE (R_{MOE}) as the means of comparison reduces the uncertainties related to non-uniform experimental conditions, including air content in hardened state, specimen size, test device, loading rate, and test protocol, etc., typical of databases.

$$Relative\ MOE\ (R_{MOE}) = \frac{MOE\ of\ the\ concrete\ made\ with\ RCA}{MOE\ of\ the\ reference\ concrete\ without\ any\ RCA} \quad (6\text{-}4)$$

where relative performance value of 1.0 was considered for the reference mixture of each study, proportioned without any RCA.

6.2.2. Laboratory Investigation.

6.2.2.1 Material properties. In total, 43 different concrete mixtures were produced in laboratory. A type I/II Portland cement, a Class C fly ash (FA-C), and a ground granulated blast furnace slag (GGBS) were used as binder materials. The mixtures were proportioned with either a binary or a ternary cement. The binary cement was composed of 75% (by mass) OPC and 25% FA-C. The ternary system incorporated 35% FA-C and 15% GGBS. The binary cement was adopted from the concrete mixture design employed by the Missouri Department of Transportation (MoDOT) for rigid pavement construction (Sadati and Khayat, 2016). The ternary system was optimized based on the mechanical properties and shrinkage of concrete equivalent mortar prepared with w/cm of 0.40, which was optimized by the authors (Khayat and Sadati, 2016). Three different values of water-to-cementitious materials ratio (w/cm) of 0.37, 0.40, and 0.45 were considered in designing the concrete mixtures. Coarse RCA procured from six different sources, including five recycling centers and one type of a laboratory produced RCA was considered for production of concrete mixtures. A single source of siliceous river sand was incorporated as fine aggregate. Table 6.2 summarizes the aggregate properties. Air entraining agent was used to secure 6%±1% air in fresh concrete. Water reducing admixture was incorporated to adjust initial slump values (ranging from 25 to 175 mm). Table 6.3 offers a summary of the mixture proportions and obtained MOE values obtained in the laboratory.

6.2.2.2 Concrete preparation and testing. A drum mixer with 110-l capacity was used for preparing the concrete. Slump and air content in fresh state were determined according to ASTM C143 (2015) and ASTM C231 (2014), respectively. Cylindrical specimens measuring 100×200 mm were employed for determining the compressive strength and MOE according to ASTM C39 (2001) and ASTM C469 (2010), respectively. A vibrating table was employed to secure proper consolidation of the concrete. Extracted samples were covered with wet burlap and plastic sheets up to 24 hours after casting. The specimens were cured in lime-saturated of 21±2 ºC up the testing time at 28 days.

Table 6.2 Aggregate properties

Aggregate	Source	Specific gravity	Absorption (%)	LA abrasion (%)	NMAS (mm)
Virgin coarse 1	Crushed dolomite	2.73	0.80	28	19
Virgin coarse 2	Crushed dolomite	2.72	0.98	43	19
Virgin coarse 2	Crushed limestone	2.64	0.50	24	19
Sand	River-bed sand	2.63	0.40	-	4
RCA 1	Laboratory produced RCA	2.35	4.56	41	19
RCA 2	Residual concrete, airfield	2.35	4.46	33	19
RCA 3	Residual concrete, airfield	2.38	4.20	33	19
RCA 4	Commercial recycling, MO	2.25	5.75	39	19
RCA 5	Commercial recycling, KS	2.24	6.05	38	19
RCA 6	Commercial recycling, MO	2.17	7.58	44	19
RCA 7	Commercial recycling, MO	2.21	7.13	53	12.5

6.2.3. Model Development. Being inspired by biological nervous system, the artificial neural networks are information analysis paradigms widely used as computational tools. The modeling using ANN involves five main steps: (1) problem representation and data acquisition; (2) defining the architecture; (3) determining the learning process; (4) network training; and (5) testing the developed network to ensure robustness and generalization. Neural networks are composed of a large number of interconnected artificial processing units, known as neurons. Each neuron typically consists of five different parts: inputs, weights, transfer function, activation function, and output as illustrated in Figure 6.2. The x_is represent the input applied to each neuron and w_is represent the weight attributed to each input. The transfer function used in this study is the weighted sum presented in Equation (6-5).

$$net_j = \sum_{i=0}^{n} w_{ij} x_i \tag{6-5}$$

where net_j is the weighted sum of the j^{th} neuron based on the weights and input values from n neurons of the preceding layer, w_{ij} is the weight factors between the j^{th} neuron and

the i^{th} neuron of the preceding layer, x_i is the output of the i^{th} neuron, and $b=w_{0j}x_0$ is the bias ($x_0=1$).

Table 6.3 Summary of concrete mixture properties

		Feature	Min.	Max.	Scenario			
					I	II	III	IV
Input Parameters	1	Binder content (kg/m^3)	317	323	*	*	*	*
	2	Binder type	2	2	*	*	*	*
	3	Virgin coarse content (kg/m^3)	0	1136	*	*	*	*
	4	Coarse RCA content (kg/m^3)	0	964	*	*	*	*
	5	water/binder (w/b)	0.37	0.45	*	*	*	*
	6	water/cement (w/c)	0.53	0.80	*	*	*	*
	7	Fine content (kg/m^3)	772	795	*	*	*	*
	8	Coarse aggregate absorption (%)	0.50	0.98	*	*	*	*
	9	C-RCA absorption (%)	4.20	7.58	*	*	*	*
	10	Coarse specific gravity, OD	2640	2730	*	*	*	*
	11	C-RCA specific gravity, OD	2170	2380	*	*	*	*
	12	Coarse aggregate NMAS (mm)	19	19	*	*	*	*
	13	Coarse RCA NMAS (mm)	13	19	*	*	*	*
	14	Coarse aggregate LA abrasion (%)	24	43			*	*
	15	C-RCA LA abrasion (%)	33	53			*	*
	16	water content (kg/m^3)	120	143		*		*
	17	Total coarse aggregate content (kg/m^3)	907	1136		*		*
	18	Coarse combination absorption (%)	0.50	7.13		*		*
	19	Coarse combination specific gravity, OD	2210	2730		*		*
	20	Coarse combination LA abrasion (%)	24	53				*
	21	Coarse RCA replacement ratio	0	1		*		*
Output		Relative MOE ($\boldsymbol{R_{MOE}}$)	0.67	1.05				

The activation function translates the net value to the neuron output. A variety of activation functions are available, such as linear, sigmoid, and hyperbolic tangent sigmoid. The latter was employed in this study; it takes the net values ranging anywhere between minus and plus infinite and converts it into an output in the interval [-1, 1].

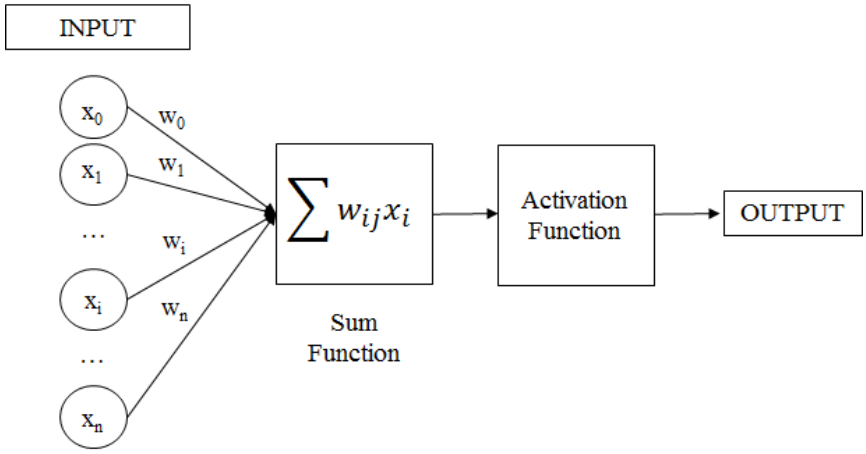

Figure 6.2 Schematic structure of a simple neuron model

The neural network toolbox provided by a commercial software (MATLAB 2016a) was used to develop the model. A multilayer perceptron network with one hidden layer was used to form the ANN architecture. The adjustment of the weight to ensure developing the desired output based on experimental data is defined as the training process. Given the acceptable performance in solving problems related to concrete materials (Duan et al. 2013, Ghafari et al. 2015), the back-propagation learning algorithm was employed for training the system. This learning process consists of two main steps: (1) a forward flow of the signal from input layer towards the output layer and calculation of error based on comparison between the output and the target value, i.e. experimental data; (2) backward propagation to minimize the error, which is done by adjustment of the weights and bias values in the input and hidden layers. Levenberg-Marquardt back-propagation with regularizing parameter equal to 0.001 was incorporated. The dimension of the input layer was equal to the number of input features incorporated in each analysis scenario (13, 15, 18, or 21), as discussed in previous sections. The output layer consisted of one neuron. The approach discussed in (Ghafari et al. 2015) was followed to select the number of neurons in hidden layer. The number of neurons in the hidden layer was varied to select the architecture with the best performance, with a parameter sweep within the range of 1 to 30. In other words, 30 different architectures were investigated for each input scenario, varying the number of neurons in hidden layer within the range of 1 to 30

to ensure best performance. For each investigated architecture 100 trials were performed by randomly initializing the weights and keeping the architecture with the smallest validation set error to address the local optima issues common to this types of neural networks. Each combination of optimized architecture and input scenario was replicated five times to ensure uniform performance of the models. Finally, based on the data obtained from various architectures, the one with the best performance in terms of minimum mean square error (MSE) and the highest correlation coefficient (R) between estimation and target values was finally selected.

A total number of 436 data samples, corresponding to 90% of the data available in developed database were randomly selected for training the neural network. The 43 data samples obtained from laboratory investigations (discussed in previous sections) were used for model validation. The remaining 10% of the data from database were used for testing the selected model.

6.3. RESULTS AND DISCUSSION

6.3.1. Model Selection. Table 6.4 summarizes the networks' performance metrics, i.e. the regression results and error associated with each network, summarizing the correlations between the estimated values (Output) and the experimental observation (Target). For each case, the optimal number of neurons for the training, validation and test subsets were incorporated as defined earlier to investigate the different subsets of features including 13, 15, 18 or 21 input parameters. Strong correlations were observed for the investigated models. The correlation values ranging from 0.68 to 0.94 for training, from 0.82 to 0.91 for validation, and from 0.77 to 0.91 for testing phase, with validation mean square error ranging from 0.00144 to 0.00260. In addition to the R and MSE values, the uniformity of data distribution around the equity line (X=Y) for validation and testing sets was also incorporated as a measure to select the models with best performance from each scenario.

Results presented in Figure 6.3 to Figure 6.6 illustrate the correlations between the predictions obtained from the selected models and the experimental targets, obtained through training, validation, and testing along with the validation MSE associated with

each model. Each of the selected models correspond to one of the investigated input scenarios.

Given the requirements for proper prediction are met, it is generally recommended to select regression models with lower number of input parameters. It is also recommended to avoid dependent variables as input parameters to avoid multi-collinearity, unless it is proved that the incorporation of such features can enhance the model performance. Considering the aforementioned model selection guidelines, and given the comparable performance of the four selected models presented in (Figure 6.3, Figure 6.4, Figure 6.5, and Figure 6.6), it was finally decided to use the models with 13 and 15 input features (Scenarios I and III).

Table 6.4 Summary of model performances

Scenario	Replication	Training R	Validation R	Testing R	Validation MSE
13 Features	1	0.89	0.82	0.87	0.00259
	2	0.93	0.85	0.83	0.00237
	3	0.91	0.85	0.85	0.00225
	4	0.86	0.85	0.84	0.00242
	5**	0.93	0.83	0.91	0.00244
18 Features	1**	0.91	0.83	0.87	0.00260
	2	0.91	0.85	0.84	0.00259
	3	0.93	0.84	0.85	0.00232
	4	0.90	0.84	0.85	0.00237
	5	0.92	0.86	0.87	0.00235
15 Features*	1	0.81	0.89	0.84	0.00158
	2	0.68	0.89	0.86	0.00174
	3**	0.91	0.88	0.88	0.00204
	4	0.78	0.84	0.77	0.00237
	5	0.90	0.88	0.82	0.00186
21 Features*	1	0.90	0.91	0.86	0.00144
	2	0.91	0.87	0.84	0.00198
	3**	0.94	0.90	0.89	0.00183
	4	0.85	0.88	0.87	0.00191
	5	0.93	0.90	0.86	0.00164

*Including LA abrasion values

**Selected model

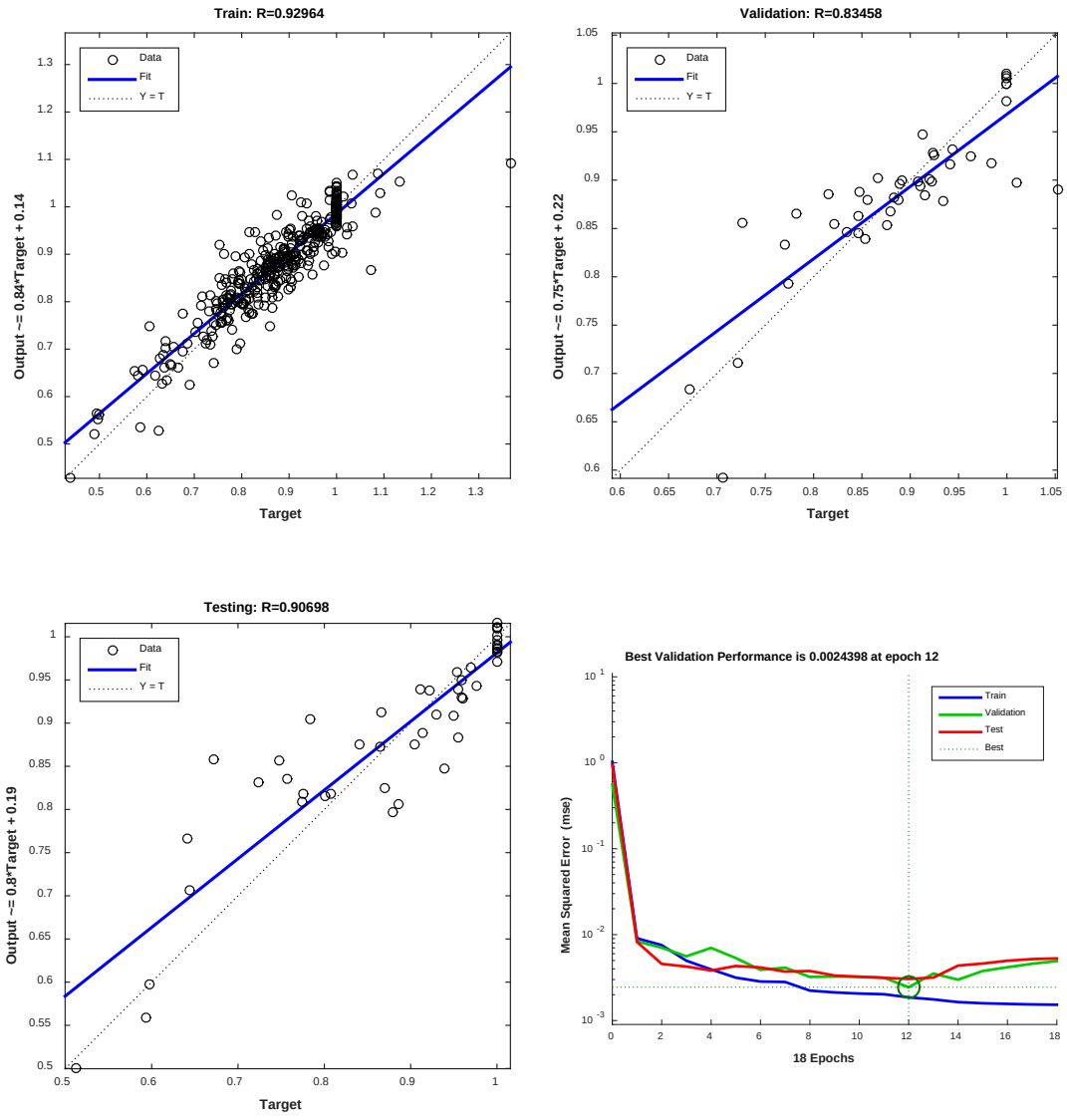

Figure 6.3 Model performance with 13 input features (Scenario I)

6.3.2. Case Study. The selected models were employed to quantify the effect of RCA incorporation on MOE of concrete for transportation infrastructure. The concrete used by the Missouri Department of Transportation (MoDOT) was used as the test bed. The test scenario involved investigating the rate of variation in MOE of concrete prepared with 323 kg/m^3 of cementitious materials and 0.40 w/cm. The simulated mixture was made with virgin coarse aggregate with 0.8% water absorption, specific gravity of 2.73, and LA abrasion of 28%. The range of the investigated RCA properties were: (1)

water absorption of 1.8%-8.5%, oven-dry specific gravity of 2.1-2.5 for the simulation according to Scenario (I); (2) water absorption of 3.2%-8.5%, oven-dry specific gravity of 2.1-2.4, and LA abrasion of 25%-53% for the simulation based on Scenario (III).

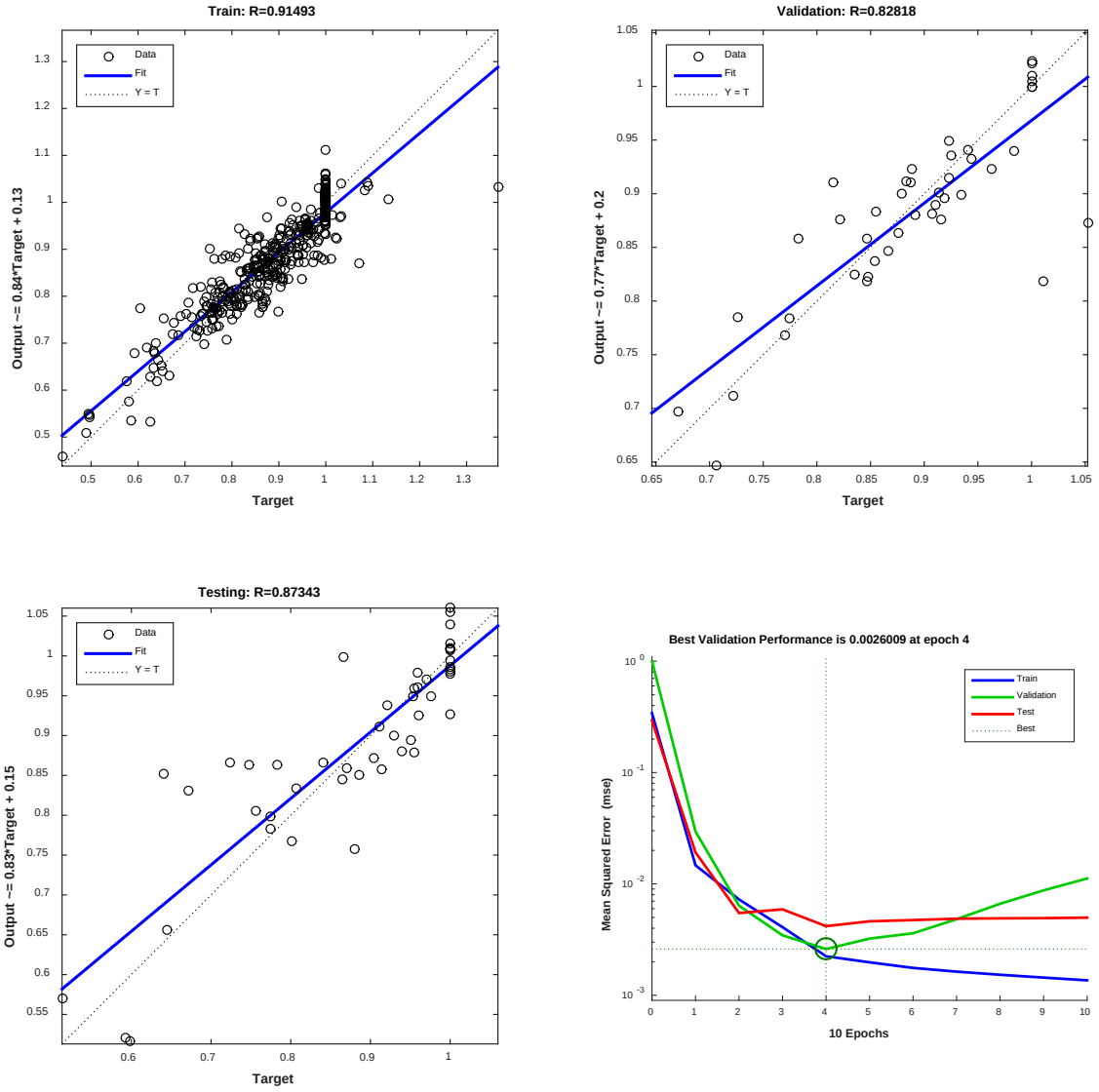

Figure 6.4 Model performance with 18 input features (Scenario II)

Figure 6.7 presents the effect of RCA specific gravity on of MOE concrete investigated in scenario I. Results indicate reduction in MOE due to the use of higher RCA content and with the use of RCA with lower specific gravity. Figure 6.8 illustrates

the effect of RCA water absorption on MOE based on scenario I. Decrease in MOE due to the use of RCA with higher water absorption was observed. For instance, the use of 20% and 50% (by mass) of RCA with 6.0% water absorption is shown to reduce the MOE by 10% and 20%, respectively. These findings are in line with the previous findings based on the obtained experimental results, discussed in previous sections.

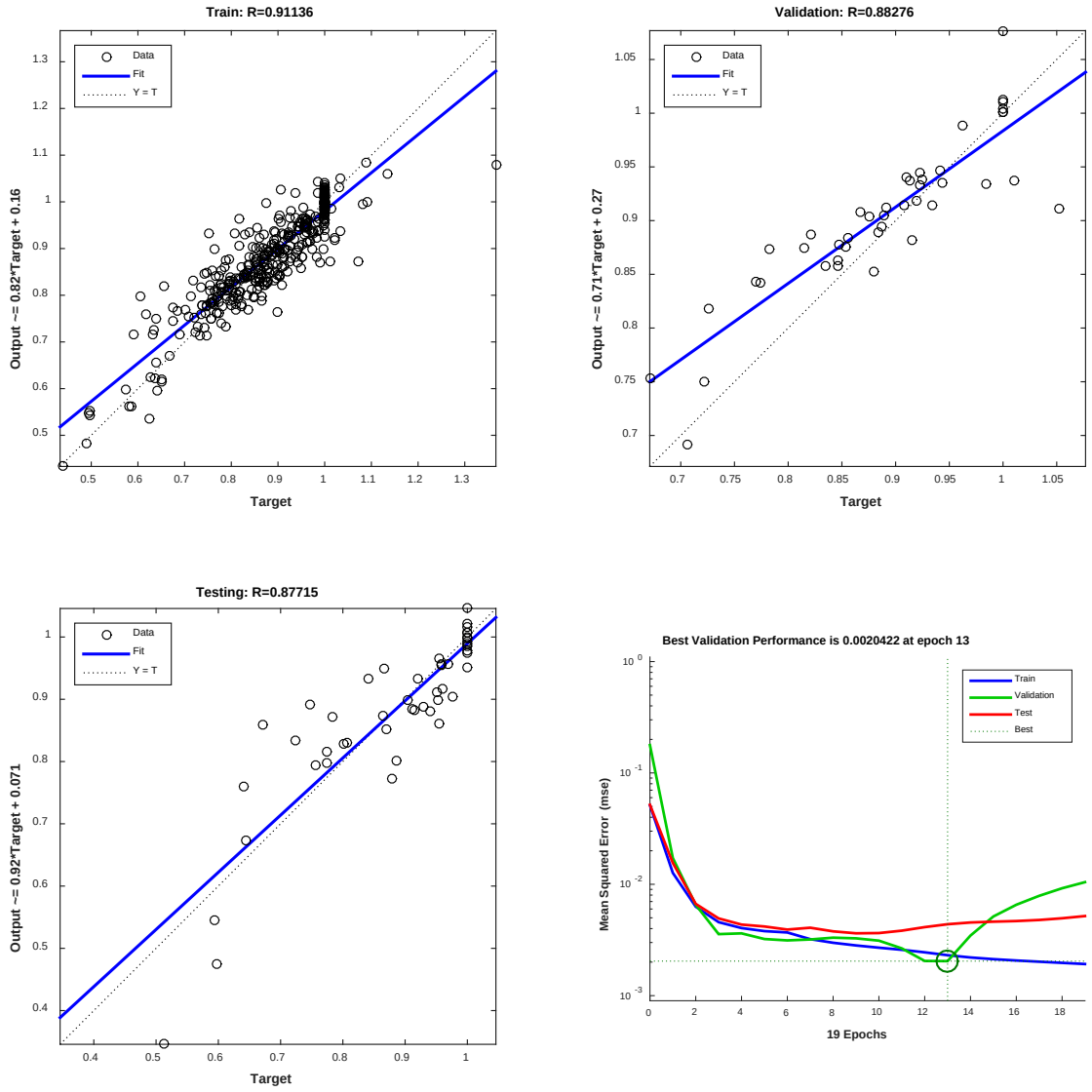

Figure 6.5 Model performance with 15 input features (Scenario III)

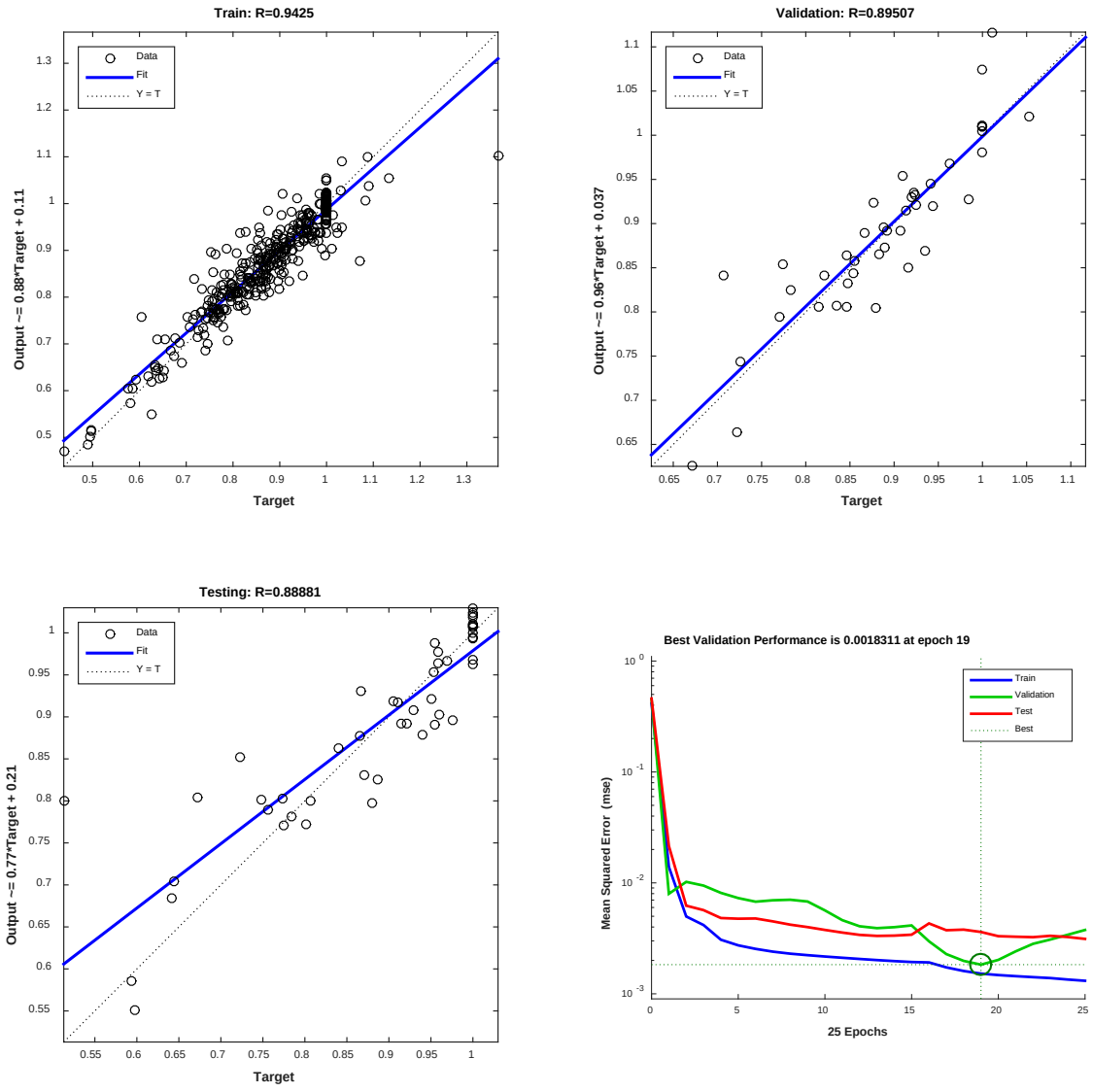

Figure 6.6 Model performance with 21 input features (Scenario IV)

Figure 6.9 presents the effect of RCA water absorption on variations in MOE of concrete based on scenario III. Similar to the data obtained from scenario I, it was observed that the use of RCA with higher water absorption reduces the MOE. Results indicate 30% reduction in MOE of simulated pavement concrete with full replacement of coarse aggregate with RCA with 7.0% water absorption.

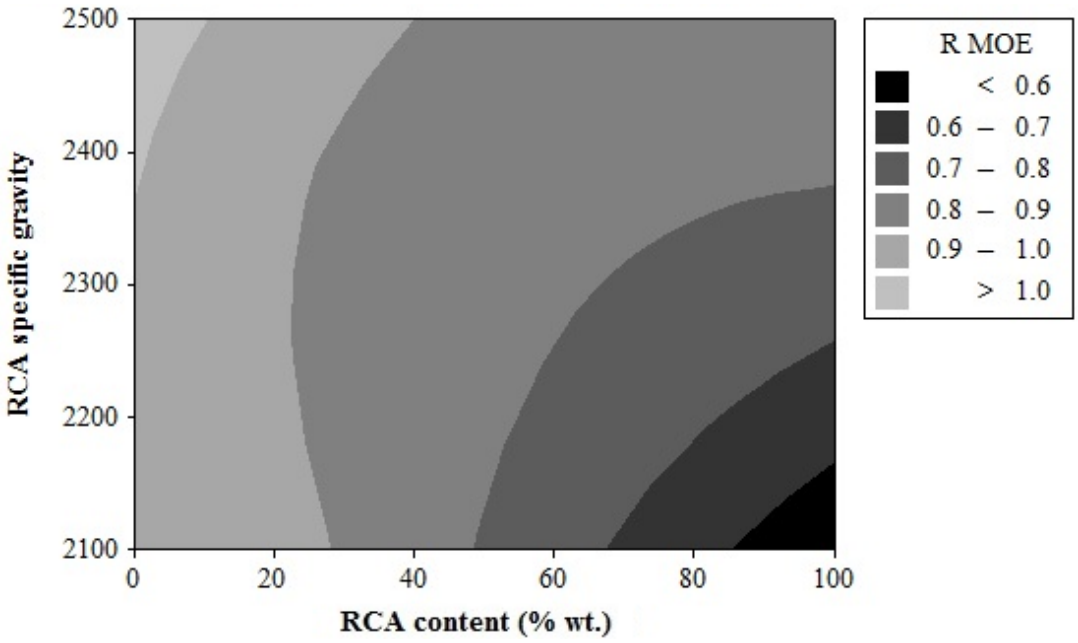

Figure 6.7 Effect of RCA specific gravity on MOE of concrete designated for rigid pavement construction, Scenario I

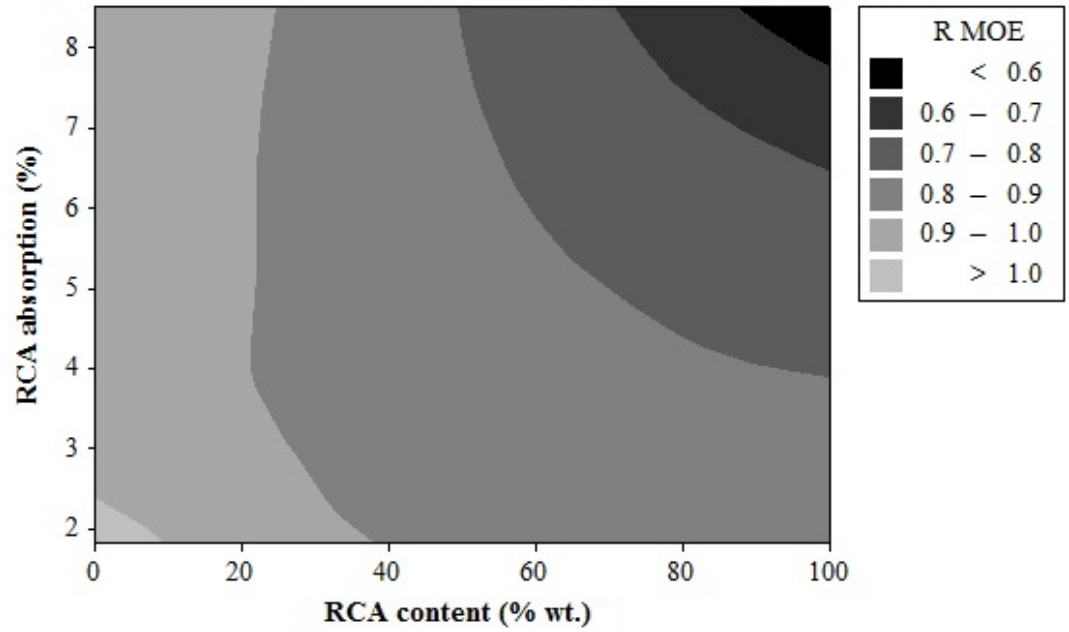

Figure 6.8 Effect of RCA absorption on MOE of concrete designated for rigid pavement construction, Scenario I

In general and based on the data obtained through the ANN modeling, it can be concluded that the simulation results follow the same trends as those observed for the

experimental investigations presented in previous sections. Results verify the viability of the proposed model and the feasibility of using the data for estimating the variations in MOE of concrete designated for rigid pavement construction.

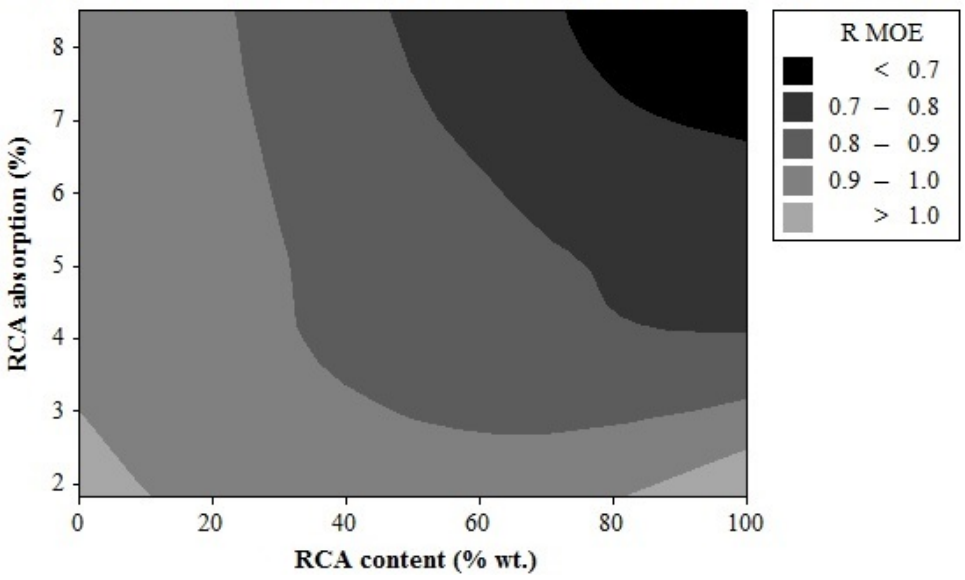

Figure 6.9 Effect of RCA water absorption on MOE of concrete designated for rigid pavement construction, Scenario III

Figure 6.10 presents the variations in MOE of the investigated concrete as a function of the RCA specific gravity. Results indicate that the use of 20% RCA with specific gravity of 2.1, or the use of over 40% RCA with specific gravity of 2.45 can lead to 10% reduction in MOE of the investigated concrete while compared to the mixture prepared without any RCA. Figure 6.11 illustrates the effect of RCA LA abrasion on MOE. As expected, results indicate a tendency to reduction in MOE as a results of using RCA with higher LA abrasion values. For instance, the use of 30% and 60% (by weight) of RCA with 40% LA abrasion was shown to reduce the MOE by about 10% and 20%, respectively, while compared to the case of the reference mixture prepared with 100% virgin coarse aggregate.

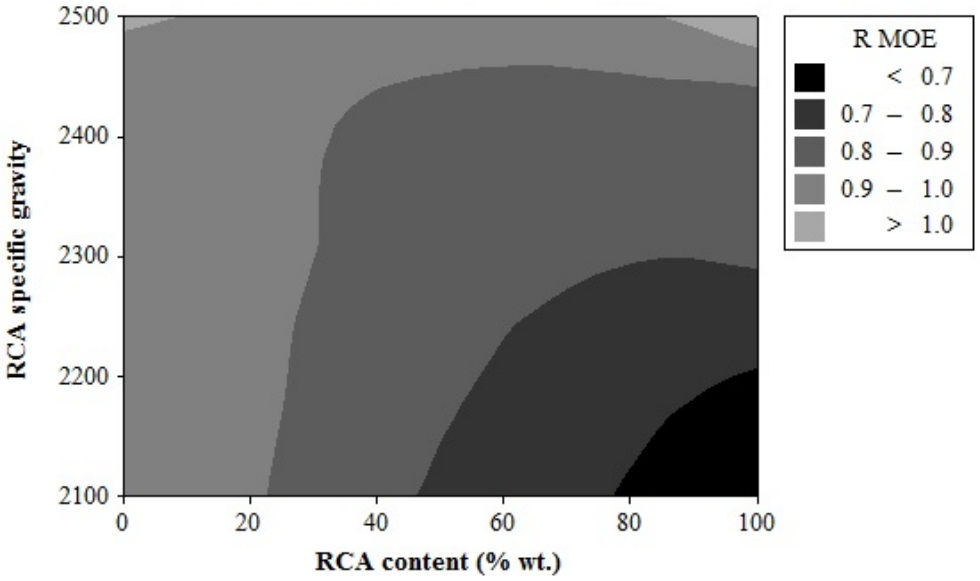

Figure 6.10 Effect of RCA specific gravity on MOE of concrete designated for rigid pavement construction, Scenario III

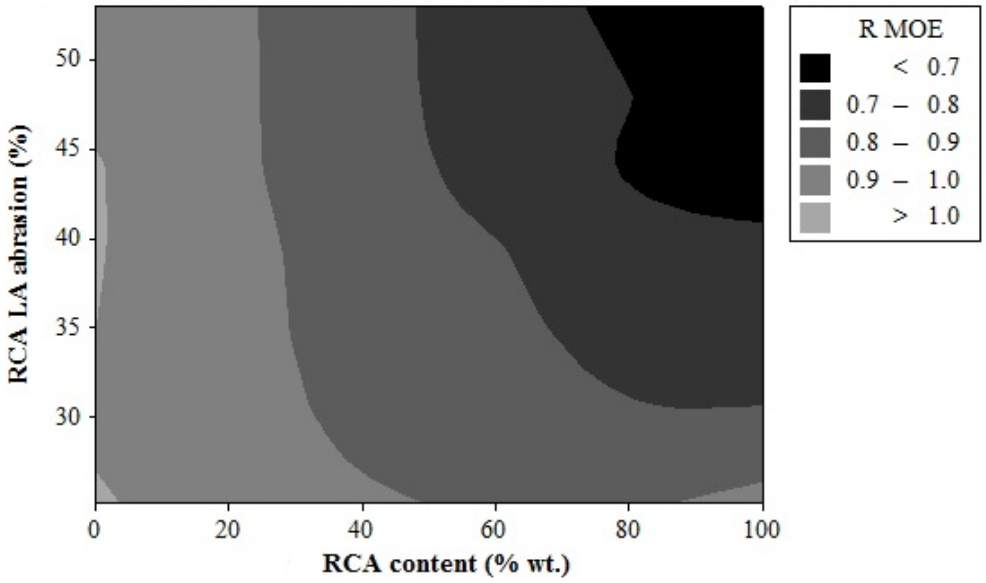

Figure 6.11 Effect of RCA LA abrasion on MOE of concrete designated for rigid pavement construction, Scenario III

6.4. REMARKS

- A database was developed in this section to investigate the effect of coarse RCA on MOE of concrete. Over 480 data series were extracted from 52 technical

papers, summarizing the key physical properties of coarse RCA and the proportions of the investigated mixtures.

- Artificial neural networks were employed for the analysis of the database. Four main scenarios were considered to investigate different combinations of the input parameters.
- Data obtained from 43 concrete mixtures investigated in the laboratory were incorporated for model validation. Results indicated strong correlation between the experimental target values and data obtained through the simulation. Strong correlations were observed for the selected models with correlation factors ranging from 0.83 to 0.94 for training, validation, and testing of the selected models.
- The availability of such a tool makes it possible to quantify the extents of the variation in MOE of different types of concrete mixtures compared to corresponding reference mixtures prepared with similar mixture proportions, i.e. same binder type and content, same water content, etc., made with different types and amounts of coarse RCA.
- The developed model was incorporated to simulate the effect of RCA characteristics on variations in MOE of concrete designated for rigid pavement construction. Depending on the RCA quality, Results indicate up to 20% reduction in MOE of the pavement concrete due to 50% coarse RCA replacement.

7. DRYING SHRINKAGE OF PAVEMENT CONCRETE MADE WITH RECYCLED CONCRETE AGGREGATE

7.1. RESEARCH SIGNIFICANCE

The research presented in this section addresses the effect of RCA on drying shrinkage of concrete designated for rigid pavement construction. A comprehensive laboratory investigation was considered to evaluate the effect of RCA content and key physical properties on drying shrinkage. Six types of coarse RCA procured from different sources and a single source of fine RCA were employed for replacement of virgin coarse an fine aggregate. The mixtures were prepared with two different binder systems, a binary and a ternary cement, and three w/cm ranging from 0.37 to 0.45. The effect of RCA replacement level, interactions with w/cm, binder type, and overall paste quality were investigated. The data obtained from laboratory investigations were incorporated to establish correlations between RCA properties and concrete shrinkage. The results presented here should be of interest to owner agencies and engineers considering the design and use of RCA in concrete for transportation infrastructure.

7.2. EXPERIMENTAL PROGRAM

7.2.1. Material Properties. The cementitious materials used for the development of the investigated concrete included a Type I/II Portland cement (OPC), a Class C fly ash (FA-C), and a ground granulated blast furnace slag (GGBS). The mixtures were proportioned with either a binary or a ternary cement. The binary cement was composed of 75% (by mass) OPC and 25% FA-C. The ternary system incorporated 35% FA-C and 15% GGBS. The binary cement was adopted from the concrete mixture design employed by the Missouri Department of Transportation (MoDOT) for rigid pavement construction (Sadati and Khayat, 2016). The ternary system was optimized based on the mechanical properties and shrinkage of concrete equivalent mortar prepared with w/cm of 0.40, as discussed in previous sections.

Two types of crushed dolomite coarse aggregate with nominal maximum size of 19 mm were incorporated in proportioning the concrete mixtures. Well-graded siliceous river-bed sand with fineness modulus of 2.47 was employed. Coarse RCA procured from

six different sources, including five commercial recycling centers and one type of a laboratory produced RCA, were considered. One source of commercially produced RCA was used for partial replacement of sand in selected mixtures. RCA particles were saturated before mixing. Table 7.1 presents the physical properties of the fine and coarse aggregates. A lignum-based water reducing admixture (WRA) with specific gravity of 1.2 and 40% solid content, and an air-entraining admixture (AEA) were incorporated.

Table 7.1 Aggregate properties

Aggregate	Source	Specific gravity	Absorption (%)	Los Angles abrasion (%)	NMAS (mm)
Virgin coarse 1	Dolomite (DOL1)	2.73	0.80	28	19
Virgin coarse 2	Dolomite (DOL2)	2.72	0.98	43	19
Sand	River-bed sand	2.63	0.40	-	4
Fine RCA1	Residual concrete, airfield	2.41	6.80	-	4
RCA 1	Laboratory produced RCA	2.35	4.56	41	19
RCA 2	Residual concrete, airfield	2.35	4.46	33	19
RCA 3	Commercial recycling, Missouri	2.25	5.75	39	19
RCA 4	Commercial recycling, Kansas	2.24	6.05	38	19
RCA 5	Commercial recycling, Missouri	2.17	7.58	44	19
RCA 6	Commercial recycling, Missouri	2.21	7.13	53	12.5

7.2.2. Concrete Mixture Proportions. In total, 38 concrete mixtures were produced with w/cm of 0.37, 0.40, and 0.45. All mixtures were proportioned using the DOL1 coarse aggregate, except for the ones cast with w/cm of 0.45, where DOL2 was used as the virgin coarse aggregate. The AEA was used to secure 6%±1% air and the WRA was incorporated to attain required initial slump values. Table 7.2 presents a summary of key mixtures proportions and fresh properties of the investigated concrete. More details on concrete mixture proportions are presented in Section 4 of this document. A coding system was adapted to label the concrete mixtures, which indicates the RCA type and content, the binder type, and the w/cm. For instance, the “RCA2-50-B-40”

mixture refers to the concrete containing 50% (by vol.) of “RCA2”, binary cement (B), and 0.40 w/cm.

Table 7.2 Summary of concrete mixture proportioning and fresh properties

Binder content (kg/m^3)	317-323
Binder type (% mass)	Binary: 75% OPC + 25% FA-C
	Ternary: 50% OPC + 35% FA-C + 15% GGBS
w/cm	037, 0.40, 0.45
C-RCA content (% vol.)	0, 30, 50, 70, 100
F-RCA1 content (% vol.)	0, 15, 30, 40
Air (%)	6±1
Slump (mm)	50±25, 150±25

7.2.3. Specimen Preparation and Testing. A drum mixer with 110-l capacity was used for preparing the concrete. The batching sequence consisted of: (1) mixing the aggregates and one third of the water at low speed for 3 min to ensure homogenized distribution and saturation of the particles; (2) AEA diluted in one third of the mixing water was added and agitation continued at high speed for 1 min; (3) introducing the cementitious materials and mixing for 1 min at high speed; (4) WRA was diluted in rest of the water and added to the batch and mixed for 2 min at high speed. After 2 min of rest, mixing was resumed for 3 min at high speed. Slump and air content in fresh state were determined according to ASTM C143 (2015) and ASTM C231 (2014), respectively. Drying shrinkage was monitored using 75×75×285 mm prisms according to ASTM C157 (2008). A vibrating table was used to secure proper consolidation of the concrete. The specimens were covered with wet burlap and plastic sheets up to 24 hours after casting. Two curing regimes were considered, where specimens were cured in lime-saturated of 21±2 ºC for either three or seven days, followed by air drying at 23±1 ºC and 50%±3% relative humidity.

7.3. RESULTS AND DISCUSSION

7.3.1. Mixtures Cast without RCA. Figure 7.1 presents the variations in drying shrinkage of the concrete mixtures cast without any RCA. The Reference concrete made with dolomite coarse aggregate (DOL1-B-40) proportioned with binary cement and 0.40 w/cm, exhibited 28-, 56-, and 90-day drying shrinkage values of 320, 430, and 440 με, respectively. Reducing the curing duration from seven to three days resulted in slightly higher shrinkage at first 28 days (11.3 vs. 13.9 με/day). However, no significant effect was observed after 90 days of drying (440 vs. 450 με).

The incorporation of ternary cement in the concrete made with virgin aggregate (DOL1-T-40) reduced the shrinkage to 340 με at 90 days. This could be attributed to lower OPC content, and modifications in pore structure in light of pozzolanic reaction caused by the use of 50% SCM. As expected, further reduction in drying shrinkage was observed in the case of the mixture cast with ternary cement and 0.37 w/cm, where the 28- and 90-day shrinkage were limited to 250 and 315 με. Increasing the w/cm from 0.40 to 0.45 increased shrinkage of the DOL2-B-45 mixture, with 90-day value of 480 με. This could also be in part attributed to lower overall quality of coarse aggregate (LA abrasion of 28% vs.43% and absorption of 0.80% vs. 0.98%).

Figure 7.2, Figure 7.3, and Figure 7.4 present the drying shrinkage results of the various mixtures made with 0.40 w/cm and binary cement (B-40), and incorporating 30%, 50%, and 100% RCA, respectively. The mixtures with lowest drying shrinkage values included the Reference concrete cast without any RCA, RCA1-30-B-40, and RCA3-30-B-40 with 90-day shrinkage of 440-470 με. Up to 100 με increase in 90-day shrinkage was observed when 30% of RCA4, RCA5, and RCA6 was used. These results correspond to 2%-23% increase in 90-day shrinkage due to 30% RCA replacement in B-40 mixtures. Despite of the use of 50% RCA replacement of virgin aggregate, the B-40 concrete made with RCA1 and RCA3 exhibited relatively low shrinkage values of 480 and 520 με at 90 days, respectively, which corresponds to 40 and 80 με increase compared to the Reference mixture. However, similar concrete made with rest of the RCA types had up to 40% higher 90-day shrinkage values. An increase in the RCA content from 0 to 100% resulted in significantly greater drying shrinkage at early age and 90 days. The concrete proportioned with 100% RCA exhibited shrinkage rate of 27-31

με/day for the first 10 days of drying, compared to 20 με/day for the Reference concrete. The maximum 90-day shrinkage of such concrete was 650 με for the RCA6-100-B-40 mixture compared to 450 με for the Reference mixture.

Figure 7.5 and Figure 7.6 present the shrinkage results obtained for mixtures made with ternary cement and 0.37 w/cm (T-37), and containing 30% and 50% RCA, respectively, from different sources. Again the lowest shrinkage was observed for the mixture cast without any RCA, with 90-day value of 315 με. The incorporation of 30% RCA resulted in an increase of 22% to 45% of the 90-day shrinkage, corresponding to 70 to 140 με increase, compared to the concrete without any RCA. Significant increase (34% to 80%) in 90-day shrinkage of the mixtures cast with ternary cement and w/cm of 0.37 was observed in concrete with 50% RCA. The mixtures proportioned with 50% RCA6 exhibited the maximum 90-day shrinkage values of 560 με. This can be attributed to the significantly higher LA abrasion and absorption rate of the RCA6, along with the reduced maximum size and rigidity of the aggregate skeleton. It should be noted that reduction in maximum aggregate size can result in reduced slump. In this case slump was kept constant with adjustment of WRA dosage.

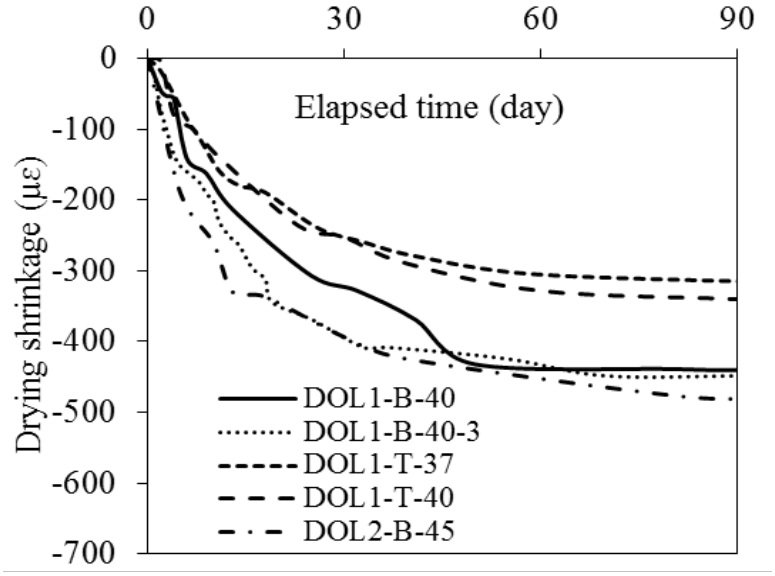

Figure 7.1 Variations in drying shrinkage of the mixtures prepared without any RCA

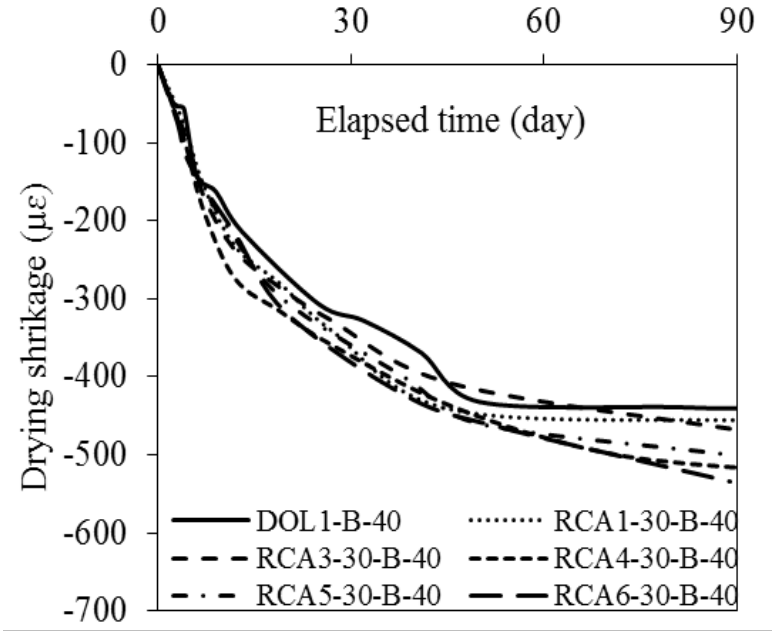

Figure 7.2 Variations in drying shrinkage of the mixtures prepared with 30% C-RCA, binary cement, and 0.40 w/cm

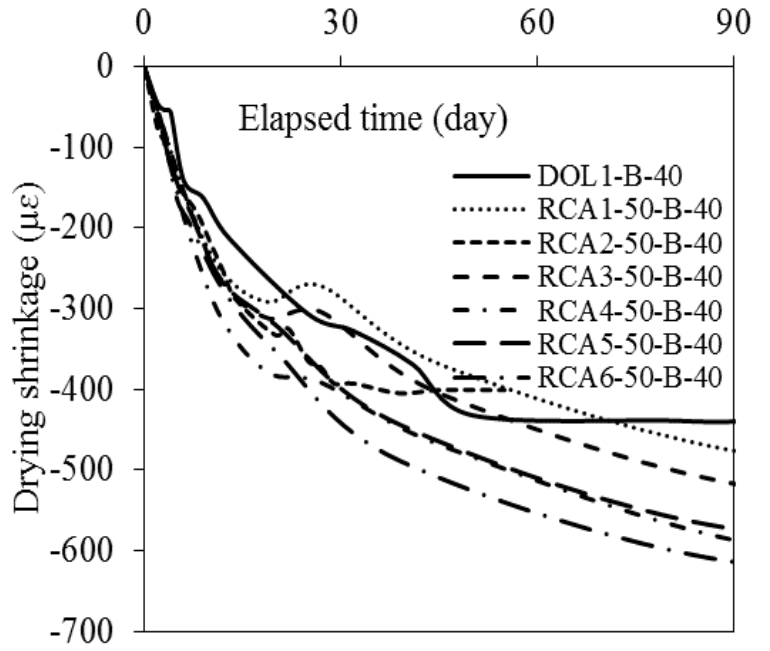

Figure 7.3 Variations in drying shrinkage of the mixtures prepared with 50% C-RCA, binary cement, and 0.40 w/cm

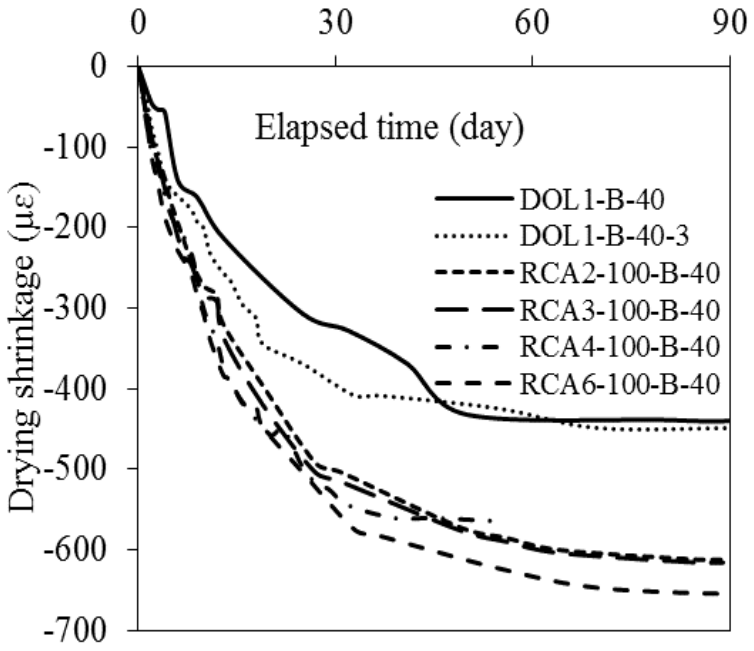

Figure 7.4 Variations in drying shrinkage of the mixtures prepared with 100% C-RCA, binary cement, and 0.40 w/cm

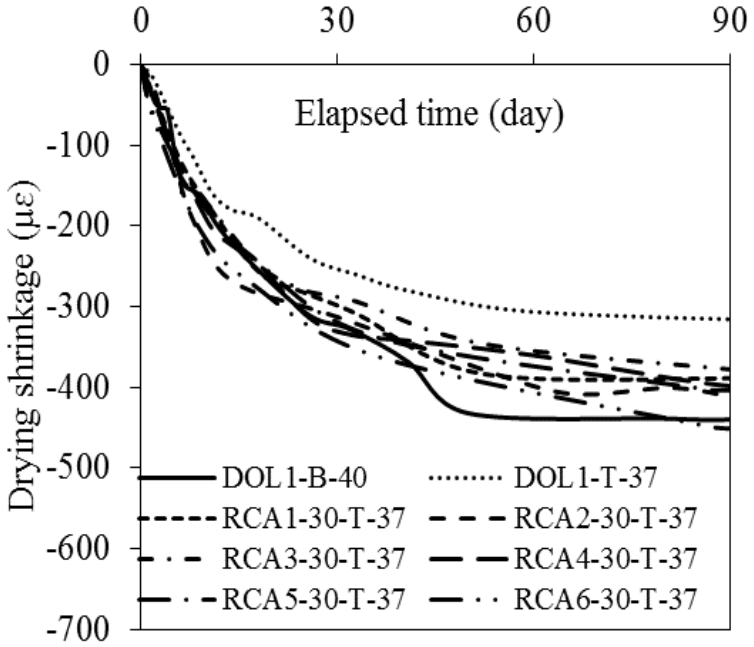

Figure 7.5 Variations in drying shrinkage of the mixtures prepared with 30% C-RCA, ternary cement, and 0.37 w/cm

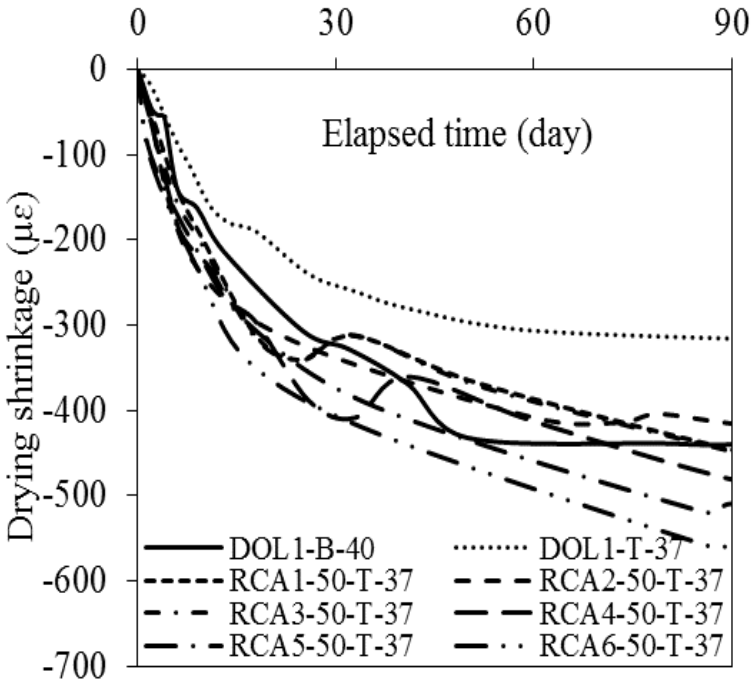

Figure 7.6 Variations in drying shrinkage of the mixtures prepared with 50% C-RCA, ternary cement, and 0.37 w/cm

7.3.2. Effect of RCA Content. Figure 7.7 presents the relative shrinkage values, defined as the ratio of drying shrinkage of concrete made with RCA to values for the corresponding mixture cast with virgin dolomitic aggregate (concrete with the same w/cm and binder type). In general, an increase in RCA content led to greater shrinkage. Considerable spread in relative shrinkage was obtained for each corresponding RCA content. These values ranged from 0.62 to 1.70, 0.89 to 2.10, 1.16 to 2.10, and 1.25 to 1.60 for concrete with 30%, 50%, 70%, and 100% RCA, respectively. Such variations in relative shrinkage reveal the fact that RCA content is not the only factor to govern shrinkage; instead, interaction with the other parameters, such as mixture proportions, and RCA quality should be considered in the analysis. The average relative shrinkage was 1.44, 1.28, 1.24, and 1.17 for the various mixtures determined at 7, 28, 56, and 90 days, respectively. This indicates that shrinkage starts with a higher rate in concrete incorporating RCA, as shown previously.

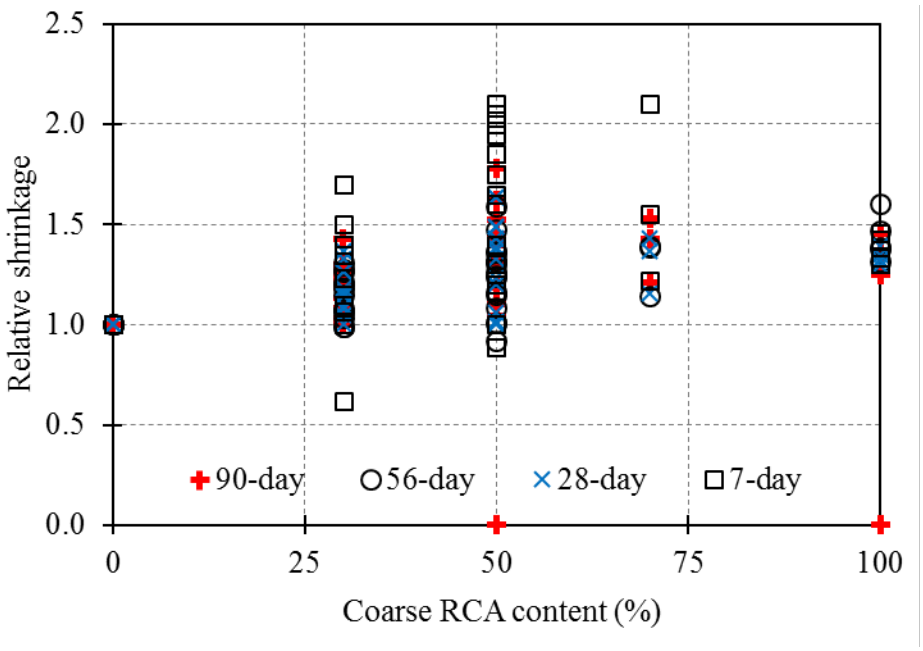

Figure 7.7 Relative shrinkage as a function of RCA content

7.3.3. Effect of Mixture Properties. Figure 7.8 presents the shrinkage results obtained for mixtures cast with 0 to 70% of RCA2 and 0 to 50% of RCA1 made with either ternary binder with 0.37 and 0.40 w/cm or binary system with 0.40 and 0.45 w/cm. The reduction in the 90-day shrinkage due to reducing the w/cm from 0.40 to 0.37 in mixtures made with up to 30% RCA2 was limited to 30 με. However, increasing the replacement ratio to 50% and 70% enhanced the degree of sensitivity to variations in w/cm where the 90-day spread was up to 85 με. For mixtures cast with RCA1, increasing the w/cm from 0.40 to 0.45 did not have any significant effect on drying shrinkage. The results suggest that shrinkage was more sensitive to variations in w/cm with higher quality paste, especially at 90 days and replacement levels greater than 50%. Considering the data presented in Figure 4, it can be suggested that the effect of RCA on drying shrinkage of mixtures proportioned with w/cm of 0.40 or less (e.g. 0.37) can be more sensitive to variations in w/cm, compared to those cast with higher than 0.40.

Figure 7.9 presents the variations in drying shrinkage of the mixtures cast with 0 and 50% of RCA2, proportioned with fixed w/cm of 0.40, and binary or ternary cement. Mixtures prepared with ternary binder were more sensitive to the use of RCA compared to those with binary cement. The use of 50% RCA in the mixture made with binary

cement increased the 7-, 28-, and 56-day shrinkage from 150 to 165, 320 to 385, and from 435 to 460 με, respectively. However, using 50% RCA in mixtures with the ternary cement increased the 7-, 28-, and 56-day drying shrinkage from 100 to 205, 245 to 365, and from 325 to 430 με, corresponding to 105%, 52%, and 32% increase, respectively. In the case of the 90-day results, using 50% RCA in concrete cast with ternary binder increased the drying shrinkage from 340 to 500 με, corresponding to 47% increase. It can be concluded that even though the shrinkage results were generally lower in mixtures with ternary system, the concrete proportioned with ternary system was more sensitive to use of 50% RCA. The degree of sensitivity to binder composition was higher in mixtures cast without any RCA where the 90-day results were 440 and 340 με for the binary and ternary systems, corresponding to 23% reduction.

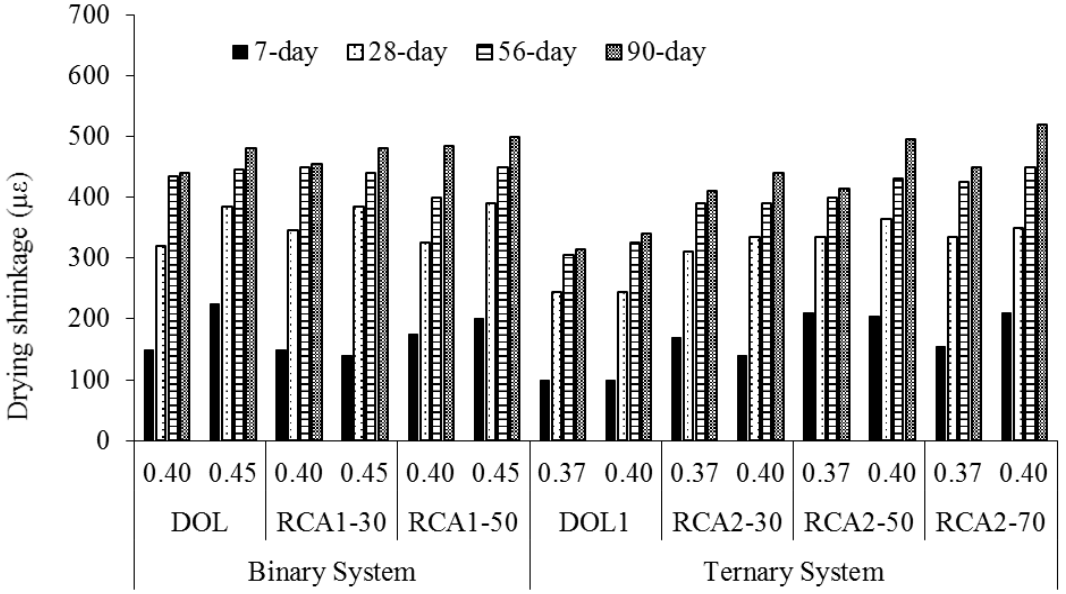

Figure 7.8 Effect of w/cm on drying shrinkage

In summary it can be concluded that concrete with enhanced paste quality, i.e. reduced w/cm and/or that made with ternary binder can exhibit higher sensitivity of increase in drying shrinkage with using RCA. However, results suggest that the partial replacement of higher quality RCA with water absorption less than 5% and LA abrasion mass loss limited to 40%, can minimize any negative effect. As an example, the RCA1-

50-T-37, RCA2-50-T37, and RCA3-50-T-37 mixtures proportioned with ternary cement and w/cm of 0.37 exhibited 90-day shrinkage values of 415, 445, and 450 με, respectively, which were comparable to 440 με for concrete cast with virgin aggregate, binary cement, and 0.40 w/cm.

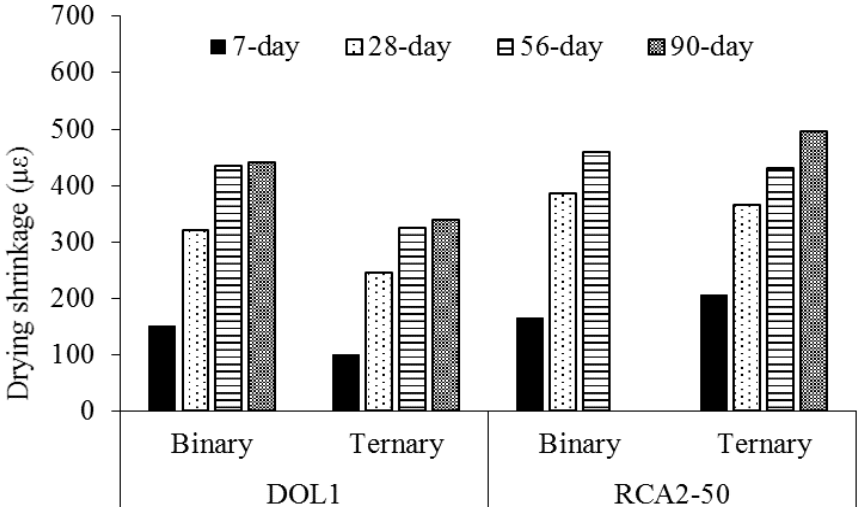

Figure 7.9 Effect of binder type on shrinkage of concrete with 50% RCA

7.3.4. Mixtures Made with Fine RCA. Figure 7.10 presents the effect of 15% (by vol.) fine RCA1 replacement on concrete made with 30% and 50% coarse RCA2, prepared with ternary cement and 0.37 and 0.40 w/cm. Regardless of the w/cm, it was generally observed that the use of 15% fine RCA increased the drying shrinkage of the investigated mixtures at all investigated ages. For instance, the 15% fine RCA replacement in concrete made with 30% coarse RCA2 and 0.40 w/cm, increased the 90-day shrinkage by about 10%; from 440 to 480 με. An increase in 90-day shrinkage from 495 to 550 με was observed due to the use of 15% fine RCA1 in concrete made with 50% coarse RCA2 and 0.40 w/cm.

Figure 7.11 presents the shrinkage results obtained for concrete made with 50% and 70% coarse RCA2, with 0 to 40% fine RCA1. All mixtures were prepared with 0.40 w/cm and ternary cement. Similar to the previous results, the increase in fine RCA content resulted in greater shrinkage values. The use of 15%, 30%, and 40% fine RCA in concrete made with 50% coarse RCA2 increased the 90-day shrinkage from 495 to 550,

560, and 650 με, respectively, corresponding to up to 31% increase in 90-day shrinkage. Trends were similar in the case of the mixtures made with 70% coarse RCA2, where the use of 15% and 30% fine RCA increased the 90-day shrinkage from 520 to 560 and 540 με.

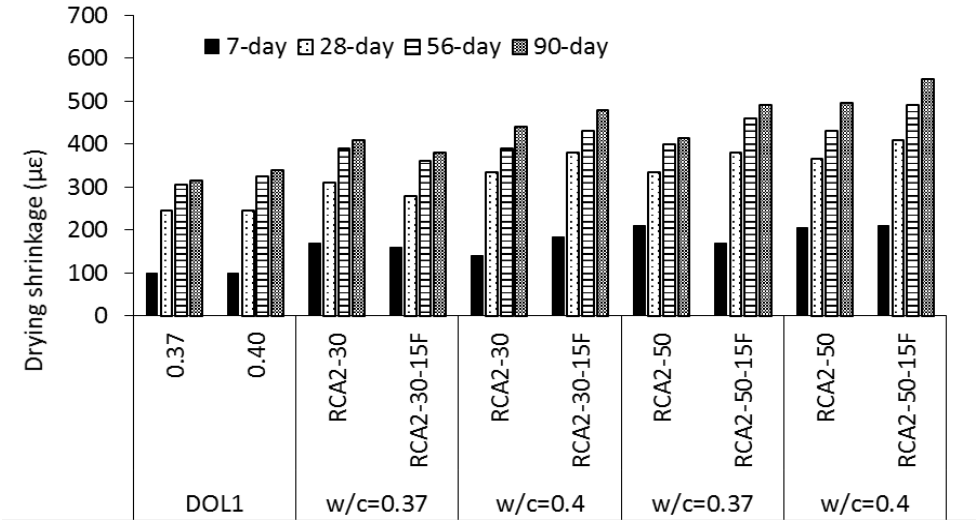

Figure 7.10 Effect of 15% fine RCA on concrete made with 30% and 50% coarse RCA2

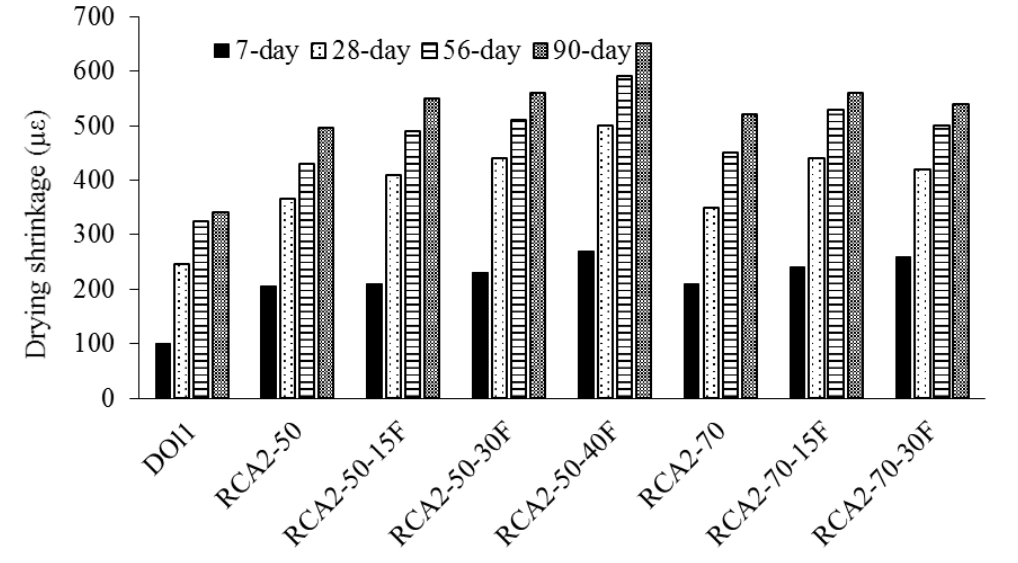

Figure 7.11 Effect of fine RCA on shrinkage of concrete made with 50% and 70% coarse RCA2

7.3.5. Quantifying the Effect of RCA Properties. As presented in Figure 7.7, a considerable spread in relative shrinkage can be observed for a given RCA content, thus indicating that the shrinkage is affected by the properties of RCA. The main physical properties include water absorption, specific gravity, and mass loss due to LA abrasion, which are employed by the standards, recommendations, and guidelines to define RCA quality (Butler et al. 2013; ASHTO 2015; Mc Neil and Kang 2012).

The residual mortar phase available in RCA particles is the main source of difference in properties of RCA compared to virgin aggregate (Silva et al., 2014). A higher content of residual mortar is normally expected to cause greater impact on engineering properties of RCA, i.e. lower specific gravity, higher absorption rate, and higher mass loss due to LA abrasion. An aggregate skeleton formed by the combination of virgin and recycled aggregate is therefore expected to exhibit relatively higher water absorption, greater LA abrasion, and lower specific gravity, compared to virgin aggregate. This is in agreement with data reported by Omary et al. (2016) that describe the properties of an aggregate blend as a linear combination of the properties of the blend constituents. Such a concept can be incorporated to calculate the properties of the aggregate combination as a function of the relative mass/volume of the fractions found in the composition. The following were used to determine the oven-dry specific gravity, water absorption, and mass loss due to LA abrasion of a given combination of coarse aggregate, respectively, as suggested by Omary et al. (2016).

$$Coarse_{SG} = [(Mass_{RCA} \times RCA_{SG}) + (Mass_{NC} \times NC_{SG})]/(Mass_{Rca} + Mass_{NC}) \quad (7\text{-}1)$$

$$Coarse_{Abs} = [(Mass_{RCA} \times RCA_{Abs}) + (Mass_{NC} \times NC_{Abs})]/(Mass_{Rca} + Mass_{NC}) \quad (7\text{-}2)$$

$$Coarse_{LA} = [(Mass_{RCA} \times RCA_{LA}) + (Mass_{NC} \times NC_{LA})]/(Mass_{Rca} + Mass_{NC}) \quad (7\text{-}3)$$

where $Mass_{RCA}$ is the RCA content (kg/m^3), $Mass_{NC}$ is the virgin coarse aggregate content (kg/m^3), RCA_{SG} is the oven-dry specific gravity of RCA, NC_{SG} is the oven-dry specific gravity of the virgin coarse aggregate, RCA_{Abs} is the water absorption of the RCA (%), NC_{Abs} is the virgin coarse aggregate absorption rate (%), RCA_{LA} is the mass loss due to LA abrasion of RCA (%), NC_{LA} is the mass loss due to LA abrasion of the

virgin coarse aggregate (%), and $Coarse_{SG}$, $Coarse_{Abs}$, and $Coarse_{LA}$ are the oven-dry specific gravity, water absorption rate (%), and LA abrasion (%) of the coarse aggregate combination, respectively.

Data obtained from testing of the concrete mixtures subjected to seven days of initial moist curing were incorporated to establish the correlations between combined aggregate physical properties and drying shrinkage at 7, 28, 56, and 90 days. Two main scenarios were investigated: (1) concrete prepared with 323 kg/m^3 of binary cement and 0.40 w/cm; (2) concrete made with 323 kg/m^3 of ternary cement and 0.37 w/cm.

Figure 7.12 and Figure 7.13 present the correlation between the oven-dry specific gravity of coarse aggregate combination and drying shrinkage at 7, 28, 56, and 90 days. As expected, shrinkage was decreased as a function of increase in specific gravity of combined coarse aggregate. The coefficient of determination (R^2) values of the linear correlations obtained between the shrinkage results and the combined specific gravity, ranged from 0.51 to 0.74 and 0.76 to 0.81 for the T-37 and B-40 mixtures, respectively. Higher R^2 values were observed for the B-40 mixtures compared to the T-37 concrete for corresponding ages. Comparing the slope of the regression lines in these figurs suggests that shrinkage values are more sensitive to reduction in combined specific gravity, i.e. higher RCA content and/or lower quality RCA, at later ages. As an instance, a reduction of 0.1 in specific gravity of coarse aggregate combination could lead to 47 με increase in 90-day shrinkage of the mixtures cast with binary cement and w/cm of 0.40. Such a reduction was 19 με at 7 days. This was in line with data presented in Figure 2 where shrinkage of RCA mixtures were significantly higher than those of corresponding Reference mixtures at later ages. The trend lines for the T-37 mixtures had higher slopes than the B-40 ones, suggesting that the increase in RCA content and/or use of lower RCA quality can have a more pronounced effect on shrinkage.

Figure 7.14 and Figure 7.15 present the correlation between the water absorption of the combined coarse aggregate and drying shrinkage at 7, 28, 56, and 90 days. Increase in shrinkage was observed as a result of higher absorption rate of the combined coarse aggregate. Values of R^2 obtained for the linear correlation between the shrinkage results and the combined water absorption ranged between 0.51 and 0.85 for the 7-day and 90-

day measurements of the T-37 mixtures, respectively. Such values ranged from 0.77 to 0.80 for the B-40 mixtures.

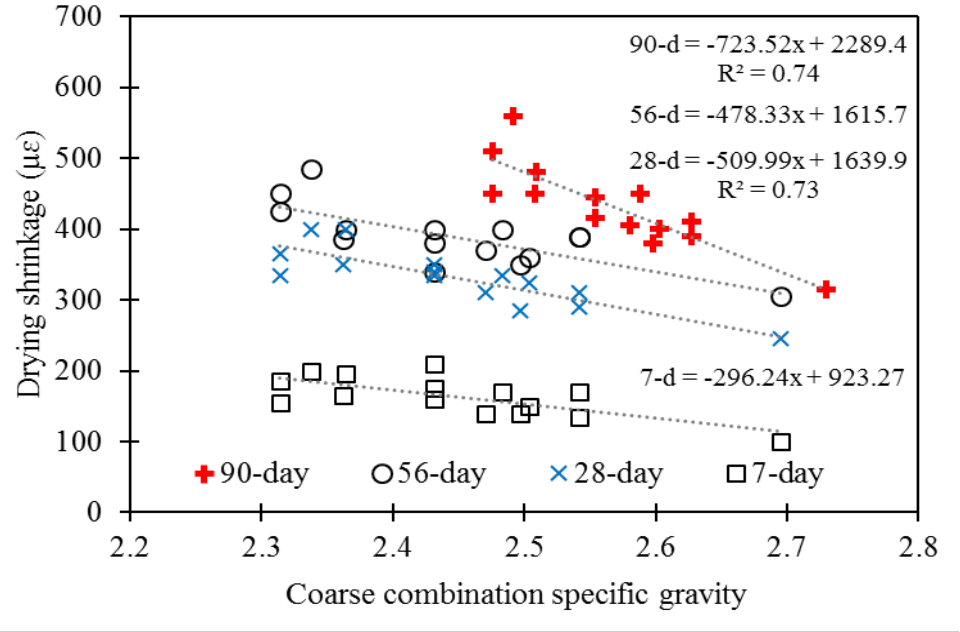

Figure 7.12 Effect of combined coarse aggregate specific gravity on drying shrinkage of concrete made with ternary cement and 0.37 w/cm

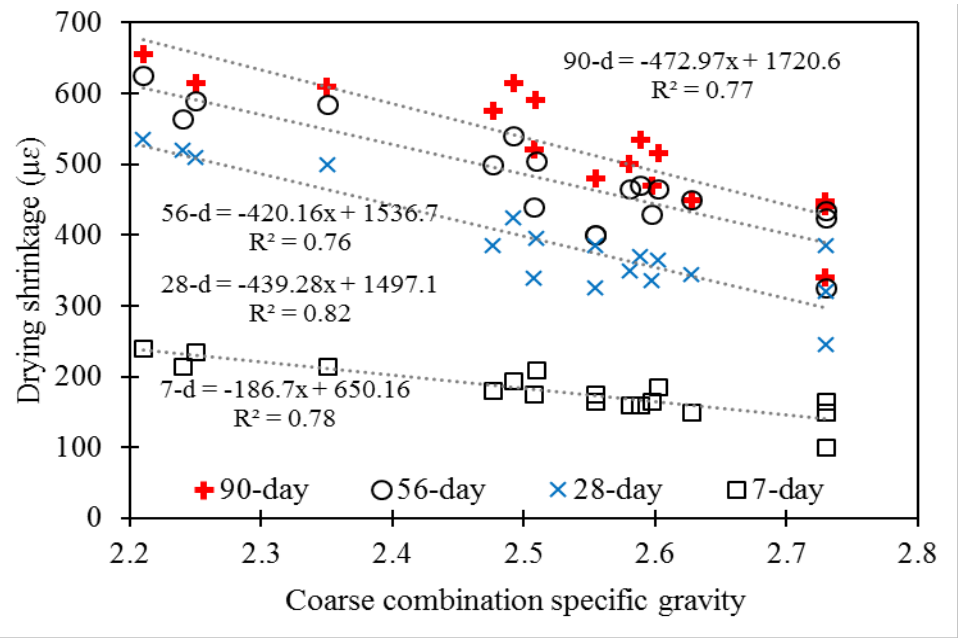

Figure 7.13 Effect of combined coarse aggregate specific gravity on drying shrinkage of concrete made with binary cement and 0.40 w/cm

Higher slope of the 90-day trend lines suggest that the degree of sensitivity to absorption, is increasing with elapsed time from drying. As an instance, an increase of 1% in water absorption of coarse aggregate combination in mixtures made with binary cement and w/cm of 0.40 could increase the 90-day shrinkage by 42 με. Such an increase is expected to be limited to 17 με for 7-day results. Even though the shrinkage values of the T-37 mixtures were generally lower than those of the B-40 ones, higher slopes of the trend lines obtained for the T-37 mixtures reveal the fact that the T-37 mixtures were more sensitive to RCA incorporation, which was in line with previous observations.

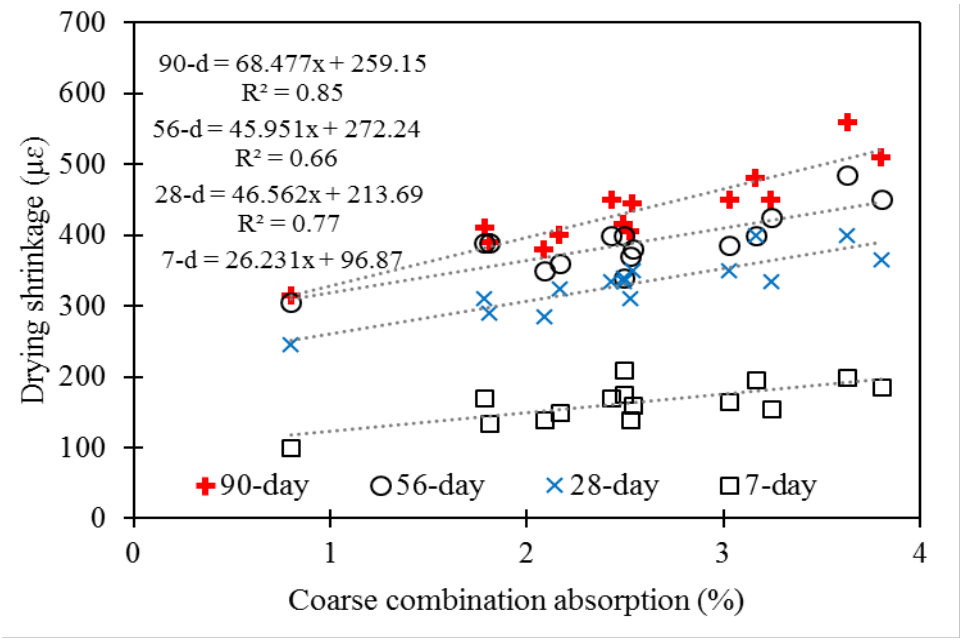

Figure 7.14 Effect of combined coarse aggregate water absorption on drying shrinkage of concrete made with ternary cement and 0.37 w/cm

Figure 7.16 and Figure 7.17 present the correlation between the LA abrasion of the combined coarse aggregate and drying shrinkage at 7, 28, 56, and 90 days. Shrinkage was reduced with a decrease in LA abrasion value of the coarse aggregate combination. Values of R^2 ranged from 0.28 to 0.81 and 0.54 to 0.57 for the T-37 and B-40 mixture, respectively. Similar to previous observations, slopes of the trend lines were higher in the case of the T-37 mixtures, indicating that the increase in RCA content and/or use of RCA of lower quality can have a stronger impact on shrinkage. Higher slope of the 90-day

trend lines suggest that the degree of sensitivity to LA abrasion, is increasing at later ages. As an instance, an increase of 5% in LA abrasion of coarse aggregate combination in mixtures cast with ternary cement and w/cm of 0.37 could increase the 90-day shrinkage by 95 με. Such an increase is expected to be limited to 28 με for 7-day results.

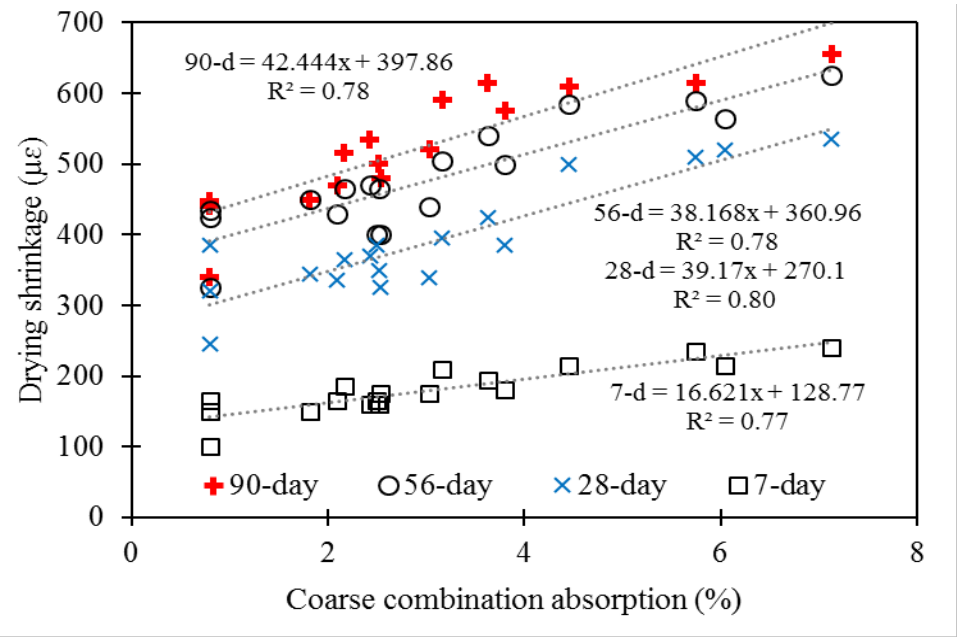

Figure 7.15 Effect of combined coarse aggregate water absorption on drying shrinkage of concrete made with binary cement and 0.40 w/cm

Comparing the regression results for the 90-day data presented in Figure 7.12 to Figure 7.17, where less variability was obtained, it can be concluded that the combined specific gravity and combined absorption are better predictors for drying shrinkage of the B-40 mixtures. In the case of the B-40 concrete, the R^2 values were 0.77 and 0.78 for the combined specific gravity and combined absorption compared to 0.57 for the combined LA abrasion results. Combined absorption rate and combined LA abrasion values resulted in more accurate predictors of the 90-day shrinkage of the T-37 mixtures. The R^2 values were 0.85 and 0.81 for the combined absorption and combined LA abrasion of the T-37 mixtures, compared to R^2 of 0.74 for the combined specific gravity. In summary, it can be concluded that regardless of the w/cm and binder type, the water absorption and

replacement rate of RCA can be considered as the main factors governing the drying shrinkage of a RCA concrete.

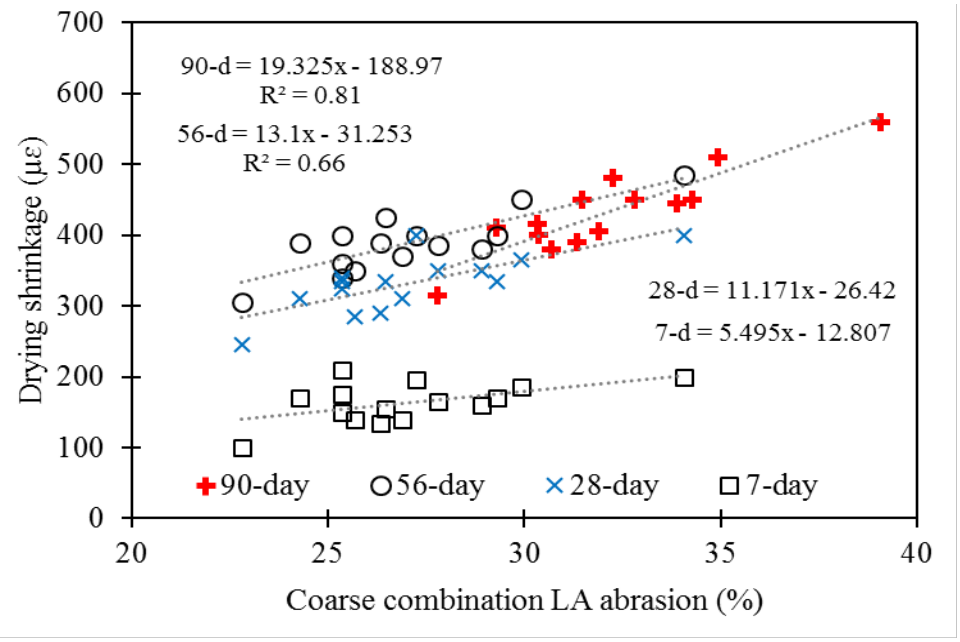

Figure 7.16 Effect of combined coarse aggregate Loss Angeles abrasion on drying shrinkage of concrete made with ternary cement and 0.37 w/cm

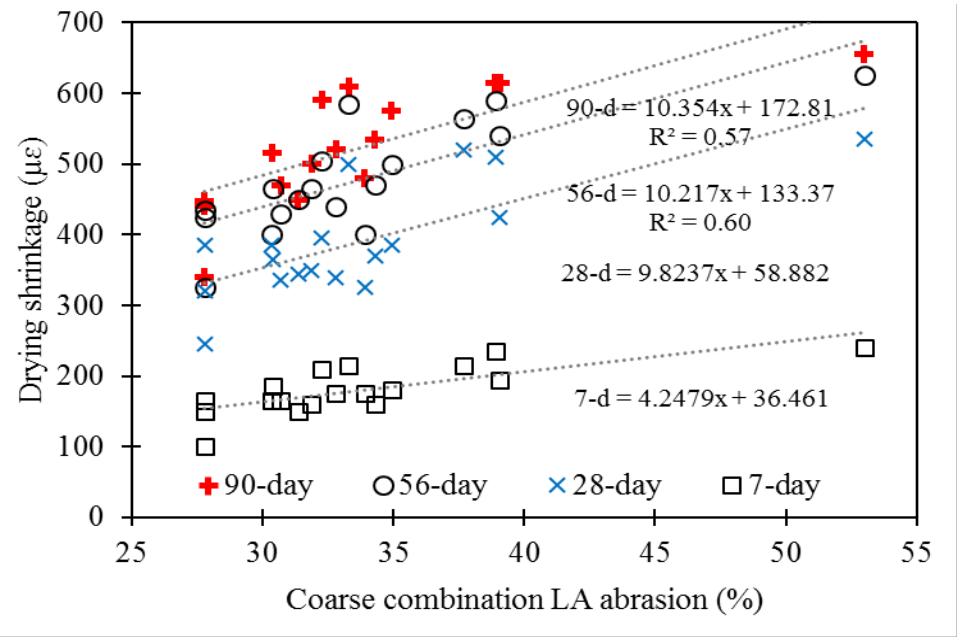

Figure 7.17 Effect of combined coarse aggregate Loss Angeles abrasion on drying shrinkage of concrete made with binary cement and 0.40 w/cm

Evaluating the coupled effect of the factors presented in in Figure 7.12 to Figure 7.17, did not present any significant effect. Figure 7.18 and Figure 7.19 present examples of contour diagrams generated based on the results of the 90-day drying shrinkage results for the B-40 mixture. The virgin coarse aggregate considered in this example has an absorption of 0.8% and an oven-dry specific gravity of 2.73.

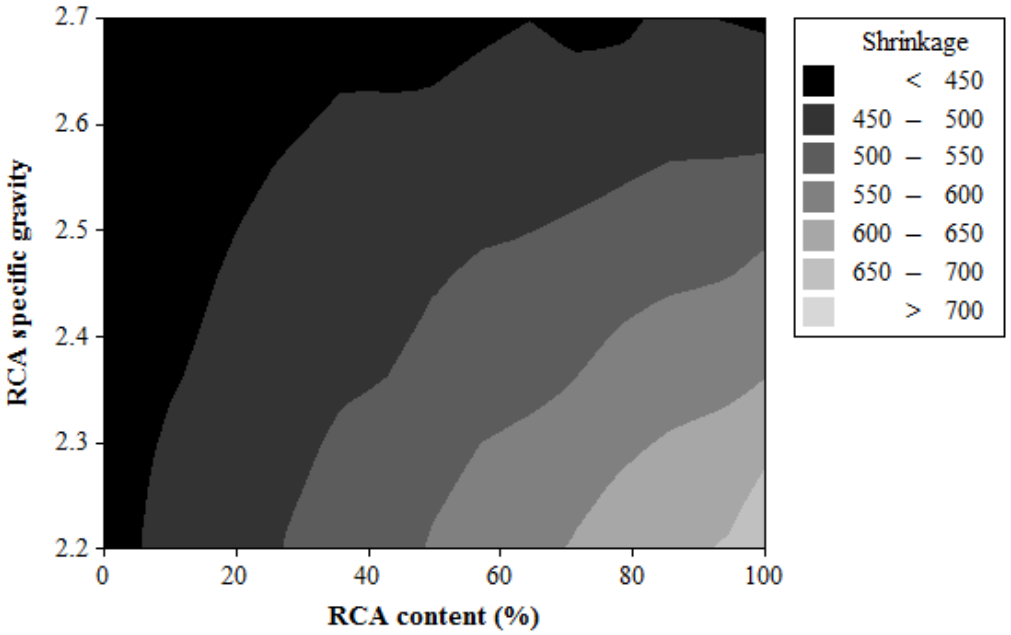

Figure 7.18 Variations in 90-day drying shrinkage of concrete made with binary cement and 0.40 w/cm as a function of RCA specific gravity

Based on the results presented in Figure 7.18, the incorporation of 20%, 40%, 60%, 80%, and 100% RCA with specific gravity of 2.50 can result in 90-day shrinkage of 460, 480, 500, 520, and 540 με, compared to about 440 με for the mixture without any RCA. For a mixture cast with 50% RCA, increasing the specific gravity of RCA from 2.20 to 2.45 and 2.70 is shown to reduce the 90-day shrinkage from 560 to 500 and <450 με, respectively. Using the data presented in Figure 7.19, it can be concluded that the incorporation of 30%, 50%, 80%, and 100% RCA with 6.0% absorption rate, could lead to an increase in 90-day shrinkage from <450 to approximate values of 500, 550, 600, and 650 με, respectively. In the case of a concrete proportioned with 50% RCA, the increase in RCA absorption from 3.0% to 5.0% and 8.0% can lead to greater shrinkage of 475 to 525 and 575 με, respectively.

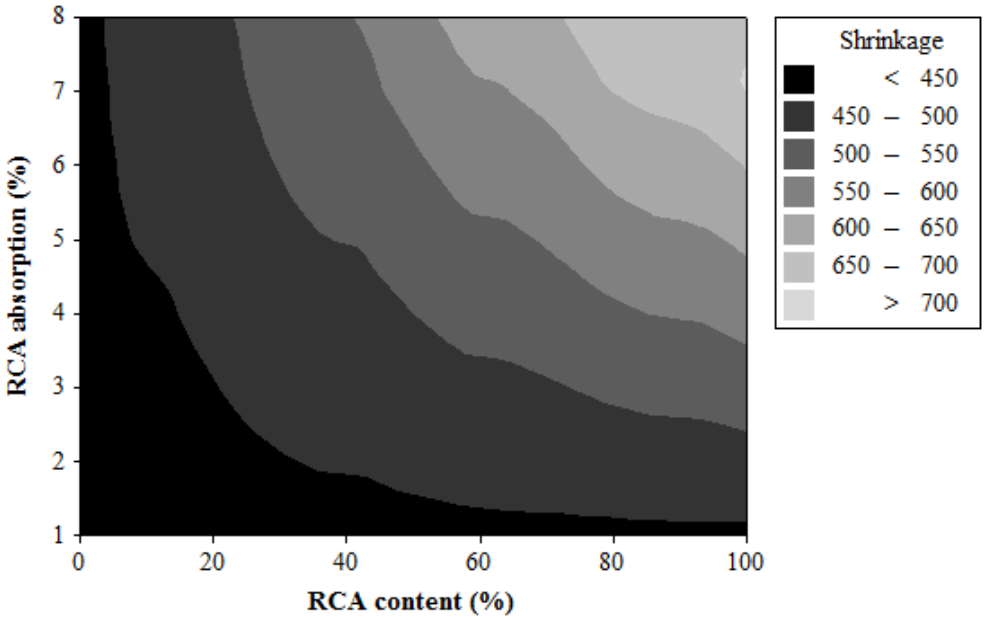

Figure 7.19 Variations in 90-day drying shrinkage of concrete made with binary cement and 0.40 w/cm as a function of RCA specific gravity

These results indicate that for a typical RCA replacement of 30%, drying shrinkage can increase to values of up to 525 με, compared to a Reference concrete with 90-day shrinkage of about 450 με. In an extreme case where 100% RCA with absorption of up to 8.0% or specific gravity as low as 2.2 is used, there is a potential for up to 50%-55% increase in drying shrinkage for the B-40 mixture, which corresponds to MoDOT Reference pavement concrete. This is in agreement with the survey conducted by (NCHRP 2013) and the correction factors presented in literature review in Section 2.

7.4. REMARKS

The effect of RCA on drying shrinkage of concrete designated for transportation infrastructure was investigated. A binary cement containing 25% Class C fly ash and a ternary system with 35% Class C fly ash and 15% GGBS were incorporated. The mixtures were proportioned with w/cm of 0.37, 0.40, and 0.45. RCA procured from five commercial recycling centers along with one laboratory produced RCA were employed at 30% to 100% replacement. Based on the results presented in this paper, the following conclusions are warranted:

- The use of fine RCA increased the drying shrinkage significantly. The use of up to 40% fine RCA in concrete made with 50% coarse RCA2 increased the 90-day shrinkage from 495 to 650 με, corresponding to up to 31% increase in 90-day shrinkage. On the average, the use of coarse RCA increased the drying shrinkage by 44% and 17% at 7 and 90 days, respectively.
- Key physical properties of RCA, including water absorption, specific gravity, and LA abrasion affect shrinkage. For example, in the case of a mixture proportioned with binary cement and 0.40 w/cm and 50% RCA, increasing the absorption of the RCA from 3.0% to 5.0% and 8.0% increased shrinkage from 475 to 525 and 575 με, respectively.
- The properties of the concrete mixture also affect the sensitivity to using RCA. The use of higher quality paste given a lower w/cm (0.37 vs. 0.40) and a ternary cement vs. binary system was more sensitive to the rate of RCA replacement. As an instance, the increase in 90-day shrinkage due to increasing the w/cm from 0.37 to 0.40 in mixtures with up to 30% RCA2 was limited to 30 με. However, increasing the replacement ratio to 50% and 70% enhanced the degree of sensitivity to variations in w/cm with a 90-day spread of 85 με due to increase in w/cm from 0.37 to 0.40.
- The water absorption, specific gravity, and LA abrasion of the combined RCA and virgin coarse aggregate have significant effect on drying shrinkage. The water absorption characteristics yielded the highest R^2 values of 0.78 and 0.85 for mixtures cast with 0.40 and 0.37 w/cm, respectively.
- The RCA replacement level (% mass), water absorption rate, and specific gravity were used as input parameters to develop contour graphs to enable prediction of 90-day shrinkage of concrete typically used by State DOTs for rigid pavement construction. Results indicate up to 17% increase (from 450 to 525 με) in 90-day shrinkage of such a mixture due to incorporation of 30% RCA with specific gravity of 2.2 and water absorption of 8.0%. Up to 55% increase in 90-day drying shrinkage due to full replacement of such RCA in these pavement mixtures could be expected.

8. RESTRAINED SHRINKAGE CRACKING OF CONCRETE MADE WITH RECYCLED AGGREGATE

8.1. RESEARCH SIGNIFICANCE

Cracking can lead to pavement distress, resulting in significant reduction in service life. Greater drying shrinkage as a result of high surface-to-volume ratio, along with high degree of restraint exerted by the base layer and adjacent slabs can increase cracking potential in rigid pavement. The interaction between the tensile stresses induced by shrinkage, material's tensile strength, and stress relaxation in a viscoelastic material, like concrete, governs cracking under restrained conditions (Monteiro 2006, Shah and Weiss 2006, Weiss and Shah 2002, Loser and Leemann 2009). The incorporation of RCA can affect these material characteristics. Variations in volume stability, modulus of elasticity (MOE), and tensile properties of concrete due to the use of RCA can alter the cracking resistance under restrained conditions. Cracking potential under restrained shrinkage conditions is reduced with the decrease in drying shrinkage and MOE and the increase in tensile strength (Monteiro 2006). Compared to virgin aggregate, the use of RCA can decrease tensile strain capacity and increase drying shrinkage, leading to greater risk of cracking. However, the use of RCA can also reduce the MOE of the concrete, thus enhancing stress relaxation and reducing the risk of cracking (Hwang and Khayat 2010).

Availability of residual mortar in RCA particles reduces the overall stiffness of the coarse aggregate skeleton and increases the absolute volume of mortar in the hardened state. This reduces the rigidity of the concrete, resulting in lower MOE compared to the mixtures prepared with virgin aggregate (Knaack and Kurama 2014, Fonseca et al. 2011, Vieira et al. 2011). The existence of micro-cracks and defected interfacial transition zone (ITZ), typical of RCA materials, can significantly affect the MOE (Monteiro 2006).

The porosity of adhered mortar, along with higher content of fines and dust in RCA, can increase the water absorption of the RCA compared to virgin aggregate. Results of a survey (FHWA 2004) reveal the fact that coarse RCA sources typically exhibit absorption of 2% to 6% compared to typical values of lower than 2% for virgin

aggregate. Such increase in water absorption, along with the reduced restraining capacity of the less rigid RCA can lead to greater shrinkage (Henry et al. 2011, Corinaldesi 2010).

The decrease in tensile strength of concrete as a result of RCA can also enhance the risk of cracking. The presence of deleterious materials (e.g. bituminous and organic materials), weakened ITZ and micro-cracks in RCA can lower tensile properties of the concrete. On the other hand, rough surface texture and typically angular shape of RCA particle can have beneficial effect on tensile strength of mixtures incorporating RCA (Kim and Yun 2013, Yang et al. 2008, Kang et al. 2014).

The above properties of concrete made with RCA can indeed influence the potential for cracking of concrete using RCA under restrained conditions. The present research investigates the effect of RCA on cracking under restrained shrinkage. Concrete mixtures made with either 50% or 100%, by volume, of RCA were investigated using RCA from four different sources. A Reference concrete corresponding to mixture used for rigid pavement construction was evaluated. The concrete was produced with either binary or ternary cements with 0.40 or 037 w/cm. Mechanical properties, drying shrinkage, and cracking potential due to restrained shrinkage were investigated.

8.2. EXPERIMENTAL PROGRAM

8.2.1. Material Properties. Two binder systems including a binary cement containing Type I/II Portland cement and 25% (by mass) FA-C and a ternary system with 35% FA-C and 15% ground granulated blast furnace slag (GGBS) were incorporated. The ternary binder was optimized based on enhanced mechanical properties and reduced drying shrinkage of concrete equivalent mortar made with w/cm of 0.40 as discussed in previous sections. Crushed dolomite with a nominal maximum size of 19 mm was used for the virgin aggregate. Well-graded siliceous river-bed sand with a fineness modulus of 2.47 was incorporated. Four types of coarse RCA procured from different commercial recycling centers in states of Missouri and Kansas were employed. Table 8.1 presents the physical properties of the fine and coarse aggregates. A lignum-based water reducing admixture (WRA) with specific gravity of 1.2 and 40% solid content and an air-entraining admixture (AEA) were incorporated to secure required fresh properties.

Table 8.1 Aggregate properties

Aggregate	Source/Type	Specific gravity	Absorption (%)	Los Angles abrasion (%)	NMAS (mm)
Virgin Coarse	Dolomite	2.73	0.80	28	19
Fine	River-bed sand	2.63	0.40	-	4
RCA 1	Airfield, Missouri	2.35	4.46	33	19
RCA 2	Waste concrete, MO	2.21	7.13	53	12.5
RCA 3	Waste concrete, KS	2.24	6.05	38	19
RCA 4	Waste concrete, MO	2.25	5.75	39	19

8.2.2. Mixture Proportions. All investigated mixtures were proportioned with natural river-bed sand and a binder content of 323 kg/m^3. The binder content was kept relatively low to reduce shrinkage. The Reference concrete was prepared using the binary cement, a 0.40 w/cm, and virgin coarse aggregate. Four mixtures were produced with 100% RCAs procured from different sources (RCA1 to RCA4). RCA1 that corresponds to recycled concrete from airfield in St. Louis, Missouri was used for the development of three mixtures containing 50% RCA. These mixtures were proportioned with w/cm of 0.37 or 0.40 and binary or ternary binder composition. All RCAs were saturated before mixing.

The admixture dosages were adjusted to secure an initial slump value of 125 ± 25 mm and an air content of 6% ± 1%, respectively. A slump value of 50 ± 15 mm is typically recommended for slip form paving (Sadati and Khayat 2016). However, higher values of slump were considered in this research to ensure proper consolidation of the ring specimens. Table 8.2 summarizes the mixture proportions of the investigated concrete. The air content in fresh state and the slump value at the end of the mixing procedure is also included in this table. The target air contents was 6%±1%. The target slump value was 125±25 mm.

Table 8.2 Proportions and fresh properties of the investigated concrete mixtures

Mixture ID	Ref.	C1-50-T37	C1-50-T40	C1-50-B40	C1-100-B40	C2-100-B40	C3-100-B40	C4-100-B40
Cement (kg/m^3)	243	162	162	243	243	243	243	243
FA-C (kg/m^3)	81	113	113	81	81	81	81	81
GGBS (kg/m^3)	-	48	48	-	-	-	-	-
w/cm	0.40	0.37	0.40	0.40	0.40	0.40	0.40	0.40
Sand (kg/m^3)	782	793	782	782	782	782	782	782
Virgin coarse (kg/m^3)	1121	560	560	560	-	-	-	-
RCA 1 (kg/m^3)	-	489	482	482	965	-	-	-
RCA 2 (kg/m^3)	-	-	-	-	-	907	-	-
RCA 3 (kg/m^3)	-	-	-	-	-	-	920	-
RCA 4 (kg/m^3)	-	-	-	-	-	-	-	923
WRA (kg/m^3)	1.45	2.90	2.21	1.62	2.11	1.22	1.79	1.29
AEA (kg/m^3)	0.08	0.06	0.06	0.04	0.04	0.07	0.05	0.08
Slump (mm)	150	100	115	115	100	135	100	115
Air content (%)	5.5	6.0	4.5	7.2	5.0	7.0	6.0	5.0
Unit weight (kg/m^3)	2390	2350	2360	2230	2280	2200	2230	2240

8.2.3. Specimen Preparation and Testing. A drum mixer with 110-liter capacity was used for preparing concrete. Slump and air content were determined according to ASTM C143 (2015) and ASTM C231 (2014), respectively. Cylindrical specimens measuring 100×200 mm were employed for the determination of compressive strength in accordance with ASTM C39 (2001), and for testing the modulus of elasticity and splitting tensile strength in accordance with ASTM C469 (2010) and ASTM C496 (2011), respectively. Drying shrinkage was monitored using 75×75×285 mm prisms according to ASTM C157 (2008).

The specimens were covered with wet burlap and plastic sheets up to three days, followed by storage at 23±1ºC and 50%±3% relative humidity. The companion cylinders were demolded 24 hours after casting and cured in lime-saturated water of 21±1ºC for two days. By the end of the curing period, specimens were transported to the environmental chamber conditioned at 23±1ºC and 50%±3% relative humidity up to the testing age.

Restrained shrinkage cracking was evaluated using ring-type specimens complying with ASTM C1581 (2016). The test consists of casting concrete in the annular space between two concentric cylinders to form a shell element. An inner rigid steel ring of a uniform thickness of 12.5 mm with an inside diameter of 300 mm and height of 150 mm was used. Ring specimens were cast in three layers. The consolidation process consisted of rodding each layer for 75 times, followed by vibration on a vibrating table and tapping on the sides. Two concrete rings were prepared for each concrete type. Rings were demolded 24 hours after casting and subjected to two days of curing under wet burlap and plastic sheets. A layer of aluminum adhesive tape was employed to seal the top section of the rings to ensure drying from the ring circumference only.

A data acquisition system was incorporated to monitor the strain development in the steel ring due to restrained shrinkage of the concrete. Data logging started immediately after casting, with a frequency of 20 minutes up to cracking time. Figure 8.1 presents a schematic view of a diagonal section of the ring setup.

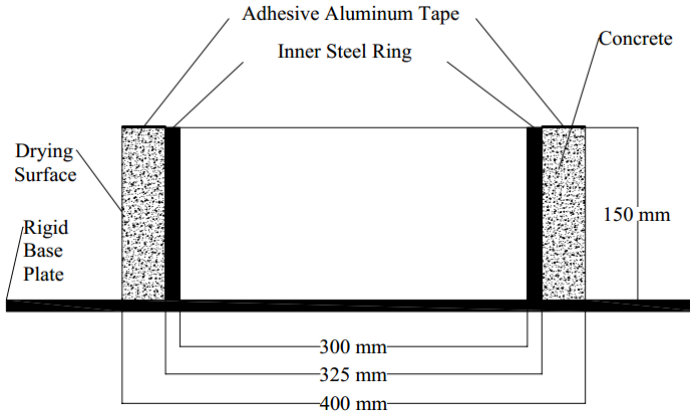

Figure 8.1 Schematic view and dimensions of the ring test setup

8.3. RESULTS AND DISCUSSION

8.3.1. Hardened Properties. Figure 8.2 presents the compressive strength results of the investigated concrete mixtures. Comparable compressive strength at the initiation of drying of 3 days, ranging from 26.4 to 28.0 MPa was observed for the Reference concrete and the mixtures prepared with binary cement and 50% or 100% RCA. The 3-day compressive strengths of the mixtures with ternary binder with 50% SCM dropped to 18.7 and 19.7 MPa. The mixtures proportioned with 50% SCM and 50% RCA exhibited 28-day compressive strength values of 50.7 and 51.6 MPa, compared to 44.5 MPa for the Reference concrete, with the rest of values ranging from 35.4 to 47.1 MPa. For the 56-day results, mixtures cast with 50% RCA and ternary cement developed compressive strength of 50.3 and 51.6 MPa, which was up to 9% higher than that of the Reference concrete with 47.3 MPa. The mixtures proportioned with 100% RCA exhibited compressive strength ranging from 39.5 (C2-100-B40) to 44.5 MPa (C4-100-B40), indicating up to 16% reduction compared to the Reference concrete at 56 days.

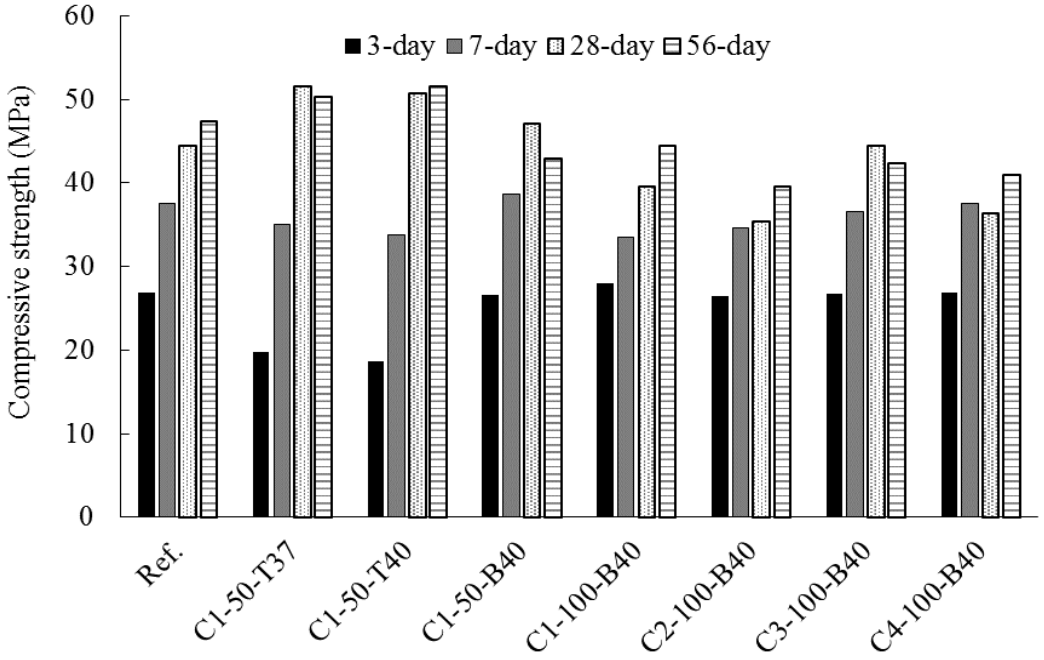

Figure 8.2 Compressive strength measurements

Figure 8.3 presents the MOE results. The Reference mixture exhibited the highest values of MOE at all investigated ages. A drop in 3-day MOE of up to 10% and 19% was observed due to 50% and 100% RCA incorporation, respectively. Trends were similar at 7 days, with highest MOE of 37.6 GPa obtained for the Reference concrete, compared to values ranging from 32.9 to 33.8, and 27.8 to 30.3 GPa for the mixtures with 50% and 100% RCA, respectively. At 28 days, the Reference concrete had a MOE of 41.0 GPa, followed by 36.9 GPa for the ones cast with 50% RCA and ternary cement. No significant increase in MOE of the mixtures cast with binary system and RCA was observed at 28 days. Trends were similar at 56 days, indicating reduction in MOE with use of RCA. The mixtures prepared with 50% RCA had MOE of 38±1 GPa compared to 42.8 GPa for the Reference concrete. Reduction in MOE was more pronounced with 100% RCA replacement, were the 56-day MOE ranged from 31.2 to 32.8 GPa.

Regression analysis was conducted to present the variations in MOE as a function of time. A logarithmic model introduced in Equation (8-1) was employed with the regression results summarized in Table 8.3. Good correlations were obtained with R^2 values ranging between 0.96 and 0.99.

$$MOE = a \times \ln(t) + b \tag{8-1}$$

where *t* was age of test (day) and *a* and *b* were the regression coefficients.

Figure 8.4 presents the variations in drying shrinkage of the investigated mixtures. In general, higher early-age shrinkage of 26 με/day was observed for the first 14 days for the 100% RCA mixtures. A similar rate of 20 με/day was obtained for the Reference concrete and for mixtures with 50% RCA. Most of the shrinkage occurred during the first 28 days of drying, with values tending to stabilize at about 400-450 με for the Reference and 50% RCA mixtures, and in the range of 650-750 με for mixtures with 100% RCA. The 28-day shrinkage of the C1-50-B40 was 375 με, compared to 385 and 500 με for the Reference and the C1-100-B40 mixtures, respectively. The incorporation of the ternary system with 50% SCM was effective in reducing the shrinkage at later ages, where the 28-day shrinkage was reduced from 385 for the Reference concrete to 360 and 340 με for the C1-50-T40 and C1-50-T37 mixtures, respectively. The minimum 56-day shrinkage was observed for the mixtures cast with ternary cement, with 330 and 370 με at 0.37 and

0.40 w/cm, respectively. The mixture cast with 50% RCA and binary cement exhibited similar 56-day shrinkage to that of the Reference concrete. Significantly higher 56-day shrinkage was observed the mixtures cast with 100% RCA, with values ranging from 585 to 620 με, corresponding to 39% to 48% increase compared to the Reference concrete.

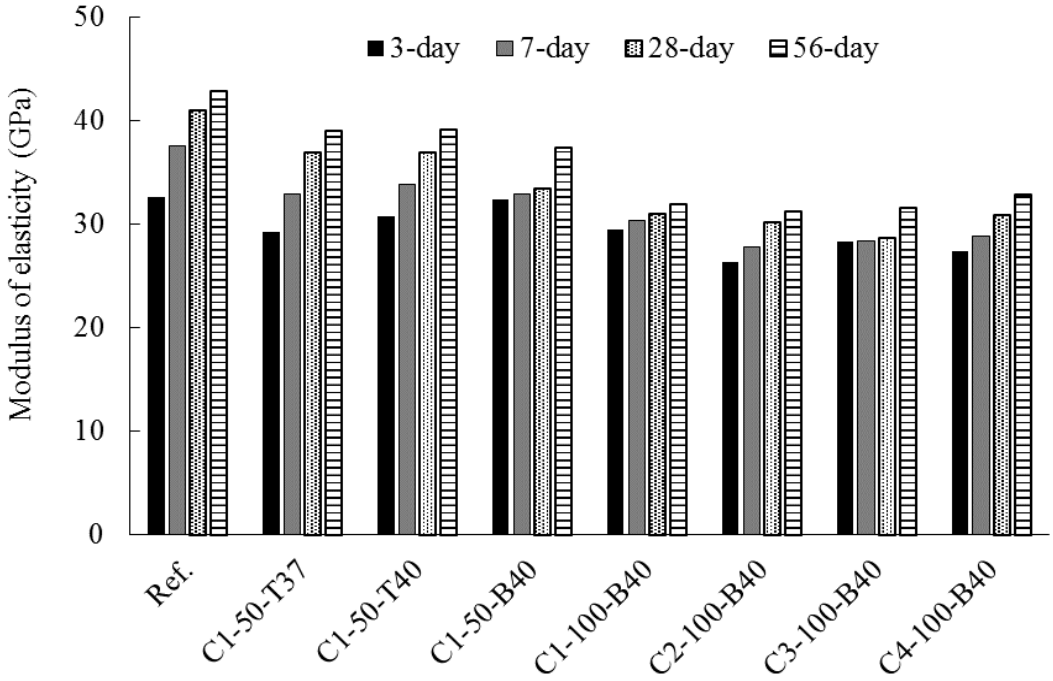

Figure 8.3 Modulus of elasticity measurements

Table 8.3 Variations in drying shrinkage and modulus of elasticity as a function of time

Mixture ID		Ref.	C1-50-T37	C1-50-T40	C1-50-B40	C1-100-B40	C2-100-B40	C3-100-B40	C4-100-B40
MOE (GPa)	*a*	3.33	3.23	2.75	0.46	0.69	1.70	0.18	1.54
	b	29.85	26.14	28.01	31.93	28.87	24.49	28.08	25.76
	R^2	0.96	0.99	0.99	0.99	0.96	0.99	0.99	0.99
Drying shrinkage (με)	*k*	-70.5	-65.3	-70.5	-69.9	-87.3	-99.0	-95.6	-90.6
	R^2	0.97	0.97	0.98	0.98	0.97	0.98	0.98	0.97

Regression analysis was conducted to present the variations in drying shrinkage as a function of the square root of the drying time, as presented in Equation (8-2). Regression results are presented in Table 8.3. Good correlations were obtained with R^2 values ranging between 0.97 and 0.99.

$$\varepsilon_{sh} = k \times \sqrt{t} \tag{8-2}$$

where ε_{sh} was the drying shrinkage (με), *t* was the time from initiation of drying (day), and *k* was the regression coefficient.

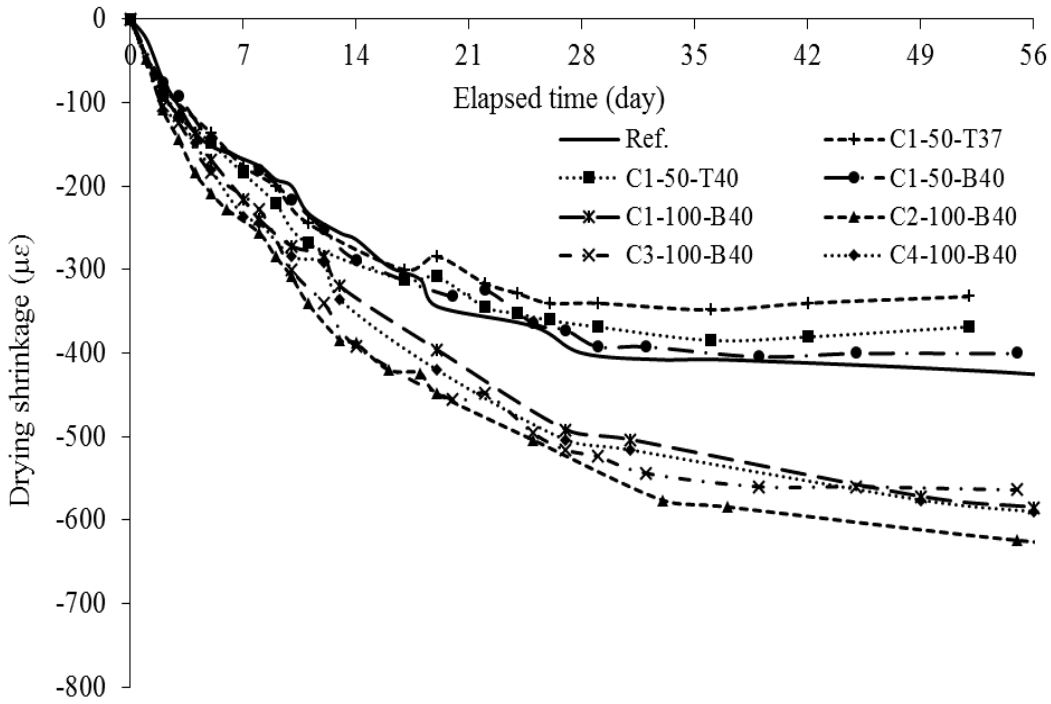

Figure 8.4 Variations in drying shrinkage after three days of curing

8.3.2. Cracking Potential. Figure 8.5 presents the variations of net strain in the steel ring, with drying time. Compressive strain development in the steel ring was monitored up to the time of an abrupt jump in compressive strain values, corresponding to cracking of concrete shell (ASTM C1581 2016). In general, it was observed that mixtures cast with 100% RCA exerted higher strain compared to the Reference concrete. The C1-50-B40 mixture had steel strain similar to that of the Reference concrete up to 14

days, with an increase limited to 5 με up to 28 days. The mixtures proportioned with 50% RCA and ternary cement developed the minimum steel strain values of up to 21 days, while exhibiting slight increase with about 5 με higher than that of the Reference concrete afterwards. Same steel strain values were observed for the mixtures with ternary cement, regardless of the w/cm, which was in agreement with drying shrinkage results obtained for these mixtures. For the mixtures cast with 100% RCA, the values of strain in steel ring were up to 10 με higher than that of the Reference concrete at 9 to 11 days, corresponding to 15%-17% increase at the time of cracking.

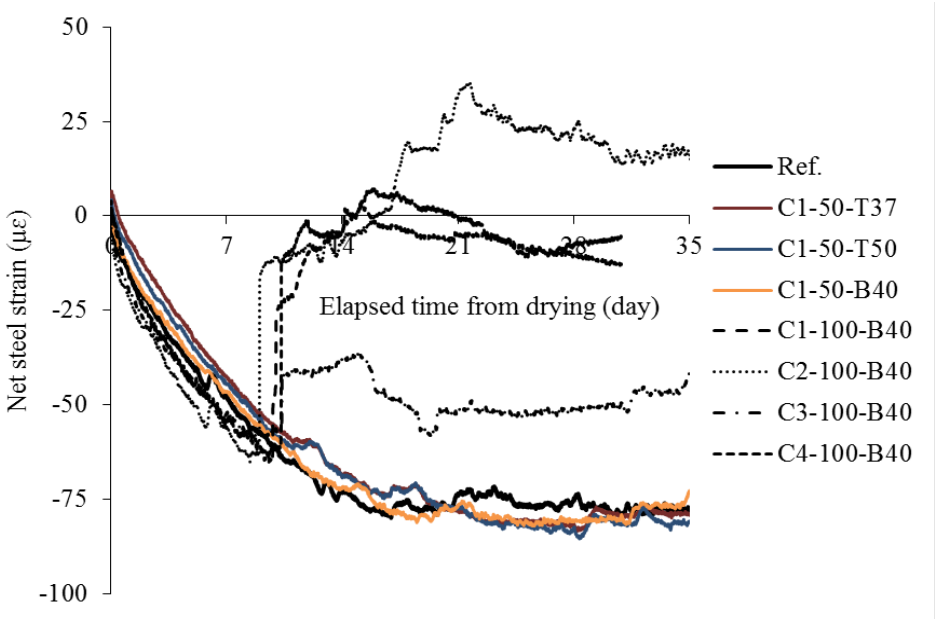

Figure 8.5 Variations in steel ring strain recorded from the drying initiation

Equation (8-3) (Hwang and Khayat 2008) was incorporated to quantify the cracking potential during the first 35 days from the initiation of drying, based on their cracking time. Table 8.4 offers a summary of results. A 35-day cracking potential of 0 can be attributed to the Reference mixture, and those cast with 50% RCA, given the fact that these mixtures did not exhibit any cracking before 35 days (Hwang and Khayat 2008). The incorporation of 100% RCA on the other hand increased the cracking potential by up to 74%.

$$Cracking\ potential\ (\%) = \left(1 - \frac{t_{cr}}{t_{cr,max}}\right) \times 100 \quad (8\text{-}3)$$

where the t_{cr} is the time to cracking for the investigated mixtures (day) and $t_{cr,max}$ is the maximum observed time to cracking, capped at 35 days in here.

The rate of strain development in steel ring was plotted as a function of the square root of time (day), as recommended by (ASTM C1581 2016), which leads to a linear trend. The slope of such linear variations (α), i.e. the strain rate factors (mm/day$^{0.5}$), were determined. The average strain rate factors (α_{avg}) obtained for each ring (2 to 3 sensors per ring) were incorporated for calculating the stress rate (MPa/day) using Equation (8-4) (ASTM C1581 2016). Table 8.4 offers a summary of the test results.

$$q = \frac{G|\alpha_{avg}|}{2\sqrt{t_r}} \quad (8\text{-}4)$$

where α_{avg} is the average strain rate factor (mm/day$^{0.5}$), t_r is the time to cracking (day), and G was a factor reflecting the sample geometry and is equal to 72.2 GPa.

Table 8.4 Tensile properties and time to cracking of concrete mixtures

Mixture ID	Ref.	C1-50-T37	C1-50-T40	C1-50-B40	C1-100-B40	C2-100-B40	C3-100-B40	C4-100-B40
28-day splitting tensile strength (MPa)	2.96	3.47	3.17	2.79	2.35	2.22	2.83	2.26
Time to crack (day)	>35	>35	>35	>35	9.75	9.00	10.50	11.00
28-day stress rate (MPa/day)	0.10	0.12	0.12	0.12	0.28	0.34	0.26	0.25
28-day cracking potential (%)	0	0	0	0	72	74	70	69

The Reference mixture did not exhibit cracking within the investigation period of 35 days and developed an average stress rate of 0.10 MPa/day after 28 days of drying. This concrete is corresponding to “low” risk of cracking. No cracking was observed in the case of the mixtures proportioned with 50% RCA and ternary system. This was expected based on the laboratory data, where up to 45 με reduction in shrinkage, up to 6% and 10% decrease in 3- and 28-day MOE, and up to 40% higher 28-day splitting

tensile strength values were observed compared to the Reference concrete. No cracking was observed in the case of the C1-50-B40 mixture, proportioned with 50% RCA, binary system, and w/cm of 0.40. Comparable shrinkage to that of the Reference concrete, higher splitting tensile strength of 2.79 vs. 2.46 MPa at 28 days, and reduction in MOE could be the reason for the resistance to cracking in this mixture. In summary all mixtures cast with 50% RCA exhibited low potential of cracking due to shrinkage in restrained conditions, suggesting the feasibility of use in rigid pavement construction. The incorporation of 100% RCA reduced the time to cracking to values ranging from 9.0 to 11 days, with stress rates of 0.25 to 0.34 MPa/day for the C2-100-B40, C3-100-B40, and C4-100-B40 mixtures. These mixtures exhibited “moderate-high” risk of cracking, as indicated by (ASTM C1581 2016).

Equation (8-5) (Hwang and Khayat 2008) was employed to calculate the degree of restraint of the investigated ring specimens, defined as the stiffness of the steel ring, relative to the overall stiffness of the ring and concrete setup. Results are presented in Figure 8.6.

$$R_m = \frac{\varepsilon_{sh} - \varepsilon_{st}}{\varepsilon_{sh}} = 1 - \frac{\varepsilon_{st}}{\varepsilon_{sh}} \tag{8-5}$$

where ε_{sh} is the drying shrinkage, and ε_{st} is the elastic compressive strain of the steel ring.

Higher degree of restrain was observed in the case of mixtures proportioned with 100% RCA, while compared to the Reference concrete. Concrete proportioned with 50% RCA developed higher degree of restraint up to 17 days, corresponding to the lower strain in the steel ring compared to the Reference concrete. Trend changed after 17 days, where a higher degree of restrain was observed for the Reference concrete, coinciding with the lower steel strain reported in Figure 8.5.

8.3.3. Tensile Creep Behavior. The drying shrinkage in a restrained condition is balanced with a combination of elastic concrete strain, tensile creep strain, and elastic contraction strain of the steel ring, as summarized in Equation (8-6) (See et al. 2003).

$$\varepsilon_{sh}(t) = \varepsilon_e(t) + \varepsilon_{cp}(t) + \varepsilon_{st}(t) \tag{8-6}$$

where $\varepsilon_e(t)$ is the elastic concrete strain and $\varepsilon_{cp}(t)$is the tensile creep strain at time *t*.

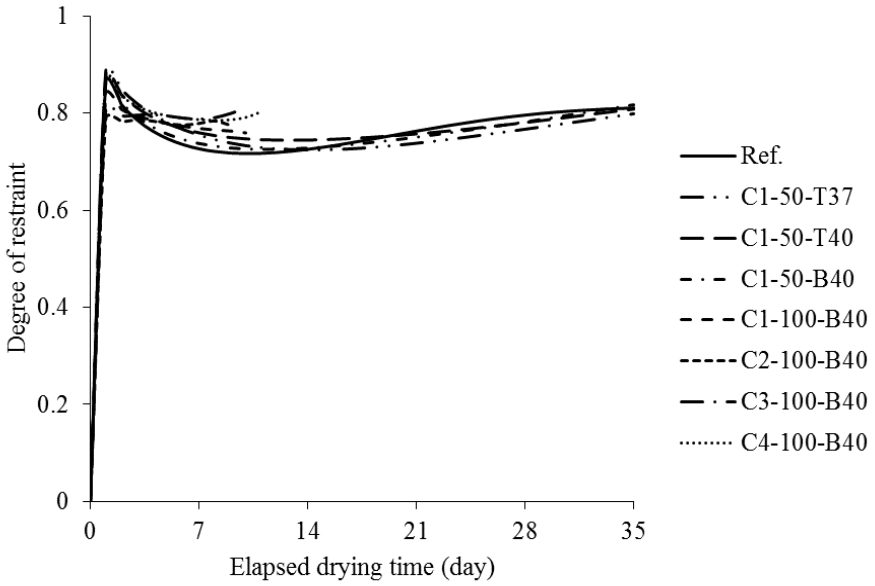

Figure 8.6 Variations of degree of restraint of tested mixtures

Balancing the radial pressure between the steel ring and concrete shell at time *t* results in Equation (8-7) for calculation of the average tensile stress in the concrete (See et al. 2003), from which the elastic concrete strain can be calculated, as follows:

$$\sigma_t(t) = \frac{E_{st} r_{ic} h_{st}}{r_{is} h_c} \varepsilon_{st}(t) \tag{8-7}$$

$$\varepsilon_e(t) = \frac{\sigma_t(t)}{E_c(t)} \tag{8-8}$$

where E_{st} is the modulus of elasticity of the steel (200 GPa), E_c is the concrete modulus of elasticity, h_{st} and h_c are the thicknesses of the steel ring and the concrete, equal to 12.5 and 37.5 mm, respectively, and r_{ic} and r_{is} are the inner radii of the steel ring and the concrete shell, equal to 162.5 and 150 mm, respectively.

The tensile creep coefficient at time *t*, $C_r(t)$, can be expressed as the ratio of the creep strain to elastic concrete strain as summarized in Equation (8-9). Having the tensile strain in concrete calculated using Equations (8-7) and (8-8), Equation (8-9) can be re-written as a function of the specimen geometry and measured properties, i.e. E_c, ε_{sh} , and ε_{st} as summarized in Equation (8-10) (Hwang and Khayat 2008, 2010).

$$C_r(t) = \frac{\varepsilon_{cp}(t)}{\varepsilon_s(t)} \tag{8-9}$$

$$C_r(t) = \frac{E_c(t) r_{is} h_c}{E_{st} r_{ic} h_{st}} \left[\frac{\varepsilon_{sh}(t)}{\varepsilon_{st}(t)} - 1\right] - 1 \tag{8-10}$$

Figure 8.7 and Figure 8.8 present the variations in elastic concrete strain and tensile creep strain, initiating from the start of drying. The Reference concrete exhibited the minimum values of elastic concrete strain, while the maximum values were obtained for the C2-100-B40 mixture, up to the time of cracking. An increasing trend in elastic concrete strain of up to 140 με was observed for the Reference mixture, up to 21 days of drying, where the strain in steel ring was stabilized as presented in Figure 8.5. Elastic concrete strain was increasing as a function of time for the 50% RCA mixtures, capped at 200 με for up to 35 day measurements. Such an increasing trend was also observed in the case of the mixtures with 100% RCA, with values ranging from 110 to 170 με at the time of cracking.

The tensile creep strain was increasing for the Reference concrete up to 35 days, with maximum value of 200 με. The same trend was observed for the 100% RCA mixture up to the time of cracking. The increase in tensile creep strain up to 35 days was also observed for the mixtures with 50% RCA, with a maximum value of 230 με for C1-50-T40 mixture.

Table 8.5 presents the variations in tensile creep coefficient as a function of elapsed time since the initiation of drying. In general, an increase in tensile creep coefficient of the Reference concrete was recorded over time, which is in agreement with the resistance to cracking observed for this mixture. A tendency to increase in tensile creep coefficient of the mixtures cast with 100% RCA replacement was observed up to the time of cracking.

The tensile creep coefficient of the 100% RCA mixtures at the time of cracking were higher than that of the Reference concrete at the same age. The tensile creep coefficient at the time of cracking was 0.34, 0.38, 0.78, and 0.68 for the C1-100-B40, C2-100-B40, C3-100-B40, and C4-100-B40 mixtures, respectively, compared to values ranging from 0.34 to 0.36 for the Reference concrete at the same period of time, i.e. 9 to

11 days. This is believed to be mainly due to the lower elastic modulus and higher relaxation capacity of mixtures incorporating RCA. However, the reduced tensile properties of concrete due to the availability of non-homogenous zones of weakness in concrete attributed to the availability of deleterious materials and micro-cracks in RCA, can be a reason for crack initiation of concrete made with 100% RCA.

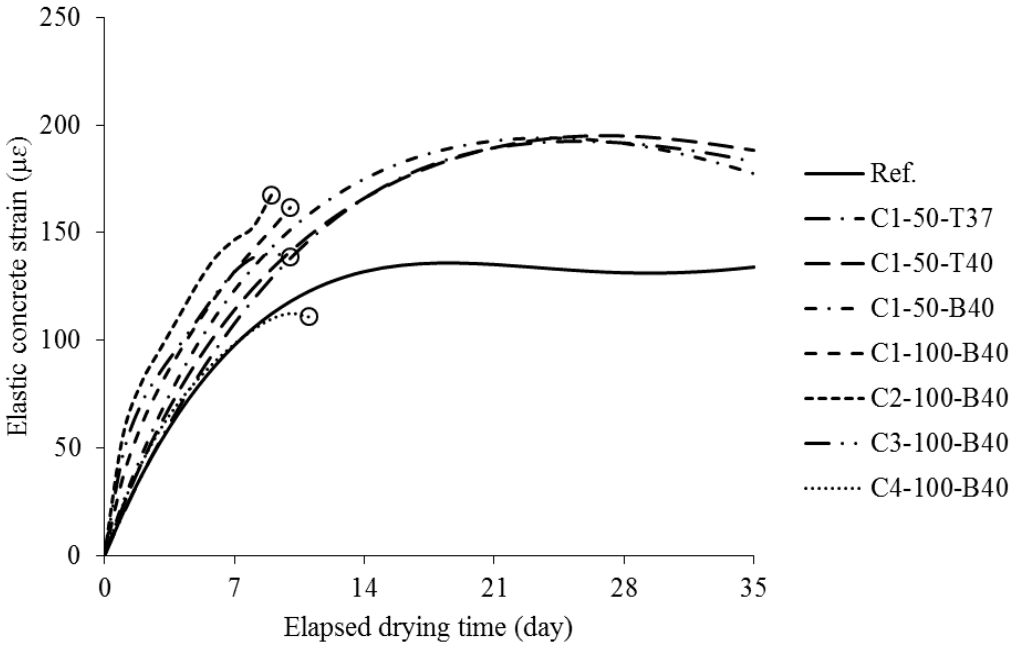

Figure 8.7 Variations in elastic concrete strain

The same observation can be drawn for the C1-100-B40, C2-100-B40, and C3-100-B40 mixtures. The increasing trend of tensile creep coefficient from 0.34 to 0.38 and 0.78, did not necessarily lead to increase in time to cracking with values of 9.75, 9.0 and 10.5 days, which is contrary to what normally expected (Monteiro 2006, Shah and Weiss 2006, Weiss and Shah 2002, Loser and Leemann 2009). This is also in line with observed values of splitting tensile strength where the 28-day splitting tensile strength was 2.35, 2.22, and 2.83 MPa at 28 days for the C1-100-B40, C2-100-B40, and C3-100-B40 mixtures, respectively, compared to 2.96 MPa for the Reference concrete. In general, it may be concluded that even though the mixtures with RCA can exhibit higher stress relaxation, the susceptibility to cracking may be increased if proper measures to reducing

shrinkage were not taken. This is in line with the “moderate-high” risk of cracking of the 100% RCA mixtures and “low” risk of cracking for the mixtures cast with 50% RCA, where reduced w/cm and higher content of SCM were helpful in reducing shrinkage and cracking.

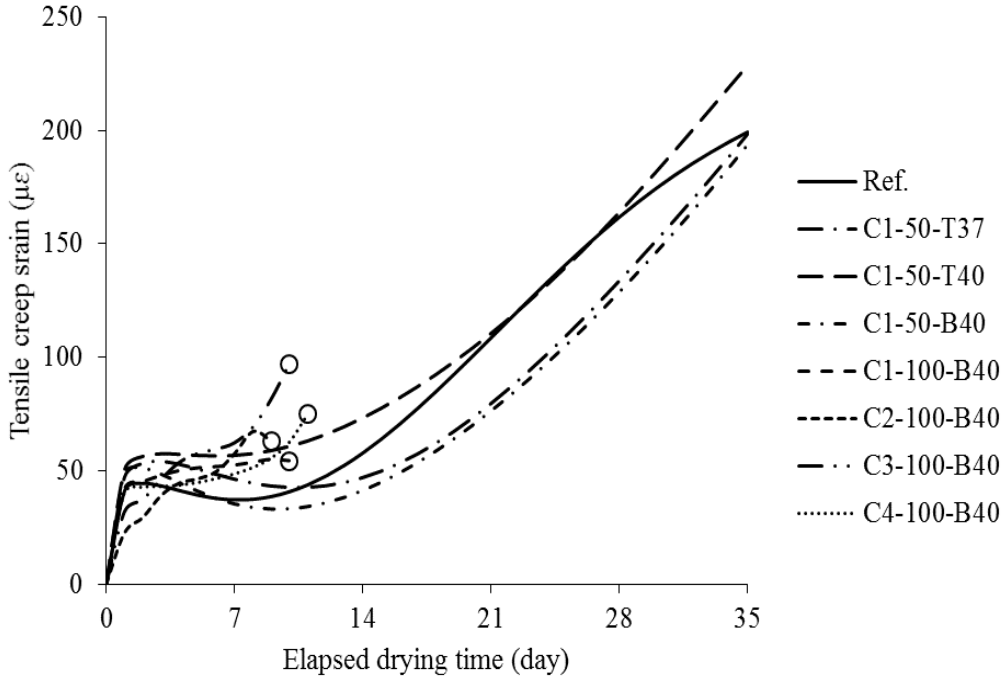

Figure 8.8 Variations in tensile creep strain

Table 8.5 Variations in tensile creep coefficient

Time (day)	Ref.	C1-50-T37	C1-50-T40	C1-50-B40	C1-100-B40	C2-100-B40	C3-100-B40	C4-100-B40
5	0.50	0.62	0.63	0.42	0.47	0.37	0.53	0.55
7	0.38	0.43	0.50	0.29	0.40	0.39	0.47	0.49
9	0.34	0.34	0.44	0.23	0.36	0.38*	0.58	0.51
10	0.35	0.31	0.43	0.22	0.34*	-	0.70	0.56
11	0.36	0.29	0.43	0.22	-	-	0.78*	0.68*
21	0.80	0.42	0.58	0.40	-	-	-	-
28	1.23	0.70	0.84	0.67	-	-	-	-
35	1.49	1.08	1.21	1.09	-	-	-	-

*Time of cracking

8.4. REMARKS

Based on the data reported in this paper, the following conclusions are warranted:

- The incorporation of 50% and 100% RCA reduced the MOE by up to 10% and 20%, respectively. Drying shrinkage of mixtures with 100% RCA increased by up to 150 and 200 με after 28 and 56 days of drying, respectively, which corresponds to approximately 40% and 50% increase compared to the Reference concrete made without any RCA.
- In the restrained ring test, no cracking was observed in the case of the Reference mixture up to 35 days of drying, with stress rate limited to 0.10 MPa/day. No cracking up to 35 days of drying was observed for the mixtures with 50% RCA, which is considered as "low" potential for cracking. On the other hand, the incorporation of 100% RCA reduced the time of cracking to values ranging from 9 to 11 days, with stress rates ranging from 0.25 to 0.34, which correspond to "medium-high" risk of cracking.
- A greater RCA content can increase strain development in the steel ring. The minimum values of elastic concrete strain were observed in the case of the Reference concrete. The increase in RCA content enhanced the development of elastic strain in concrete, with the highest values observed for the mixture that developed the highest drying shrinkage.
- Concrete mixtures cast with 100% RCA developed higher tensile creep coefficient. Such values of ranged from 0.34 to 0.78 at the time of cracking compared to 0.34 to 0.36 for the Reference concrete, and 0.23 to 0.43 for the concrete with 50% RCA. This is believed to be due to higher stress relaxation, i.e. lower MOE.
- Even though the tensile creep coefficient and stress relaxation were higher in concrete made with 100% RCA, the significantly higher shrinkage and reduction in tensile strength of up to 25% led to earlier time to cracking of such mixtures.

9. DURABILITY OF CONCRETE MADE WITH RECYCLED AGGREGTAE

9.1. RESEARCH SIGNIFICANCE

Concrete durability can affect the maintenance cost and service life of transportation infrastructure significantly. The degradation mechanisms are typically tied to the environmental conditions and exposure situation, including the variations in seasonal temperature and relative humidity, availability of deleterious materials and ions, etc. Frost action, scaling caused by de-icing salts, ionic attacks, and surface damage caused by abrasion are some of the mechanisms that can result in deterioration of different segments of transportation infrastructure, including structural elements and pavement panels. Situations are more complicated while using recycled concrete aggregate (RCA) in concrete production. Typically marginal quality of the RCAs, sourced in residual mortar phase of the particles and the availability of impurities and deleterious materials, can cause uncertainties regarding the durability of concrete (NCHRP 2013).

Lower concrete quality, which can be reflected in greater porosity and water absorption, facilitates the saturation of the exposed surfaces. The water available in saturated concrete will freeze and expand in subzero environments, exerting internal pressure to the matrix that can result in cracking and degradation of concrete. Moreover, a higher porosity can result in increased rate of ion transport and greater risk of damage in aggressive environments, leading to accelerated accumulation of deteriorating agents in concrete and occurrence of chemical attacks.

It is a generally accepted fact that providing the minimum strength requirements along with securing proper air entrainment in concrete can yield to dependable durability against frost action. An efficient air entrainment requires adequate amount (% vol.) of air in fresh and hardened state and proper characteristics of the air void system in terms of spacing factor ($\bar{L}$) and specific surface (α), with recommended values of $\bar{L} < 0.2\ mm$ and $\alpha \geq 24\ mm^2/mm^3$ (ASTM C457 2016).

Rapid chloride ion permeability (RCP), water absorption, and electrical resistivity are typically considered as indicators of transport properties of concrete. Such tests are of

great interest especially in the case of reinforced concrete elements, including the structural elements and substructure members, as well as reinforced concrete pavement.

The present research investigates the effect of RCA incorporation on durability of concrete designated for transportation infrastructure. Six types of coarse RCA, and a source of fine RCA were used in the study. Two binder systems and three w/cm of 0.37, 0.40, and 0.45 were considered. Effect of RCA on concrete durability was investigated in terms of freeze and thaw resistance, resistance to scaling caused by de-icing salts, electrical resistivity, sorptivity, abrasion resistance, and coefficient of thermal expansion (CTE).

9.2. EXPERIMENTAL PROGRAM

9.2.1. Material Properties. The investigated concrete mixtures were proportioned with either a binary or a ternary cement. The former included 75% Type I/II Portland cement and 25% Class C fly ash (FA-C), by mass of total binder. The ternary system contained 35% FA-C and 15% ground granulated blast furnace slag (GGBS), by mass. The binary cement is similar to the concrete employed by the Missouri Department of Transportation (MoDOT) for rigid pavement construction (Sadati and Khayat, 2016). The ternary system was optimized to enhance the mechanical properties and reduce shrinkage of concrete equivalent mortar with 0.40 w/cm (Khayat and Sadati, 2016).

Two types of crushed dolomite with nominal maximum aggregate size (NMAS) of 19 mm were used. Different types of coarse RCA procured from six different sources, including five commercial recycling centers and one laboratory-produced RCA were considered.

The aggregate soundness test introduced by ASTM C88 was modified as proposed by Abbas et al. (2007) to determine the resistance of coarse RCA materials against freeze-thaw cycles. The method involved: (1) obtaining a representative sample of different size portions of RCA as suggested by Abbas et al. (2007); (2) washing the aggregate with tap water, drying in oven set at 110±5 ºC until constant mass; (3) aggregates were immersed in saturated solution of Sodium Sulfate; (4) samples were exposed to seven daily cycles of freezing and thawing with temperature range similar to requirements of ASTM C 672 (2012) test on de-icing salt scaling; (5) by the end of the

freeze-thaw cycles, the aggregates were washed using tap water, oven dried, and sieved on 4.75 mm mesh; (6) percentage mass loss was calculated for each size fraction and determined for each aggregate type based on aggregate particle size distribution.

Well-graded siliceous river-bed sand with fineness modulus of 2.47 was used. In addition, a fine RCA with fineness modulus of 2.47 was used. All RCA materials were in saturated state before mixing. Table 9.1 presents the physical properties of the fine and coarse aggregates.

A lignum-based water reducing admixture (WRA) with specific gravity of 1.2 and 40% solid content was used. An air-entraining admixture (AEA) was incorporated in all mixtures to secure 6%±1% air content.

9.2.2. Concrete Mixture Proportions. In total, 33 different concrete mixtures were produced in the laboratory. Three w/cm of 0.37, 0.40, and 0.45 were considered in designing these mixtures. Table 9.2 and Table 9.3 summarize the mixture proportioning of the investigated concrete. Air entraining agent was used to secure 6%±1% air in fresh state. Water-reducing admixture was incorporated to adjust the slump values of 50±25, 150±50 mm for pavement and substructure applications, respectively. All mixtures were prepared with 323 kg/m^3 of binder, except for the ones made with 0.45 w/cm, where 317 kg/m^3 of cementitious materials was used. The binder consists of a binary cement with 25% FA-C and a ternary system with 35% FA-C and 15% GGBS, A coding system was adapted to label different concrete mixtures indicating the RCA type and content, binder type, and w/cm. For instance, the “RCA1-50-B-40” mixture was proportioned with 50% (by vol.) of RCA1, using binary cement (B), and w/cm of 0.40. The “RCA2-30-T-37-15F” refers to the concrete with 30% of RCA2, ternary cement, 0.37 w/cm, and 15% fine RCA. Details regarding the mixture proportions and properties are provided in (Khayat and Sadati 2016, Volz et al. 2014).

Table 9.1 Virgin aggregate and RCA properties

Aggregate	Source	Specific gravity	Absorption (%)	Deleterious materials (% mass)	Soundness mass loss (%)	Los Angeles abrasion (%)	NMAS (mm)
NC1	Dolomite 1	2.73	0.80	-	-	28	19
NC2	Dolomite 2	2.72	0.98	-	-	43	19
Sand	River-bed sand	2.63	0.40	-	-	-	4
Fine RCA	Residual concrete, airfield	2.11	7.33	-	-	-	4
RCA 1	Laboratory produced RCA	2.35	4.56	0.3	21	41	19
RCA 2	Residual concrete, airfield	2.35	4.46	4.0	19	33	19
RCA 3	Commercial recycling, Missouri	2.25	5.75	4.5	36	39	19
RCA 4	Commercial recycling, Kansas	2.24	6.05	2.2	17	38	19
RCA 5	Commercial recycling, Missouri	2.17	7.58	1.3	23	44	19
RCA 6	Commercial recycling, Missouri	2.21	7.13	1.9	40	53	12.5

Table 9.2 Mixture proportions and fresh properties of concrete made with RCA1, and RCA3-6

Mix.	Binder (kg/m^3)	OPC	GGBS	FA-C	w/cm	Water	DOL	RCA	Sand	RCA (% vol.)	Air (%)	Slump (mm)
		(% mass)				(kg/m^3)						
DOL1-B-40	323	75	-	25	0.40	129	1120	0	782	0	6.2	85
DOL1-T-37	323	50	15	35	0.37	120	1136	0	793	0	7.2	65
DOl1-T-40	323	50	15	35	0.40	129	1120	0	782	0	5.0	85
DOL2-B-45	317	75	-	25	0.45	143	1089	0	772	0	7.2	150
RCA1-30-B-45	317	75	-	25	0.45	143	762	282	772	30	7.2	175
RCA1-50-B-45	317	75	-	25	0.45	143	544	469	772	50	6.6	135
RCA1-70-B-45	317	75	-	25	0.45	143	326	657	772	70	5.6	200
RCA1-100-B-45	317	75	-	25	0.45	143	0	939	772	100	5.4	210
RCA1-50-B-40	323	75	-	25	0.40	129	560	482	782	50	5.8	70
RCA1-50-T-37	323	50	15	35	0.37	120	568	488	793	50	6.8	65
RCA3-50-B-40	323	75	-	25	0.40	129	560	462	782	50	5.2	65
RCA3-50-T-37	323	50	15	35	0.37	120	568	466	793	50	5.4	70
RCA4-50-B-40	323	75	-	25	0.40	129	560	460	782	50	5.1	65
RCA4-50-T-37	323	50	15	35	0.37	120	568	466	793	50	5.6	35
RCA5-50-B-40	323	75	-	25	0.40	129	560	446	782	50	6.0	80
RCA5-50-T-37	323	50	15	35	0.37	120	568	451	793	50	5.2	50
RCA6-50-B-40	323	75	-	25	0.40	129	560	453	782	50	6.8	75
RCA6-50-T-37	323	50	15	35	0.37	120	568	460	793	50	6.0	50

Table 9.3 Mixture proportions and fresh properties of concrete made with coarse RCA2 with or without fine RCA

Mix.	Binder (kg/m^3)	OPC	GGBS	FA-C	w/cm	Water	DOL	C-RCA	Sand	F-RCA	C-RCA	F-RCA	Air (%)	Slump (mm)
		(% mass)				(kg/m^3)					(% vol.)			
RCA2-30-T-37	323	50	15	35	0.37	120	795	293	793	0	30	0	6.8	85
RCA2-30-T-40	323	50	15	35	0.40	129	784	290	782	0	30	0	5.0	75
RCA2-50-B-40	323	75	-	25	0.40	129	560	482	782	0	50	0	7.2	115
RCA2-50-T-37	323	50	15	35	0.37	120	568	489	793	0	50	0	7.0	85
RCA2-50-T-40	323	50	15	35	0.40	129	560	482	782	0	50	0	5.4	50
RCA2-70-T-37	323	50	15	35	0.37	120	341	685	793	0	70	0	5.5	75
RCA2-70-T-40	323	50	15	35	0.40	129	336	675	782	0	70	0	6.9	85
RCA2-30-T-37-15F	323	50	15	35	0.37	120	795	293	674	96	30	15	5.0	85
RCA2-30-T-40-15F	323	50	15	35	0.40	129	784	290	665	94	30	15	5.0	40
RCA2-50-T-37-15F	323	50	15	35	0.37	120	568	489	674	96	50	15	6.8	85
RCA2-50-T-40-15F	323	50	15	35	0.40	129	560	482	665	94	50	15	5.6	65
RCA2-50-T-40-30F	323	50	15	35	0.40	129	560	482	548	188	50	30	5.0	85
RCA2-50-T-40-40F	323	50	15	35	0.40	129	560	482	469	250	50	40	5.0	50
RCA2-70-T-40-15F	323	50	15	35	0.40	129	336	675	665	94	70	15	5.4	50
RCA2-70-T-40-30F	323	50	15	35	0.40	129	336	675	548	188	70	30	5.2	25

9.2.3. Specimen Preparation and Testing. A 110-liter drum mixer was used. The batching sequence consisted of: (1) mixing the aggregate and one third of the water at low speed for 3 min to ensure homogenized distribution and saturation of the particles; (2) introducing the AEA diluted in one third of the mixing water and agitation at high speed for 1 min; (3) introducing the cementitious materials and mixing for 1 min at high speed; (4) adding the WRA diluted with the rest of the water and mixing for 2 min at high speed. After 2 min of rest, the mixing was resumed for 3 min at high speed.

Slump and air content were determined according to ASTM C143 (2015) and ASTM C231 (2014), respectively. A vibrating table was used to ensure proper consolidation of the specimens. All specimens were covered with wet burlap and plastic sheet up to 24 hours after casting. Prismatic samples measuring 75×100×400 mm were used to determine the freeze and thaw durability of concrete according to ASTM C666-A (2015). The specimens were cured in lime-saturated water of 21±2 ºC. In the case of the mixtures cast with ternary cement, curing period was eight weeks before the start of the freezing and thawing cycles. The rest of the freeze and thaw specimens were cured for 28 days. Durability factor was monitored based on variations in ultrasonic pulse velocity as a function of freeze/thaw cycles as demonstrated in Equation (9-1):

$$DF = \left(V_n / V_0\right)^2 \tag{9-1}$$

where is V_n the ultrasonic pulse velocity after n cycles of freeze and thaw capped at 300 cycles, V_0 is the pulse velocity before starting the test cycles.

An automated image analysis system was employed to determine the air void parameters of hardened concrete, including spacing factor and specific surface. Measurements were conducted in accordance with linear-traverse method, described in ASTM C457 (2016). Black coloring and white Barium sulfate power were used for enhancing the contrast of the polished concrete surfaces.

The resistance to de-icing salt scaling was determined in accordance with ASTM C672 (2012). Slabs with surface areas of 200×225 mm and thicknesses of 75 mm were used. A dike was placed on the finished surface of the specimens for ponding with a 4.0% aqueous solution of Calcium Chloride. The specimens were subjected to 50 daily cycles of freezing and thawing. The curing regime included 28 days of curing in lime-saturated

water, followed by 14 days of drying in an environmental chamber conditioned at 23±1 ºC and 50%±3% relative humidity. The degree of surface deterioration was rated qualitatively on a scale of 0 to 5, representing the best and the lowest performances, respectively, based on the criteria suggested by ASTM C672 (2012). In addition, mass loss due to scaling was recorded as a function of test cycles and reported as a quantitative measure (g/m^2) of scaling resistance.

Bulk electrical resistivity was determined on 100×200 mm cylindrical specimens as detailed in ASTM C 1760 (2012). The specimens were cured in lime-saturated water up to the time of testing. Sorptivity measurement was conducted on two 50-mm thick slices of concrete, obtained from mid-height of 100×200 mm cylinders in accordance with ASTM C 1585 (2013). The cylinders were cured in lime-saturated water for 56 days. The extracted discs were then cured in an environmental chamber with temperature of 50±2°C and relative humidity of 80±3% for 3 days. This was followed by storage in sealed containers for 15 days to ensure uniform internal moisture distribution. Specimens were then sealed on the sides, and the top surface and placed in a container with the free surface of the samples exposed to tap water of 23±2°C. Variation in mass of the specimens due to water absorption was monitored over time.

Cylindrical specimens measuring 150 mm in diameter were employed for determining the abrasion resistance after 56 days of curing. Testing was conducted in accordance with ASTM C944 with a rotating cutter covering an area with 82.5 mm diameter under fixed pressure of 197 N. The value of mass loss normalized to the abraded area was reported.

9.3. RESULTS AND DISCUSSION

9.3.1. Durability against Freeze and Thaw Cycles.

9.3.1.1 Mixtures cast without any RCA. Table 9.4 presents the variations in durability factor of the investigated concrete. The DOL1-B-40 mixture made with 25% FA-C, dolomitic aggregate, and 0.40 w/cm exhibited the highest durability factor of 96%. The use of ternary cement with 50% SCM slightly reduced the durability factor; a marginal decrease to 94% and 93% for the concrete with w/cm of 0.37 and 0.40, respectively, was observed. The increase in w/cm from 0.40 to 0.45 had a more

pronounced effect on durability to freezing and thawing. A drop in durability factor from 96% to 86% was observed for the DOL2-B-45 concrete, where the w/cm increased from 0.40 to 0.45.

Table 9.4 Frost durability of the investigated mixtures

	Mixture	Freeze-Thaw	De-Icing Salt Scaling	
		Durability Factor (%)	Rating	Mass Loss (g/m^2)
Virgin aggregate	DOL1-B-40	96	1	100
	DOL2-B-45	86	1	-
	DOL1-T-37	94	1	415
	DOL1-T-40	93	3	730
Coarse RCA	RCA1-30-B-45	83	2	-
	RCA1-50-B-45	83	2	-
	RCA1-70-B-45	83	2	-
	RCA1-100-B-45	79	4	-
	RCA1-50-T-37	91	2	310
	RCA2-30-T-37	97	3	640
	RCA2-30-T-40	91	3	870
	RCA2-50-T-37	92	3	700
	RCA2-70-T-37	96	3	450
	RCA3-50-T-37	86	3	760
	RCA4-50-T-37	89	1	430
	RCA5-50-T-37	89	1	400
Fine and coarse RCA	RCA2-30-T-37-15F	96	3	1070
	RCA2-30-T-40-15F	95	3	1200
	RCA2-50-T-37-15F	96	3	800

9.3.1.2 Effect of coarse RCA content. Figure 9.1 summarizes the test results obtained for mixtures prepared with different contents of coarse RCA. The first set of the mixtures was proportioned with up to 100% of RCA1, a binary cement, and 0.45 w/cm. The second group was prepared up to 70% of RCA2, a ternary cement, and 0.37 /cm.

Comparable durability factor was observed for concrete prepared with 0 to 100% of RCA1 in mixtures with 0.45 w/cm and binary cement. The reduction in durability factor was limited to 3%, i.e. decrease from 86% to 83%, with up to 70% RCA1 replacement, while the full replacement of RCA1 reduced the durability factor to 79%. The air void system of concrete made with up to 100% RCA1 and 0.45 w/cm was investigated. Results are summarized in Table 9.5 for both cases of the voids with chord length of lower than 1.0 or lower than 0.5 mm.

Table 9.5 Air void properties of concrete made with 0 to 100% of RCA1

Mixture		DOL1-B-45	RCA1-30-B-45	RCA1-50-B-45	RCA1-70-B-45	RCA1-100-B-45
Fresh air (%)		7.2	7.2	6.6	5.6	5.4
<0.5 mm	Air (%)	4.3	6.8	6.3	6.5	8.6
	$\bar{L}$ (mm)	0.17	0.09	0.10	0.12	0.08
	α (mm^{-}	29.1	38.2	37.2	30.1	37.5
< 1.0 mm	Air (%)	6.3	8.8	9.6	9.4	11.2
	$\bar{L}$ (mm)	0.17	0.09	0.08	0.11	0.07
	α (mm^{-}	21.9	30.75	31.1	22.5	30.0

Results indicated excellent air void properties for the investigated concrete, with spacing factor values lower than 0.2 mm and α of over 0.24 mm^{-1}. Even though the air content in fresh state ranged between 5.4% and 7.2% for all concrete types, the air content in hardened state was increasing with greater RCA content. This is believed to be due to the availability of air voids in residual mortar phase of the RCA particles. Such a mechanism also led to reduction in spacing factor and increase in specific surface area. For instance ad in the case of chords smaller than 0.5 mm, the highest spacing factor of 0.17 mm was observed for DOL1-B-45 concrete made without any RCA. However, the use of 100% RCA1 reduced the spacing factor to 0.08 mm. Similar trends were observed when all chords smaller than 1.0 mm were investigated. A reduction in spacing factor from 0.17 to 0.07 mm was observed as a result of 100% RCA incorporation. These observations were in line with the theory of pressure dissipation due to the use of RCA

from air-entrained source, proposed by Gokce et al. (2004). Given the proper air void system of the mixtures prepared with 0 to 100% RCA1, reduction in durability factor of concrete made with RCA1 can be attributed to the propagation of micro-cracks already available in residual mortar phase of RCA particles.

Concrete with RCA2 achieved excellent freeze-thaw durability. Durability factor of 97%, 92%, and 96% was obtained for the mixtures prepared with 30%, 50%, and 70% RCA2, respectively, compared to 94% for the corresponding concrete made with 100% dolomitic aggregate.

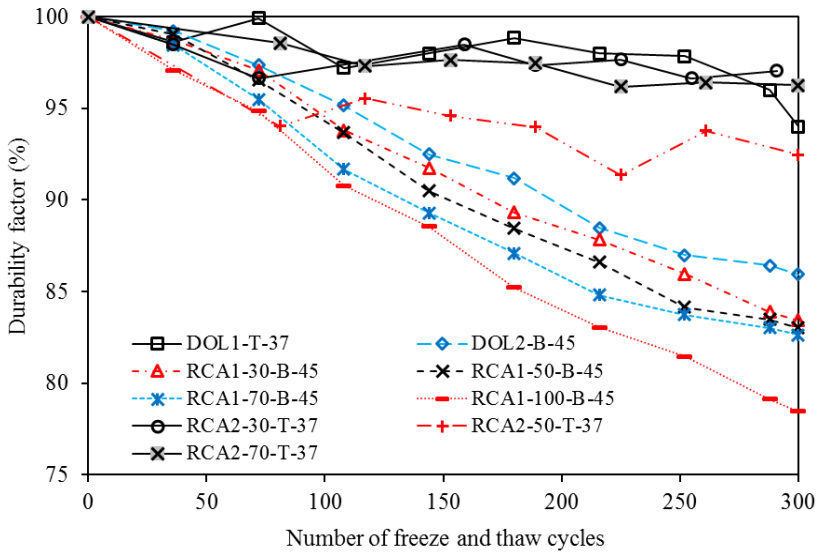

Figure 9.1 Effect of coarse RCA content on durability factor

9.3.1.3 Effect of coarse RCA type. Table 9.4 presents the variations in durability factor for concrete made with ternary cement, 0.37 w/cm, and 50% of different types of RCA. All mixtures made with 50% RCA exhibited excellent freeze-thaw resistance with durability factor ranging from 86% to 92%. Even though the RCA4 was procured from an area with aggregate generally known as susceptible to frost damage, the RCA4-50-T-37 mixture exhibited an acceptable resistance to freeze and thaw cycles, with durability factor of 89%. This was in agreement with RCA soundness test results presented in Table 9.1, where RCA4 exhibited the lowest mass loss of 17%. The durability factor of 86% was obtained for the concrete made with RCA3. This RCA exhibited the highest

concentration of deleterious materials (4.5%) mainly composed of masonry, and the maximum mass loss obtained from soundness test. Based on the findings, the incorporation of up to 50% coarse RCA can result in slight variations (limited to 2% to 8%) in durability factor of concrete proportioned with w/cm of 0.37, regardless of the RCA source.

9.3.1.4 Concrete with fine RCA. Data obtained from testing concrete with up to 15% fine RCA are presented in Table 4. The investigated mixtures were prepared with 30% or 50% coarse RCA2, ternary cement, and 0.37 or 0.40 w/cm. Excellent performance was obtained for such concrete, with durability factor ranging between 91% and 97%. Similar results were reported by Bogas et al. (2016) who investigated the effect of 0, 20%, 50%, and 100% fine RCA in mixtures prepared with w/c of 0.35. The author reported durability factor ranging from 89% to 93%, with slight increase with the use of fine RCA (Bogas et al. 2016). Results presented in Table 4 also indicate that the increase in w/cm from 0.37 to 0.40 resulted in 1% to 6% lower durability factor for the mixtures prepared with dolomitic aggregate, 30% coarse RCA, or a combination of 30% coarse and 15% fine RCA.

In summary, frost durability factor results suggest that the use of 50% coarse RCA from unknown sources, or the use of up to 70% coarse RCA obtained from air-entrained concrete can yield in concrete with proper resistance to freeze-thaw cycles.

9.3.2. De-icing Salt Scaling.

9.3.2.1 Effect of coarse RCA content. Table 9.4 presents a summary of surface damage ratings after 50 cycles of exposure to scaling caused by de-icing salts. Mixtures prepared with binary cement exhibited the best resistance to scaling. For instance, DOL1-B-40 concrete made with binary cement and 0.40 w/cm, exhibited accumulative mass loss of 100 g/m^2. The use of ternary cement with 50% SCM increased the degree of sensitivity to scaling, leading to an increase in scaling from 100 to 730 g/m^2. However, the reduction in w/cm from 0.40 to 0.37 in such concrete enhanced the resistance to scaling damage, with mass loss reduced from 730 to 415 g/m^2.

Despite of the satisfactory durability factor values, a slight increase in scaling was observed due to 70% RCA1 replacement in concrete with binary cement and 0.45 w/cm.

Slight to moderate scaling with damage rate of 2 was obtained for such mixtures compared to slight scaling for the DOL2-B-45 mixtures prepared without any RCA.

The use of up to 70% RCA2 in concrete with ternary cement and 0.37 w/cm increased the degree of surface damage caused by scaling. An increase from 415 to 640, 700, and 450 g/m^2 was observed with the use of 30%, 50%, and 70% RCA2, respectively, in concrete made with ternary cement and 0.37 w/cm.

9.3.2.2 Effect of coarse RCA type. Figure 9.2 presents the variations in mass loss due to scaling as a function of test cycles for concrete prepared with 50% of different coarse RCA types. The mixtures prepared with 50% RCA1, RCA4, and RCA5 exhibited similar performance to that of the corresponding reference concrete, with accumulative values limited to 430 g/m^2. As stated earlier (Table1), these RCA sources contained relatively low (limited to 2.2%) deleterious materials and exhibited comparable soundness values, ranging from 17% to 23%.

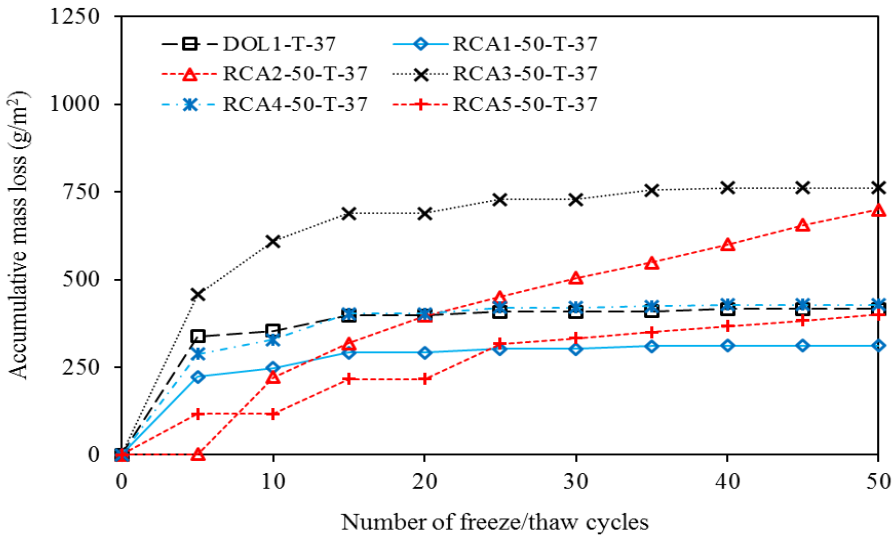

Figure 9.2 Effect of coarse RCA type on accumulative mass loss of de-icing salt scaling samples

The concrete made with 50% of RCA3, with the highest deleterious materials content of 4.5% and highest soundness value of 36%, exhibited mass loss of 760 g/m^2. In general, it may be concluded that the use of 50% coarse RCA I concrete with 0.37 w/cm resulted in acceptable resistance against de-icing salt scaling, with mass loss mainly

limited to 500 g/m^2. However, care must be taken regarding the scaling resistance of such concrete especially in the case of the RCA with over 4% deleterious materials content or high mass loss due to soundness test.

9.3.2.3 Effect of fine RCA. Results presented in Figure 9.3 indicate that the use of up to 15% fine RCA can lead to greater mass loss due to de-icing salt scaling. The incorporation of 15% fine RCA increased the scaling in mixture with 30% of RCA2, ternary cement, and 0.40 w/cm from 870 to 1190 g/m^2. Similar trends were observed for the mixtures with 30% or 50% of RCA2, ternary cement, and 0.37 w/cm, where the use of 15% fine RCA increased the accumulative mass loss from 640 to 1080 and from 700 to 800 g/m^2, respectively. In summary it can be concluded that even though the incorporation of up to 15% fine RCA did not have a negative impact on durability factor, resistance to scaling can be affected by fine RCA incorporation.

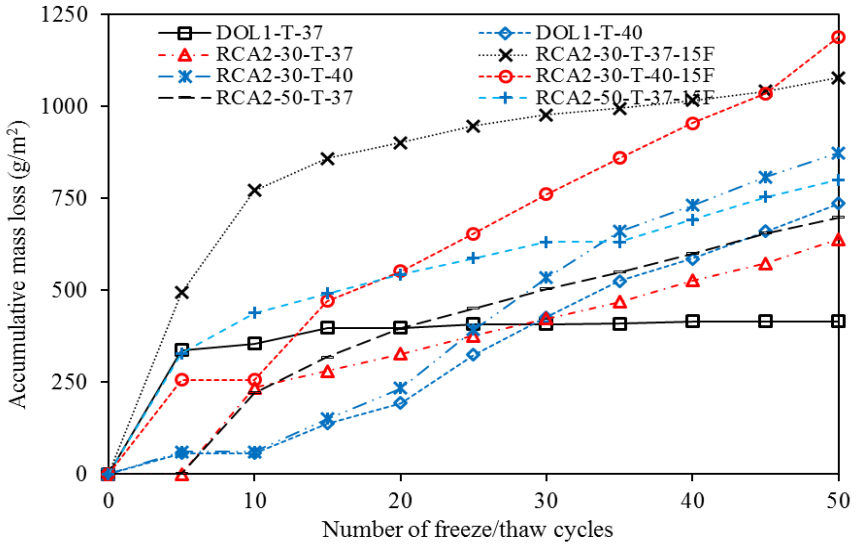

Figure 9.3 Effect of fine RCA on accumulative mass loss of de-icing salt scaling samples

9.3.3. Electrical Resistivity.

9.3.3.1 Effect of coarse RCA content. Figure 9.4 presents the effect of coarse RCA content on electrical resistivity. Two RCA types were used in two groups of concrete mixtures prepared with either a ternary cement and 0.37 w/cm or a binary cement and 0.45 w/cm. Increase in electrical resistivity was observed with time,

regardless of the RCA content. Such a time-dependent rate of increase in electrical resistivity was more significant in the case of the T-37 mixtures, which could be attributed to advanced pozzolanic activity in later ages. For instance and in the case of the mixtures prepared with 50% RCA, the resistivity values were enhanced from 7.4 to 11.1 KΩ.cm for the concrete made with binary cement and 0.45 w/cm, compared to the increase from 16.5 to 31.2 KΩ.cm for mixture prepared with ternary cement and 0.37 w/cm.

In general and regardless of the binder system, a tendency to decrease in electrical resistivity was observed with greater RCA content. The reduction in electrical resistivity was more pronounced concrete prepared with ternary cement and 0.37 w/cm. In other words, the sensitivity to RCA incorporation was higher for the concrete prepared with higher quality binder. For instance, the use of 70% coarse RCA reduced the 91-day electrical resistivity from 35.0 to 29.2 KΩ.cm in concrete made with ternary cement and 0.37 w/cm. Such a reduction was limited to 2.8 KΩ.cm (from 13.1 to 10.3 KΩ.cm) for concrete made with 0.45 w/cm and binary cement.

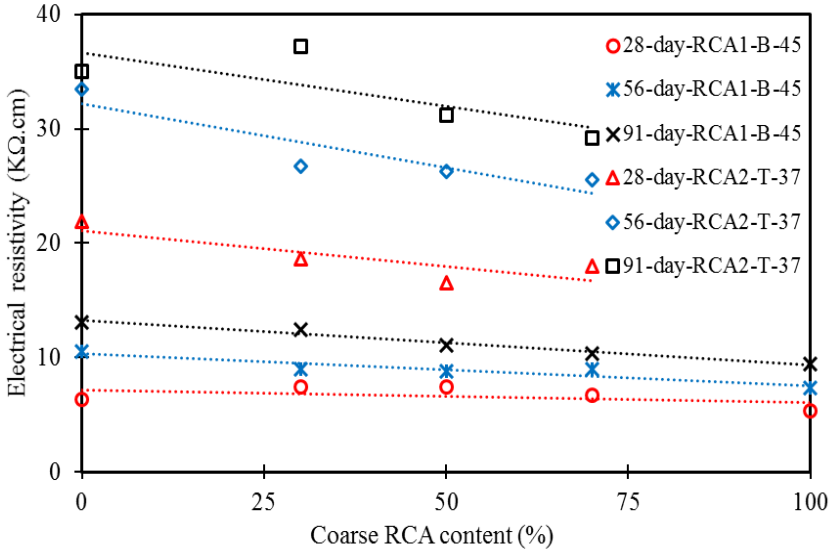

Figure 9.4 Effect of coarse RCA content on electrical resistivity

9.3.3.2 Effect of coarse RCA type. Figure 9.5 presents the electrical resistivity measurements for concrete made with 50% RCA from various sources, proportioned with

either binary cement and 0.40 w/cm, or ternary cement and 0.37 w/cm. The mixtures made with 0.40 and 0.37 w/cm and dolomitic aggregate exhibited 91-day electrical resistivity of 18.7 and 35.0 KΩ.cm, respectively. Results obtained for 91-day measurements of the B-40 mixtures with 50% coarse RCA ranged from 14.8 to 19.1 KΩ.cm, corresponding to up to 21% reduction or up to 2% increase in resistivity. The resistivity results of the T-37 mixtures made with 50% coarse RCA on the other hand were constantly lower than that of the concrete without any RCA, with values ranging from 27.4 to 31.2 KΩ.cm, corresponding to 11%-22% decrease compared to the DOL1-T-37 mixture. Even though the linear relation was not very strong, it was observed that the increase in water absorption of the RCA reduces the 91-day resistivity. This was in line with observations of Duan and poon (2014) and Kou et al. (2012).

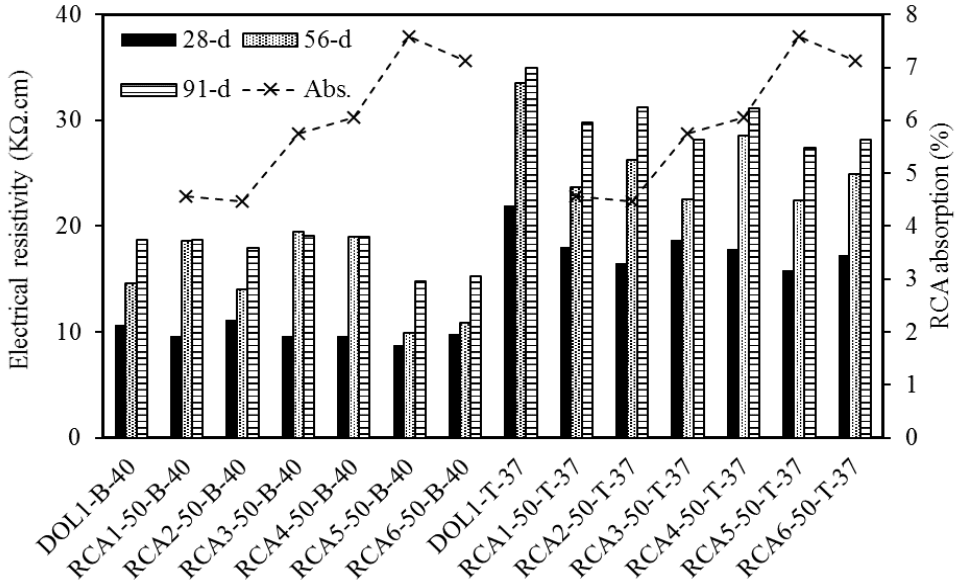

Figure 9.5 Electrical resistivity of concrete made with 50% coarse RCA

In general, it may be concluded that the electrical resistivity of concrete made with 50% coarse RCA can be up to 32% lower than that of the mixture prepared with virgin coarse aggregate, regardless of the RCA source. Such a behavior can be attributed to the presence of potentially porous and cracked residual mortar, potential ionic contamination, and the availability of damaged ITZ in RCA materials. However, the incorporation of 0.37 w/cm and ternary cement were effective in mitigating the negative

impacts of RCA on electrical resistivity compared to the case of concrete made with binary cement, 0.40 w/cm, and 100% dolomitic coarse aggregate. The minimum 91-day resistivity of concrete made with ternary cement, 0.37 w/cm, and 50% of coarse RCA (27.4 KΩ.cm) was higher than that of the concrete made with binary cement, 0.40 w/cm, and without any RCA (18.7 KΩ.cm).

9.3.3.3 Effect of fine RCA content. Figure 9.6 presents the effect of fine RCA on electrical resistivity of concrete proportioned with ternary cement and 0.40 w/cm. It was generally observed that the use of fine RCA tends to reduce the electrical resistivity especially at earlier ages. However, the rate of reduction was not significant for up to 40% fine RCA replacement. The use of up to 40% fine RCA in concrete made with 50% coarse RCA reduced the 56- and 91-day electrical resistivity from 25.4 to 22.2 KΩ.cm, and from 29.7 to 26.4 KΩ.cm, corresponding to 13% and 11% reduction, respectively. This might be due to the advanced hydration of the ternary cement at 91 days that results to a more densified pore structure, hence compensating for the potential impacts of the fine RCA. Another justification for such observations can be the fact the incorporated fine RCA was obtained from airfield concrete, where chloride bearing salts are not typically used during the cold season.

9.3.4. Sorptivity. Figure 9.7 presents the results of sorptivity measurement on concrete made with ternary cement and different amounts of coarse and fine RCA. Results were compared to concrete prepared without any RCA, proportioned with binary or ternary cement and 0.40 w/cm. The highest water absorption was observed for DOL1-B-40 concrete, with initial and secondary sorptivity values of 2.30×10^{-7} and 8.90×10^{-7} $mm.s^{-0.5}$, respectively. Such values were 1.49×10^{-7} and 5.50×10^{-7} $mm.s^{-0.5}$ for the initial and secondary sorptivity of DOL1-T-40 concrete, respectively. Slight increase in sorptivity was observed with the use of 30% coarse RCA or a combination of 30% coarse RCA and 15% fine RCA in concrete with 0.40 w/cm. The secondary sorptivity values were 6.0×10^{-7} and 6.2×10^{-7} $mm.s^{-0.5}$ for the RCA2-30-T-40 and RCA2-30-T-40-15F mixtures, respectively, corresponding to up to 13% increase. The use of greater amount of coarse RCA in mixtures with 0.37 w/cm resulted in a slight rate of increase in water absorption rate, with secondary sorptivity values of 5.1×10^{-7}, 5.0×10^{-7}, and 5.3×10^{-7} $mm.s^{-0.5}$ for the concrete made with 30%, 50%, and 70% coarse RCA, respectively. This

was in agreement with observations of Medina et al. (2014) who reported increase in 28-day sorptivity due to RCA use in concrete made with 323 kg/m^3 OPC and 0.65 w/c. The authors reported sorptivity values of 0.68, 0.67, and 0.79 mm/h$^{0.5}$ for concrete made with 0, 30%, and 50% coarse RCA (Medina et al. 2014). It is worth mentioning that the sorptivity values obtained for concrete made with ternary cement, 0.37 w/cm, and various amounts of RCA were generally lower than that of concrete made with binary cement, 0.40 w/cm, and 100% virgin aggregate.

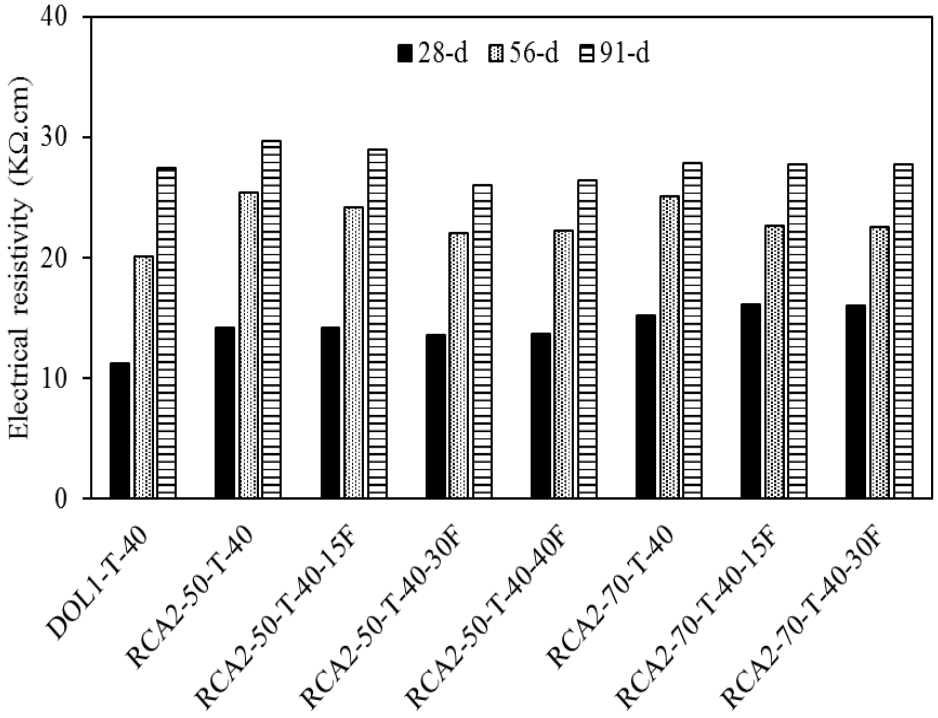

Figure 9.6 Effect of fine RCA content on electrical resistivity

9.3.5. Abrasion Resistance. Table 9.6 summarizes the abrasion resistance data obtained for mixtures prepared with different amounts of coarse RCA2, with or without fine RCA. The mixtures prepared with 100% virgin aggregate and 0.40 w/cm exhibited similar mass loss of 225 g/m^2, regardless of the binder type. An increase in mass loss from 225 to 245 g/m^2, corresponding to 9% increase was observed with 30% coarse RCA incorporation in concrete with 0.40 w/cm and ternary cement. However, all mixtures prepared with 0.37 w/cm had lower mass loss regardless of the fine and coarse RCA

content. For instance, the mass loss obtained for the RCA2-70-T-37 mixture was limited to 130 g/m^2, corresponding to 42% reduction in comparison with DOL1-T-40 concrete. In addition to the higher paste quality, such an observation can be due to the high quality of the incorporated coarse RCA with Los Angeles abrasion value of 33% in comparison with the virgin coarse aggregate with Los Angeles resistance of 28%. Based on the obtained data, it can be concluded that reducing the w/cm and the use of high quality RCA with low Los Angeles value can be considered as effective means of reducing the risk of severe surface damage due to abrasion.

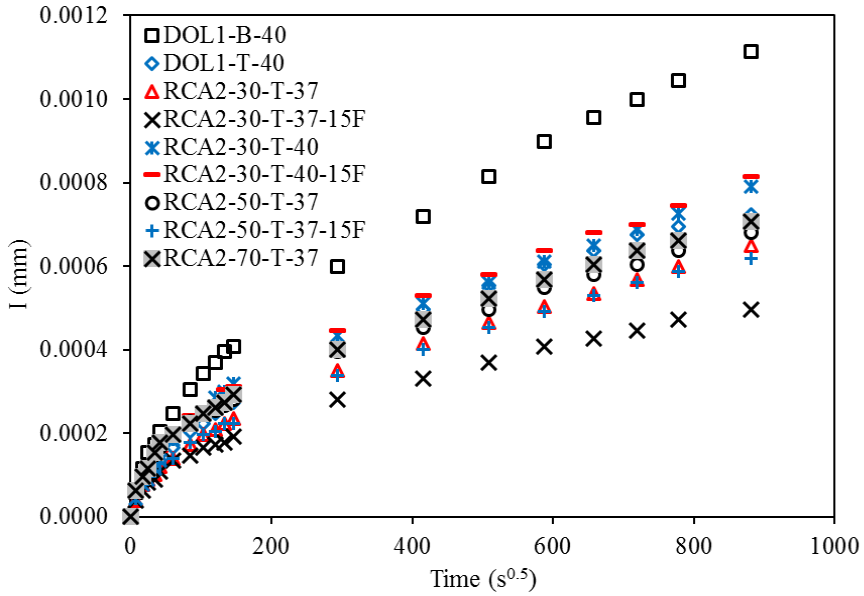

Figure 9.7 Effect of coarse and fine RCA on sorptivity results

9.3.6. Coefficient of Thermal Expansion. Table 9.6 summarizes the CTE values obtained for mixtures prepared with different amounts of coarse RCA2, with or without fine RCA. Slight variations, with a spread limited to 0.66×10^{-6} m/m/ºC was observed for the investigated mixtures. The concrete prepared with dolomitic aggregate, binary cement, and 0.40 w/cm exhibited the highest CTE value of 9.40×10^{-6} m/m/ºC. The use of ternary cement reduced the CTE to 9.07×10^{-6} m/m/ºC. In general, lower coefficient of thermal expansion was observed for the mixtures prepared with RCA, with the lowest CTE of 8.74×10^{-6} m/m/ºC obtained for the concrete made with 70% coarse RCA, ternary cement, and 0.37 w/cm. Results were contrary to the previous findings where increase in

56-day CTE from 7.88×10^{-6} to 8.68×10^{-6} m/m/ºC was observed with 40% coarse RCA replacement in concrete with limestone virgin coarse aggregate, binary cement, and 0.40 w/cm (Sadati and Khayat, 2016).

Table 9.6 Mass loss due to abrasion and coefficient of thermal expansion

Mixture	Mass loss (g/m^2)	CTE (E-6 m/m/ºC)
DOL1-B-40	225	9.40
DOL1-T-40	225	9.07
RCA2-30-T-37	150	9.34
RCA2-30-T-40	245	9.14
RCA2-30-T-37-15F	130	9.12
RCA2-30-T-40-15F	205	8.90
RCA2-50-T-37	95	9.25
RCA2-50-T-37-15F	130	-
RCA2-70-T-37	130	8.74

9.4. REMARKS

The effect of RCA on durability of concrete was investigated. RCA from five commercial recycling centers, along with one laboratory-produced source were employed at replacement rates of 30%, 50%, 70%, and 100%, by volume. Up to 40% fine RCA was also used. The reference concrete mixtures were proportioned without any RCA and with 0.40 and 0.45 w/cm using 25% fly ash. Other mixtures with lower w/cm of 0.37 and ternary cement were prepared to compensate for anticipated loss of durability stemming from the use of RCA. Based on the results of this study, the following conclusions are warranted:

- The use of up to 70% coarse RCA from a high quality air-entrained concrete source used in airfield or laboratory produced air-entrained concrete did not cause any significant variation in frost durability factor. The use of 50% commercially produced RCA in concrete with 0.37 w/cm reduced the durability factor from 94% to 86%, though both values are considered provide adequate frost durability.

On the other hand, such concrete exhibited greater de-icing salt scaling, with an increase in accumulative mass moss from 415 to up to 760 g/m^2.

- Air content in hardened state was shown to increase with the use of RCA obtained from air-entrained concrete. An increase in volume of air voids with chord length of lower than 1.0 mm from 6.3% to 11.2% was observed with full replacement of such coarse RCA. Reduction in spacing factor from 0.17 to 0.07 mm, and increase in specific surface from 21.9 to 30 mm^{-1} was observed for such concrete.
- No reduction in frost durability factor was observed when the fine RCA volume was limited to 15%, regardless of the w/cm. However, the use of 15% fine RCA in concrete with ternary cement and 0.40 w/cm increased the mass loss due to scaling from 870 to 1190 g/m^2.
- The increase in fine and coarse RCA reduced the electrical resistivity, depending on the RCA content, binder type, and w/cm. The use of up to 40% fine RCA in concrete prepared with ternary cement and 0.40 w/cm reduced the 91-day electrical resistivity by up to 10%. Concrete with lower w/cm (0.37) and ternary cement was more sensitive to the use of RCA. Up to 32% reduction in electrical resistivity was observed with 50% coarse RCA replacement in such mixtures. However, resistivity values of mixtures made with ternary cement, 0.37 w/cm, and 50% coarse RCA were higher than that of the concrete prepared with binary cement, 0.40 w/cm, and without any RCA.
- Slight increase in sorptivity was observed with the use of RCA, where using 30% coarse RCA in concrete with ternary cement and 0.40 w/cm increased the secondary sorptivity from 5.5×10^{-7} mm.s$^{-0.5}$ to 6.0×10^{-7} mm.s$^{-0.5}$. However, the use of lower w/cm and ternary cement was effective in reducing the sorptivity. The mixture prepared with 70% coarse RCA, ternary cement, and 0.37 w/cm exhibited secondary sorptivity of 5.3×10^{-7} mm.s$^{-0.5}$, compared to 8.9×10^{-7} mm.s$^{-0.5}$ in the case of concrete with 100% dolomitic aggregate, binary cement, and 0.40 w/cm.
- The concrete made with RCA exhibited greater abrasion damage. However, the use of lower w/cm of 0.37 was effective in reducing the abrasion damage. The mass loss dropped from 225 g/m^2 in the case of concrete with 0.40 w/cm and

100% virgin aggregate to 130 g/m^2 for concrete with 0.37 w/cm and 70% coarse RCA. A slight reduction, limited to 7%, was observed in CTE of concrete made with up to 70% coarse RCA.

10. FIELD PERFORMANCE OF CONCRETE PAVEMENT INCORPORATING RECYCLED CONCRETE AGGREGATE

10.1. RESEARCH SIGNIFICANCE

Given the variable characteristics of RCA compared to virgin aggregate, there still exists a conservative approach that limits the use of RCA in field applications (Surya et al. 2013). Therefore, most of the application of RCA involves the use of RCA as aggregate in base and subbase layers, backfill, embankment, stabilization, erosion control (riprap), and landscaping (ACPA 2009). According to a survey published by the Federal Highway Administration (FHWA 2004), 41 states recycled concrete for use as aggregate in new construction in United States. Thirty eight of these states allow the use of RCA as aggregate in base layer applications. Of these states, however, only 11 were using RCA in new Portland cement concrete production (FHWA 2004).

With the increasing interest in the use of sustainable concrete made with RCA, more information regarding the performance of such materials in field applications is required. The research presented here contributes to the evaluation of properties of pavement concrete proportioned with partial replacement of RCA. The results presented should be of interest to owner agencies and engineers considering the design and use of eco-friendly concrete for transportation infrastructure.

The objective of the study reported in this section is to investigate the material properties and performance of the rigid pavement cast with RCA. The investigation is divided in two phases. The first phase investigates the properties of concrete mixtures produced with fine and coarse RCA for pavement application. Several concrete mixtures proportioned with different fly ash replacement levels, fine and coarse RCA contents, and w/cm were investigated in the laboratory. The mixtures were tested to determine mechanical properties, durability, and shrinkage. Two mixtures produced with 30% and 40% coarse RCA replacement and a reference concrete proportioned without any RCA were employed at second phase for the construction of a pavement section in St. Louis, Missouri. Sampling was conducted at the job site, and core samples were extracted to evaluate in-situ properties of the sustainable concrete. Instrumentation was also employed to monitor early age and long-term deformation of different pavement sections.

10.2. EXPERIMENTAL PROGRAM

10.2.1. Material Properties. The investigated concrete was proportioned with binary cement containing Type I/II Portland cement and Class C fly ash. Crushed limestone with a maximum size of 25 mm was used for the virgin aggregate. Well-graded siliceous river-bed sand was used. Coarse and fine RCA procured from a commercial recycling center were employed as a partial replacement of the virgin aggregate. The RCA (both fine and coarse) were produced by recycling old concrete available at Lambert International Airport area in St. Louis, Missouri. Table 10.1 presents the physical properties of the fine and coarse aggregates. The residual mortar content of the RCA was determined by a combination of thermal stress and chemical degradation testing as suggested by Abbas et al. (2009). RCA was soaked in a saturated solution of sodium sulfate and subjected to cycles of freezing and thawing to detach the adhered mortar from the old virgin aggregate particles Abbas et al. (2009).

Table 10.1 Physical properties of the virgin and recycled concrete aggregate

Aggregate	Specific gravity	Dry rodded unit weight (kg/m^3)	Absorption (%)	Los Angles abrasion (%)	Residual mortar (% mass)
River sand	2.63	-	0.34	-	-
Fine RCA	2.41	-	6.8	-	-
Limestone	2.64	1602	0.5	24	-
Coarse RCA	2.38	1458	4.2	33	36

10.2.2. Mixture Proportions. An initial laboratory investigation was conducted at phase I to evaluate the performance of candidate mixtures. A mixture recommended by the Missouri Department of Transportation (MoDOT) for rigid pavement applications was used as a reference concrete. This concrete was prepared with 323 kg/m^3 of cementitious materials that included 25% Class C fly ash, by mass, a w/cm of 0.40, and virgin aggregate. The initial laboratory investigation involved the variation of w/cm, fly ash, and fine RCA content. Class C fly ash was incorporated at a replacement rate of 25% to 40%, by mass of cementitious materials. The w/cm varied from 0.37 to 0.42. Fine RCA replacement ranged from 0 to 20%, by volume, and coarse RCA replacement was

fixed at 30%. This was carried out to evaluate engineering properties and durability of concrete containing fine RCA and to investigate the feasibility of producing an environmentally friendly, yet durable, pavement material.

Table 10.2 summarizes the mixture proportions and fresh properties of the concrete developed and evaluated in phase I. All mixtures were proportioned with sand-to-aggregate ratio (S/A) of 40% (by volume) and total cementitious material content of 323 kg/m^3, except for the equivalent mortar volume (EMV) mixture (Fathifazl et al. 2009). The total mortar of the RCA-made concrete is considered as the summation of residual mortar content attached to the RCA particles and the fresh mortar of the new mixture. The second condition of the EMV method is that the total virgin coarse aggregate content in the reference concrete should be equal to the total virgin coarse aggregate content of the RCA-concrete, i.e. the summation of the old coarse aggregate available in RCA particles and virgin aggregate of the RCA-made concrete (Fathifazl et al. 2009).

A lignum-based water reducing admixture (WRA) with specific gravity of 1.2 and 40% solid content, and an air-entraining admixture (AEA) were incorporated to secure an initial slump value of 50 ± 15 mm and an air content of 6% ± 1%, respectively. A coding system was developed for labeling the different mixtures. The codes are composed of three numbers indicating the fly ash content, fine RCA content, and w/cm. As an example, code “25-15-40” refers to a mixture made with 25% of fly ash, 15% of fine RCA, and w/cm of 0.40.

The mixtures developed for phase II (field implementation) were proportioned with 323 kg/m^3 of binary binder composition of Type I/II Portland cement and 25% of Class C fly ash by mass of binder. The w/cm was fixed at 0.4 with S/A of 0.42. Aggregate sources incorporated in the field implementation were the same as those used in laboratory investigations.

The concrete was produced at the contractor’s ready mix plant located 30 minutes from the job site. The batching plant used a wet 9-m^3 electric gear portable central mix. The materials were mixed in the drum mixer with speed of 15 rpm for one minute and hauled in 6-m^3 deliveries in dump trucks.

Table 10.2 Mixture proportions of concrete investigated in phase I

Mixture ID		Ref.	35-0-40	35-15-37	40-20-37	35-10-42	25-15-40	25-10-37	25-0-40	EMV
Cementitious materials (kg/m^3)		323	323	323	323	323	323	323	323	282
Type I cement (kg/m^3)		243	210	210	194	210	243	243	243	212
Class C fly ash, by mass (%)		25	35	35	40	35	25	25	25	25
Class C fly ash (kg/m^3)		81	113	113	129	113	81	81	81	71
w/cm		0.4	0.4	0.37	0.37	0.42	0.4	0.37	0.4	0.4
Water (kg/m^3)		129	129	120	120	136	129	120	129	113
Fine RCA, by volume (%)		-	-	15	20	10	15	10	-	-
Fine RCA (kg/m^3)		-	-	102	136	68	102	68	-	-
Sand (kg/m^3)		745	745	633	596	670	633	670	745	692
Coarse virgin aggregate (kg/m^3)		1121	785	785	785	785	785	785	785	841
Coarse RCA (kg/m^3)		-	303	303	303	303	303	303	303	371
Mechanical properties batch	Air content (%)	5.5	5.2	5.5	5.3	5.3	5.2	6.0	5.9	5.5
	Slump (mm)	65	90	50	50	65	50	40	40	25
	Unit weight (kg/m^3)	2392	2358	2347	2334	2353	2337	2327	2334	2392
Durability batch	Air content (%)	5.3	5.1	5.3	5.0	5.2	5.3	5.9	5.6	6.0
	Slump (mm)	50	75	65	40	75	65	40	65	40
	Unit weight (kg/m^3)	2404	2345	2342	2323	2326	2364	2352	2382	2350

Table 10.3 summarizes the properties of the concrete used for casting various pavement sections. All mixtures had air contents of 6% ± 1%. Slump values were within the desired range of 50 ± 15 mm. No signs of edge slump and no problems with casting and finishing and tinning of the concrete mixtures were reported at the job site.

Table 10.3 Properties of concrete mixtures used in field study

Mixture ID	Reference	30% RCA	40% RCA
Type I cement (kg/m^3)	243	243	243
Class C fly ash (kg/m^3)	81	81	81
Water (kg/m^3)	129	129	129
Coarse aggregate (kg/m^3)	1075	755	645
Coarse RCA (kg/m^3)	-	335	445
Sand (kg/m^3)	795	795	795
WRA (l/m^3)	2.0	2.2	2.2
Slump (mm)	40	35	35
Air content (%)	5.5	6.5	6.5
Unit weight (kg/m^3)	2380	2320	2290

10.2.3. Details of Field Implementation. The field implementation was planned in collaboration with MoDOT and involved the construction of a 6.6-m wide ramp approach to a bridge in St. Louis, Missouri. The experimental sections were placed within the 300-m length of the project in three different sections. In total, 450 m^3 of concrete was used. The concrete was hauled by dump trucks, placed with a slip-form paver, and finished with transverse tinning. A liquid curing compound was sprayed on the finished surfaces after finishing. More details about the site conditions are available in (Khayat and Sadati 2014).

The rigid pavement was cast on a 100-mm thick base layer made with a standard aggregate composition (Type 5 aggregate) complying with MoDOT specification Number 1007 (Missouri Department of Transportation 1999). The base was constructed on a compacted subgrade soil. The various concrete materials were used to construct a

JPCP system that had a uniform thickness of 215 mm. The experimental pavement section consisted of a 3.6-m wide traffic lane, a 3.0-m wide concrete shoulder, and a 150-mm wide ditch. The traffic lane was tied to an existing lane cast with MoDOT's reference concrete a few weeks in advanced, as shown in Figure 10.1. Longitudinal joints were saw-cut between the travel lane and the shoulder. Transverse joints were saw-cut at 4.5-m spacing where dowel bars were pre-placed. This resulted in 3.6×4.5 m pavement panels along the traffic lane. Saw-cutting was performed about 6 to 8 hours after concrete casting.

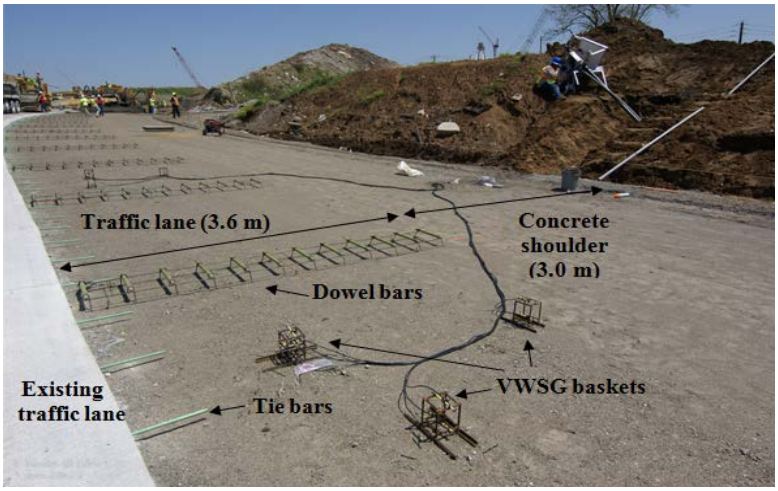

Figure 10.1 General view of the construction site

10.2.4. Specimen Preparation and Testing. A drum mixer with 110 liter capacity was used for preparing the mixtures in the laboratory. The samples were demolded 24 hours after casting and cured in lime-saturated water at 21±1ºC until the time of testing. For the determination of compressive strength, 100×200 mm cylindrical specimens were employed in accordance with ASTM C39 (2001). Three samples were tested for compressive strength values. Similar samples were used for testing the modulus of elasticity (MOE) and splitting tensile strength in accordance with ASTM C469 (2010) and ASTM C496 (2011), respectively. The flexural strength was measured on

150×150×535 mm beams in accordance with ASTM C78 (2010). Two specimens were tested for each mixture at each testing age.

Shrinkage was monitored using 75×75×285 mm prisms according to ASTM C157 (2008). Samples were cured in lime-saturated water for seven days before storage at 23±1ºC and 50%±3% relative humidity. The bulk electrical resistivity was determined on 100×200 mm cylindrical specimens according to ASTM C1760 (2012). Samples were cured in lime-saturated water and tested until the age of 91 days. Rapid chloride ion permeability test was conducted on 50-mm thick slices obtained from cutting 100×200 mm cylindrical specimens in accordance with ASTM C1202 (2012).

Two sets of specimens were employed to measure frost durability according to ASTM C666, Procedures A and B (ASTM C666 2003). For Procedure A, specimens were cured in lime saturated water for 28 days before being subjected to freeze and thaw cycles. The curing period was 35 days in the case of the Procedure B. CTE was determined using cylindrical specimens measuring 100×200 mm, based on AASHTO T336 (2011). Samples were cured in lime-saturated water up to the testing age. Core samples were extracted and tested for abrasion resistance in accordance with ASTM C779-C (2012).

10.3. RESULTS AND DISCUSSION

10.3.1. Test Results of Mixtures Investigated in Phase I. Table 10.2 presents the fresh properties of these mixtures. Values of the measured air content in fresh concrete ranged from 5.2% to 6.0%. All mixtures exhibited slump values within the range of 50±15 mm, except for the 35-0-40 and EMV mixtures with slump values of 90 and 25 mm, respectively. The increase in residual mortar content of the RCA coincides with the decrease in the amount of fresh mortar according to the EMV method. Given the reduction in fresh mortar content, reducing the workability of the concrete can be considered as a drawback for the EMV method.

10.3.1.1 Mechanical properties. Table 10.4 presents the mechanical properties of the mixtures investigated in phase I. The minimum 1-day compressive strength of 17

MPa was observed for the mixture prepared with 40% fly ash which was lower than the minimum requirement of 19 MPa. The EMV samples exhibited the highest 1-day compressive strength of 24 MPa. All mixtures had 28-day compressive strength values higher than the targeted minimum value of 28 MPa. The highest 56-day strength was observed for the concrete with w/cm of 0.37 and 40% fly ash. Comparing the results of the reference and 25-0-40 mixtures, a 7% decrease in 91-day strength was observed as a result of 30% coarse RCA replacement. The highest 91-day strength values were observed for the mixtures made with 35% and 40% fly ash replacement due to the pozzolanic reaction at later ages. Up to 20% fine RCA replacement did not have a significant effect on compressive strength. A slight decrease of up to 4% in compressive strength was observed at 91 days in the case of mixtures 35-15-37, 40-20-37, and 25-15-40. Similar results were reported by (2007) who found that the incorporation of up to 30% RCA replacement does not have a significant effect on compressive strength of concrete.

The highest 7-day splitting tensile strength value of 3.7 MPa was observed for the EMV samples, which is believed to be due to good aggregate interlock, followed by the 25-10-37 mixture proportioned with w/cm of 0.37, 25% fly ash, and 10% fine RCA. Variations in fly ash content and w/cm did not have a major effect on 7-day splitting tensile strength of the rest of specimens with results varying from 2.5 to 2.8 MPa.

Increase in coarse RCA content from 0 to 30% did not have a significant effect on 7-day splitting tensile strength. However, a decrease of 6% in 56-day results was observed while comparing the reference concrete with mixture 25-0-40 that incorporated 30% coarse RCA. Increasing the fine RCA content from 0 to 15% resulted in only 3% decrease in the 56-day tensile strength of the 25-15-40 mixture in comparison with the 25-0-40 concrete. The highest 56-day value of 4.0 MPa was observed for the 40-20-37 and EMV mixtures, indicating that a combination of 40% fly ash and reducing w/cm to 0.37 was efficient in enhancing the splitting tensile strength of the mixture made with 20% fine RCA and 30% coarse RCA. Similar results were observed by Volz et al. (2014) who found that up to 8% decrease in splitting tensile strength can be obtained when 50%

RCA replacement is used in concrete with 0.45 w/cm and 315 kg/m^3 of cementitious materials.

All mixtures had flexural strength values of higher than 4.1 MPa at 28 days, as presented in Table 10.4. A 5% decrease in flexural strength was observed as a result of increasing the coarse RCA content from 0 (reference) to 30% (mixture 25-0-40). Mixture 25-10-37 made with w/cm of 0.37, 10% fine RCA, and 25% fly ash had the highest 28-day flexural strength of 5.9 MPa.

Comparing the 56-day flexural strength of mixture 25-15-40 to that of 25-0-40 reveals 7% decrease as a result of 15% fine RCA replacement. Reducing the w/cm to 0.37 and incorporation of 25% fly ash in concrete with 10% fine RCA was beneficial in improving the 56-day flexural strength by 6% compared to the reference concrete. However, in the case of the mixture made with 40% fly ash, w/cm of 0.37 and 20% fine RCA replacement, flexural strength was reduced by 9% compared to the reference specimens. The highest 56-day flexural strength was observed for the EMV mixture followed by the 25-10-37 mixture; this was in agreement with the splitting tensile strength observations. For both testing ages, the minimum results were observed in the case of the mixture 35-10-42 with w/cm of 0.42.

As presented in Table 10.4, the reference, 40-20-37, and 35-0-40 mixtures had the highest 56-day MOE results of about 40.5 GPa followed by the EMV mixture (38.5 GPa). The 56-day MOE of concrete with 30% coarse RCA replacement (mixture 25-0-40) was 8% lower than the reference concrete. The replacement of up to 15% sand by fine RCA did not lead to considerable drop in elastic modulus (4% decrease at 91 days). Similar results were observed in the case of mixture 40-20-37 made with 0.37 w/cm and 20% of fine RCA replacement. This is in agreement with Silva et al. (2016) who reported 15% to 20% decrease in MOE as a result of 30% to 50% RCA replacement, respectively.

10.3.1.2 Shrinkage and durability. As indicated in Table 10.2, all mixtures had fresh air contents of 5% to 6%. Slump values were within the targeted range of 50±15 mm, except for the 30-0-40 and 35-10-42 mixtures with initial slump value of 75 mm.

Table 10.4 Mechanical properties of laboratory made concrete

Mixture ID		Ref.	35-0-40	35-15-37	40-20-37	35-10-42	25-15-40	25-10-37	25-0-40	EMV
Property	Age (d)									
Compressive strength (MPa)	1	19.8	20.2	18.7	17.3	19.8	22.2	21.3	18.7	24.4
	7	35.4	35.6	35.5	37.9	33.1	37.6	34.0	34.1	36.1
	28	43.5	52.1	53.6	48.5	42.7	49.5	48.8	42.1	41.7
	56	48.1	53.2	54.8	55.7	49.5	52.4	50.0	46.6	44.6
	91	51.8	56.7	53.2	54.3	50.9	50.3	52.2	48.0	48.7
Splitting tensile strength (MPa)	7	2.65	2.80	2.70	2.75	2.80	2.50	3.15	2.70	3.70
	28	3.50	3.30	3.60	3.50	3.70	3.60	3.45	3.25	3.80
	56	3.85	3.85	3.40	4.05	3.30	3.50	3.50	3.60	4.05
Flexural strength (MPa)	28	4.50	4.20	5.55	4.60	4.15	4.70	5.90	4.40	5.30
	56	5.50	4.65	5.55	5.00	4.40	4.85	5.85	5.20	6.05
MOE (MPa)	28	35.5	36.5	36.5	36.0	34.0	35.5	36.0	34.5	37.0
	56	40.5	40.0	37.5	40.5	37.0	36.0	35.0	37.5	38.5
Durability factor (%), Procedure A		91	87	91	88	88	88	89	90	87

The shrinkage results are illustrated in Figure 10.2. All mixtures had drying shrinkage values limited to 600 με after 180 days of drying. The minimum shrinkage was recorded for the EMV mixture, with 300 με at six months of age. This was due to the lower amount of fresh mortar, along with higher content of coarse aggregate in this mixture. Similar observations were reported by Fathifazl et al. (2011) who showed that the EMV method was effective in reducing the 220-day shrinkage of concrete with w/cm of 0.45 by more than 150 με. Increasing the coarse RCA content from 0 to 30% (Ref. vs. 25-0-40) increased the 180-day shrinkage from 450 to 520 με.

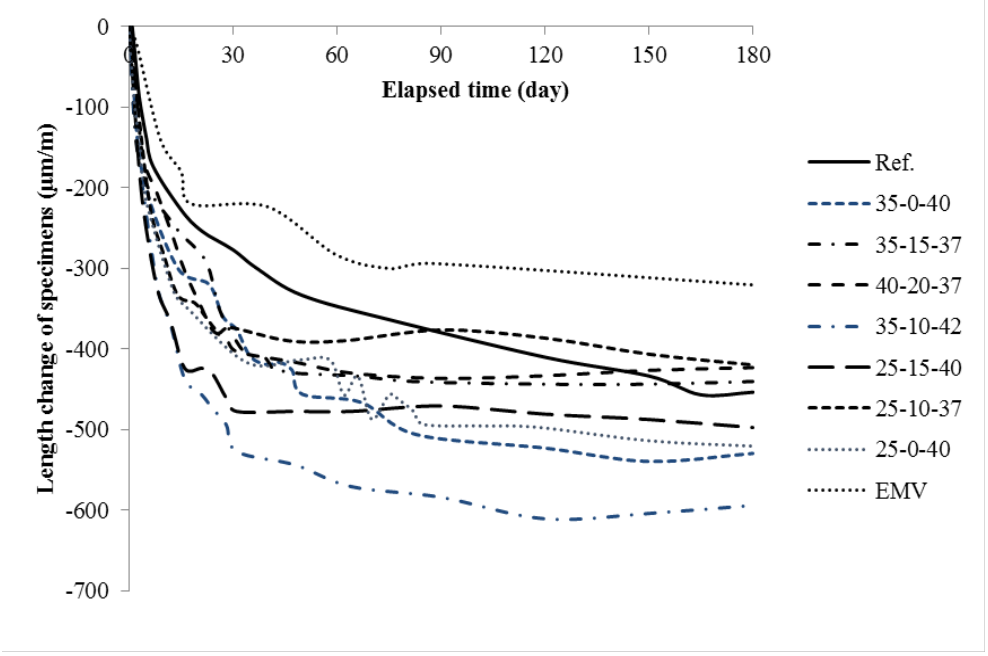

Figure 10.2 Shrinkage deformation of laboratory made concrete

Increasing the fine RCA content from 0 to 15% had no significant effects on drying shrinkage of the 25-15-40 mixture in comparison with that of the 25-0-40. Using 40% fly ash while reducing the w/cm to 0.37 was helpful in reducing the 180-day shrinkage of the mixture proportioned with 20% fine RCA to 425 με. Increasing the

w/cm to 0.42, on the other hand, increased the 180-d shrinkage of the mixture made with 15% fine RCA and 35% fly ash to 590 με.

As indicated in Figure 10.3, the 56-day resistivity values were slightly higher than the 28-day observations. However, 80% to 110% increase in 91-day resistivity was observed in comparison with 28-day results, which is believed to be due to pozzolanic reaction of fly ash available in mixtures. The maximum 28-day bulk resistivity was observed for the reference concrete produced without any RCA. The incorporation of 30% coarse RCA reduced the 28-day resistivity slightly (4%). The increase in fine RCA content from 0 to 15%, on the other hand, resulted in 22% decrease in 28-day resistivity of the 25-15-40 mixture in comparison with 25-0-40 specimens.

The minimum 28-day resistivity of 9.3 KΩcm was observed for the EMV specimens. The highest 91-day resistivity was recorded for the 40-20-37 mixture, demonstrating the potential for compensating for impacts of RCA on the resistivity by means of fly ash and low w/cm. the incorporation of 30% coarse RCA reduced the 91-day resistivity by 6%. Increase in fine RCA from 0 to 15% reduced the 91-day resistivity by 18%. The minimum 91-day resistivity of 17.9 KΩcm was observed for the 25-15-40 mixture.

Results of the durability factor measurements after 300 cycles of freezing and thawing according to ASTM C666, Procedure A are presented in Table 10.4. All mixtures exhibited good frost resistance with a durability factor higher than 87%. No difference was observed when incorporating 30% coarse RCA replacement (25-0-40) compared to the reference concrete.

Increasing the fine RCA content from 0 to 15% reduced the durability factor from 90% to 88% (mixture 25-0-40 vs. 25-15-40). Durability factor of 88% in the case of mixture 40-20-37 indicates that using up to 20% fine RCA does not have a significant effect on frost durability. Similar performance was observed in the case of mixtures 35-0-40 and 35-10-42 with w/cm of 0.4 and 0.42 and durability factors of 87% and 88%, respectively. Results are in agreement with observations of Richardson et al. (2011) who reported that given the similar strength grade, there is no significant difference in

freeze/thaw resistance of the RCA-made and conventional concrete, providing that adequate air entrainment is secured.

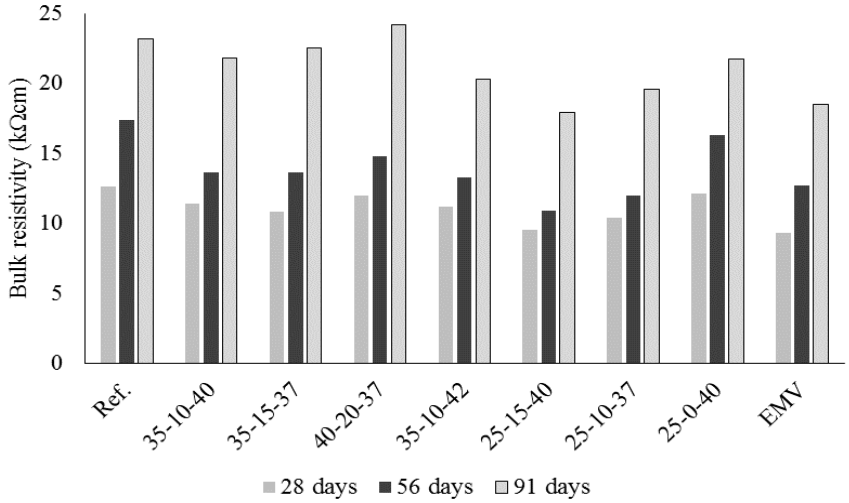

Figure 10.3 Electrical resistivity data of laboratory made concrete

10.3.2. Proposed Candidates for Field Implementation. Based on the laboratory investigations, the performance of concrete made with coarse RCA up to 30% was comparable with that of the reference concrete in most cases. The strength criteria required by MoDOT limit the 1-day and 28-day compressive strength of a 215-mm pavement to 19 and 28 MPa, respectively. All mixtures investigated in laboratory developed 28-day compressive strength values higher than the required criteria. Increasing the fly ash content to 40% reduced the 1-day strength of the 40-20-37 mixture to 17 MPa. In order to reduce the risk of drop in 1-day compressive strength and to avoid frost related problems, it was decided to keep the fly ash replacement level at 25% for site implementation. Given the reductions observed in flexural strength and negative effects on shrinkage and durability, it was decided to exclude incorporation of fine RCA and limit the w/cm to 0.40 in field implementation. Therefore, concrete mixtures produced with 30% and 40% coarse RCA replacements (by mass) were used along with the reference mixture without any RCA for the field work in phase II.

10.3.3. Test Results of Mixtures Investigated in Phase II.

10.3.3.1 Control samples. Sampling was conducted at the job site during placement. A vibrating table was incorporated to ensure proper consolidation of all specimens. Wet burlap and plastic sheets were incorporated to cover the samples for one day at job site. Field-sampled specimens were transported to the laboratory afterwards and moist cured until the age of testing. A summary of mechanical property measurements is reported in Table 10.5.

The highest 1-day compressive strength of 18.2 MPa was observed for the reference concrete, which was slightly less than the required minimum of 19 MPa. This was followed by the 30%RCA and 40%RCA mixtures with 16.3 and 14.0 MPa, respectively. The compressive strength of the 30%RCA mixture was 12%, 13%, and 7% less than that of the reference concrete at 7, 28, and 56 days, respectively. For the 40%RCA mixture, 11%, 11%, and 5% decrease in compressive strength was observed at 7, 28, and 56 days, respectively. The reference concrete made without any RCA exhibited the highest compressive strength of 42.6 MPa at 91 days. The 30%RCA and the 40%RCA mixtures had 91-day strength values of 39.8 and 37.5 MPa, respectively. No significant difference was observed in compressive strength for the 30% and 40% RCA mixtures.

The reference concrete and the mixture made with 40%RCA developed the same 7-day splitting tensile strength of approximately 3.0 MPa. At 28 days, slightly higher tensile strength of 3.15 MPa was recorded for the reference specimens, followed by 3.05 MPa for the 30% and 40% RCA mixtures. Similar results were observed for the splitting tensile strength of the reference and RCA mixtures with 56-day results of 3.30 to 3.45 MPa.

All three types of mixtures exhibited similar flexural strength results at 28 days which is in line with splitting tensile strength data. At 56 days, the mixtures made with 30% and 40% of RCA replacement had results similar to that of the reference mixture, varying from 5.70 to 5.85 MPa.

The MOE was the most affected mechanical property due to the incorporation of RCA. At 28 days, 7% and 18% decrease in MOE was observed with the use of 30% and 40% RCA replacements, respectively. Compared to the reference mixture, a decrease of 22% and 14% in MOE was recorded as a result of incorporating 30% and 40% RCA at 56 days, respectively.

Table 10.5 Mechanical properties of concrete used in field study

Mixture	Age (day)	Reference	30%RCA	40%RCA
Compressive strength (MPa)	1	18.2 (4.8*)	16.3 (7.0)	14.0 (5.0)
	7	31.8 (3.6)	27.9 (6.0)	28.3 (3.0)
	28	37.6 (1.2)	32.7 (4.0)	33.3 (5.0)
	56	39.0 (3.7)	36.3 (10.0)	37.1 (7.0)
	91	42.6 (2.2)	39.8 (4.0)	37.5 (3.0)
Splitting tensile strength (MPa)	7	2.95	2.60	3.00
	28	3.15	3.05	3.05
	56	3.30	3.45	3.40
Flexural strength (MPa)	28	5.55 (6.5)	5.20 (8.8)	5.35 (4.1)
	56	5.80 (6.7)	5.85 (0.6)	5.70 (2.4)
	after F/T	4.40 (7.8)	4.45 (10.9)	3.80 (7.6)
Modulus of elasticity (GPa)	28	33.6 (2.0)	31.4 (3.0)	27.6 (12.0)
	56	38.8 (-)	30.4 (9.0)	33.2 (-)
Permeability (Coulomb)	28	2,040	2,020	2260
	56	1,395	1,425	1,515
	91	990	1230	1320
Durability factor (%)	Procedure A	92	92	91
	Procedure B	90	92	87
Coefficient of thermal expansion (μm/m/ºC)	2	7.88	8.24	8.68
	11	7.56	7.74	7.88

*COV (%)

Figure 10.4 shows the variation of drying shrinkage with time. The reference and 30%RCA mixtures exhibited similar shrinkage values, which were approximately 100 με

lower than those for the 40%RCA mixture. The increase in drying shrinkage of the 40%RCA concrete is due to the lower restraining capacity of the RCA particles, given the residual mortar, and decreases in the concentration of stiff virgin aggregate in the mixture (Xiao et al. 2012). The shrinkage findings are in line with data reported in (Volz et al. 2014, Xiao et al. 2012).

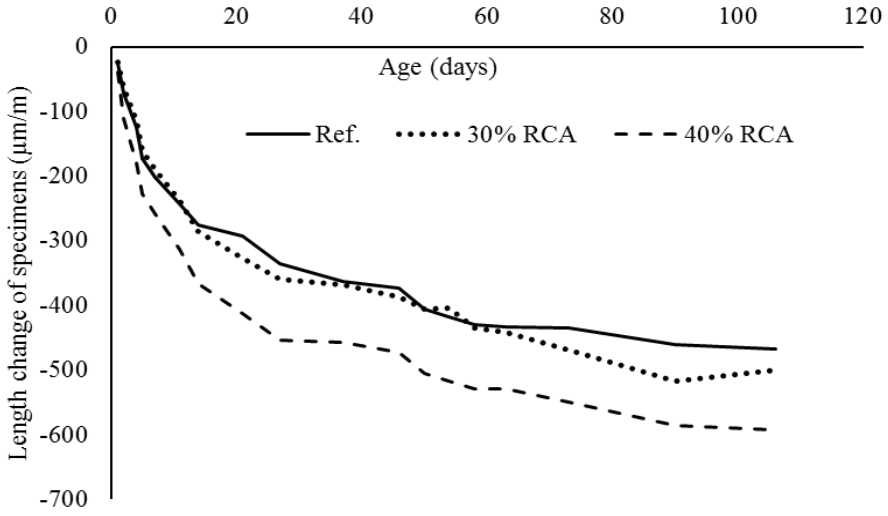

Figure 10.4 Variation of drying shrinkage with time

The rapid chloride-ion permeability test (RCPT) was performed at 28, 56, and 91 days of age. Results of permeability test are presented in Table 10.5. For 28 and 56-day measurements, the reference and 30%RCA mixtures had similar performance with a spread of 200 Coulomb in the case of the 40%RCA mixture compared to the reference samples, which is negligible. The effect of RCA incorporation on RCPT was slightly higher at 91 days where the reference concrete had very low permeability of 900 Coulomb, compared to low permeability of 1300 Coulomb for the RCA mixtures, according to (ASTM C1202 2012).

The values of durability factor measured at the end of test cycles are presented in Table 10.5. Results obtained from both procedures are in good agreement. All mixtures

exhibited acceptable frost durability with durability factors ranging between 87% and 92%.

Specimens evaluated through Procedure B were tested for residual flexural strength after frost cycles to evaluate the extent of internal damage. Results are presented in Table 10.5. No significant difference was observed in residual flexural strength of the reference and the 30%RCA specimens. However, a drop of 14% was detected for the 40% RCA mixture. Comparing the flexural strength after the frost cycles with 56-day field measurements reveals 24%, 24%, and 33% drop in residual flexural strength for the reference, 30% RCA, and 40% RCA specimens. Xiao et al. (2012) also observed that the loss of strength due to freeze/thaw cycles is more significant in concrete mixtures produced with RCA.

Table 10.5 summarizes the CTE values of concrete specimens. Regardless of the age of testing, the CTE increased slightly as a function of RCA content. Measurements were more sensitive to RCA content at 2 months, with 5% and 10% increase in CTE when using 30% and 40% RCA replacements, respectively. The CTE values increased by 2% and 5% as a result of 30% and 40% RCA replacement at 11 months. Kim et al. (2003) studied effect of 100% RCA replacement on CTE of concrete proportioned with w/cm of 0.45. Authors reported 8%, 26%, 21%, and 8% increase in CTE while compared to concrete produced with virgin coarse aggregate from granite, andesite, sandstone, and gneiss sources, respectively. The CTE affects pavement deformation caused by variations in temperature. Higher CTE corresponds to larger slab deformations, joint openings, and more cracking potential.

Based on the data obtained from testing the control samples, RCA-made concrete exhibited slightly lower mechanical properties and up to 100 με higher shrinkage. However, the performances of the mixtures in terms of durability were similar. This was in line with the laboratory investigations of phase I.

10.3.3.2 In-situ mechanical properties. Core samples measuring 100 mm in diameter were extracted four months after field construction of the pavement sections to investigate in-situ mechanical properties. The core samples were maintained in moist

conditions until the time of testing. Table 10.6 summarizes the test results of the core samples at the age of 120 days. In-situ results are compared to 91-day compressive strength and 56-day splitting tensile strength and MOE for standard samples. No correction factors were employed to the data obtained from testing core samples.

The reference mixture developed 5% and 20% greater compressive strength compared to the 30%RCA and 40%RCA core samples, respectively. Same trends were observed for the splitting tensile strength with 20% higher values for the reference and 30%RCA concrete compared to the 40%RCA mixture. The MOE values were comparable for all mixtures. The reference and 30%RCA cores had compressive strength results similar to that of 91-day laboratory results and approximately 10% higher tensile strength compared to the 56-day laboratory cured specimens, which may be attributed to the hydration progress and pozzolanic reactions of fly ash. The 40%RCA cores had 8% lower splitting tensile strength results compared to the 56-day measurements. The MOE value obtained for the reference concrete was 14% lower than the results obtained at 56 days, which may be due to the experimental errors or micro-cracks during the coring process. For other tested mixtures, slight increase (up to 7%) in MOE was observed, while comparing to 56-day results.

Table 10.6 Properties of core samples at 120 days

Mixture	Reference	30%RCA	40%RCA
Compressive strength (MPa)	41.6 (97*)	39.6 (99)	32.9 (88)
Splitting tensile strength (MPa)	3.70 (111)	3.80 (110)	3.10 (92)
Modulus of elasticity (GPa)	33.2 (86)	32.4 (107)	33.8 (102)
Abrasion depth- top surface (mm)	2.5	2.3	2.2

*****Ratio of core data to last measurement on field samples with standard curing

An additional set of core samples measuring 150 mm in diameter were used to determine the abrasion resistance in accordance with ASTM C 779-C. Results are summarized in Table 10.6. No difference in the abrasion depth was observed for the top

and bottom surfaces of the cores. It should be noted that the top part of the cores were the tined surface of the pavement. The bottom parts were saw cut surfaces. No difference was observed in the abrasion resistance of the reference and RCA mixtures.

Results obtained for the core samples were comparable to those obtained from testing the control samples. In general, incorporation of RCA resulted in slight reductions in mechanical properties in comparison with the reference concrete. However, all three implemented mixtures exhibited proper in-situ properties.

10.3.3.3 Long-term deformation. Vibrating wire strain gauges (VWSG) with length of 170 mm were placed in pavement sections constructed with different concrete mixtures to monitor long-term deformation. For each mixture, the VWSGs were placed at different locations. The sensors were capable of determining the value of total strain in the pavement caused by a combination of temperature variations, concrete shrinkage, warping, and curling. Figure 10.5 offers a schematic view of the pavement section along with the locations of the sensor baskets. Instrumentation details are summarized in Table 10.7.

The iso-thermal deformation determined at the top surface of the pavement at the wheel path parallel to traffic direction at sections corresponding to the concrete mixtures in use (location A1) are presented in Figure 10.6. All deformation values are quite small. The total deformation is a combination of shrinkage deformation and environmental effects. All mixtures had similar deformation patterns during the first 140 days of the pavement life (up to mid-September). The concrete exhibited an initial expansion of about 10 μm/m before exhibiting negative deformation caused by shrinkage and compressive stress (and strain) due to warping during the summer time.

The deformation pattern is changed by the beginning of cold season (September). This indicates that the environmental effects (warping and curling) are the main factors governing the deformation characteristics, as shown in Figure 10.6, where negative strain values are changing to positive strains caused by tensile stresses due to cold weather. This pattern, however, tends to be cyclic and repeating through the year.

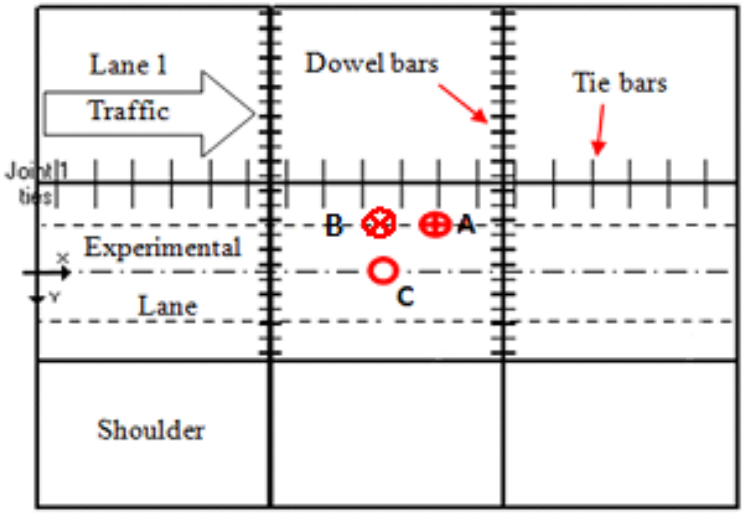

Figure 10.5 Schematic view of the pavement panels

Table 10.7 Instrumentation details and configurations

Location	Symbol	Location	Number of gauges	Distribution in height	Direction of gauges
A	⊕	Wheel path	4	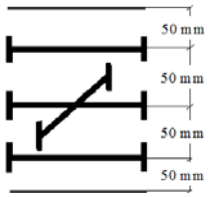	Top: one, parallel to traffic Mid-height: one parallel to traffic, one perpendicular to the traffic flow Bottom: one parallel to traffic
B	⊗	Wheel path	2	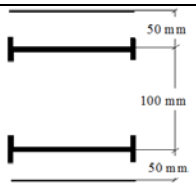	Top: one, parallel to traffic
C	◯	Center line	2	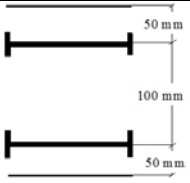	Top: one, parallel to traffic

The highest variations in strain due to seasonal effects were observed in the case of 40%RCA mixture with an approximately 100 μm/m spread. The minimum value was

about 60 µm/m for the reference mixture. This might be in part due to the higher CTE and lower MOE of the 40%RCA mixture compared to the reference and the 30%RCA concrete, as demonstrated by the following equation (Huang 2004):

$$\delta_x = \left(C_x + \mu C_y\right) E\alpha(\Delta T)/2(1-\mu^2) \quad (10\text{-}1)$$

where δ_x is the warping stress in longitudinal direction, E is the modulus of elasticity of the concrete, α is the coefficient of thermal expansion, µ is the Poisson's ratio, and C_x and C_y are the correction factors for infinite slab length.

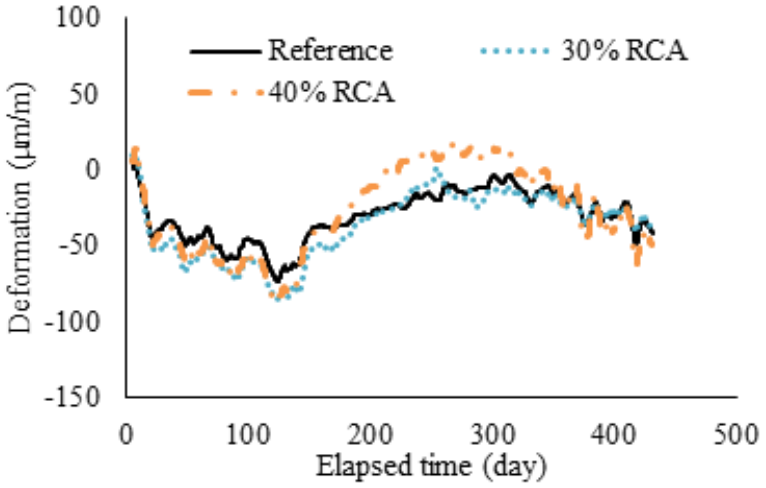

Figure 10.6 Long-term iso-thermal in-situ deformations at top, wheel path, parallel to traffic

Given the similar panel dimensions and base conditions, it is usually expected that a decrease in MOE and an increase in the CTE increase the warping stress and strain in rigid pavement. Figure 10.7 presents the strain recorded at mid-height of the pavement parallel to the traffic direction (locations A2) at wheel path. The lowest deformation was observed in the case of 30%RCA mixture up to the start of cold season (140 days of age). The maximum variations in strain during the cold season was observed for the 30%RCA mixture with about 80 µm/m change in strain direction. This was the lowest for the reference mixture with spread of about 50 µm/m.

Figure 10.8 shows the strains recorded at the mid-height of the pavement perpendicular to the traffic direction (locations A3) at the wheel path. Deformations were similar for all mixtures up to 140 days. The minimum seasonal effect, i.e. change in strain direction due to reversed warping stress direction at cold season, was observed for the reference mixture. It seems that the variation in stress and strain direction after the peak in winter (about 300 days of age) tends to be slower compared to the same location but parallel to the traffic flow (A2 location).

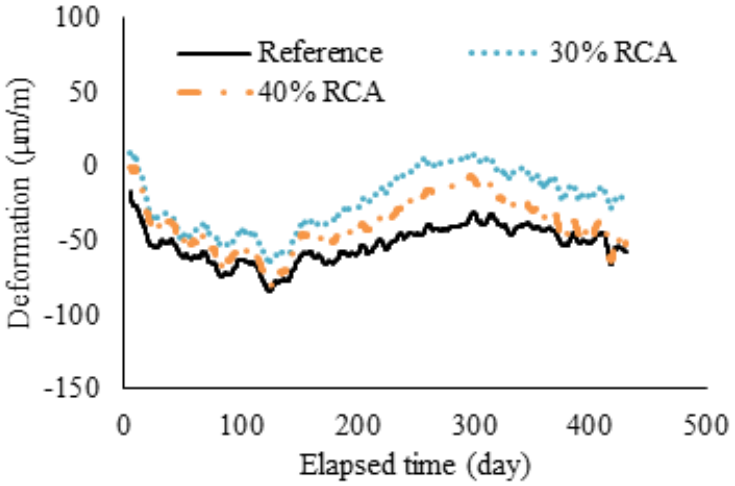

Figure 10.7 Long-term iso-thermal in-situ deformations at mid-height, wheel path, parallel to traffic

Figure 10.9 shows iso-thermal concrete deformation registered at location A4, which is the bottom part of the pavement at wheel path, parallel to the traffic direction. For the deformations at the bottom part of the pavement, it was observed that the reference concrete and the mixture with 40%RCA replacement had comparable deformations. The mixture with 30% RCA had the minimum strain up to 140 days which might be due to experimental errors in installation or performance of the gauge. Again, lower seasonal effects were recorded for the reference mixture in comparison with the 40%RCA section.

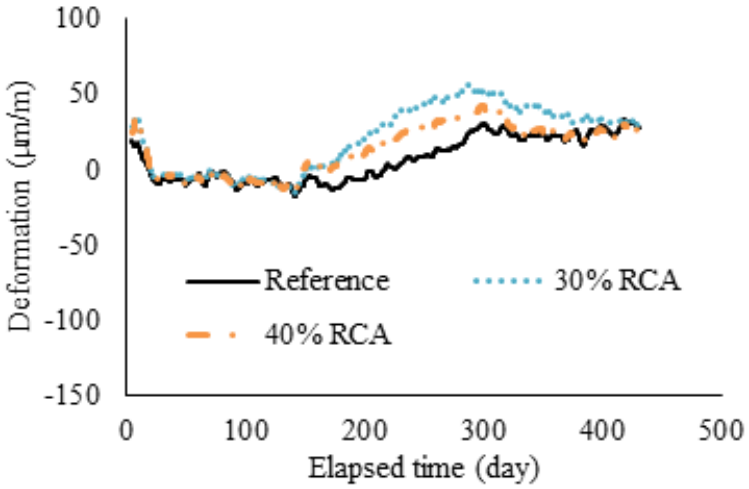

Figure 10.8 Long-term iso-thermal in-situ deformations at mid-height, wheel path, perpendicular to traffic

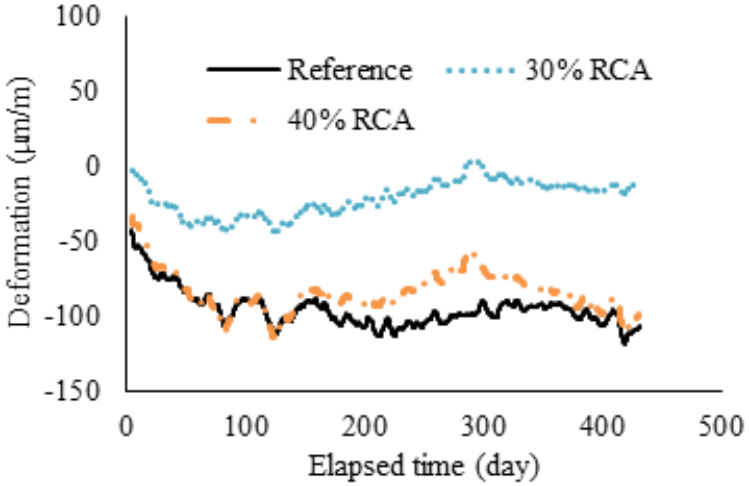

Figure 10.9 Long-term iso-thermal in-situ deformations at bottom, wheel path, parallel to traffic

Figure 10.10 shows the strains at C1 gauges at top part of pavement at the center line of the traffic lane, parallel to the traffic direction. The 40%RCA and reference mixtures had the lowest deformation, and the 30%RCA mixtures had the highest strain up to 140 days. The minimum seasonal effect was observed for the 30%RCA mixture. Deformation at the C2 location, at centerline, at the bottom part of the pavement and

parallel to the traffic are presented in Figure 10.11. The maximum deformation was obtained with the 40%RCA mixture by the end of the first summer (140 days). Very slight seasonal effect was observed in the case of the reference mixture and the maximum effect was proved to be for the 40%RCA concrete.

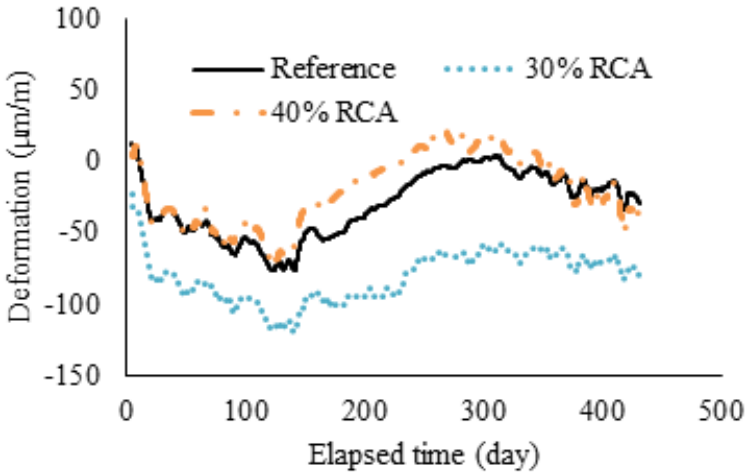

Figure 10.10 Long-term iso-thermal in-situ deformations at top, center line, parallel to traffic

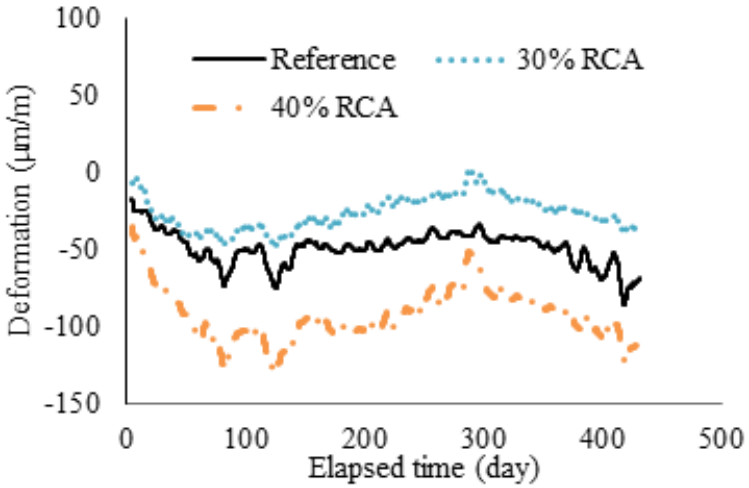

Figure 10.11 Long-term iso-thermal in-situ deformations at bottom, center line, parallel to traffic

In summary, a cyclic pattern of in-situ strain values ranging from tension to compression and vice versa was observed with change in seasonal weather conditions for the concrete pavement. Strain values at sensor locations were limited to 150 με. This verifies the performance of RCA-made sections regarding the long-term deformations due to shrinkage and environmental effects. However, the concrete sections made with RCA tend to have slightly higher deformation due to seasonal changes, i.e. curling and warping in addition to shrinkage. Overall, the long-term in-situ performance of the RCA-made pavement was comparable to that with virgin coarse aggregate.

10.3.3.4 Controlled traffic loading. The truck was modeled according to its measured geometry and weight. Figure 10.12 provides a schematic of the truck configuration. For all loading scenarios, the wheel plane over sensors A and B corresponding to that at the driver side were used for loading the sensors. In the case of the tandem axle, the outer tires were placed on instrumented spots. The weights of both the driver and passenger sides of the front and the rear axles were determined in a weigh station. Table 10.8 includes the weights of the axles and the pressure applied to the pavement surface based on the contact area beneath the tires.

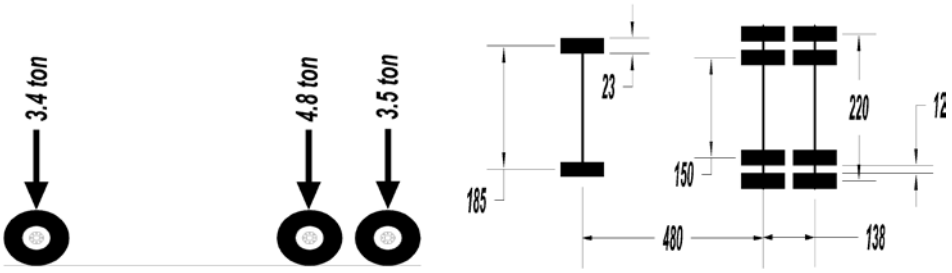

Figure 10.12 Truck configuration, dimensions in cm

The various steps involved in the truck loading included static, slow moving, and high speed loading. The first step consisted of positioning the front wheel of the truck on instrumented spots to simulate the effect of static single-axle loading. After registration of the deformation data, the truck was moved forward to position the tires of the rear tandem axle over the sensor locations. In order to investigating the effect of speed on

pavement deformation, truck was then allowed to pass on top of the marked sensor locations at different speeds of 1, 14, 23, and 35 km/h. The sensors located at wheel path (locations A and B in Figure 2) were employed for loading purpose. Two sensors were considered for each depth (top and bottom) for all mixtures. Top and bottom sensors were located approximately 50 mm from the top surface and bottom part of the pavement section, respectively. All sensors were aligned parallel to the traffic flow.

Table 10.8 Axle weight and pressure values at tire-pavement contact area (driver side)

Axle type	Single	Tandem	
Tire position	Front tire	Front tires	Rear tires
Tire load (Ton)	3.4	4.8	3.5
Contact pressure (KPa)	570	1010	730

All sensor readings were set to zero before the loading. Time history deformation was registered for all the loading scenarios, and the maximum deflection caused by the single and the tandem axle loadings was compared as suggested by Goulias et al., (2011). As an example, the deformations subjected to the slow moving load at top and bottom part of the pavement section cast with the 30% RCA mixture are presented in Figure 10.13.

For every loading spot, it was found that for the tension areas, stresses are compressive just before the tire reaches the top of the sensor, and then the stresses change to tension and vise versa. Time needed for change stress between compression and tension varied with the speed of truck. An example for this behavior is presented in Figure 10.14 where the time history deformation of sensors located at the bottom part (tension zone) of the pavement cast with 30% RCA for both the static and high speed loading. Similar patterns for the stress type during dynamic loading was also observed by Kumara (2005).

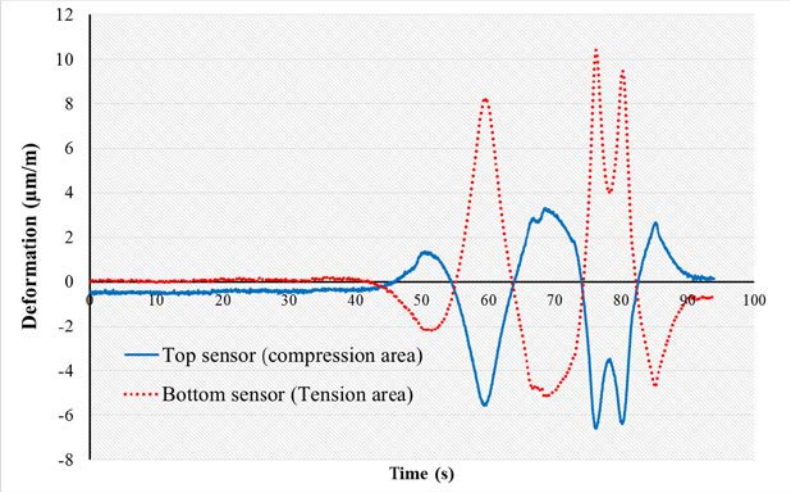

Figure 10.13 Sample deformations registered at top and bottom of the pavement due to slow moving truck

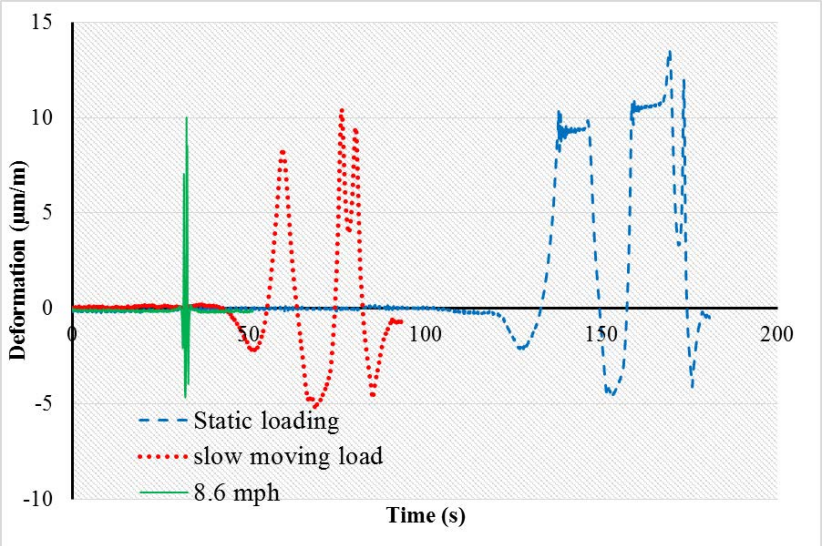

Figure 10.14 Variations in stress direction during the truck movement – bottom part of pavement

The values of the maximum deformation at different sensor locations are summarized in Table 10.9 to Table 10.11. Negative values represent deformation in the compression zone (pavement surface), and positive data refer to the tensile strain

measurements at the bottom part of pavement sections. Based on the data, it was clear that the deformation values registered at mid-height of the pavement section are significantly lower than those of the top or bottom parts. This is expected given the fact that the mid-height sensors are placed close to the neutral axis of the section, thus resulting in deformation values close to zero.

Table 10.9 Peak deformation registered through Static loading (µm/m)

- : compression, +: tension						
Axle type	Mixture type	Sensor location				
		Top 1	Bot. 1	Mid-height	Top 2	Bot. 2
Single	Ref	-3.2	5.3		-3.1	5.8
	30% RCA	-6.9	10.2	0.6	-	-
	40% RCA	-6.4	10.6		-6.2	14.1
Tandem	Ref	-2.5	4.2		-4.1	7.5
	30% RCA	-7.7	13.6	1.8	-	-
	40% RCA	-7.8	13.1		-6.1	13.9

Table 10.10 Peak deformation registered for slow moving load (µm/m)

-: compression, +: tension						
Axle type	Mixture type	Sensor location				
		Top 1	Bot. 1	Mid-height	Top 2	Bot. 2
Single	Ref	-3.1	4.9		-3.0	5.7
	30% RCA	-5.1	8.0	0.4	-	-
	40% RCA	-4.4	6.7		-4.3	7.9
Tandem	Ref	-3.0	4.7		-3.7	6.9
	30% RCA	-6.1	10.4	0.7	-	-
	40% RCA	-6.0	10.5		-4.6	9.2

Table 10.11 Peak deformation registered for high speed moving load (µm/m)

-: compression, +: tension					
Speed (km/h)	Axle type	Mixture	Sensor location		
			Top 1	Bot. 1	Mid-eight
14	Single	30% RCA	-4.4	7.7	0.4
	Tandem	30% RCA	-5.7	10.1	0.6
23	Single	30% RCA	-3.9	7.1	0.5
	Tandem	30% RCA	-6.0	10.1	0.4
35	Single	30% RCA	-3.5	5.9	0.3
	Tandem	30% RCA	-4.9	8.1	0.3

In general it can be concluded that the increase in truck speed reduced the strain values. All mixtures exhibited similar performance where measured strain values were limited to 15 με at the sensor location. These observations further verify the feasibility of using RCA as a partial replacement for virgin aggregate for rigid pavement construction.

10.4. REMARKS

This section presents the results of a field-oriented study carried out to demonstrate the suitability of RCA for use in the construction of rigid concrete pavements. Fresh and hardened properties of eight RCA-made concrete mixtures were compared to those of a reference concrete produced in the laboratory. The investigated mixtures were proportioned with 30% coarse RCA replacement, 0 to 20% fine RCA, 25% to 40% fly ash replacement, and w/cm of 0.37 to 0.42. Two mixtures proportioned with 30% and 40% of coarse RCA along with reference concrete made without any RCA were then implemented in a field project. Samples were taken during the casting. In addition, cores were extracted 120 days after pavement placement to determine the in-situ properties. Instrumentation was incorporated to monitor the long-term deformation of different pavement sections. Based on the results obtained in this study, the following conclusions are warranted:

- All laboratory produced mixtures met the 28-day compressive strength requirement of 28 MPa. Increasing the coarse and fine RCA content to 30% and 20% did not have a significant effect on 91-day compressive strength. Reductions in splitting tensile and flexural strength were limited to 6% and 7%, respectively. Incorporation of 30% coarse and 15% fine RCA reduced the 56-day MOE by 8% and 4%, respectively.
- The specimens cast with the EMV mixture exhibited minimum 180-day shrinkage of 300 με. Incorporation of fly ash and reducing the w/cm was helpful in controlling shrinkage of RCA-made mixtures. The six-month shrinkage of the majority of the investigated mixtures was limited to 500 με in comparison to 450 με for the reference concrete.

- No signs of edge slump, and no problems with placement, finishing, and tinning of RCA-made mixtures were observed at the job site, which included casting 450 m^3 of concrete in a length of 300 m.
- Incorporation of 30% and 40% RCA reduced the 1-day compressive strength by 10% and 23%, respectively. Reduction rate was limited to 7% and 12% at 91 days. The 56-day MOE was reduced by 22% and 14% due to 30% and 40% RCA replacement, respectively. However, the 56-day splitting tensile strength and flexural strength values were similar for the reference, 30%RCA, and 40%RCA mixtures.
- The reference and 30% RCA mixtures had similar shrinkage and chloride ion permeability performance. An increase of 100 με in shrinkage and 300 Coulomb increase in total passed charged was observed for the 40%RCA samples. All mixtures had good freeze thaw resistance with durability factors higher than 87%.
- All investigated pavement sections had similar patterns of iso-thermal deformation, which were limited to 150 με at sensor locations. No significant difference in deformation of various mixtures was observed.
- In general it can be concluded that the increase in truck speed reduced the strain values. All mixtures exhibited similar performance where measured strain values were limited to 15 με at the sensor location.

11. SUMMARY AND CONCLUSIONS

The objective of this study is to investigate the feasibility of using high performance concrete made with high-volume of recycled materials in sustainable transportation infrastructure. Development of environmentally friendly mixtures for rigid pavement construction was the main subject of interest. The feasibility of replacing 50% of Portland cement with industrial by-products and supplementary cementitious materials (SCMs) was evaluated. Several sources of fine and coarse recycled concrete aggregates (RCA) were considered for concrete production. A comprehensive experimental program was conducted to evaluate the effect of concrete mixture design and RCA characteristics on mechanical properties, drying shrinkage, cracking potential, and durability of concrete. Based on the obtained data, the following conclusions are drawn.

11.1. BINDER OPTIMIZATION

Concrete equivalent mortar (CEM) designed based on the concrete mixture design used for construction of rigid pavement was employed for optimization of binder compositions. The w/cm was fixed at 0.40. Several binary and ternary combinations of cement (OPC), Class C fly ash (FA-C), Class F fly ash (FA-F), slag (GGBS), and ground glass fiber (GGF) were investigated for rheological properties, heat of hydration, compressive strength development, drying shrinkage, cost, and emissions.

The use of high volume SCM a replacement rates of over 50% reduced the early age strength development. However, the long-term compressive strength values were mostly higher than that of the mixture made with 100% OPC (34.1 MPa), with maximum value of 61.5 MPa for CEM made with 15% GGBS and 35% FA-C. The use of 15% and 25% GGF in ternary blends was effective in enhancing the compressive strength. The best performances were observed in the case of the GGF/FA-C mixtures, followed by the GGF/GGBS, and GGF/FA-F, with up to 45%, 28%, and 10% increase in 91-day compressive strength compared to the Reference mixture.

Both the early age and long-term shrinkage values reduced with the use of SCMs. The maximum 7- and 120-day shrinkage values of 850 and 1030 με were observed for the mixture made with 100% OPC. Reduction in 120-day shrinkage to values as low as 500 με was observed with high-volume SCM incorporation, with replacement rates of up to 70%.

Multi criteria decision making was conducted to rank the overall performance of binary and ternary mixtures prepared with various amounts of GGBS, FA-C, and FA-F. Given the technical considerations, cost, emissions, and considering the performance of the investigated mixtures, it was decided to use a ternary blend of 50% OPC, 15% GGBS, and 35% FA-C as a candidate binder for concrete production. The CEM made with this binder exhibited 91-day compressive strength of 61.5 MPa and 120-day drying shrinkage of 700 με, and electrical resistivity of 14.2 KΩ.cm.

Considering the overall performance of the mixtures cast with GGF, it was decided to limit the use of GGF to 15% in concrete production. Given the acceptable performance, a ternary blend of 50% OPC, 35% FA-C, and 15% GP was also added to the test matrix of the concrete phase. The CEM made with this binder exhibited 91-day compressive strength of 47.7 MPa and 120-day drying shrinkage of 900 με, and electrical resistivity of 24.9 KΩ.cm.

11.2. AGGREGATE CHARACTERIZATION

Several sources of fine and coarse RCA were procured from various recycling centers in the state of Missouri, Kansas, and Illinois. Moreover, a source of coarse RCA was produced in the laboratory. Key engineering properties of the aggregates, including particle size distribution, specific gravity, water absorption, Los Angeles abrasion, deleterious materials content, residual mortar content, and soundness were investigated in the laboratory.

Several combinations of fine and coarse aggregates were investigated for particle packing density. Results were analyzed for a variety of investigated combinations of

virgin and recycled aggregates. A sand to aggregate ratio of 42% (by vol.) was selected for concrete production.

11.3. MECHANICAL PROPERTIES

Different types of fine and coarse RCA were used for development of concrete mixtures in the laboratory. The concrete mixtures were proportioned with w/cm ranging from 0.37 to 0.45, with binary and ternary cements. The mixtures were investigated for compressive strength, splitting tensile strength, flexural strength, and Modulus of elasticity. Results indicated that the adjustments in mixture design parameters, including the reduction in w/cm and the use of ternary cements were effective in mitigating the negative impacts of using RCA and securing proper mechanical properties. Strong correlations were established between the key physical properties of aggregate, including water absorption, oven-dry specific gravity, and LA abrasion with investigated mechanical properties. Contour diagrams were developed to illustrate the effect of coarse RCA on mechanical properties of concrete designated for rigid pavement construction.

In general, it was observed that the variations in LA abrasion and water absorption of the combined coarse aggregate can be considered as proper means of estimating the effect of coarse RCA on compressive strength of concrete. Based on the results obtained for the investigated mixtures, the use of 50% coarse RCA with water absorption of 3% and 6% can result in approximate compressive strength of 56.0 and 50.0 MPa, respectively, compared to values of about 57.5 MPa for concrete made without any RCA, 0.37 w/cm, and ternary cement with 15% GGBS and 35% FA-C. The use of 50% coarse RCA with LA abrasion of 35% and 45% can result in approximate compressive strength of 53.0 and 49.0 MPa, respectively, compared to values of higher than 55.0 MPa for concrete made without any RCA, 0.37 w/cm, and ternary cement with 15% GGBS and 35% FA-C.

Results indicate that the variations in LA abrasion and water absorption of the combined coarse aggregate can be considered as proper means of estimating the effect of coarse RCA on splitting strength of concrete. Based on the results obtained for the

investigated mixtures, the use of 50% coarse RCA with LA abrasion of 40% and 50% can result in approximate splitting tensile strength of 3.15 and 3.0 MPa, respectively, compared to values of higher than 3.3 MPa for concrete made without any RCA, 0.40 w/cm, and binary cement with 25% FA-C. The use of 50% coarse RCA with water absorption of 3% and 7% can result in approximate splitting tensile strength of 3.25 and 3.1 MPa, respectively, compared to values of about 3.3 MPa for concrete made without any RCA, 0.0 w/cm and binary cement with 25% FA-C.

It was observed that the variations in water absorption and specific gravity of the combined coarse aggregate can be considered as proper means of estimating the effect of coarse RCA on flexural strength of concrete. Based on the data obtained through laboratory investigation, the use of 50% coarse RCA with water absorption of 4% and 7% can result in approximate flexural strength of 4.95 and 4.80 MPa, respectively, compared to values of about 5.10 MPa for concrete made without any RCA, binary cement, and 0.40 w/cm. For the same type of concrete mixtures, the use of 50% coarse RCA with oven-dry specific gravity of 1.80 and 2.45 can result in approximate flexural strength of 4.50 and 5.10 MPa, respectively, compared to values of about 5.25 MPa for concrete made without any RCA.

In general it was observed that the water absorption and the oven dry specific gravity were better predictors for estimation of MOE. For the investigated concrete made with binary cement and 0.40 w/cm, the use of 50% coarse RCA with water absorption of 3% and 7% can result in approximate MOE of 38.5 and 34.0 GPa, respectively, compared to values of about 40.0 GPa for concrete made without any RCA. The use of 50% coarse RCA with oven-dry specific gravity of 1.80 and 2.40 can result in approximate MOE of 38.0 and 30.0 GPa, respectively, compared to values of about 40.0 GPa for concrete made without any RCA.

Given the significant impact of MOE on design and performance of rigid pavements, artificial neural networks were incorporated for estimating the variations in MOE of concrete made with coarse RCA. A database summarizing the mixture

proportions and RCA characteristics of over 480 concrete mixtures was developed and investigated using artificial intelligence.

Several scenarios were investigated for the input parameters. Strong correlations were observed for the selected models with correlation factors ranging from 0.83 to 0.94 for training, validation, and testing of the selected models. MOE of concrete designated for rigid pavement construction was investigated as a case study. Depending on the RCA quality, Results indicate up to 20% reduction in MOE of the pavement concrete due to 50% coarse RCA replacement.

11.4. DRYING SHRINKAGE

Different types of fine and coarse RCA were used for development of concrete mixtures in the laboratory. The concrete mixtures were proportioned with w/cm ranging from 0.37 to 0.45, with binary and ternary cements. The mixtures were investigated for drying shrinkage.

Strong correlations were established between the key physical properties of aggregate, including water absorption, oven-dry specific gravity, and LA abrasion with drying shrinkage of concrete at different ages. The water absorption characteristics yielded the highest R2 values of 0.78 and 0.85 for mixtures cast with 0.40 and 0.37 w/cm, respectively.

The RCA replacement level (% mass), water absorption rate, and specific gravity were used as input parameters to develop contour graphs to enable prediction of 90-day shrinkage of concrete typically used by State DOTs for rigid pavement construction. Results indicate up to 17% increase (from 450 to 525 με) in 90-day shrinkage of such a mixture due to incorporation of 30% RCA with specific gravity of 2.2 and water absorption of 8.0%. Up to 55% increase in 90-day drying shrinkage due to full replacement of such RCA in these pavement mixtures could be expected.

11.5. CRACKING POTENTIAL

Different types of coarse RCA were employed at 505 and 100% replacement rates to evaluate the cracking potential under re-strained shrinkage conditions. Ring type specimens were incorporated.

In the restrained ring test, no cracking was observed in the case of the Reference mixture up to 35 days of drying, with stress rate limited to 0.10 MPa/day. No cracking up to 35 days of drying was observed for the mixtures with 50% RCA, which is considered as “low” potential for cracking. On the other hand, the incorporation of 100% RCA reduced the time of cracking to values ranging from 9 to 11 days, with stress rates ranging from 0.25 to 0.34, which correspond to “medium-high” risk of cracking.

Concrete mixtures cast with 100% RCA developed higher tensile creep coefficient. Such values of ranged from 0.34 to 0.78 at the time of cracking compared to 0.34 to 0.36 for the Reference concrete, and 0.23 to 0.43 for the concrete with 50% RCA. This is believed to be due to higher stress relaxation, i.e. lower MOE. Even though the tensile creep coefficient and stress relaxation were higher in concrete made with 100% RCA, the significantly higher shrinkage and reduction in tensile strength of up to 25% led to earlier time to cracking of such mixtures.

11.6. CONCRETE DURABILITY

Concrete made with different types of coarse and fine RCA procured from different sources was investigated for durability. Durability against freeze/thaw cycles, de-icing salt scaling, electrical resistivity, abrasion resistance, and sorptivity were investigated.

The use of up to 70% coarse RCA from a high quality air-entrained concrete source used in airfield or laboratory produced air-entrained concrete did not cause any significant variation in frost durability factor. The use of 50% commercially produced RCA in concrete with 0.37 w/cm reduced the durability factor from 94% to 86%, though both values are considered provide adequate frost durability. On the other hand, such concrete exhibited greater de-icing salt scaling, with an increase in accumulative mass

moss from 415 to up to 760 g/m^2. No reduction in frost durability factor was observed when the fine RCA volume was limited to 15%, regardless of the w/cm. However, the use of 15% fine RCA in concrete with ternary cement and 0.40 w/cm increased the mass loss due to scaling from 870 to 1190 g/m^2.

Air content in hardened state was shown to increase with the use of RCA obtained from air-entrained concrete. An increase in volume of air voids with chord length of lower than 1.0 mm from 6.3% to 11.2% was observed with full replacement of such coarse RCA. Reduction in spacing factor from 0.17 to 0.07 mm, and increase in specific surface from 21.9 to 30 mm^{-1} was observed for such concrete.

The increase in fine and coarse RCA reduced the electrical resistivity, depending on the RCA content, binder type, and w/cm. The use of up to 40% fine RCA in concrete prepared with ternary cement and 0.40 w/cm reduced the 91-day electrical resistivity by up to 10%. Concrete with lower w/cm (0.37) and ternary cement was more sensitive to the use of RCA. Up to 32% reduction in electrical resistivity was observed with 50% coarse RCA replacement in such mixtures.

Slight increase in sorptivity was observed with the use of RCA. However, the use of lower w/cm and ternary cement was effective in reducing the sorptivity. The concrete made with RCA exhibited greater abrasion damage. However, the use of lower w/cm of 0.37 was effective in reducing the abrasion damage.

11.7. FILED IMPLEMENTATION

Two mixtures produced with 30% and 40% coarse RCA replacement and a reference concrete proportioned without any RCA were employed at second phase for the construction of a pavement section in St. Louis, Missouri, which included casting 450 m^3 of concrete in a length of 300 m. Sampling was conducted at the job site, and core samples were extracted to evaluate in-situ properties of the sustainable concrete. Instrumentation was also employed to monitor early age and long-term deformation of different pavement sections.

No problems with placement and finishing of RCA-made mixtures were observed at the job site. The incorporation of 30% and 40% RCA reduced the 1-day compressive strength by 10% and 23%, respectively. Reduction rate was limited to 7% and 12% at 91 days. The 56-day MOE was reduced by 22% and 14% due to 30% and 40% RCA replacement, respectively. However, the 56-day splitting tensile strength and flexural strength values were similar for the reference, 30%RCA, and 40%RCA mixtures.

The reference and 30% RCA mixtures had similar shrinkage and chloride ion permeability performance. An increase of 100 με in shrinkage and 300 Coulomb increase in total passed charged was observed for the 40%RCA samples. All mixtures had good freeze thaw resistance with durability factors higher than 87%.

All investigated pavement sections had similar patterns of iso-thermal deformation, which were limited to 150 με at sensor locations. No significant difference in deformation of various mixtures was observed. All mixtures exhibited similar performance where measured strain values were limited to 15 με at the sensor location.

11.8. FUTURE RESEARCH

Based on the data obtained through this research, the following aspects are recommended for further research in future:

- Given the variable nature of RCA, it is required to establish analytical methods to quantify the key engineering properties of concrete made with RCA. It is necessary to develop comprehensive databases to investigate the mixture proportions, aggregate characteristics, and performance of concrete made with fine and coarse RCA. Statistical data analysis techniques and artificial intelligence can be used for the analysis of databases, aiming at development of analytical models for prediction of properties of concrete made with RCA.
- The residual mortar phase of RCA can contain a variety of chemical contaminations, including chloride ions, etc. Further research is required to establish simplified test methods for quantifying such ionic contaminations. In

additions, potential quantifying the correlations between such contaminations and durability of concrete made with RCA should be investigated.

- The availability of porous mortar in RCA particles can alter the air void system of the concrete made with RCA. Further investigation is required to quantify the effect of RCA replacement ratio, RCA residual mortar content, and properties of the residual content on air void system of concrete made with RCA.
- Development of cost-effective and user friendly techniques for enhancing the RCA properties can reduce the uncertainties related to the use of RCA and increase the market share of recycled materials. The use of organic agents, coatings, and chemical treatments can be considered as effective means of enhancing the RCA properties. Further research is required to establish guidelines and recommendations.

APPENDINX A.

SHEAR PERFORMANCE OF REINFORCED CONCRETE BEAMS INCORPORATING RECYCLED CONCRETE AGGREGATE AND HIGH-VOLUME FLY ASH

NOTATIONS

A_s = area of non-prestressed tension reinforcement (mm^2)

a_s = shear span of beam (m)

b_w = web width (mm)

d = distance from extreme compression fiber to centroid of longitudinal tension reinforcement (mm)

d_a = maximum aggregate size (mm)

d_{max} = maximum aggregate size (mm)

d_v = effective shear depth (mm)

E_s = modulus of elasticity of reinforcing steel (MPa)

f'_c = specified compressive strength of concrete for use in design (MPa)

f_{ck} = characteristic compressive cylinder strength of concrete (MPa)

f_{cm} = mean compressive strength of concrete (MPa)

M_u = factored moment at section (KN.mm)

V = shear strength provided by concrete (KN)

V_u = factored shear force at section (KN)

w/c = water to cement ratio

α_0 = 1 for rounded aggregate and 1.44 for crushed or angular aggregate

ε_s = strain in non-prestressed longitudinal tension reinforcement (mm/mm)

ρ = longitudinal reinforcement ratio

RESEARCH SIGNIFICANCE

Concrete is the most widely used construction material. Efforts aimed at producing environmentally friendly concrete can play a major role in securing environmentally friendly construction. Candidate technologies for sustainable concrete materials include the incorporation of supplementary cementitious materials (SCMs), such as fly ash as a partial replacement for portland cement, the incorporation of recycled materials in concrete production, and, in particular, recycled concrete aggregate (RCA), as well as the use of highly durable concrete to increase service life.

Portland cement production accounts for a significant portion of the total greenhouse gas emission. The production of Portland cement is responsible for about 7% of total worldwide CO_2 emissions (Nuaklong et al., 2015). Therefore, replacing Portland cement with an alternative cementitious material and/or industrial by-products can decrease the carbon footprint of the concrete.

Over 900 million tons of construction and demolition waste is produced annually in Europe, the U.S., and Japan (WBCSD, 2012). Although the use of RCA does not significantly reduce CO_2 emissions, it can significantly contribute to reducing the depletion of natural resources (virgin aggregate) and decreasing the need for landfills.

When using a high volume of RCA and SCMs, it is necessary to understand the structural performance of this new class of concrete materials. Limited studies regarding the structural performance of high-volume fly ash concrete (HVFAC) are available. Arezoumandi et al. (2013) replaced 70% of cement with Class C fly ash in full-scale beams with longitudinal reinforcement ratios of 1.27%, 2.03%, and 2.71%. The concrete had compressive strengths at 28 days of 31 MPa. Results of the studies showed that the HVFAC beams can develop a shear strength that is around 12% higher than the reference beam made without any fly ash, which had a 28-day strength of 29 MPa. Rao et al. (2011) replaced 50% of cement with Class F fly ash in reinforced concrete (RC) beams made with longitudinal reinforcement ratios of 0.6% to 2.9% and reported a slightly lower shear strength than the reference specimens without any fly ash.

A number of studies were conducted to evaluate the shear behavior of concrete made with RCA. Sogo et al. (2004) used RCA from foundation concrete of 10 to 40 years of age. Concrete mixtures were proportioned with a water-to-cementitious materials ratio (w/cm) of 0.3 to 0.6 and a RCA replacement of 100%. Beam specimens with a longitudinal reinforcement ratio varying between 2.39% and 4.22% with different shear reinforcement ratios of 0, 0.26%, and 0.53% were studied. The authors found that the shear strengths of beams made with RCA were up to 20% lower than those of the control beams in which RCA and virgin fine were used. A decrease in shear capacity of up to 30% was observed for concrete made with both fine and coarse RCA (Sogo et al., 2004).

Yagashita et al. (1994) used three different types of RCA of relatively low, medium, and high quality as a full replacement of virgin coarse aggregate. The authors reported an 8% lower shear strength for the beams made with high-grade RCA compared to concrete made with virgin aggregate. Gonzalez-Fonteboa et al. (2007) tested beams made with a 50% RCA replacement. Beams were cast with 2.39% of longitudinal reinforcement and four shear reinforcement ratios ranging from 0 to 0.22%. Concrete mixtures with slump values of 50 to 100 mm, proportioned with w/cm of 0.55 and containing 8% silica fume were prepared. The average compressive strength at 115 days was 40 MPa. No significant difference in the shear strength was observed between the RCA-made and control beams. Table 1 offers a summary of various studies of the shear strength of concrete made with RCA.

The study reported in this paper investigates the shear capacity of 24 full-scale RC beams fabricated with high volume fly ash and RCA. Four concrete mixtures were employed for casting the beams: conventional concrete (CC) without any fly ash or RCA as the reference; fly ash concrete with 50% of Class C fly ash replacement (FA50 beams); RCA concrete with 50% of coarse RCA replacement (RCA50 beams); and sustainable concrete (SC) proportioned with 50% Class C fly ash and 50% RCA. The beams were fabricated with three different longitudinal reinforcement ratios of 1.27%, 2.03%, and 2.71%. The test results were compared with theoretical models provided by six different design codes as well as a shear database for CC. The experimental results were also compared to analytical approaches based on fracture mechanics as well as the modified compression field theory approach. Parametric and non-parametric statistical data analyses were conducted to compare the shear strength characteristics of the various beam elements.

With the increasing use of sustainable concrete made with RCA and fly ash, more information regarding the structural behavior of such sustainable materials is required for safe implementation. The research presented here contributes to the evaluation of the structural performance of concrete containing high-volume fly ash and RCA in shear. The results presented here should be of interest to owner agencies and engineers

considering the design and use of sustainable concrete for structural applications. It should be noted that the research presented in this appendix was conducted in collaboration with Dr. Jeffery Volz and his research group at Missouri University of Science and Technology. More details on experimental program and test results are presented by Volz et al. (2014) and Arezoumandi et al. (2014).

EXPERIMENTAL PROGRAM

As stated earlier, the experimental program involved the testing of four concrete mixtures and three longitudinal reinforcement ratios with two replicate beams per mixture. The constituent materials and mixture proportioning of the four mixtures are elaborated below.

Materials and Mixture Proportions.

The CC mixture was proportioned with ASTM Type I portland cement, crushed limestone aggregate with a maximum aggregate size of 25mm, and natural siliceous riverbed sand. The SC and FA50 mixtures incorporated Class C fly ash from a local source in Missouri. The RCA used for the production of the SC was obtained by crushing 30-to 40 year old concrete pavement mixed with 60-to 120 day old ready mix concrete residuals. The RCA employed for casting RCA50 beams was produced in the laboratory. The physical properties of the virgin aggregate and RCA are presented in Table 2. Table 3 summarizes the characteristics of the cement and fly ash. Grade 60 (414 MPa) longitudinal and shear reinforcement steel complying with ASTM A615 (2012) was used.

Table 4 summarizes the concrete mixture proportions. The CC, SC, and RCA50 mixtures were proportioned with a w/cm of 0.40. The FA50 concrete had a w/cm of 0.35. Gypsum and calcium hydroxide were added to the FA50 mixture to enhance the early age strength development (Bentz, 2010). Concrete was delivered by a local ready mix concrete supplier. Table 5 presents the properties of the investigated mixtures.

Specimen Design.

All specimens were cast with rectangular cross sections measuring 4.2 m in length, 305 mm in width, and 460 mm in height, and had a shear span-to-depth ratio of 3.0 or greater, as presented in Figure 1. The beams were designed with various longitudinal reinforcement ratios ranging from 1.27% to 2.71% to prevent failure in flexure. Care was taken to ensure the reinforcement amount was maintained within the criteria introduced by ACI 318 (2011). The designation codifications of the beams in Figure 1 (NS-4, NS-6, and NS-8) indicate the use of no stirrups (NS) in shear regions and the number of #22 bars at the bottom of the beams.

Fabrication and Curing of Test Specimens.

Beam fabrication and testing were conducted at the High-Bay Structural Research Laboratory in the Department of Civil Engineering at Missouri University of Science and Technology. The concrete was delivered to the laboratory by ready mix trucks in batches measuring 0.7 m^3. The beams were cast in two layers and properly consolidated using internal vibration. At the end of casting, wet burlap and plastic sheeting were used to cover the specimens. Such a curing regime continued until the beams were tested, which was at the age of 28 days. For the FA50 and RCA50 beams, the curing regime included four days of moist curing using wet burlap, followed by storage at 21±3ºC and a relative humidity of 40%±10% up to the age of testing.

Test Setup and Procedure.

A load frame was designed for the four-point loading of the beams. The set up was equipped with a pair of 490 KN servo-hydraulic jacks. A displacement controlled mode at a rate of 0.50 mm/min was selected for applying the load. The beams were supported with a combination of a roller-type and a pin support at a distance of 300 mm from the two ends. The combination of the two point loads and the two supports resulted in the desired four-point loading system. A linear variable differential transformer (LVDT) was employed for measuring the mid-span deflection. Strain gauges were also incorporated to monitor the strain in reinforcing bars. In order to determine the reinforcement strain at the maximum flexural moment location, the first set of gauges

was attached to the bottom layer of the flexural reinforcement at mid-span. Another set of gauges was employed to determine strain at the middle of the shear test area (i.e., at quarter points of the span). The loading configuration and positions of the strain gauges are depicted in Figure 1. More details on the experimental program and test set up are available in (Volz et al., 2014).

The formation of cracks was monitored, and cracks were marked at load increments of 22 KN. Deformation and registered strain values were also monitored up to failure.

TEST RESULTS, ANALYSIS, AND DISCUSSION

The performances of the various beams are discussed in this section. The shear strength and steel strain were compared to values that can be deducted from various standards as well as a database proposed by Reineck et al. (2003). A statistical data analysis was conducted to evaluate the shear strength results that were normalized to the square and cube root of compressive strength.

General Observations.

No significant difference was distinguished in crack patterns, crack propagation, and load-deflection patterns of the various beams. In all cases, failure in shear was the governing mechanism that took place when the inclined flexural-shear crack reached the compression zone of the beams close to the loading plate. Based on the data obtained from strain gauges, it was observed that none of the longitudinal reinforcing bars reached yield stress at the time of failure. Crack patterns and distributions at the time of failure are shown in Figure 2.

Figure 3 presents the measured mid-span deflection as a function of the applied load. A steep linear elastic trend was observed before the initiation of flexural cracks, which is indicated by point A for each load-deflection diagram. However, increasing the load resulted in critical flexural-shear cracks, which led to failure in shear.

Comparison of Test Results with Structural Design Codes.

Table 6 presents the compressive strength results obtained from the testing of the companion cylinders measuring 100×200 mm at the time of beam testing. This table also summarizes the shear force results at the time of failure (V_{test}). The V_{test}/ V_{code} values that correspond to AASHTO LRFD (2010), ACI 318 (2011), AS 3600 (2009), CSA (2004), Eurocode 2 (2005), and JSCE (2007) codes are also presented in Figure 4 to 9.

For the CC beams, the average V_{test}/ V_{code} values ranged from 1.0 in the case of the AASHTO LRFD (2010) and CSA (2004) to 1.5 for the ACI 318 (2011). The average V_{test}/ V_{code} value for the FA50 beams ranged from 1.01 for AASHTO LRFD (2010) to 1.34 for the ACI 318 (2011) code. In the case of the RCA50 beams, the average test-to-code ratio varied from 1.05 for CSA to 1.37 for ACI. The same comparisons for SC beams showed that V_{test}/ V_{code} varied from 0.90 to 1.25 for AASHTO and ACI, respectively. The maximum V_{test}/ V_{code} values were observed for the ACI 318 (2011) prediction, indicating that this standard can underestimate (conservatively) the shear capacity of the investigated beams. The JSCE (2007) standard was also conservative and resulted in average test-to-code ratios ranging from 1.14 to 1.28. The predictions obtained through the AS-3600 (2009) and Eurocode 2 (2005) are also in good agreement with experimental data with most of the average V_{test}/ V_{code} values slightly higher than 1.0. The AASHTO LRFD (2010) and CSA (2004) on the other hand, resulted in test-to-code shear ratios close to or slightly less than 1.0. In other words, care must be taken while incorporating these codes to determine the shear capacity of such concrete.

The average values of V_{test}/ V_{code} were 1.12, 1.13, 1.17, and 1.03 for the CC, FA50, RCA50, and SC beams, respectively. A 10% decrease in the test-to-code ratio of the SC specimens indicated that the existing codes overestimated the shear capacity of the SC beams in comparison with other mixtures.

Comparing Test Results with Shear Test Database.

The main factors that affect the shear strength of a reinforced concrete element are the depth of member (d), the shear span to depth ratio (a/d), the compressive strength of the concrete (f'_c), and the amount of longitudinal reinforcement (ρ). The experimental

results were compared with the shear test database presented by Reineck et al. (2003) to evaluate the effect of the aforementioned factors on the shear capacity of the beams. The database summarizes 439 test results obtained by testing the shear performance of the beam specimens with a wide range of properties, including: (1) concrete compressive strength ranging from 12.0 to 110 MPa; (2) member depth varying from 100 to 2000 mm; (3) shear span to depth ratio of 2.4 to 8.0; as well as (4) longitudinal reinforcement ratio of 0.5% to 7.0%.

Figure 10 plots the shear stress as a function of f'_c, ρ, d, and a/d, respectively. A regression analysis was conducted to fit a nonlinear curve through the data points. The figure indicates that the results obtained through this study fall within the middle part of the data points and are in line with the general trends of the database.

It was observed that the shear strength exhibited a slight increasing trend due to the increase in compressive strength. This is in line with the general behavior of the data represented by the trend line. The highest compressive strength of 35.5 MPa was observed for the RCA50 concrete, followed by FA50, SC, and CC concrete with compressive strength values of 32.4, 30.8, and 29.0 MPa at the time of testing, respectively. A similar trend was observed for the shear strength values, where the highest and the lowest average shear strength values were observed for the RCA50 and CC beams, respectively.

Regarding the effect of d on shear strength, it was observed that the experimental data followed the trend of the database, and the increase in d from 375 to 400 mm resulted in an average decrease in shear strength from 1.33 to 0.97 MPa. According to the data presented in the database, it may be concluded that an increase in a/d tends to reduce the shear strength. However, considering the data obtained through experiments, it may be concluded that a slight increase in shear strength is observed due to an increase in a/d from 3.1 to 3.25. The variations in shear strength due to the longitudinal reinforcement ratio also follow the trends obtained for the database. Studying the plotted experimental data reveals the fact that an increase in ρ from 1.27% to 2.71% enhances the average shear strength of the beams.

Comparison of Measured Reinforcement Strains with AASHTO LRFD (2010).

AASHTO LRFD Standard (2010) proposed Equation 1 to determine the tensile strain in the longitudinal reinforcing steel:

$$\varepsilon_s = \frac{\left(\frac{|M_u|}{d_v} + |V_u|\right)}{E_s A_s} \quad (1)$$

Table 6 presents strain gauge measurements at the center of the shear test zone compared to the values obtained from Equation (13-1). The AASHTO LRFD (2010) equation makes an acceptable prediction of strain values for the SC, CC, and the FA50 beams. Figure 11 also presents the ratios of the code-to-experiment steel strain values ($\frac{\varepsilon_s - Eq}{\varepsilon_s - Exp}$). The average code-to-experiment values for these concrete types varied from 0.87 to 0.93. This means that the AASHTO LRFD (2010) model is applicable for the SC beams as well as the CC and FA50 beams. The best prediction was observed for the RAC50 beams with an average equation-to-experiment ratio of 1.00.

Comparison of Test Results with Fracture Mechanics Approaches.

Gastebled and May (2001), Bazant and Yu (2005), and Xu et al. (2012) suggested employing a fracture mechanics approach to assess the shear capacity of reinforced concrete beams that are not reinforced with stirrups in the shear zone. The model proposed by Bazant and Yu (2005) determines the shear capacity of reinforced concrete beams cast without stirrups (Equation 2). Equation 3, developed by Gastebled and May (2001) is based on fracture energy for splitting crack propagation that leads to releasing the longitudinal reinforcing bars from the surrounding concrete. Moreover, Equation 4, proposed by Xu et al. (2012) is originated from the fracture energy needed to release the interface bond between the rebar and concrete.

$$V_c = 10\rho^{\frac{1}{3}}\left(1 + \frac{d}{a_s}\right)\sqrt{\frac{f'_c}{1 + \frac{f'_c}{f'^{\frac{2}{3}}_c\,(3800\sqrt{d_a})}}}\, b_w d \quad (2)$$

$$V_c = \frac{1.109}{\sqrt{d}}\left(\frac{d}{a_s}\right)^{\frac{1}{3}}\rho^{\frac{1}{6}}\left(1 - \sqrt{\rho}\right)^{\frac{2}{3}} f'^{0.55}_c \sqrt{E_s}\, b_w d \quad (3)$$

$$V_c = \frac{1.018}{\sqrt{d}}\left(\frac{d}{a_c}\right)^{\frac{1}{8}}\rho^{\frac{1}{6}}\left(1-\sqrt{\rho}\right)^{\frac{2}{3}}(0.0255f_c' + 1.24)b_w d \quad (4)$$

Figure 12 compares the V_{test}/V_{Eq} values for the introduced models. Most of the investigated models predicted the shear capacity of the beams conservatively. The ratio of the experimental-to-predicted results (V_{test}/V_{Eq}) from the models developed by Bazant and Yu (2005), Gastebled and May (2001), and Xu et al. (2012) ranged from 1.04 to 1.45, 1.0 to 1.60, and 0.89 to 1.54, respectively (Figure 12). Furthermore, this comparison shows that, similar to the design code shear strength comparisons, the V_{test}/V_{Eq} for the majority of SC beams are generally lower than those for the rest of the beams. More importantly, it seems that the various fracture mechanics models are applicable for all beam types.

Comparison of Test Results with the Modified Compression Field Theory Method.

The modified compression field theory (MCFT) evaluates the load-deformation behavior of two-dimensional cracked reinforced concrete in shear. Several codes, including the AASHTO-LRFD (2010) and CSA (2004), have recommended simplified versions of this method. The results predicted by the MCFT are compared to the experimental data in this section. Based on the data presented in Figure 12, it can be observed that the MCFT method underestimates the shear capacity of the investigated beams. Similar to both shear provisions of the codes and the fracture mechanics approaches, the MCFT method shows lower ratios (V_{test}/V_{Eq}) for the SC beams compared with the rest of the beams. The test-to-equation values range from 1.19 to 1.37, 1.2 to 1.49, 1.04 to 1.43, and 1.03 to 1.28 in the case of the CC, FA50, RCA50, and SC beams, respectively.

Statistical Data Analysis.

A statistical data analysis was conducted to determine the statistically significant variations between the normalized shear strength results. Such an analysis enables us to make sure that the conducted comparisons and derived conclusions are robust and not due to experimental errors and noise in data. The effect of compressive strength on shear capacity is taken into account by normalization to the results of f'_c. It is generally

believed that shear capacity is a function of the square root of f'_c (ACI 318-11, AASHTO LRFD-10, CSA-04, and JSCE-07) or cube root of f'_c (AS 3600 -09 and Eurocode 2-05).

Analysis of variance (ANOVA) was conducted based on F-test as means of comparing the normalized shear strength values. A statistical analysis software (SAS 9.3) was used to test the following hypotheses at α=0.05 significance level:

H_0: there is no significant difference in the mean shear strength of the CC beams and that of the SC ones

H_a: the assumption of H_0 is not correct

Statistical analysis relies on the fact that a calculated P-value less than the significance level means that the factor or the interaction between factors will be statistically significant, while a P-value greater than the α=0.05 threshold reveals the fact that such a particular factor or interaction will not be statistically significant (Sadati and Khayat, 2014). In other words, a P-value less than 0.05 means that there is less than a 5% chance that the observed behavior is due to noise, ensuring that the effect will be statistically significant. It should be noted that conducting ANOVA requires the data to follow a normal distribution (Montgomery, 2008). Therefore, the Kolmogorov-Smirnov and Anderson-Darling methods of testing for normality were incorporated using a statistical software (Minitab 17) to make sure that the data follow a normal distribution.

The P-values obtained for the cube root and square root normalized values were higher than 0.15 according to Kolmogorov-Smirnov. Moreover, the P-values were 0.237 and 0.355 based on Anderson-Darling method, respectively. These observations indicate that the data are normally distributed and ANOVA results would be valid. A summary of the ANOVA results is presented in Table 7.

Based on the data presented in Table 7, it can be concluded that, for both the square root and cube root normalizations, the concrete type (CC vs. SC) plays a significant role in normalized shear strength with P-values less than 0.05. In other words, the null hypothesis will be rejected, and it could be concluded that the normalized shear strength of the SC beams is statically less than that of the CC beams.

Given the observed P-values for the steel content, it can be observed that the longitudinal reinforcement ratio also plays a significant role for the shear strength of beams, and an increase in ρ enhances the shear capacity of the beams. This is in line with the observations of Lee and Kim (2008) who reported an increase in the shear capacity of reinforced concrete beams cast with minimum shear reinforcement due to an increase in the longitudinal reinforcement ratio. However, there is no significant interaction between the concrete type and ρ with P-values higher than a significance level of 0.05.

Several sets of contrast vectors were incorporated to compare the normalized shear capacity of the CC, SC, FA50, and RCA50 beams in the SAS software as summarized in Table 8. This was conducted to determine if there is any statistically significant difference between the normalized shear strength of different beams fabricated with various concrete types. In the case of the square root normalizations according to ACI 318 (2011), AASHTO LRFD (2010), CSA (2004), and JSCE (2007), it was observed that the shear capacity of the SC beams is statistically less than that of the CC and FA50 beams with P-values of 0.0084 and 0.0153, respectively. None of the other contrasts were significant at a 0.05 significance level. In other words, the differences between the shear strength of the CC and FA50, CC and RCA50, FA50 and RCA50, and SC and RCA50 beams are not statistically significant.

Regarding the cube root comparisons that comply with AS-3600 and Eurocode 2, it was observed that the mean shear capacity of the SC beams is statistically less than those of the CC, FA50, and RCA50 beams with P-values of 0.0121, 0.0045, and 0.0209, respectively. None of the other contrasts were significant. This means that there is no statistically significant difference in the cube root normalized shear strength of the CC and RCA50, CC and FA50, and FA50 and RCA50 beams.

Based on the statistical data analysis, it can be concluded that the shear strength of the SC was statistically lower than the CC beams. On average, a 10%, 18%, and 16% decrease in shear capacity was observed for the SC beams in comparison with CC, FA50, and RCA50 specimens, respectively.

REMARKS

This paper compares the shear strength of concrete proportioned with 50% fly ash and 50% RCA, which is referred to as sustainable concrete (SC), to conventional concrete, concrete with 50% fly ash, and concrete with 50% RCA. The results presented in this study are providing a better understanding of the performance of such sustainable concrete mixtures for potential structural applications. The data obtained through testing 24 full-scale beams were analyzed. The beams had a longitudinal reinforcement ratio ranging between 1.27% and 2.71%. Based on the results obtained in this study, the following conclusions are warranted:

- The compressive strength of the concrete at the time of testing at 28 days was 29.0, 30.8, 32.4, and 35.5 for the CC, SC, FA50, and RCA50 specimens, respectively.
- The values of strain in the longitudinal reinforcement bars were in good agreement with theoretical measurements based on AASHTO LRFD. The average registered strain varied from 772 to 948, 870 to 1147, 866 to 1088, and 875 to 1232 με, for the CC, FA50, RCA50, and SC concrete types, respectively.
- A statistical data analysis indicates that there is no significant difference between the normalized shear strength values when comparing the behavior among the CC, FA50, and RCA50 beams. However, the comparison of the shear strength of the SC beams to the CC, FA50, and RCA50 specimens, indicated a 10%, 18%, and 16% reduction in shear strength, respectively.
- All beams exhibited similar load-deflection trends, crack patterns, and crack propagation.
- The shear strength values were conservatively predicted using the ACI 318 (2011) and JSCE (2007); the shear strength of the SC beams was overestimated by up to 10% using the AASHTO LRFD (2010) and CSA (2004).

- The experimental results obtained for the specimens were slightly higher than the values estimated by the fracture mechanics approaches, suggesting that these methods can provide a safe estimation of shear strength. The ratios of experimental-to-predicted shear strength results (Vtest/VEq) based on the models developed by Bazant and Yu (2005), Gastebled and May (2001), and Xu et al. (2012), varied from 1.04 to 1.45, 1.0 to 1.60, and 0.89 to 1.54, respectively.
- Slightly higher shear strength results were observed for the four tested concrete types compared to the MCFT predictions. The average ratio of experimental-to-predicted shear strength (Vtest/VEq) based on the MCFT approach was 1.31, 1.33, 1.27, and 1.15 in the case of the CC, FA50, RCA50, and SC beams, respectively.
- Evaluating the shear performance of sustainable concrete based on both the fracture mechanics and MCFT approaches for design and/or control applications is recommended.
- The results presented here should be of interest to owner agencies and engineers who are considering the design and use of sustainable concrete for structural applications.

REFERENCES

American Association of State and Highway Transportation Officials (AASHTO), 2010. AASHTO LRFD Bridge design specifications, 4th Ed., Washington, D.C., 72-84.

American Concrete Institute ACI Committee, 2011. Building code requirements for structural concrete (ACI 318-11/318R-11), Farmington Hills, MI: American Concrete Institute, 155-168.

Arezoumandi, M., Volz, J. S., and Myers, J. J., 2013. Shear behavior of high-volume fly ash concrete versus conventional concrete. Journal of Materials in Civil Engineering, Vol. 25, No. 10, 1506-1513.

Arezoumandi, M., Volz, J. S., Ortega, C. A., & Myers, J. J., 2014. Shear behavior of high-volume fly ash concrete versus conventional concrete: Experimental study. Journal of Structural Engineering, 141(3), B4014006.

Arezoumandi, M., Smith, A., Volz, J. S., and Khayat, K. H., 2014. An experimental study on shear strength of reinforced concrete beams with 100% recycled concrete aggregate. Construction and Building Materials, 53, 612-620.

AS 3600, 2009. Concrete structures, Standards Australia, Sydney, pp. 105-109.

ASTM A615/A615M, 2012. Standard specification for deformed and plain carbon-steel bars for concrete reinforcement, ASTM, West Conshohocken, PA.

Bažant, Z. P., and Yu, Q., 2005. Design against size effect on shear strength of reinforced concrete beams without stirrups, Journal of Structural Engineering, ASCE, V. 131, No. 12, 1877-1885.

Behnood, A., Olek, J., & Glinicki, M. A. (2015). Predicting modulus elasticity of recycled aggregate concrete using M5′ model tree algorithm. Construction and Building Materials, 94, 137-147.

Bentz D.P., 2010. Powder additions to mitigate retardation in high-volume fly ash mixtures. ACI Materials Journal, 107(5):508–14.

Canadian Standards Association (CSA), 2004. Design of concrete standards for buildings. CAN3-A23.3, Rexdale, Ontario, Canada, 53-61.

European Committee for Standardization, Eurocode No. 2, 2005. Design of concrete structures. Part 1: general rules and rules for buildings, 84-92.

Etxeberria, M., Mari, A. R., & Vazquez, E., 2007. Recycled aggregate concrete as structural material. Materials and Structures, 40(5), 529-541.

Fathifazl, G., Razaqpur, A. G., Burkan Isgor, O., Abbas, A., Fournier, B., and Foo, S., 2011. Shear capacity evaluation of steel reinforced recycled concrete (RRC) beams. Engineering Structures, 33(3), 1025-1033.

Gastebled, O. J., and May, I. M., 2001. Fracture mechanics model applied to shear failure of reinforced concrete beams without stirrups, ACI Structural Journal, V. 98, No. 2, 184-190.

Gonzalez-Fonteboa, B., and Martinez-Abella, F., 2007. Shear strength of recycled concrete beams. Construction and Building Materials, 21(4), 887-893.

Han, B. C., Yun, H. D., & Chung, S. Y., 2001. Shear capacity of reinforced concrete beams made with recycled aggregate. ACI Special publication, 200.

Japan Society of Civil Engineers (JSCE), 2007. Standard specification for concrete structure, JSCE No. 15, Tokyo, Japan, 154-159.

Ji, S. K., Lee, W. S., & DoYun, H., 2008. Shear strength of reinforced concrete beams with recycled aggregates. Tailor Made Concrete Structures – Walraven & Stoelhorst (eds) Taylor & Francis Group, London, ISBN 978-0-415-47535-8

Knaack, A. and Kurama, Y., 2014. Behavior of reinforced concrete beams with recycled concrete coarse aggregates. Journal of Structural Engineering, 10.1061/ (ASCE) ST.1943-541X.0001118 , B4014009, 1-12.

Lee, J. Y., & Kim, U. Y., 2008. Effect of longitudinal tensile reinforcement ratio and shear span-depth ratio on minimum shear reinforcement in beams. ACI Structural Journal, V. 105, No. 2, 134-144.

Montgomery, D. C., 2008. Design and analysis of experiments. 7th ed. John Wiley & Sons Inc., New York.

Nuaklong, P., Sata, V., & Chindaprasirt, P., 2015. Influence of recycled aggregate on fly ash geopolymer concrete properties, Journal of Cleaner Production, http://dx.doi.org/10.1016/j.jclepro.2015.10.109

Rao, R. M., Mohan, S., and Sekar, .S.K., 2011. Shear resistance of high volume fly ash reinforced concrete beams without web reinforcement, International Journal of Civil and Structural Engineering, V. 1, No. 4, 986-993.

Reineck, KH, Kuchma, DA, Kim, KS, and Marx, S., 2003. Shear database for reinforced concrete members without shear reinforcement, ACI Structural Journal, V. 100, No. 2, 240-249.

Sadati S. and Khayat K. H., 2014. Field performance of concrete pavement made with recycled concrete aggregate. In International Symposium on Environmentally Friendly Concrete- ECO-CRETE, Reykjavik, Iceland, 385-392.

Sogo, M., Sogabe, T., Maruyma, I., Sato, R., & Kawai, K., 2004. Shear behavior of reinforced recycled concrete beams. In Proceedings of the International RILEM Conference on the Use of Recycled Materials in Building and Structures, 610-618.

Vecchio, F.J. and Collin, M. P., 1986. The modified compression field theory for reinforced concrete elements subjected to shear, ACI Structural Journal, V.83, No.2, 219-23.

Volz, J. S., Khayat, K. H., Arezoumandi, M., Drury, J., Sadati, S., Smith, A, and Steele, A., 2014. Recycled concrete aggregate (RCA) for infrastructure elements. National University Transportation Center (NUTC), Missouri University of Science and Technology, Rolla, MO, USA, (NUTC R312).

World Business Council for Sustainable Development (WBCSD) Report, 2012. Recycling concrete, http://www.wbcsdcement.org/index.php/key-issues/sustainability-with-concrete/54, (accessed date: August 21, 2014).

Xu, S., Zhang, X., and Reinhardt, H.s W., 2012. Shear capacity prediction of reinforced concrete beams without stirrups using fracture mechanics approach, ACI Structural Journal, V. 109, No. 5, 705-714.

Yagishita, F., Sano, M., and Yamada, M., 1994. Behavior of reinforced concrete beams containing recycled coarse aggregate, Demolition and Reuse of Concrete & Masonry Rilem Proceeding 23, E&FN Spon, 331-342.

Table 1 Summary of shear performance of RCA-made concrete

Author	RCA (%)	b (mm)	d (mm)	h (mm)	a/d	dmax (mm)	ρ (mm)	f'_c (MPa)	V (kN)
Han et al. (2001)	100	170	270	300	1.5	25	1.1	39.6	83.5
		170	270	300	2.0	25	1.1	30.6	65.2
		170	270	300	2.0	25	1.1	32.6	60.6
		170	270	300	3.0	25	1.1	31.2	42.7
		170	270	300	4.0	25	1.1	31.9	31.7
Belén and Fernando (2007)	50	200	303	350	3.3	25	3.0	39.7	90.6
Etxeberria and Vazquez, (2007)	25	200	303	350	3.3	25	2.9	42.4	104.0
	50	200	303	350	3.3	25	2.9	41.3	89.0
	100	200	303	350	3.3	25	2.9	39.8	84.0
Ji et al. (2008)	100	170	270	300	2.2	-	1.1	39.7	60.0
Fathifazl et al. (2011)	63.5	200	300	375	1.5	19	1.0	41.6	186.7
		200	300	375	2.0	19	1.5	41.6	169.5
		200	309	375	2.7	19	1.62	41.6	103.9
		200	305	375	4.0	19	2.46	41.6	83.2
	74.3	200	300	375	1.5	19	1.0	49.1	195.3
		200	300	375	2.0	19	1.5	49.1	179.0
		200	305	375	4.0	19	2.46	49.1	105.6
	63.5	200	201	250	2.7	19	2.0	41.6	89.3
		200	309	375	2.6	19	1.6	41.6	103.9
		200	381	450	2.7	19	1.8	41.6	99.5
		200	476	550	2.7	19	1.7	41.6	104.6
	74.3	200	201	250	2.7	19	2.0	49.1	122.6
		200	381	450	2.7	19	1.8	49.1	111.7
		200	476	550	2.7	19	1.7	49.1	119.6

Table 1 Summary of shear performance of RCA-made concrete (cont.)

Knaack and Kurama (2014)	50	150	200	230	3.8	19	1.3	41.8	44.0
		150	200	230	3.8	19	1.3	41.8	39.1
		150	200	230	3.8	19	1.3	37.4	43.7
		150	200	230	3.8	19	1.3	37.4	41.2
	100	150	200	230	3.8	19	1.3	39.1	36.4
		150	200	230	3.8	19	1.3	39.1	38.0
		150	200	230	3.8	19	1.3	39.2	39.9
		150	200	230	3.8	19	1.3	39.2	36.1
Arezoumandi et al. (2014)	100	305	400	460	3.1	25	1.27	30.0	114.8
		305	375	460	3.25	25	1.27	30.0	143.2
		305	375	460	3.25	25	2.03	30.0	131.4
		305	400	460	3.1	25	2.03	34.1	113.0
		305	375	460	3.25	25	2.71	34.1	124.1
		305	375	460	3.25	25	2.71	34.1	140.3

Table 2 Aggregate properties

	Coarse aggregate	Coarse aggregate**	Sand	RCA*	RCA**
Bulk specific gravity	2.52	2.72	2.63	2.23	2.35
Absorption (%)	3.20	0.98	0.4	6.30	4.56

*Beams with 50% RCA and 50% fly ash (SC beams)

**Beams with 50% RCA (RCA50 beams)

Table 3 Chemical composition and physical properties of cement and fly ash

Property	Cement	Fly ash
SiO_2, %	21.98	33.46
Al_2O_3, %	4.35	19.53
Fe_2O_3, %	3.42	6.28
CaO, %	63.97	26.28
MgO, %	1.87	5.54
SO_3, %	2.73	2.40
Na_2O eq., %	0.52	1.43
Blaine surface area, m^2/kg	410	490
Specific gravity	3.15	2.73
LOI, %	0.6	0.34

Table 4 Concrete mixture proportions

Mixture	Water (kg/m^3)	Cement (kg/m^3)	w/cm	Class C fly ash (kg/m^3)	Gypsum (kg/m^3)	Calcium hydroxide (kg/m^3)	Coarse aggregate (kg/m^3)	Recycled coarse aggregate (kg/m^3)	Sand (kg/m^3)	HRWR (l/m^3)	AEA (l/m^3)
CC	134	337	0.40	-	-	-	1103	-	735	0.66	0.20
FA50	160	210	0.35	210	10	22	1040	-	705	-	-
RCA50	127	317	0.40	-	-	-	581	502	743	2.10	0.77
SC	134	169	0.40	169	-	-	529	468	735	0.44	0.15

Table 5 Fresh and hardened concrete properties

Property		CC	FA50	RCA50	SC
Slump (mm)		115	115	155	120
Air content (%)		5.5	4.1	6.5	6.0
Unit weight (kg/m3)		2306	2395	2259	2300
Compressive strength (MPa)	3 days	-	-	-	20.6 (4*)
	28 days	29.0 (4)	32.4	35.5 (6)	30.8 (2)
	56 days	-	-	-	35.3 (5)
Splitting tensile strength (MPa)	28 days	2.9 (20)	3.0	3.0 (17)	1.8 (18)
	56 days	-	-	-	2.2 (8)
Flexural strength (MPa)	28 days	2.8	3.5	3.1	3.3
	56 days	-	-	-	3.4
*COV (%)					

Table 6 Summary of the test results

Concrete type	Beam type	Replicate	f'_c (MPa)	V_{test} (kN)	ε_s quarter-point (με)	
					Experiment	AASHTO LRFD (2010)
CC	NS-4	1	29.0	119.7	*	1004
		2	26.5	113.9	844	954
	NS-6	1	29.0	153.5	989	892
		2	26.5	144.6	906	840
	NS-8	1	29.0	147.7	726	645
		2	26.5	143.7	818	626
FA50	NS-4	1	32.4	127.0	1231	1029
		2	33.5	134.1	1063	1088
	NS-6	1	32.4	163.9	1012	928
		2	33.5	133.7	727	752
	NS-8	1	32.4	164.8	1037	912
		2	33.5	163.7	806	725
RCA50	NS-4	1	32.0	117.4	1001	1154
		2	35.5	111.6	912	973
	NS-6	1	32.0	151.2	1080	1064
		2	35.5	148.6	1095	1087
	NS-8	1	32.0	171.7	897	821
		2	35.5	168.6	834	768
SC	NS-4	1	30.8	120.5	1257	1277
		2	26.6	99.9	1206	1066
	NS-6	1	30.8	140.8	1229	1037
		2	26.6	134.6	1102	989
	NS-8	1	30.8	136.3	854	751
		2	26.6	116.8	896	647

*: Non-reliable strain gage data

Table 7 ANOVA results at 0.05 significance level

Analysis	Source	Type III SS	Mean Square	F Value	Pr > F
Square root normalization	Concrete	22.77	22.77	27.15	0.0020
	Steel	69.56	34.78	41.47	0.0003
	Concrete×Steel	2.99	1.49	1.79	0.2462
Cube root normalization	Concrete	62.38	62.38	16.14	0.0070
	Steel	211.08	105.54	27.31	0.0010
	Concrete×Steel	9.01	4.50	1.17	0.3735

Table 8 Contrast results at 0.05 significance level

Analysis	Contrast	Contrast SS	Mean Square	F Value	Pr > F
Square root normalization	CC vs. SC	22.77	22.77	9.91	0.0084
	CC vs. FA50	0.24	0.24	0.10	0.7530
	CC vs. RCA50	3.51	3.51	1.53	0.2400
	FA50 vs. SC	18.35	18.35	7.99	0.0153
	RCA50 vs. SC	8.40	8.40	3.66	0.0800
	FA50 vs. RCA50	1.92	1.92	0.84	0.3785
Cube root normalization	CC vs. SC	62.38	62.38	8.71	0.0121
	CC vs. FA50	2.00	2.00	0.28	0.6067
	CC vs. RCA50	0.62	0.62	0.09	0.7734
	FA50 vs. SC	86.73	86.73	12.11	0.0045
	RCA50 vs. SC	50.55	50.55	7.06	0.0209
	FA50 vs. RCA50	4.85	4.85	0.68	0.4264

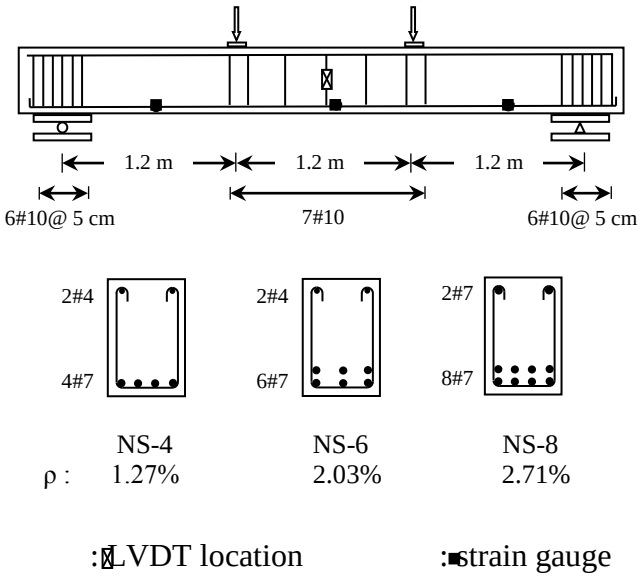

Figure 1 Four-point loading setup, location of instrumentation, and typical reinforcement, including stirrup over support area and in mid-span region

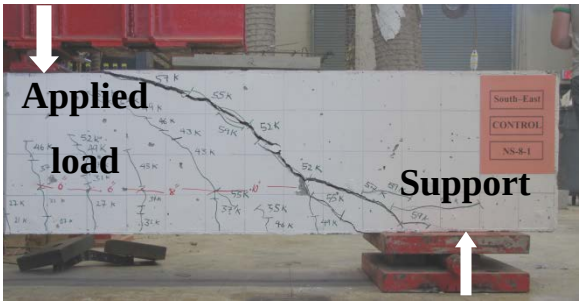

CC

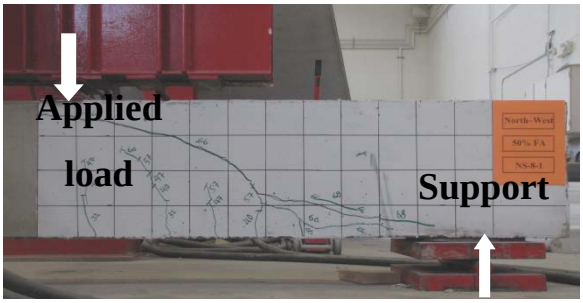

FA50

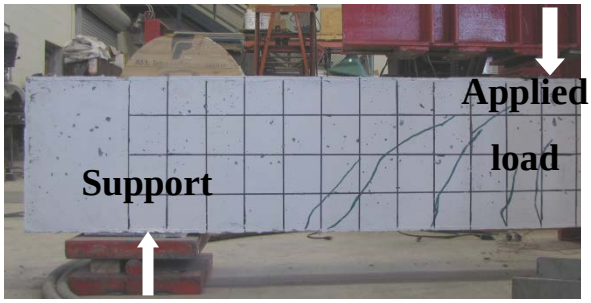

RCA50

SC

Figure 2 Crack patterns at the time of failure

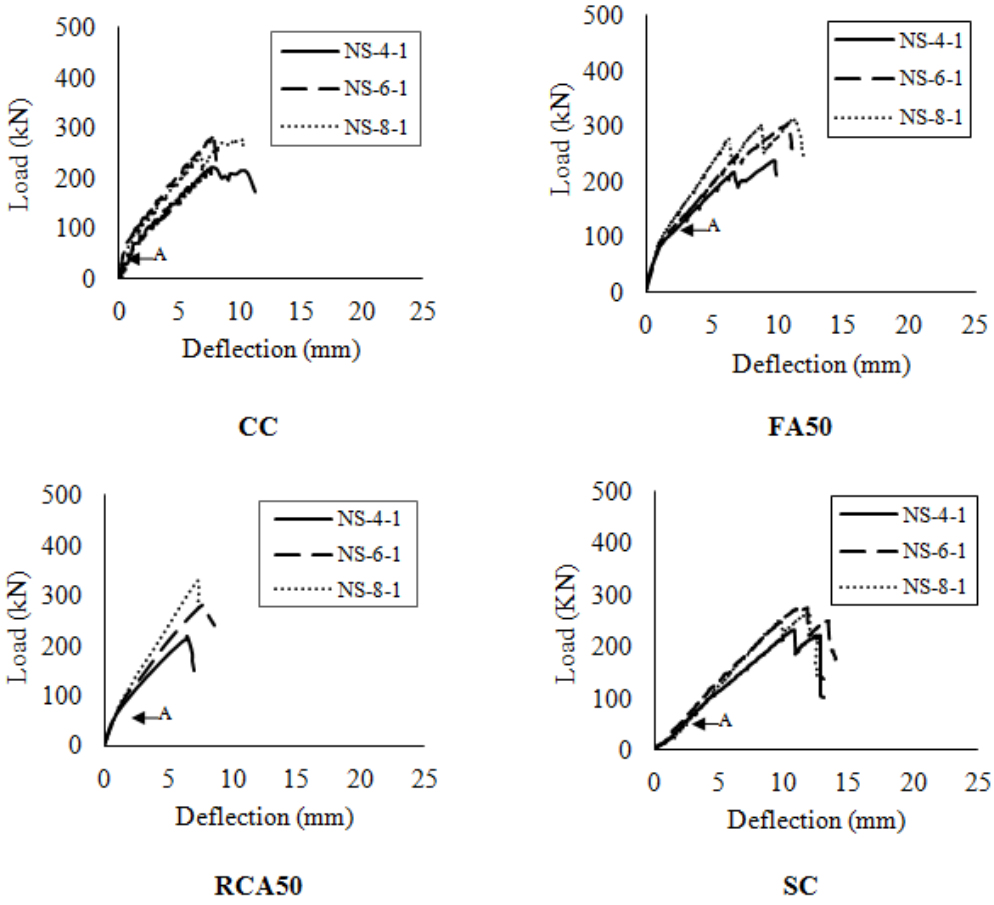

Figure 3 Mid-span load-deflection of various beam specimens

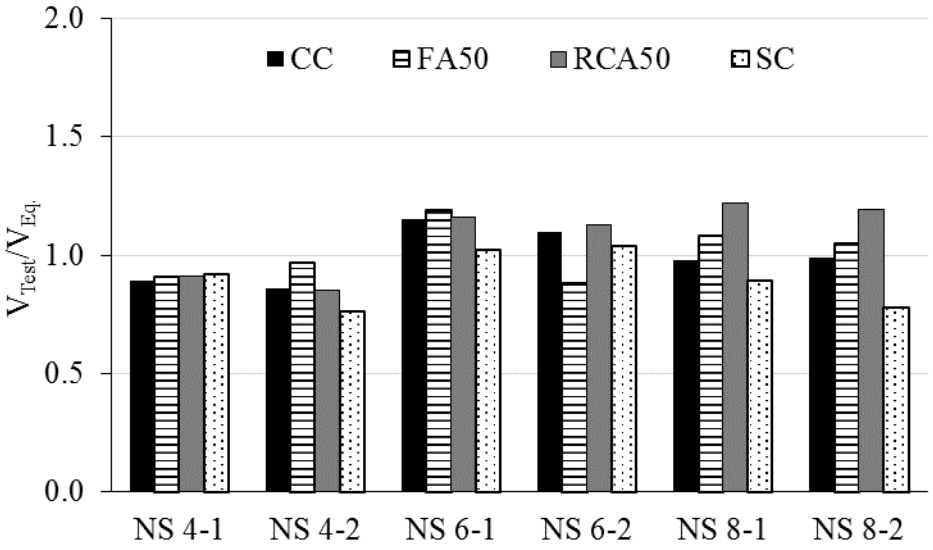

Figure 4 Comparing experiment-to-code values derived from AASHTO LRFD (2010)

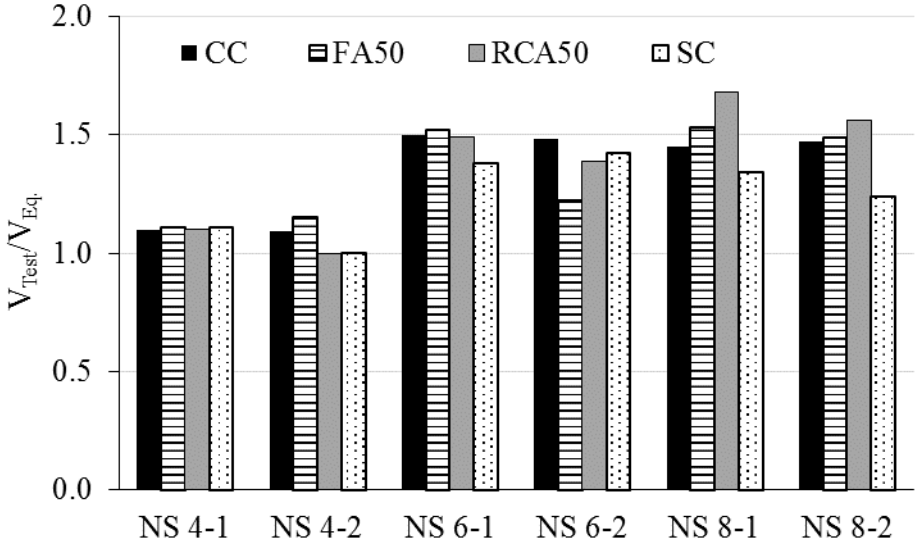

Figure 5 Comparing experiment-to-code values derived from ACI-318 (2011)

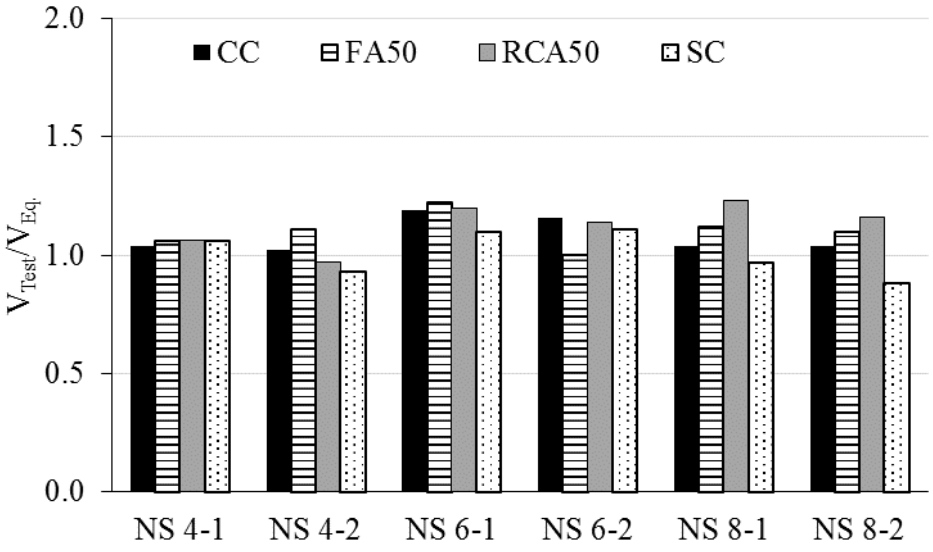

Figure 6 Comparing experiment-to-code values derived from AS-3600 (2009)

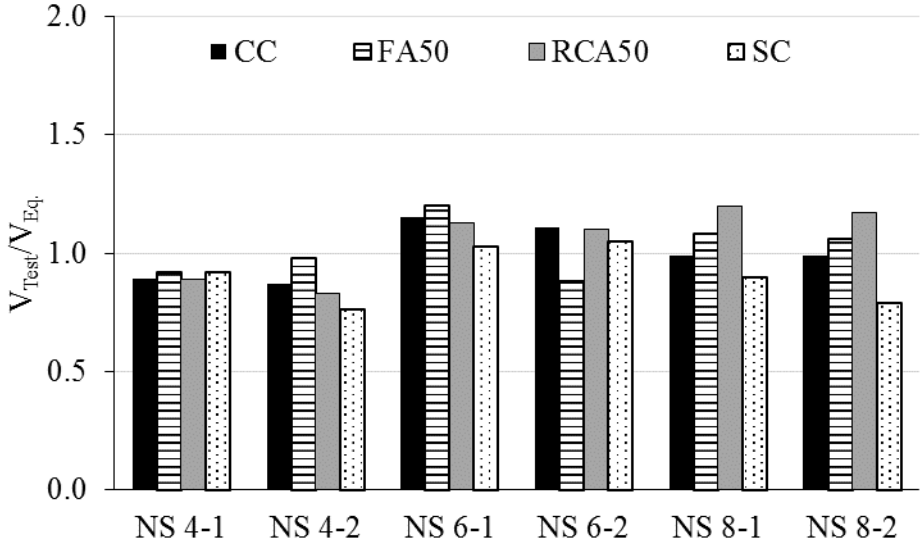

Figure 7 Comparing experiment-to-code values derived from CSA (2004)

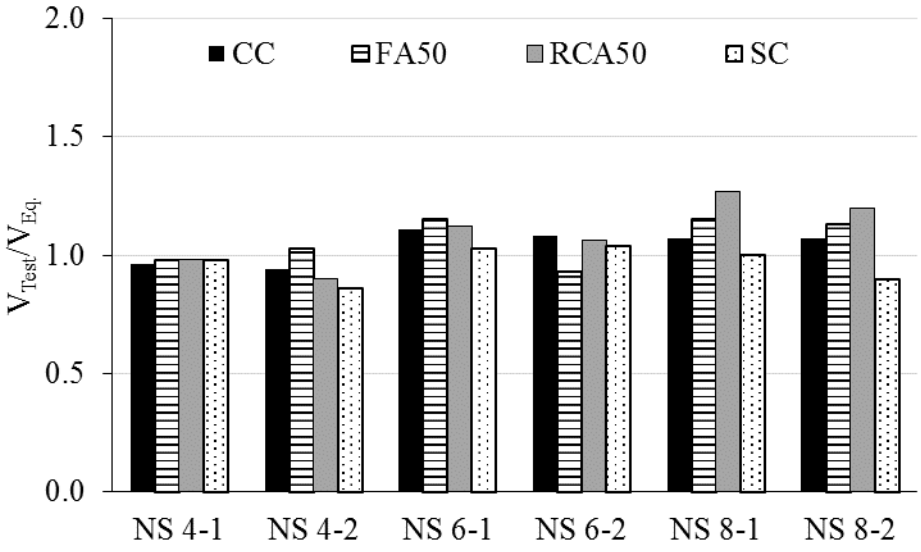

Figure 8 Comparing experiment-to-code values derived from Eurocode 2 (2005)

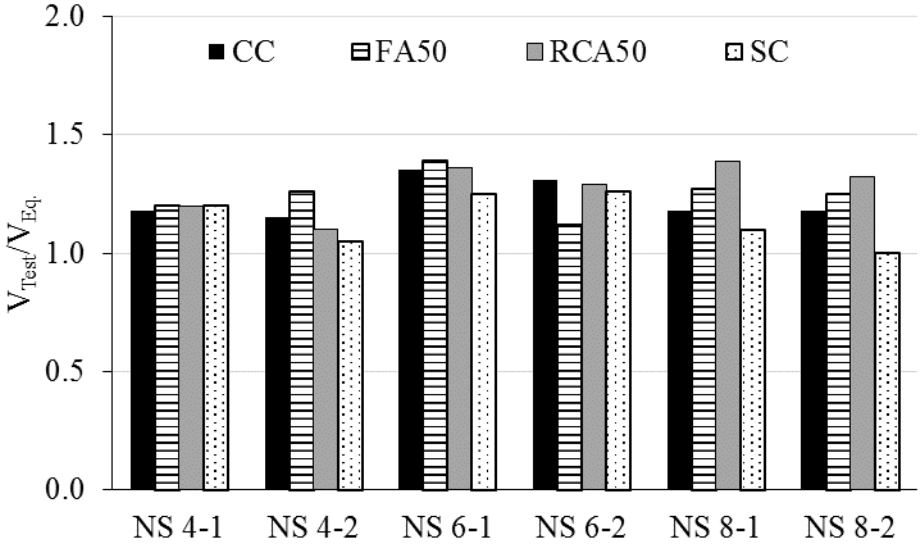

Figure 9 Comparing experiment-to-code values derived from JSCE (2007)

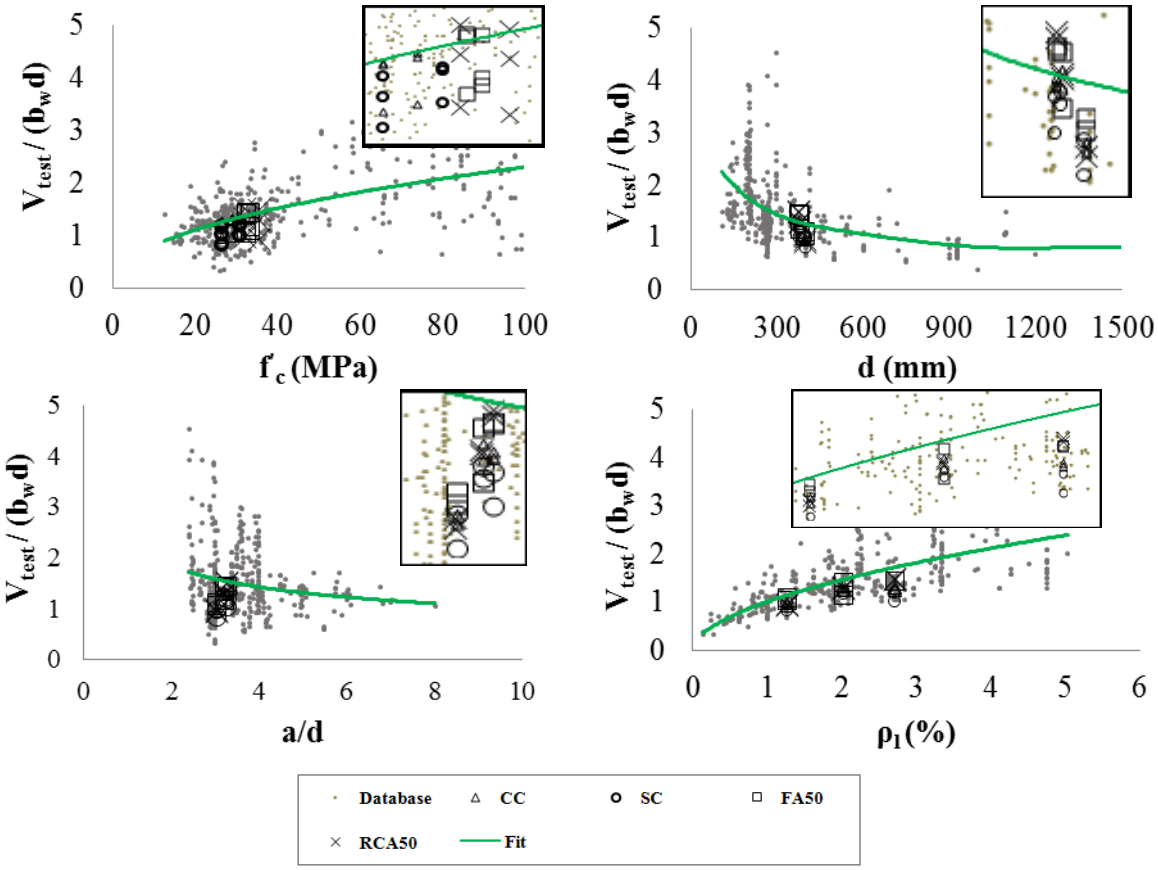

Figure 10 Comparison of experimental data with database reported by Reineck et al. (2003)

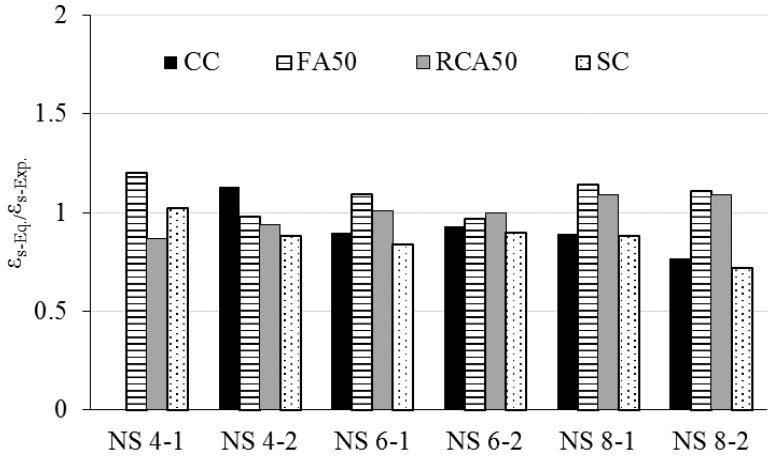

Figure 11 Comparing equation-to-experiment steel strain values derived from comparison to AASHTO LRFD (2010)

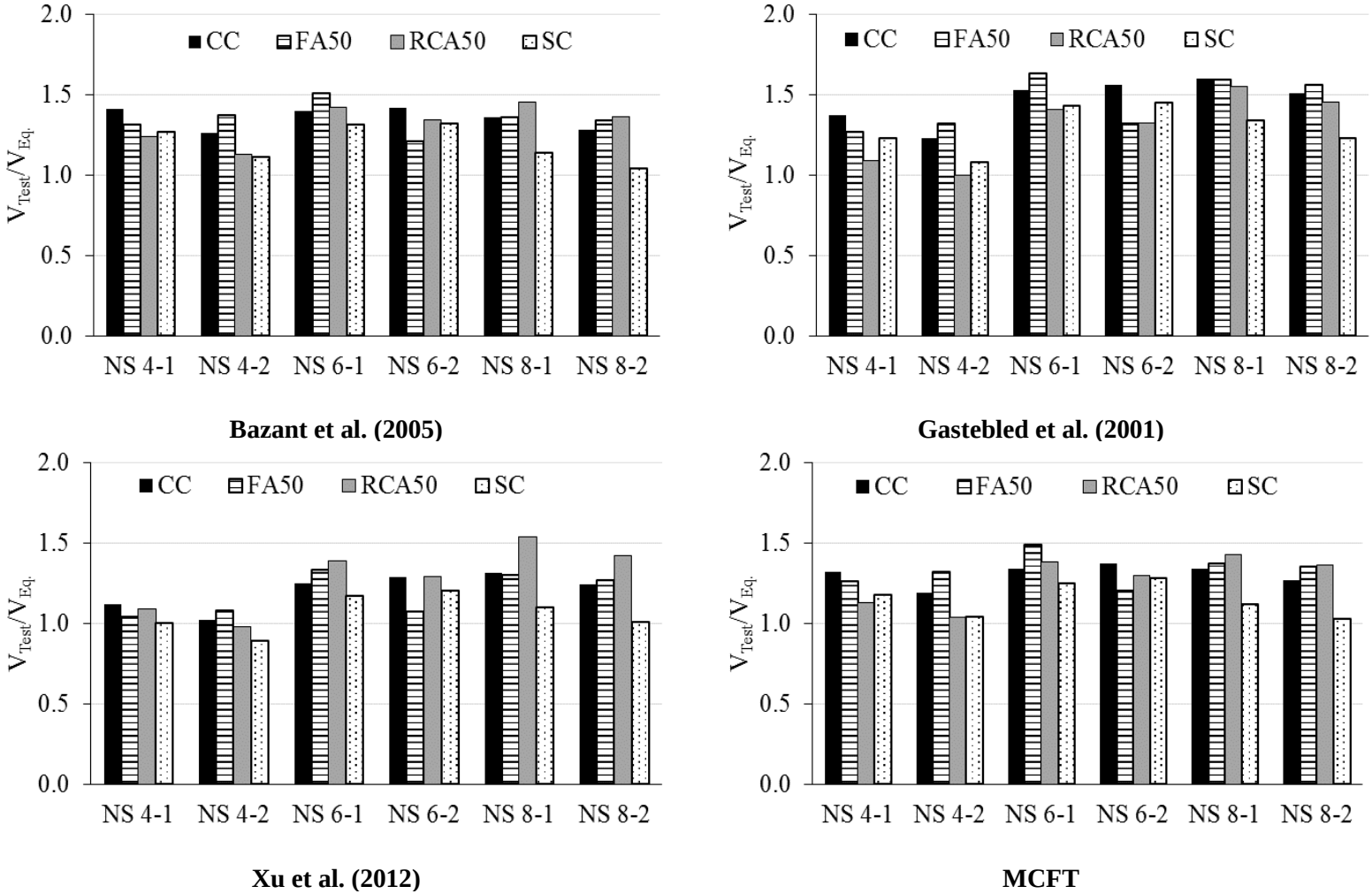

Figure 12 Comparison of experimental shear strength data with fracture mechanics approaches and MCFT method predictions

APPENDIX B.

BOND PERFORMANCE OF SUSTAINABLE REINFORCED CONCRETE BEAMS

RESEARCH SIGNIFICANCE

Concrete is the most widely used construction material. Efforts aimed at producing environmentally friendly concrete can play a major role in securing sustainable construction. Candidate technologies for sustainable concrete materials include the incorporation of supplementary cementitious materials (SCMs), such as fly ash as a partial replacement for Portland cement, the incorporation of recycled materials in concrete production, and in particular recycled concrete aggregate (RCA), use of high strength concrete to reduce dimensions of structural sections, as well as the use of highly durable concrete to increase service life.

The production of Portland cement is responsible for about 7% of the total worldwide CO_2 emission (Shen et al. 2015). Therefore, partial replacement of Portland cement with alternative cementitious materials and/or industrial by-products can decrease the carbon footprint of concrete. Over 900 million tons of construction and demolition waste is produced yearly in Europe, the U.S., and Japan (WBCSD 2012). Although using RCA does not lead to significant reduction in CO_2 emission, it can significantly contribute to the reduction of the depletion of natural resources (virgin aggregate) and decrease the need for landfills.

When using high volume of RCA and SCMs, it is necessary to understand the structural performance of such new class of concrete materials. Given the importance of force transfer between the reinforcing bars and surrounding concrete, it is necessary to study the effect of such modifications in concrete mixture on bond strength. Bond strength between the concrete and reinforcing steel affects the transverse crack development, tension stiffening, flexural curvature, strength of end anchorages, lapped joints, and rotation capacity of plastic hinges (Zhao et al. 2015).

Bond strength is a function of chemical adhesion, friction between the rebar surface and surrounding concrete, and interlocking between the concrete and ribs on rebar surface (Desnerck et al. 2015). The chemical bond between the concrete and steel surface is the result of chemical reactions that take place during the curing period and is the governing mechanism in the case of plain reinforcing bars. The initiation of cracks in

the interface between the rebar and concrete reduces the chemical bonding drastically. The mechanical mechanisms of stress transfer between the reinforcement and surrounding concrete, i.e. the friction and interlocking are the governing mechanisms afterwards, especially for deformed reinforcing bars (FIB 2010, Eligehausen et al. 1983, Taerwe and Stijn 2013, Rehm and Rolf 1979, Bazant and Sener 1988). Depth of concrete cover, concrete properties, bar diameter, quality of rebar surface in terms of corrosion status, confinement, casting position (top-bar effect), etc. affect the bond strength (Alonso et al. 1998, Cairns et al. 2007, Mangat and Elgarf 1999, Vidal et al. 2004, Khayat and shutter 2013).

There are four test methods that are most commonly used for determining the bond strength between reinforcement and concrete; (1) pull out specimens, (2) modified cantilever beam, or beam-end tests, (3) beam anchorage, and (4) splice specimens (ACI 408 2003). For the pull out specimens, the concrete surrounding the rebar will experience compressive stresses while the rebar is in tension. Moreover, formation of compressive struts between the support points for the concrete and the rebar surface will exert compressive stresses to the bar surface. These conditions may affect the results obtained through the pull out test method. The beam-end testing is considered as a simple test method that generally duplicates the stress state of the concrete members; the rebar and cover concrete are exposed to tensile stresses at the same time. Results obtained through testing beam-end tests are typically higher than those of the splice beams (ASTM A944 2015). The last two methods, i.e. the anchorage beam and the splice beams are providing the most realistic estimations of the bond strength between the reinforcing bars and concrete. However, these methods necessitate the fabrication and testing of large scale reinforced concrete beams (ACI 408 2003).

Several studies are devoted to investigating the bond between concrete and reinforcement in concrete mixtures produced with recycled concrete aggregate (RCA) using pull out and beam-end tests. However, limited data are available for full-scale beam tests. Xiao and Falkner (2007) used pull out samples to investigate bond strength of concrete made with 0, 50%, and 100% RCA replacement. Three different RCA sources

were incorporated to produce concrete mixtures with water-to-cementitious materials ratio (w/cm) of 0.43. The total cementitious materials content was 430 kg/m^3 (725 lb/yd^3) for investigated mixtures and both the plain and ribbed reinforcing bars were employed. The compressive strength of concrete was 44, 40, and 35 MPa (6380, 5800, and 5075 psi) for the Reference, 50% RCA, and 100% RCA mixtures, respectively. The authors reported similar load-slip relations for control samples and those cast with RCA. It was reported that with the increase in RCA content to 50% and 100%, the normalized bond strength reduced by 7% and increased by 5%, respectively for the samples fabricated with plain bars. However, in the case of the specimens cast with deformed bars, the normalized bond strength increased by 4% and 12% with 50% and 100% RCA replacement, respectively. Breccolotti and Materazzi (2013) investigated bond strength of concrete produced with 0, 50%, and 100% RCA. RCA was produced from crushing the test residuals of a concrete laboratory. Initial compressive strength of 30 to 33 MPa (4350 to 4785 psi) was reported for parent concrete specimens. Concrete mixtures were proportioned with w/cm of 0.45 and 0.50. The compressive strength of the samples ranged between 37 and 56 MPa (5365 and 8120 psi). Authors reported no significant difference between the normalized bond strength of the Reference concrete and the mixtures proportioned with 50% and 100% RCA. Butler et al. (2011) investigated bond strength of concrete produced with 100% RCA replacement. Two types of commercial RCA were used for producing concrete mixtures with target compressive strength of 30 and 50 MPa (4350 and 7250 psi). Beam-end specimens were fabricated to determine the bond strength between the concrete and reinforcing bars with 25 mm (#8) diameter. The authors reported that bond strength of the Reference samples proportioned without any RCA were between 9% and 19% higher than those of mixtures made with 100% RCA (Butler et al. 2011).

Limited studies are devoted to the bond strength of high-volume fly ash concrete (HVFAC). Arezoumandi et al.[20] studied the bond strength of HVFAC made with 70% of Class fly ash C replacement. The authors used pull out specimens fabricated with deformed bars of 13 and 19 mm (#4 and #6) diameter. Splice beams were also cast both

with and without confinement to determine the bond strength between concrete and deformed bars measuring 19 mm (# 6) in diameter. Concrete mixtures were proportioned with w/cm of 0.45. The 28-d compressive strength of the Reference and 70% fly ash mixtures were 39 and 31 MPa (5655 and 4500 psi), respectively. No significant difference was reported between the pull out results of the Reference samples and those cast with 70% fly ash. However, 17% and 20% increase in normalized bond strength was observed due to the incorporation of 70% fly ash for the unconfined and confined beams, respectively. Similar crack pattern, load-deflection, and load-slip behavior was reported for both the Reference and high-volume fly ash (HVFA) mixtures.

Zhao et al. (2015) studied the bond strength of concrete proportioned with Class F fly ash contents ranging from 0 to 70%. Concrete mixtures were produced with w/cm of 0.30, 0.34, and 0.41 to determine bond strength using pull out samples. Plain steel bars measuring 12 mm (#4) in diameter and deformed rebars of 12 and 20 mm (#4 and #6) diameter were used for casting 150 mm (6 in.) cubic pull out samples. Authors reported that the specimens fabricated with plain and deformed 12 mm (#4) bars cast with w/cm of 0.41 exhibited pull out failure. Samples cast with w/cm of 0.3 failed due to yielding of the reinforcement. However, in the case of the w/cm of 0.34, samples with fly ash contents of more than 50% exhibited pull out failure and those cast with less than 50% of fly ash failed due to yielding of the steel (Bazant and Sener 1988). The authors reported that all samples cast with deformed 20 mm (#6) bars failed due to splitting of concrete. Regarding the bond-slip behavior, it was reported that in the case of the plain bars of 12 mm (#4) diameter, increasing the fly ash content up to 70% reduced bond strength. It was observed that the residual bond strength decreased from 50% to 23% of the ultimate bond strength due to increase in fly ash content from 0 to 70%. In the case of the deformed 12 mm (#4) bars, variation in fly ash content had no significant effect on bond-slip behavior. The residual bond strength was also constant (about 25% of ultimate bond strength) (Zhao et al. 2015). Regarding the effect of fly ash content on normalized ultimate bond strength, no significant effect was detected due to increasing the replacement ratio from 0 to 30%. The increase in fly ash content from 30% to 60% resulted in up to 40% increase

in normalized ultimate bond strength followed by up to 17% decrease due to increasing the fly ash content from 60% to 70% (Zhao et al. 2015).

With the increase in use of sustainable concrete made with RCA and fly ash, more information regarding the structural behavior of such material is required for safe implementing. The research presented here contributes to the evaluation of bond strength of concrete containing HVFA and high volume of RCA. Most of the studies concerning the bond strength of RCA-made concrete are based on simple pull out specimens. There are limited studies that consider the fabrication of full-scale splice beams for determining the bond strength of reinforced concrete with RCA. Results obtained from testing full-scale splice beams prepared with 50% Class C fly ash and 50% RCA are compared to those of beams cast with no RCA or fly ash or only one of these two components. This study is part of an effort to investigate the performance of sustainable concrete materials produced with at least 50% replacement of industrial by-products and recycled aggregate for transportation infrastructures. Therefore, the limits of 50% RCA and 50% fly ash were employed. The results presented here should be of interest to owner agencies and engineers considering the design and use of sustainable concrete for structural applications. It should be noted that the research presented in this appendix was conducted in collaboration with Dr. Jeffery Volz and his research group at Missouri University of Science and Technology. More details on experimental program and test results are presented by Volz et al. (2014) and Arezoumandi et al. (2015).

EXPERIMENTAL PROCEDURE

Materials and Mixture Proportions.

The CC mixture was proportioned with ASTM Type I portland cement, crushed limestone aggregate with a maximum aggregate size of 25 mm (1 in.), and natural siliceous river-bed sand. The SC and FA50 mixtures incorporated Class C fly ash from a local source in Missouri. The RCA used for the production of the SC was obtained from crushing 30-to-40 year old concrete pavement mixed with 60-to-120 day old ready mix concrete residuals. The RCA employed for casting RCA50 beams was produced in the

laboratory. Figure 1 presents the particle size distribution of the coarse aggregate. Two different types of RCA were used to examine the effect, if any, of the type of recycled aggregate. Physical properties of the virgin aggregate and RCA are presented in Table 1. Table 2 summarizes the characteristics of the selected cement and fly ash. Grade 420 (Grade 60) longitudinal and shear reinforcement steel complying with ASTM A615 (2012) was used. The properties of the steel bars are summarized in Table 3.

Table 4 summarizes the concrete mixture proportions. The CC, SC, and RCA50 mixtures were proportioned with w/cm of 0.40. The FA50 concrete had w/cm of 0.35. In the case of the FA50 mixtures, gypsum and calcium hydroxide were added to enhance early age strength development (Bentz 2010). These two powder additives result in the formation of calcium-silicate-hydrate (C-S-H) to compensate for potential reductions in C-S-H concentration as a result of 50% fly ash replacement (Bentz 2010). Concrete was delivered by a local ready mix concrete supplier. Table 5 presents the properties of the investigated mixtures. The RCA50 and SC concrete mixtures have higher air content compared to the FA50 and CC mixtures. In addition to the incorporation of air-entraining admixture in these two mixtures, the higher air content in the fresh state, may be due to the higher water absorption (void structure) within the recycled concrete aggregate, given the residual mortar phase of RCA. Air content directly affects material properties, including compressive strength. The values of compressive strength were employed to normalize bond test values.

Specimen Design.

All specimens were cast with rectangular cross sections measuring 3,000 mm (120 in.) in length, 300 mm (12 in.) in width, and 460 mm (18 in.) in height, as presented in Figure 2. Three beams were considered for each mixture type. Two of these beams were cast as replications for each concrete mixture with splice located at bottom part of beam, and an additional beam was cast upside down to simulate the top-bar effect for all mixtures (except for the RCA50 concrete). A splice in longitudinal reinforcement was located in the middle of the span, within the area of the maximum flexural stress. Beams were designed with constant longitudinal reinforcement ratios of 0.62% to prevent failure

in flexure. Care was taken to ensure maintaining the reinforcement amount within the criteria introduced by ACI-318 (2014). Three reinforcing bars measuring 19 mm (#6) in diameter were employed for tensile reinforcement, as illustrated in Figure 2. Besides, U type stirrups were employed for shear reinforcement, as depicted in Figure 2. However, no stirrups were considered for the splice area to ensure unconfined splice conditions. Clear concrete cover of 38 mm (1.5 in.) was considered for the longitudinal reinforcement. A splice length of 360 mm (14.5 in.) was selected corresponding to 70% of the development length proposed by ACI-318 (2014) to ensure that failure in bond would occur. Equation 1 proposed by ACI-318 (2014) was incorporated for the calculation of the development length:

$$l_d = \frac{3}{40}\frac{f_y}{\sqrt{f_c'}}\frac{\Psi_t\Psi_e\Psi_s}{\left(\frac{c_b + k_{tr}}{d_b}\right)}d_b \quad (1)$$

Fabrication and Curing of Test Specimens.

Beam fabrication and testing was conducted at the High-Bay Structural Research Laboratory at the Civil, Architectural, and Environmental Engineering Department at Missouri University of Science and Technology. The concrete was delivered to the laboratory by ready mix trucks in batches measuring 0.75 m^3 (1.0 yd^3). The measured concrete slump was 115, 125, 165, and 110 mm (4.5, 5.0, 6.5, and 4.5 in.) for CC, FA50, RCA50, and SC mixtures, respectively. The beams were cast in two layers and properly consolidated using internal vibration. At the end of casting, wet burlap and plastic sheet were used to cover the specimens. Knowing that compressive strength may reduce in SC mixture, such a curing regime was extended for the beams cast with SC mixture to secure comparable strength gain with rest of the investigated mixtures. In the case of the CC, FA50 and RCA50 beams, the curing regime included four days of moist curing using wet burlap, followed by storage at 21 ± 3ºC (70 ± 5ºF) and relative humidity of 40% ± 10% up to the age of testing.

Test Setup and Procedure.

A load frame was designed for the four-point loading of the beams. The set up was equipped with a pair of 490 KN (110 kips) servo-hydraulic jacks. Displacement controlled mode at a rate of 0.50 mm/min (0.02 in./min) was selected for applying the load. Beams were supported with a combination of a roller-type and a pin support, at distance of 300 mm (12 in.) from the two ends. The combination of the two point loads and the two supports resulted in the desired four-point loading system. A linear variable differential transformer (LVDT) was employed for measuring mid-span deflection. Strain gauges were also incorporated to monitor strain in reinforcing bars at both ends of the splice region. The loading configuration and positions of the strain gauges are depicted in Figure 2. Formation of cracks was monitored, and cracks were marked at load increments of 22 KN (5 kips). Deformation and registered strain values were also monitored up to failure.

EXPERIMENTAL RESULTS AND DISCUSSION

The performance of the various beams is discussed in this section. The steel strain values measured by the strain gauges and the modulus of elasticity of the reinforcing bars were used to determine the stress values in longitudinal reinforcement. The bond strength was then calculated by dividing the stress to the surface area of the reinforcing bars in contact with surrounding concrete. Measured steel strain values are compared to predicted values derived from models developed by Popovic et al. (1973) and ACI-408 (2003). Ultimate bond strength results are compared to values that can be deducted from various analytical models as detailed in Equations 4 to 9. Experimental data are also compared to the database developed through the literature survey on bond strength of concrete made with RCA as well as the database proposed by ACI-408 (2003) for CC specimens.

General Observations.

In all cases, splitting failure of the concrete was the governing mechanism. Based on the data obtained from strain gauges, it was observed that none of the longitudinal

reinforcing bars reached yield stress at the time of failure. Crack patterns and distributions at the time of failure are shown in Figure 3. The first cracks occurred at the area of maximum flexural stress, i.e. maximum moment at the central part of the beam. Cracks were then propagated all over the area between the two loading points which led to splitting failure due to the increase in applied load. Figure 4 presents the measured mid-span deflection as a function of applied load. No significant variation in trends was observed as a result of incorporation of 50% RCA or 50% fly ash or the combination of the both, and all beams exhibited similar load-deflection pattern, and the main difference for various concrete types was the ultimate load at the time of failure.

Analysis of Stress in Reinforcing Steel.

The values of tensile stress at reinforcing bars are reported in Table 6. These values are derived from the average strain values recorded by the gauges installed at the start of each splice as illustrated in Figure 2. Results are compared to the analytical data deducted from models derived from moment-curvature method. The first model is suggested by Popovic et al. (1973) and the second one is the Hognestad stress-strain curve as suggested by ACI-408 (2003), as detailed in following equations.

$$f_2 = f_c' \frac{n(\varepsilon_2/\varepsilon_c')}{n-1+(\varepsilon_2/\varepsilon_c')^{nk}} \quad (2)$$

$$f_c = f_c' \left[\frac{2\varepsilon_c}{\varepsilon_0} - \left(\frac{\varepsilon_c}{\varepsilon_0}\right)^2\right] \quad (3)$$

It was observed that the model proposed by Popovic et al. (1973) underestimates the steel stress by 22%, 18%, 15%, and 8% for the CC, FA50, RCA50, and SC beams, respectively. Similar conclusion applies for beams tested for top-bar effect, where the model proposed by Popovic et al. (1973) underestimated the steel stress by 19%, 14%, and 6% for the CC, FA50, and SC beams, respectively. In other words, this model predicts the force transfer between concrete and steel conservatively. The ACI-408 (2003) recommended model (Hognestad stress-strain curve), is in good agreement with experimental data and slightly overestimated the steel stress of the CC and FA50 (around 2%). In the case of the RCA50 and SC specimens, this model underestimated the steel

stress by 15% and 5%, respectively. Similar trends were observed for the top-bar effect samples, where 5% and 3% overestimation was observed for the CC and FA50 beams respectively, followed by 4% underestimation for the SC ones.

Table 6 presents the ultimate longitudinal reinforcement stress values normalized to the square root and the fourth root of compressive strength. Several design codes, including the ACI 318 (2014), AASHTO LRFD (2010), AS-3600 (2009), Canadian Standard (CSA 2014), and standard of the Japan Society of Civil Engineers (JSCE 2007) consider the bond strengths as a function of the inversed square root of the concrete compressive strength. ACI-408[15], on the other hand, offers an example of the codes that consider bond strength as a function of inversed fourth root of f_c'.

Relative comparison of the average normalized steel stress values to those of the CC beams are presented in Table 6. Based on the data summarized in this table, it can be concluded that all investigated specimens (FA50, RCA50, and SC) exhibited higher average steel stress compared to the CC beams. For the square root normalized values, the average results were 10%, 17%, and 21% higher than CC for the case of FA50, SC, and RCA50 beams, respectively. Similar trends were observed for the top-bar effect results where the FA50 and SC beams exhibited 20% and 24% higher stress in reinforcing steel compared to the CC beam.

Based on the data obtained through fourth root normalization, the average normalized steel stress of the CC specimens was 21%, 15%, and 13% lower than those of the FA50, RCA50, and SC beams, respectively. The trend was the same for top-bar effect samples and the FA50 and SC beams exhibited 31% and 20% higher steel stress compared to the CC sample.

Influence of Casting Position.

The reduction of bond strength to horizontally anchored or overlapped bars located in the upper sections of structural elements as opposed to those located near the bottom is known as the top-bar effect. A high top-bar factor necessitates an increase in the anchorage length and further contributes to the congestion of some structural sections (Khayat and Shutter 2013). Top-bar effect occurs due to the accumulation of bleed water

underneath the reinforcing steel, and/or settlement of the concrete around the fixed bars. This can result in decrease in bond strength between the steel bar and surrounding concrete. In other words, under similar loading conditions, the stress transfer from concrete to reinforcing steel will be inversely affected by this phenomenon, and the registered stress is expected to be less than the normal conditions.

Variations in stress in reinforcing bars in the case of invert cast SC and FA50 beams in comparison to normal cast ones were limited to 1%. The top-bar effect values were 1.07, 0.99, and 1.01 for the CC, RCA50, and SC mixtures, respectively. This indicates that the bond strength of the top cast and bottom cast beams are similar. No bleeding was observed for the cast concrete. This could be attributed to proper casting and avoiding excessive vibration, incorporation of fly ash, use of RCA with high absorption rate, and use of air entraining admixture.

Comparison of Experimental Ultimate Bond Strength with Code Predictions.

According to ACI-408 (2003) recommendation on bond and development length, precise theoretical models for estimating the bond strength of reinforcing steel are not fully developed yet. However, effort is devoted to propose simplified models extracted from experimental data. Several analytical models are proposed in the literature and design codes to estimate bond strength. Kemp and Wilhelm (1979) proposed Equation 4 to determine the ultimate bond strength of reinforcing steel in concrete:

$$\tau_u = 0.083 \times (6.57 + 2.9\, c / d_b)\sqrt{f_c'} + 0.191\, A_s f_y / s_b \quad (4)$$

ACI-408 (2003) document proposes several descriptive models to estimate the bond strength, which are elaborated here. Equation 5 proposed by Orangun et al. (1975) provides a model for determining the ultimate bond strength as a function of geometry and compressive strength of concrete for unconfined conditions where no stirrups are provided in the overlap bond region of beams. Darwin et al. (1992) incorporated the data obtained from a large database, including 133 unconfined splice specimens as well as 166 confined ones and observed that the bond strength has a stronger relationship with the fourth root of f'_c rather than the typically recommended square root of f'_c. Based on the observations, Darwin et al.[31] recommended Equation 6 for estimating bond strength as a

function of material properties and geometry of specimens. Zuo and Darwin (1998, 2000) proposed Equation 7 for estimating bond strength of unconfined reinforcing bars which was derived from regression analysis of database composed of 171 test points. Esfahani and Rangan (1998a, 1998b) proposed Equation 8 for determining bond strength of bars that are not confined by stirrups for the case of concrete mixtures with compressive strength of no more than 50 MPa (7250 psi). ACI-408 (2003) also proposed an equation based on the database gathered by the committee (Equation 9) that is based on some slight modifications to Equation 7 proposed by Zuo and Darwin (1998, 2000). Experimental results obtained through the present study for sustainable concrete materials are compared to the models proposed through Equations 4 to 9.

$$\frac{u_c}{\sqrt{f_c'}} = 0.101 + 0.268\,\frac{c_{min}}{d_b} + 4.4\,\frac{d_b}{l_d} \tag{5}$$

$$\frac{T_c}{f_c'^{0.25}} = \frac{A_b f_s}{f_c'^{0.25}} = [1.5 l_d (c_{min} + 0.5 d_b) + 51 A_b]\left(0.1\,\frac{c_{max}}{c_{min}} + 0.90\right) \tag{6}$$

$$\frac{T_c}{f_c'^{0.25}} = \frac{A_b f_s}{f_c'^{0.25}} = [1.43 l_d (c_{min} + 0.5 d_b) + 56.2 A_b]\left(0.1\,\frac{c_{max}}{c_{min}} + 0.90\right) \tag{7}$$

$$\frac{T_c}{\sqrt{f_c'}} = \frac{A_b f_s}{\sqrt{f_c'}} = 2.7\pi l_d \frac{(c_{min} + 0.5 d_b)\left(1 + \frac{1}{M}\right)}{\left(\frac{c_{min}}{d_b} + 3.6\right)\left(1.85 + 0.024\sqrt{M}\right)}\left(0.12\,\frac{c_{med}}{c_{min}} + 0.88\right) \tag{8}$$

$$\frac{T_c}{f_c'^{0.25}} = \frac{A_b f_s}{f_c'^{0.25}} = [1.43 l_d (c_{min} + 0.5 d_b) + 57.4 A_b]\left(0.1\,\frac{c_{max}}{c_{min}} + 0.90\right) \tag{9}$$

Figure 5 compares the obtained code/experiment values. The model developed by Esfahani and Rangan (1998a, 1998b) overestimated bond strength of CC, FA50, RCA50, and SC beams by 81%, 49%, 59%, and 60%, respectively. The model proposed by Kemp and Wilhelm (1979) also overestimated the average bond strength of the investigated mixtures by 36%, 24%, 12%, and 15% for the CC, FA50, RCA50, and SC beams, respectively. The model proposed by Orangun et al. (1975) slightly overestimated the bond strength of the CC (by 3%). The rest of the predictions made by this model were

conservative, and the bond strength of the FA50, RCA50, and SC beams were underestimated by 6%, 15%, and 13%, respectively.

Models proposed by Darwin et al. (1992), Zuo and Darwin (1998, 2000), and ACI-408 (2003) were in good agreement with experimental data for the CC beams and estimated bond strength of the CC beams conservatively (about 5% difference). Predictions made by these models were also similar for the rest of beams. On the average, these models underestimated the bond strength of the FA50, RCA50, and SC beams by 21%, 17%, and 16%, respectively.

As a summary, the models developed by Orangun et al. (1975), Darwin et al. (1992), Zuo and Darwin (1998, 2000), and ACI-408 (2003) conservatively predicted the ultimate bond strength of the studied mixtures. However, the rest of the investigated models, including the one proposed by Esfahani and Rangan (1998a, 1998b) and the model proposed by Kemp and Wilhem[29] were overestimating the ultimate bond strength of the beams up to 81%.

Comparison of Experimental Results to Database.

ACI-408 database of CC specimens.

ACI-408 (2003) proposed a database illustrated in Figure 6 for splice beam specimens cast with CC. The database presents stress in longitudinal steel as a function of f'_c. Statistical analysis software (SAS 9.3) was employed to produce the 95% confidence interval of the points presented in database as well as to fit a non-linear regression curve. The upper and lower borders of the confidence interval represent the area in which it is expected with 95% certainty to observe the value of the predicted parameter of interest. It was observed that the data obtained through experiments follow the general trends of the database presented as an average trend line in Figure 6. However, only the FA50 data fell within the 95% confidence interval and data obtained for CC, RCA50, and SC beams were below the limits of the confidence interval.

Database of RCA specimens.

Literature survey was conducted to determine the effect of RCA content on bond strength (Xiao and Falkner 2007, Breccolotti and Materazzi 2013, Butler et al. 2011,

Ajdukiewicz and Kliszczewics 2002, Kim and Yun 2013, Volz et al. 2014, prince and Singh 2014, Steele 2014, Fathifazl et al. 2012). Data obtained from testing pull out specimens, splice beams, and beam-end specimens were analyzed. All investigated mixtures were proportioned with 100% Portland cement. Maximum size of aggregate ranged between 13 and 24 mm (0.5 to 1.0 in.). Rebar diameter ranged from 8 to 30 mm (#3 to #9) with yield stress values from 383 to 516 MPa (55.5 to 74.8 ksi). The RCA replacement ranged from 0 to 100% for the investigated data. Values of compressive strength ranged from 21 to 57 MPa (3045 to 8270 psi) for the investigated mixtures.

Initial observations revealed that the pull out specimens with different RCA replacement levels exhibited almost identical load–slip behavior to that of specimens cast without any RCA. No significant trend was observed for variations in bond strength as a function of RCA content in pull out data. However, most of the data obtained from beam-end tests revealed decrease in bond strength. Up to 36% reduction in bond strength of beam-end specimens was reported for concrete made with up to 100% RCA replacement.

Given the fact that most of the studied references used pull out and beam-end techniques to study bond strength, further investigating was conducted to determine the effect of RCA content on bond strength of the pull out samples. The relative RCA effect was defined as described in Equation 10:

$$R_{e-RCA} = \frac{Normalized\ bond\ strength\ of\ RCA\ mixture}{Corresponding\ value\ for\ CC\ sample} \quad (10)$$

Results obtained from Equation 10 were then plotted as a function of the RCA replacement ratio. Figure 7 illustrates the obtained data. Moreover, Table 7 was developed to summarize the minimum and maximum observed ratios for $R_{e\text{-}RCA}$ values, as well as the average values, coefficient of variations, and percentages of the data with $R_{e\text{-}RCA}$ values of higher than 1.0. Five categories of RCA replacement were investigated in the case of the pull out specimens; up to 30% replacement; 50% replacement; 60% replacement; 75% replacement; and 100% replacement. As summarized in Table 7, the $R_{e\text{-}RCA}$ values were ranging from 0.65 to 1.71 for pull out data. However, the average $R_{e\text{-}RCA}$ values obtained for different categories of RCA content were higher than 1.0 and

ranged from 1.07 to 1.19. The coefficient of variation (COV) of the $R_{e\text{-}RCA}$ values varied between 11.7% and 24%, and the majority of the data points had $R_{e\text{-}RCA}$ values higher than 1.0. Results obtained from Figure 7 approved the initial observations and suggest that there is not enough evidence to prove that the RCA content can necessarily result in decrease in bond strength obtained through pull out testing. However, in the case of the beam-end test results, investigated data points exhibited reduction in bond strength due to use of RCA. This rate of reduction in bond strength ranged from 0 to 36% at 100% replacement, with an average $R_{e\text{-}RCA}$ value of 0.86 and COV of 10.1%. Data obtained through the experiments were also compared to the database presented in Figure 7. The average value obtained for RCA50, SC, and top-bar effect of SC samples were within the central portion of the database with $R_{e\text{-}RCA}$ values ranging from 1.08 to 1.16.

REMARKS

This paper compares the bond strength of concrete proportioned with 50% Class C fly ash and 50% RCA (SC) with that of either conventional concrete, concrete made with 50% fly ash, and concrete made with 50% RCA. Data obtained through testing of 11 full-scale beams are analyzed. The beams had longitudinal reinforcement ratio of 0.62%. The compressive strength of concrete ranged from 25 to 44 MPa (3625 to 6380 psi) at age of testing. Bond strength results were compared in both qualitative and quantitative manners. Based on the results presented in this paper, the following conclusions are warranted:

- All beams exhibited similar load-deflection trend and crack patterns and propagation.
- The FA50, RCA50, and SC beams had higher average normalized longitudinal reinforcement steel stress (between 10% and 21%) compared with the CC beams.
- The two mixes containing RCA had comparable normalized bond strengths, indicating that the effect of the two different RCA sources is reflected in the compressive strength, and thus bond strength of the material.

- The model proposed by Popovic et al. (1973) underestimates the steel stress by 22%, 18%, 15%, and 8% for the CC, FA50, RCA50, and SC beams, respectively. ACI-408 (2003) model (Hognestad stress-strain curve) slightly overestimated the steel stress of the CC and FA50 (around 2%). In the case of the RCA50 and SC specimens, this model underestimated the steel stress by 15% and 5%, respectively.
- The analytical models, proposed by Orangun et al. (1975), Darwin et al. (1992), Zuo and Darwin (1998, 2000), and ACI-408 (2003) are shown to provide a conservative prediction of the ultimate bond strength of the investigated concrete made with high contents of RCA and fly ash. The use of these models is recommended for estimating bond strength of reinforced concrete cast with up to 50% RCA and 50% fly ash replacement.
- Experimental data were compared to two sets of database for CC and concrete made with RCA. The experimental data (except for the FA50 beams) fell out of the 95% confidence interval of the CC database. Due to the scatter in data of the RCA specimens, it was difficult to make conclusions on general trends. However, the experimental results fell within the central portion of the RCA database.
- Potential effect of casting position on bond strength was investigated. No sign of top-bar effect was observed for the FA50 and SC beams. However, 7% reduction in stress in flexural reinforcement of the CC beams was observed.
- Given the other design criteria are met, the use of up to 50% coarse RCA and up to 50% Class C fly ash or a combination of them can be recommended for the construction of sustainable concrete structures.
- Further investigation is recommended to establish and quantify the potential correlations between the properties of RCA from various quality grades with performance of full scale structural elements.

NOTATION

A_s = gross area of cross section of reinforcing steel bars (mm^2)

A_b = area of bar being developed or spliced (mm^2)

c = concrete cover thickness (mm)

c_b = the smaller of the distance from center of a bar to nearest concrete surface and one-half the center-to-center spacing of bars being developed (mm)

c_{max} = maximum (c_b , c_s) (mm)

c_{med} = median (c_{so}, c_b, $c_{si}+d_b/2$) (mm)

c_{min} = smaller of minimum concrete cover or ½ of the clear spacing between bars (mm)

c_s = minimum (c_{so}, $c_{si}+6.35$) (mm)

c_{si} = ½ of bar clear spacing (mm)

c_{so} = side concrete cover for reinforcing bar (mm)

d_b = nominal bar diameter (mm)

d_a = maximum aggregate size (mm)

d_{max} = maximum aggregate size (mm)

E_s = modulus of elasticity of reinforcing steel (MPa)

k = factor for loss in post peak ductility for high strength concrete

K_{tr} = the transverse reinforcement index

M = constant used in expressions for the bond strength of bars not confined by transverse reinforcement

n = curve fit parameter

l_d = development length of reinforcing bar (mm)

f_c' = specified compressive strength of concrete for use in design (MPa), peak stress from cylinder test

f_y = stress in concrete (MPa)

f_y = yield stress of reinforcing bar (MPa)

f_s = stress in reinforcing bar (MPa)

f_t = tensile strength of concrete (MPa)

S_b = spacing of traverse steel bars (mm)

T_c = concrete contribution to total bond force

u_c = average bond strength at failure of a bar not confined by transverse reinforcement

w/c = water to cement ratio

w/cm = water to cementitious materials ratio

ε_0 = strain at concrete at maximum stress

ε_2 = strain at concrete

ε_c = strain at concrete

ε_c' = strain at peak cylinder stress

λ = the lightweight concrete modification factor

ρ = longitudinal reinforcement ratio

ρ_{sv} = volumetric ratio of transverse reinforcement

τ_u = the ultimate bond strength (MPa)

Ψ_e = the reinforcement coating modification factor

Ψ_s = the reinforcement size modification factor

Ψ_t = the reinforcement location modification factor

REFERENCES

ACI 408 Committee. “Bond and development of straight reinforcing bars in tension (ACI 408R-03),” American Concrete Institute, Detroit, Michigan, US, 2003.

ACI Committee 318, “Building code requirements for structural concrete (ACI 318-11),” American Concrete Institute, 2011.

Ajdukiewicz, A., and Kliszczewicz, A., “Influence of recycled aggregates on mechanical properties of HS/HPC,” Cement and Concrete Composites, Vol. 24, No. 2, 2002, pp. 269-279.

Alonso, C., Andrade, C., Rodriguez, J., & Diez, J. M., "Factors controlling cracking of concrete affected by reinforcement corrosion," Materials and structures, Vol. 31, No. 7, 1998, pp. 435-441.

American Association of State and Highway Transportation Officials, "AASHTO LRFD bridge design specifications," 4th Ed., Washington, D.C., USA, 2010.

Arezoumandi, M., Looney, T. J., and Volz. J. S., "Effect of fly ash replacement level on the bond strength of reinforcing steel in concrete beams," Journal of Cleaner Production, Vol. 87, 2015, pp. 745-751.

AS 3600, "Concrete Structures," Standards Australia, Sydney, Australia, 2009, pp. 105-109.

ASTM A615/A615M, "Standard Specification for deformed and plain carbon-steel bars for concrete reinforcement," ASTM, West Conshohocken, PA, 2012, pp. 1-6.

ASTM A944, "Standard test method for comparing bond strength of steel reinforcing bars to concrete using beam-end specimens," ASTM, West Conshohocken, PA, 2015, pp. 1-4.

Bazant, Z. P. and Sener, S., "Size effects in pull-out tests," ACI Materials Journal, Vol. 85, No. 5, 1988, pp. 47–351

Bentz, Dale P., "Powder additions to mitigate retardation in high-volume fly ash mixtures," ACI Materials Journal, Vol. 107, No. 5, 2010, pp. 508-514.

Breccolotti, M., and Materazzi, A. L., "Structural reliability of bonding between steel rebars and recycled aggregate concrete," Construction and building materials, Vol. 47, 2013, pp. 927-934.

Butler, L., West, J. S., and Tighe, S. L., "The effect of recycled concrete aggregate properties on the bond strength between RCA concrete and steel reinforcement," Cement and Concrete Research, Vol. 41, No. 10, 2011, pp. 1037-1049.

Cairns, J., Du, Y., & Law, D., "Influence of corrosion on the friction characteristics of the steel/concrete interface," Construction and Building Materials, Issue 21, No. 1, 2007, pp. 190-197.

CSA -A23.3-14, "Design of concrete structures," Rexdale, Ontario, Canada, 2014.

Darwin, D., Steven L. M., Emmanuel K. I., and Steven P. S., “Development length criteria: bars not confined by transverse reinforcement,” ACI Structural Journal, Vol. 89, No. 6, 1992, pp. 709-736.

Desnerck, Pieter, Janet M. Lees, and Chris T. Morley. “Bond behaviour of reinforcing bars in cracked concrete,” Construction and Building Materials, Vol. 94, 2015, pp. 126-136.

Eligehausen R, Bertero V, Popov EP., “Local bond-slip relationships of deformed bars under generalized excitations,” Report No UCB/EERC 83–19, Earthquake Engineering Research center, University of California, Berkeley, CA, 1983.

Esfahani, M. R., and Rangan, B. V., “Bond between normal strength and high-strength concrete (HSC) and reinforcing bars in splices in beams,” ACI Structural Journal, Vol. 95, No. 3, 1998b, pp. 272-279.

Esfahani, M. R., and Rangan, B. V., “Local bond strength of reinforcing bars in normal strength and high-strength concrete (HSC),” ACI Structural Journal, Vol. 95, No. 2, 1998a, pp. 96-105.

Fathifazl G, Razaqpur AG, Isgor OB, Abbas A, Fournier B, Foo S., “Bond performance of deformed steel bars in concrete produced with coarse recycled concrete aggregate,” Canadian Journal of Civil Engineering, 2012, Vol.39, No. 2, pp. 128-39.

Fib Bulletin 10, “Bond of reinforcement in concrete state of the art,” Lausanne, 2010, 434

Japan Society of Civil Engineers, “Standard specification for concrete structure,” JSCE No. 15, Tokyo, Japan, 2007, pp. 154-159.

Kemp, E. L., and W. J. Wilhelm. “Investigation of the parameters influencing bond cracking,” ACI Journal Proceedings, Vol. 76, No. 1, 1979, pp. 47-71

Khayat, K., and De Schutter., G., “Mechanical properties of self-compacting concrete", State of the Art Report, RILEM Technical Committee, 2013.

Kim, S. W., & Yun, H. D., “Influence of recycled coarse aggregates on the bond behavior of deformed bars in concrete,” Engineering Structures, Vol. 48, 2013, pp. 133-143.

Mangat P. S., Elgarf M. S., “Bond characteristics of corrding reinforcement in concrete beams,” Materials and structures, 1999, Vol. 32, No. 2, pp. 89-97.

Orangun, C. O., Jirsa, J. O., and Breen, J. E., “The strength of anchored bars: a reevaluation of test data on development length and splices,” Research Report No. 154-3F, Center for Highway Research, University of Texas at Austin, 1975, pp. 1-90

Popovics, S., “A numerical approach to the complete stress-strain curve of concrete”, Cement and Concrete Research, Vol. 3, No. 5, 1973, pp. 483-599.

Prince, M. J. R., & Singh, B., “Bond behaviour between recycled aggregate concrete and deformed steel bars,” Materials and Structures, Vol. 47, No. 3, 2014, pp. 503-516.

Rehm, G., and Rolf E., “Bond of ribbed bars under high cycle repeated loads.” ACI Journal Proceedings, Vol. 76, No. 2, 1979.

Shen, W., Cao, L., Li, Q., Zhang, W., Wang, G., & Li, C. (2015). “Quantifying CO2 emissions from China’s cement industry,” Renewable and Sustainable Energy Reviews, 50, pp. 1004-1012.

Steele, A. R., “Bond performance of recycled aggregate concrete,” Master thesis, Missouri University of Science and Technology, Rolla, MO, USA, 2014.

Taerwe, L., and Stijn M., “Fib model code for concrete structures 2010,” Ernst & Sohn, Wiley, 2013.

Vidal T, Castel A, Francois R., “Analyzing crack width to predict corrosion in reinforced concrete,” Cement and Concrete Research. 2004, Vol. 34, No. 1, pp. 165-74.

Volz, J. S., Khayat K. H., Arezoumandi, M., Drury, J., Sadati, S., Smith, A., and Steele, A., “Recycled concrete aggregate (RCA) for infrastructure elements,” National University Transportation Center (NUTC), Missouri University of Science and Technology, Rolla, MO, USA. NUTC R312, 2014.

World Business Council for Sustainable Development (WBCSD) Report (2012), “Recycling concrete,” http://www.wbcsdcement.org/index.php/key-issues/sustainability-with-concrete/54, (accessed date: August 21, 2014).

Xiao, J. and Falkner, H., “Bond behaviour between recycled aggregate concrete and steel rebars,” Construction and Building Materials, Vol.21, No. 2, 2007, pp. 395-401.

Zhao, J., Gaochuang C., and Junmin Y., “Bond-slip behavior and embedment length of reinforcement in high volume fly ash concrete,” Materials and Structures, 2015, pp. 1-18.

Zuo, J., and Darwin, D., “Bond strength of high relative rib area reinforcing bars,” SM Report No. 46, University of Kansas, Center for Research, Lawrence, Kansas, 1998, 350 pp.

Zuo, J., and David D., “Splice strength of conventional and high relative rib area bars in normal and high-strength concrete,” ACI Structural Journal, Vol. 97, No. 4, 2000, pp. 630-641.

Table 1 Aggregate properties

	Coarse aggregate	Coarse aggregate**	Sand	RCA*	RCA**
Bulk specific gravity	2.52	2.72	2.63	2.23	2.35
Absorption (%)	3.20	0.98	0.4	6.30	4.56
Los Angeles abrasion	40	43	-	43	41

*Beams with 50% RCA and 50% fly ash (SC beams)

**Beams with 50% RCA (RCA50 beams)

Table 2 Chemical composition and physical properties of cement and fly ash

Property	Cement	Fly ash
SiO_2, %	21.98	33.46
Al_2O_3, %	4.35	19.53
Fe_2O_3, %	3.42	6.28
CaO, %	63.97	26.28
MgO, %	1.87	5.54
SO_3, %	2.73	2.40
Na_2O eq., %	0.52	1.43
Blaine surface area, m^2/kg	410	490
Specific gravity	3.15	2.73
LOI, %	0.6	0.34

Table 3 Properties of the incorporated longitudinal steel bars (1MPa = 145.04 psi)

	Modulus of elasticity (MPa)	Yield stress (MPa)	Elongation (%)
CC	206,250	580	13.7
FA50	206,250	580	13.7
RCA50	192,975	516	13.3
SC	192,975	516	13.3

Table 4 Concrete mixture proportions (1 kg/m3 = 1.686 lb/yd3)

Mixture	Water (kg/m^3)	Cement (kg/m^3)	w/cm	Class C fly ash (kg/m^3)	Gypsum (kg/m^3)	Calcium hydroxide (kg/m^3)	Coarse aggregate (kg/m^3)	Recycled coarse aggregate (kg/m^3)	Sand (kg/m^3)	HRWR (l/m^3)	AEA (l/m^3)
CC	134	337	0.40	-	-	-	1103	-	735	0.66	0.20
FA50	160	210	0.35	210	10	22	1040	-	705	-	-
RCA50	127	317	0.40	-	-	-	581	502	743	2.10	0.77
SC	134	169	0.40	169	-	-	529	468	735	0.44	0.15

Table 5 Fresh and hardened concrete properties (1 MPa = 145.04 psi, 1 kg/m^3 = 1.686 lb/yd^3)

Property		CC	FA50	RCA50	SC
Slump (mm)		115	125	165	110
Air content (%)		1.5	2.5	8.0	5.0
Unit weight (kg/m3)		2490	2475	2239	2415
Compressive strength (MPa)	28 days	30.9	28.3	24.5	26.6
	56 days	-	44.1	-	34.3
Splitting tensile strength (MPa)	28 days	3.0	-	2.4	2.1
	56 days	-	4.0	-	2.8
Flexural strength (MPa)	28 days	2.9	-	2.5	3.1
	56 days	-	3.9	-	3.5

Table 6 Longitudinal steel reinforcement stress (MPa) (1 MPa = 145.04 psi)

Section		f_s	$(\frac{f_{s(test)}}{f_{s(M-\phi)}})^{I}_{ave}$	$(\frac{f_{s(test)}}{f_{s(M-\phi)}})^{II}_{ave}$	$\frac{f_s}{\sqrt{\frac{f'_{c(test)}}{f'_{c(design)}}}}$	$\frac{f_s}{\sqrt[4]{\frac{f'_{c(test)}}{f'_{c(design)}}}}$	$(\frac{f_{s(...)}}{f_{s(CC)}})^{III}$	$(\frac{f_{s(...)}}{f_{s(CC)}})^{IV}$
CC	1	376	1.22	0.98	358	367		
	2	335			319	327		
	Top	332	1.19	0.95	316	324		
FA50	1	468	1.18	0.99	373	418	1.10	1.21
	2	467			372	417		
	Top	475	1.14	0.97	378	424	1.20	1.31
RCA50	1	390	1.14	1.15	416	404	1.21	1.15
	2	380			405	393		
SC	1	397	1.08	1.05	405	401	1.17	1.13
	2	381			390	385		
	Top	385	1.06	1.04	393	390	1.24	1.20

[I]: Popovic, Thorenfeldt, and Collins stress-strain curve
[II]: Hognestad stress-strain curve (ACI 408R-03[10] recommended method)
[III]: based on square root normalization
[IV]: based on fourth root normalization

Table 7 Summary of effect of RCA content on bond properties of the developed RCA database

		R_{s-RCA}				
Test	RCA content	Min.	Max.	Average	COV (%)	Values higher than 1.0 (%)
Pull Out	Up to 30%	0.65	1.71	1.07	24	74
	50%	0.85	1.31	1.07	11.7	80
	60%	0.82	1.59	1.19	19.8	85
	75%	0.86	1.24	1.09	16.5	75
	100%	0.68	1.71	1.09	20	69
Beam-end	100%	0.64	1.0	0.86	10.1	-

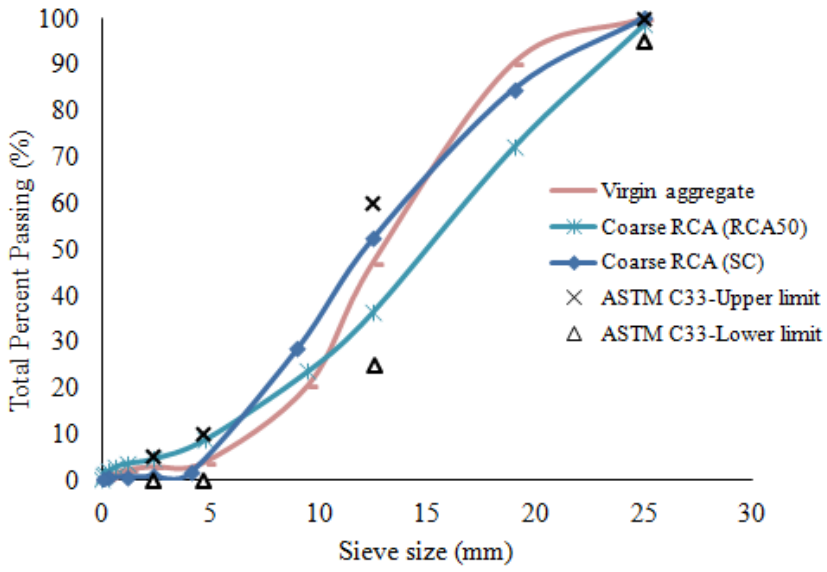

Figure 1 Particle size distribution of the coarse aggregate (1 mm=0.0394 in.)

a) Test set up and load pattern

b) Strain gauges

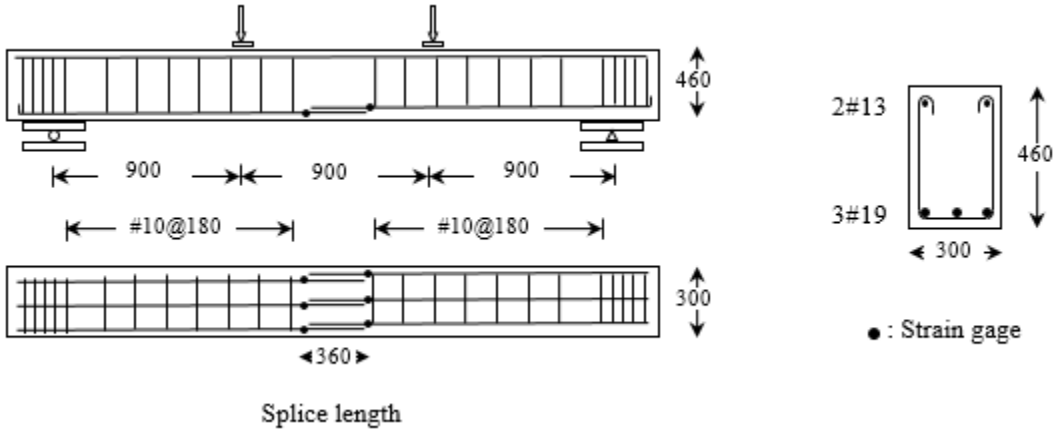

c) Splice specimen details, profile view (left, top), plan view (left, bottom), and cross section (right), all dimensions in mm

Figure 2 Details of the test set up and specimens (1 mm=0.0394 in.)

CC FA50 RCA50 SC

Bottom bar

CC FA50 SC

Top-bar

Figure 3 Crack pattern of the beams at bond failure

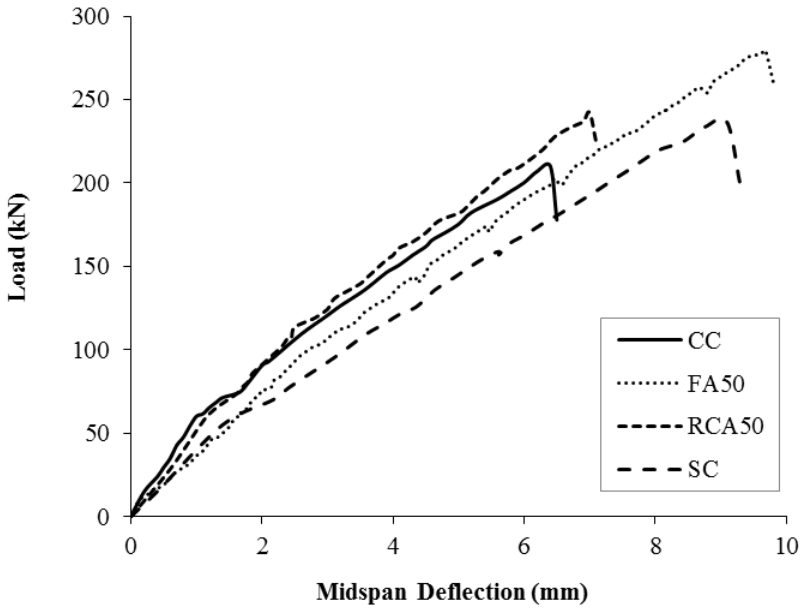

Figure 4 Load-deflection of the specimens (1 kN = 0.225 lbf, 1 mm=0.0394 in.)

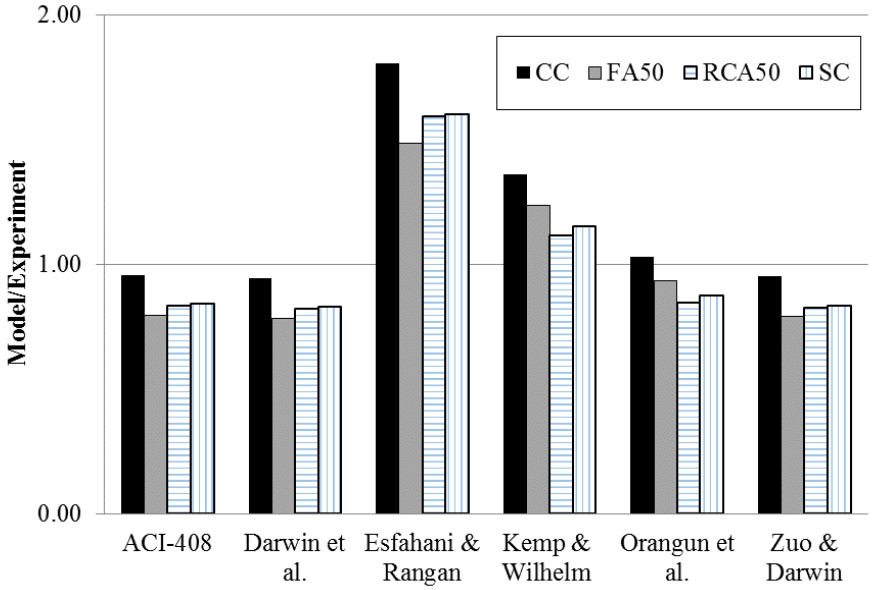

Figure 5 Comparison of ultimate bond strength results with analytical models

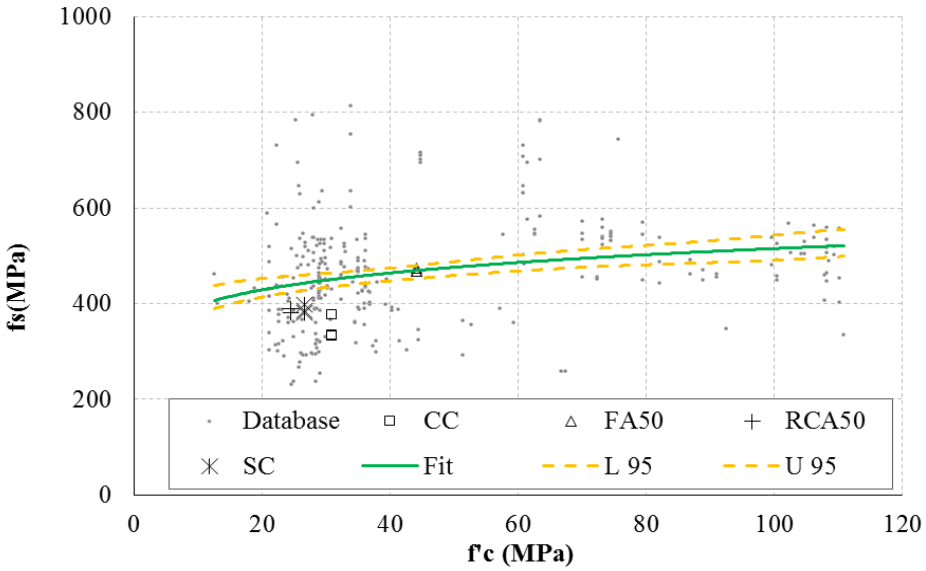

Figure 6 Longitudinal steel reinforcement stress versus compressive strength of concrete (database of ACI 408-0310 and test results of this study) (1 MPa = 145.04 psi)

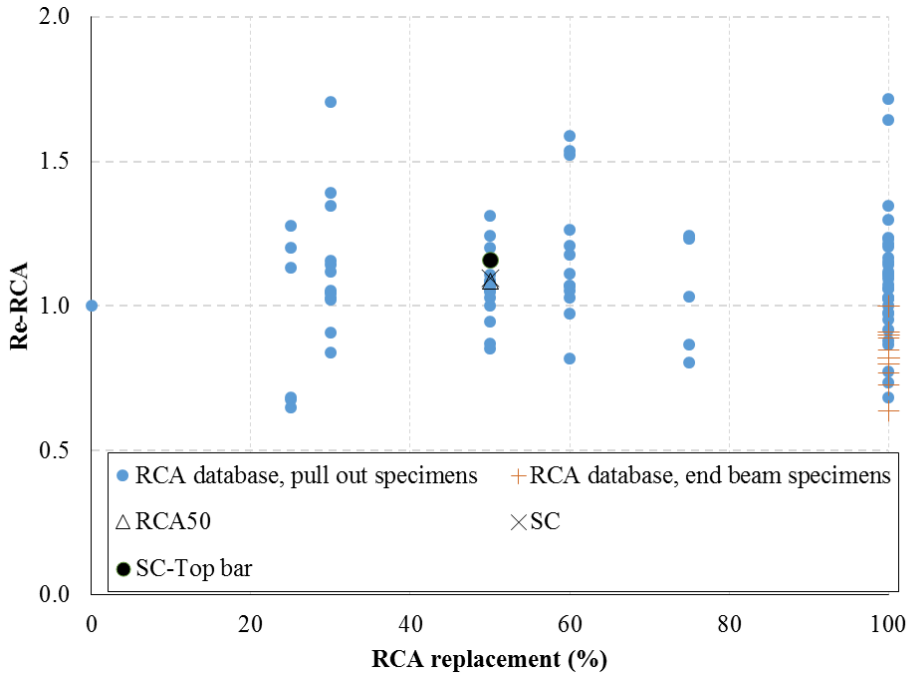

Figure 7 $R_{e\text{-}RCA}$ as a function of RCA replacement level (%)

BIBLIOGRAPHY

AASHTO MP16 (2015). Standard specification for reclaimed concrete aggregate for use as coarse aggregate in hydraulic cement concrete.

AASHTO T336-11, (2011). Coefficient of Thermal Expansion of Hydraulic Cement Concrete.

Abbas, A., Fathifazl, G., Fournier, B., Isgor, O. B., Zavadil, R., Razaqpur, A. G., & Foo, S. (2009). Quantification of the residual mortar content in recycled concrete aggregates by image analysis. Materials characterization, Vol. 60, Issue 7, 716-728.

Abbas, A., Fathifazl, G., Isgor, O. B., Razaqpur, A. G., Fournier, B., & Foo, S. (2007). Proposed method for determining the residual mortar content of recycled concrete aggregates. Journal of ASTM International, 5(1), 1-12.

Abbasi, A. F., Ahmad, M., & Wasin, M. (1987). Optimization of Concrete Mix Proportioning Using Reduced Factorial Experimental Technique. ACI Materials Journal, 84(1).

ACI Committee 318 (2014). Building code requirements for structural concrete (ACI 318-14), American Concrete Institute.

ACI Committee 555, (2001). Removal and Reuse of Hardened Concrete-ACI 555R-01. ACI Committee, Detroit.

ACPA (2009), “Recycling concrete pavement”, American concrete pavement association, Skokie, Illinois.

Adams, M. P., Fu, T., Cabrera, A. G., Morales, M., Ideker, J. H., Isgor, O. B. (2016). Cracking susceptibility of concrete made with coarse recycled concrete aggregates. Construction and Building Materials, 102, 802-810.

Afshinnia, K., & Rangaraju, P. R. (2015). Influence of fineness of ground recycled glass on mitigation of alkali–silica reaction in mortars. Construction and Building Materials, 81, 257-267.

Ahari, R. S., Erdem, T. K., & Ramyar, K. (2015). Thixotropy and structural breakdown properties of self-consolidating concrete containing various supplementary cementitious materials. Cement and Concrete Composites, 59, 26-37.

Ajdukiewicz. A., and Kliszczewicz. A. (2002), Influence of recycled aggregates on mechanical properties of HS/HPC, Cement and Concrete Composites, Volume 24, Issue 2, 269–279.

Akbarnezhad, A., Ong, K. C. G., Zhang, M. H., Tam, C. T., & Foo, T. W. J. (2011). Microwave-assisted beneficiation of recycled concrete aggregates. Construction and Building Materials, 25(8), 3469-3479.

Ali, M. B., Saidur, R., & Hossain, M. S. (2011). A review on emission analysis in cement industries. Renewable and Sustainable Energy Reviews, 15(5), 2252-2261.

American Concrete Pavement Association (ACPA) (2008), Recycled concrete in subbases: a sustainable choice, technical series, TS204.9P, ACPA, Washington, D.C.

Anderson, M. J., & Whitcomb, P. J. (1998). Find the most favorable formulations. Chemical Engineering Progress, 94(4), 63-67.

Andreu, G., & Miren, E. (2014). Experimental analysis of properties of high performance recycled aggregate concrete. Construction and Building Materials, 52, 227-235.

Arezoumandi, M., Drury, J., Volz, J. S., & Khayat, K. H. (2015). Effect of Recycled Concrete Aggregate Replacement Level on Shear Strength of Reinforced Concrete Beams. ACI Materials Journal, 112(4), 559-568.

ASTM C109, (2016). Standard Test Method for Compressive Strength of Hydraulic Cement Mortars (Using 2-in. or [50-mm] Cube Specimens).

ASTM C1202, (2012). Standard Test Method for Electrical Indication of Concrete's Ability to Resist Chloride Ion Penetration.

ASTM C143, (2015). Standard test method for slump of hydraulic-cement concrete.

ASTM C1581, (2016). Standard Test Method for Determining Age at Cracking and Induced Tensile Stress Characteristics of Mortar and Concrete under Restrained Shrinkage.

ASTM C1585, (2013). Standard Test Method for Measurement of Rate of Absorption of Water by Hydraulic-Cement Concretes.

ASTM C1760, (2012). Standard Test Method for Bulk Electrical Conductivity of Hardened Concrete.

ASTM C231, (2014). Standard test method for air content of freshly mixed concrete by the pressure method.

ASTM C39, (2001). Standard test method for compressive strength of cylindrical concrete specimens.

ASTM C457, (2016). Standard test method for microscopical determination of parameters of the air-void system in hardened concrete.

ASTM C469, (2010). Standard test method for static modulus of elasticity and Poisson’s ratio of concrete in compression.

ASTM C666, (2015). Standard test method for resistance of concrete to rapid freezing and thawing.

ASTM C672, (2012). Standard test method for scaling resistance of concrete surfaces exposed to deicing chemicals.

ASTM C779, (2012). Standard Test Method for Abrasion Resistance of Horizontal Concrete Surfaces.

ASTM C78, (2010). Standard Test Method for Flexural Strength of Concrete (Using Simple Beam with Third-Point Loading).

ASTM C157, (2014). Standard Test Method for Length Change of Hardened Cement Mortar and Concrete

Atiş, C. D. (2003). Accelerated carbonation and testing of concrete made with fly ash. Construction and Building Materials, 17(3), 147-152.

Atis, C. D., Kilic, A., & Sevim, U. K. (2004). Strength and shrinkage properties of mortar containing a nonstandard high-calcium fly ash. Cement and Concrete Research, 34(1), 99-102.

Bagragi N. K., Vidyahara H. S., and Ravandeh K., (1990), Mix design procedure for recycled aggregate concrete, Construction and Building Materials, Vol 4, No 4, 188-193.

Bogas, J. A., De Brito, J., Ramos, D. (2016). Freeze–thaw resistance of concrete produced with fine recycled concrete aggregates. Journal of Cleaner Production, 115, 294-306.

Bordelon, A., Cervantes, V., & Roesler, J. R. (2009). Fracture properties of concrete containing recycled concrete aggregates. Magazine of Concrete Research, 61(9), 665-670.

Brand, A., Amirkhanian, A., & Roesler, J. (2014). Flexural capacity of full-depth and two-lift concrete slabs with recycled aggregates. Transportation Research Record: Journal of the Transportation Research Board, (2456), 64-72.

Bravo, M., de Brito, J., Pontes, J., & Evangelista, L. (2015). Mechanical performance of concrete made with aggregates from construction and demolition waste recycling plants. Journal of cleaner production, 99, 59-74.

Burden, D. (2006). The durability of concrete containing high levels of fly ash (No. PCA R&D Serial No. 2989). University of New Brunswick, Department of Civil Engineering.

Butler, L., Tighe, S., & West, J. (2013). Guidelines for selection and use of coarse recycled-concrete aggregates in structural concrete. Transportation Research Record: Journal of the Transportation Research Board, (2335), 3-12.

Cable J. K., Frentress D. P., (2004), Two lift Portland cement concrete pavements to meet public needs, Federal Highway Administration Project 8, (Cooperative Agreement DTFH 61–01–X–00042), p. 11.

Cachim, P. B. (2009). Mechanical properties of brick aggregate concrete. Construction and Building Materials, 23(3), 1292-1297.

Carrasco-Maldonado, F., Spörl, R., Fleiger, K., Hoenig, V., Maier, J., & Scheffknecht, G. (2016). Oxy-fuel combustion technology for cement production–State of the art research and technology development. International Journal of Greenhouse Gas Control, 45, 189-199.

Casuccio, M., Torrijos, M. C., Giaccio, G., & Zerbino, R. (2008). Failure mechanism of recycled aggregate concrete. Construction and Building Materials, 22(7), 1500-1506.

Cecil Jones (2012). Recycled concrete aggregate- a sustainable choice for unbound base, Construction & Demolition Recycling Association (http://www.cdrecycling.org).

Cheng GY. (2005), Experimental study on the basic performance of recycled aggregate concrete with different displacement ratio, Chinese Concrete Journal, 11, 67–70 [only available in Chinese].

Chindaprasirt, P., Homwuttiwong, S., & Sirivivatnanon, V. (2004). Influence of fly ash fineness on strength, drying shrinkage and sulfate resistance of blended cement mortar. Cement and Concrete Research, 34(7), 1087-1092.

Chini, A.R., Muszynski, L.C., and Hicks, J., (2003), Determination of acceptance permeability characteristics for performance-related specifications for Portland cement concrete, final report submitted to Florida Department of Transportation, 116-118.

Choi S., Won M., (2009), Performance of continuously reinforced concrete pavement containing recycled concrete aggregate, GeoHunan international conference on new technologies in construction and rehabilitation of Portland cement concrete pavement and bridge deck pavement, ASCE.

Choi, W. C., & Yun, H. D. (2012). Compressive behavior of reinforced concrete columns with recycled aggregate under uniaxial loading. Engineering structures, 41, 285-293.

Construction Materials Recycling Association (2006–2009), "Case Histories" website, Concrete Recycling Organization, CMRA, Eola, Ill., 2009 [Online]. Available: http://www.concreterecycling.org/histories.html.

Corinaldesi, V. (2010). Mechanical and elastic behaviour of concretes made of recycled-concrete coarse aggregates. Construction and Building Materials, 24(9), 1616-1620.

Corinaldesi, V. (2010). Mechanical and elastic behaviour of concretes made of recycled-concrete coarse aggregates. Construction and Building Materials, 24(9), 1616-1620.

CSA -A23.3-04, (2004). Design of concrete structures, Rexdale, Ontario, Canada.

Cui, H. Z., Shi, X., Memon, S. A., Xing, F., & Tang, W. (2014). Experimental study on the influence of water absorption of recycled coarse aggregates on properties of the resulting concretes. Journal of Materials in Civil Engineering, 27(4), 04014138.

Cui, H. Z., Shi, X., Memon, S. A., Xing, F., & Tang, W. (2014). Experimental study on the influence of water absorption of recycled coarse aggregates on properties of the resulting concretes. Journal of Materials in Civil Engineering, 27(4), 04014138.

Cuttell, G., Snyder, M., Vandenbossche, J., and Wade, M. (1997). Performance of rigid pavements containing recycled concrete aggregates. Transportation Research Record: Journal of the Transportation Research Board, (1574), 89-98.

Dapena, E., Alaejos, P., Lobet, A., & Pérez, D. (2010). Effect of recycled sand content on characteristics of mortars and concretes. Journal of Materials in Civil Engineering, 23(4), 414-422.

De Juan, M. S., & Gutiérrez, P. A. (2004, November). Influence of recycled aggregate quality on concrete properties. In Conference on use of recycled materials in building and structures (pp. 9-11).

Debieb, F., Courard, L., Kenai, S., & Degeimbre, R. (2010). Mechanical and durability properties of concrete using contaminated recycled aggregates. Cement and Concrete Composites, 32(6), 421-426.

Dhir RK, Limbachiya MC, Leelawat T. Suitability of recycled aggregate for use in BS 5328 designated mixes. Proc Inst Civil Eng 1999; 134:257–74.

Dilbas, H., Şimşek, M., & Çakır, Ö. (2014). An investigation on mechanical and physical properties of recycled aggregate concrete (RAC) with and without silica fume. Construction and Building materials, 61, 50-59.

Dillmann R. Concrete with recycled concrete aggregate. In: Proceedings of international symposium on sustainable construction: use of recycled concrete aggregate, Dundee, Scotland; 1998. p. 239–53.

Domingo-Cabo A., Lázaro C., López-Gayarre F., Serrano-López M. A., Serna P., and Castaño-Tabares J.O., (2009), Creep and shrinkage of recycled aggregate concrete, Construction and Building Materials 23, 2545–2553.

Dong, J. F., Wang, Q. Y., & Guan, Z. W. (2013). Structural behaviour of recycled aggregate concrete filled steel tube columns strengthened by CFRP. Engineering Structures, 48, 532-542.

Duan, Z. H., & Poon, C. S. (2014). Properties of recycled aggregate concrete made with recycled aggregates with different amounts of old adhered mortars. Materials & Design, 58, 19-29.

Duan, Z. H., Kou, S. C., & Poon, C. S. (2013). Prediction of compressive strength of recycled aggregate concrete using artificial neural networks. Construction and Building Materials, 40, 1200-1206.

Duan, Z. H., Kou, S. C., & Poon, C. S. (2013). Using artificial neural networks for predicting the elastic modulus of recycled aggregate concrete. Construction and Building Materials, 44, 524-532.

Duan, Z., Poon, C. S., & Xiao, J. (2017). Using artificial neural networks to assess the applicability of recycled aggregate classification by different specifications. Materials and Structures, 50(2), 107.

Elahi, A., Basheer, P. A. M., Nanukuttan, S. V., & Khan, Q. U. Z. (2010). Mechanical and durability properties of high performance concretes containing supplementary cementitious materials. Construction and Building Materials, 24(3), 292-299.

Englesen C., Mehus J., Pade C., Saether D., (2005), Carbon dioxide uptake in demolished and crushed concrete, Project report 395-2005, Norwegian building research Institute, Oslo, Norway.

Eriksson, L., Johansson, E., & Wikström, C. (1998). Mixture design—design generation, PLS analysis, and model usage. Chemometrics and Intelligent Laboratory Systems, 43(1), 1-24.

Etxeberria, M., Vázquez, E., Marí, A., & Barra, M. (2007). Influence of amount of recycled coarse aggregates and production process on properties of recycled aggregate concrete. Cement and concrete research, 37(5), 735-742.

Fanghui, H., Qiang, W., & Jingjing, F. (2015). The differences among the roles of ground fly ash in the paste, mortar and concrete. Construction and Building Materials, 93, 172-179.

Fathifazl G., Abbas A., Razaqpur A. G., Isgor O. B., Fournier B., and Foo S., (2009). New mixture proportioning method for concrete made with coarse recycled concrete aggregate. Journal of Materials in Civil Engineering, Vol 10, Issue 21, 601-611.

Fathifazl, G., Razaqpur, A. G., Isgor, O. B., Abbas, A., Fournier, B., & Foo, S. (2011). Creep and drying shrinkage characteristics of concrete produced with coarse recycled concrete aggregate. Cement and Concrete Composites, 33(10), 1026-1037.

Federal Highway Administration (2004), Transportation applications of recycled concrete aggregate, FHWA state of the practice national review.

Federal Highway Administration (FHWA) (2008), Recycled Concrete Aggregate, Federal Highway Administration National Review, FHWA, Washington, D.C., http://www.fhwa.dot.gov/pavement/recycling/rca.cfm

Ferraris, C. F., Obla, K. H., & Hill, R. (2001). The influence of mineral admixtures on the rheology of cement paste and concrete. Cement and concrete research, 31(2), 245-255.

Flower, D. J., & Sanjayan, J. G. (2007). Greenhouse gas emissions due to concrete manufacture. The international Journal of life cycle assessment, 12(5), 282-288.

Fonseca, N., De Brito, J., & Evangelista, L. (2011). The influence of curing conditions on the mechanical performance of concrete made with recycled concrete waste. Cement and Concrete Composites, 33(6), 637-643.

Gabr A. R. and D.A. Cameron, (2012), Properties of recycled concrete aggregate for unbound pavement construction, Journal of Materials in Civil Engineering, 24, 754-764.

Garber S., Rasmussen R., Cackler T., Taylor P., Harrington D., Fick G., Snyder M., Van Dam T., Lobo C., (2011), A technology development plan for the use of recycled concrete aggregates in concrete paving mixtures, National Concrete Pavement Technology Center.

Geng, Y., Wang, Y., & Chen, J. (2016). Time-dependent behaviour of steel tubular columns filled with recycled coarse aggregate concrete. Journal of Constructional Steel Research, 122, 455-468.

Gesoğlu, M., Güneyisi, E., & Özbay, E. (2009). Properties of self-compacting concretes made with binary, ternary, and quaternary cementitious blends of fly ash, blast furnace slag, and silica fume. Construction and Building Materials, 23(5), 1847-1854.

Ghafari, E., Bandarabadi, M., Costa, H., & Júlio, E. (2015). Prediction of fresh and hardened state properties of UHPC: comparative study of statistical mixture design and an artificial neural network model. Journal of Materials in Civil Engineering, 27(11), 04015017.

Gokce, A., Nagataki, S., Saeki, T., Hisada, M. (2004). Freezing and thawing resistance of air-entrained concrete incorporating recycled coarse aggregate: The role of air content in demolished concrete. Cement and Concrete Research, 34(5), 799-806.

Gokce, A., Nagataki, S., Saeki, T., Hisada, M. (2011). Identification of frost-susceptible recycled concrete aggregates for durability of concrete. Construction and Building Materials, 25(5), 2426-2431.

Gomez-Soberon, J. M. (2002). Porosity of recycled concrete with substitution of recycled concrete aggregate: an experimental study. Cement and concrete research, 32(8), 1301-1311.

Gonzalez, G. P., & Moo-Young, H. K. (2004). Transportation applications of recycled concrete aggregate. FHWA state of the Practice National Review.

Gonzalez-Corominas, A., & Etxeberria, M. (2014). Properties of high performance concrete made with recycled fine ceramic and coarse mixed aggregates. Construction and Building Materials, 68, 618-626.

Gonzalez-Corominas, A., & Etxeberria, M. (2016). Effects of using recycled concrete aggregates on the shrinkage of high performance concrete. Construction and Building Materials, 115, 32-41.

Gonzalez-Corominas, A., Etxeberria, M., & Poon, C. S. (2016). Influence of steam curing on the pore structures and mechanical properties of fly-ash high performance concrete prepared with recycled aggregates. Cement and Concrete Composites, 71, 77-84.

González-Fonteboa, B., & Martínez-Abella, F. (2005). Recycled aggregates concrete: aggregate and mix properties. Materiales de construcción, 55(279), 53-66.

González-Fonteboa, B., Martínez-Abella, F., Eiras-López, J., & Seara-Paz, S. (2011). Effect of recycled coarse aggregate on damage of recycled concrete. Materials and structures, 44(10), 1759.

González-Taboada, I., González-Fonteboa, B., Martínez-Abella, F., & Carro-López, D. (2016). Study of recycled concrete aggregate quality and its relationship with recycled concrete compressive strength using database analysis. Materiales de Construcción, 66(323), 089.

Gress, D., Snyder, M., and Sturtevant, J. (2009). Performance of rigid pavements containing recycled concrete aggregate: update for 2006. Transportation Research Record: Journal of the Transportation Research Board, (2113), 99-107.

Hale, W. M., Freyne, S. F., Bush, T. D., & Russell, B. W. (2008). Properties of concrete mixtures containing slag cement and fly ash for use in transportation structures. Construction and Building Materials, 22(9), 1990-2000.

Hansen K. R. and A. Copeland (2013). Asphalt Pavement Industry Survey on Recycled Materials and Warm-Mix Asphalt Usage: 2009–2012. Information Series 138. National Asphalt Pavement

Hansen T.C., and Boegh E., (1985), Elasticity and drying shrinkage of recycled aggregate concrete, ACI Journal 82(5), 648-652.

Hansen. T.C., (1986), Recycled aggregate and recycled aggregate concrete, second state of- the-art report, developments from 1945–1985. Materials and Structures, 19(3), 201–246.

Hemmings, R. T. (2005). Process for Converting Waste Glass Fiber into Value Added Products, Final Report (No. DOE GO13015-1). Albacem LLC.

Henry, M., Pardo, G., Nishimura, T., & Kato, Y. (2011). Balancing durability and environmental impact in concrete combining low-grade recycled aggregates and mineral admixtures. Resources, Conservation and Recycling, 55(11), 1060-1069.

Hoffmann. C., Schubert. S., Leemann. A., and Motavalli. M., (2012), Recycled concrete and mixed rubble as aggregates: Influence of variations in composition on the concrete properties and their use as structural material, Construction and Building Materials, 35, 701–709.

Hossain, A., Shirazi, S., Persun, J., & Neithalath, N. (2008). Properties of concrete containing vitreous calcium aluminosilicate pozzolan. Transportation Research Record: Journal of the Transportation Research Board, (2070), 32-38.

Hu J., Wang Z., and Kim Y., (2013), Feasibility study of using fine recycled concrete aggregate in producing self-consolidating concrete, Journal of Sustainable Cement Based Materials, Vol. 2, No. 1, 20-34.

Hu MP. (2007), Mechanical properties of concrete prepared with different recycled coarse aggregates replacement rate. Chinese Concrete Journal, 2:52–4 [only available in Chinese].

Huang, Y. H. (2004). Pavement analysis and design, 2nd Ed., Pearson-Prentice Hall, Upper Saddle River, NJ.

Hwang, S. D., Khayat, K. H. (2008). Effect of mixture composition on restrained shrinkage cracking of self-consolidating concrete used in repair. ACI Materials journal, 105(5), 499.

Hwang, S. D., Khayat, K. H. (2010). Effect of mix design on restrained shrinkage of self-consolidating concrete. Materials and Structures, 43(3), 367-380.

Idir, R., Cyr, M., & Tagnit-Hamou, A. (2011). Pozzolanic properties of fine and coarse color-mixed glass cullet. Cement and Concrete Composites, 33(1), 19-29.

Ignjatović, I. S., Marinković, S. B., Mišković, Z. M., & Savić, A. R. (2013). Flexural behavior of reinforced recycled aggregate concrete beams under short-term loading. Materials and structures, 46(6), 1045-1059.

Jain, J. A., & Neithalath, N. (2010). Chloride transport in fly ash and glass powder modified concretes–influence of test methods on microstructure.Cement and Concrete Composites, 32(2), 148-156.

Jalal, M., Pouladkhan, A., Harandi, O. F., & Jafari, D. (2015). Comparative study on effects of Class F fly ash, nano silica and silica fume on properties of high performance self-compacting concrete. Construction and Building Materials, 94, 90-104.

Japan Society of Civil Engineers (2007). Standard specification for concrete structure," JSCE No. 15, Tokyo, Japan.

Jau, W. C., & Yang, C. T. (2010). Development of a modified concrete rheometer to measure the rheological behavior of conventional and self-consolidating concretes. Cement and Concrete Composites, 32(6), 450-460.

Jeong, H. (2011). Processing and properties of recycled aggregate concrete, Master's Thesis, University of Illinois at Urbana-Champaign.

Kakizaki M, Harada M, Soshiroda T, Kubota S, Ikeda T, Kasai Y. Strength and elastic modulus of recycled aggregate concrete. In: Proceedings of the 2nd international RILEM symposium on demolition and reuse of concrete and masonry, Tokyo, Japan; 1988. p. 565–74.

Kang, T. H., Kim, W., Kwak, Y. K., & Hong, S. G. (2014). Flexural testing of reinforced concrete beams with recycled concrete aggregates. ACI Structural Journal, 111(3), 607.

Kang, T. H., Kim, W., Kwak, Y. K., Hong, S. G. (2014). Flexural testing of reinforced concrete beams with recycled concrete aggregates. ACI Structural Journal, 111(3), 607.

Katz, A. (2003). Properties of concrete made with recycled aggregate from partially hydrated old concrete. Cement and concrete research, 33(5), 703-711.

Khayat, K. H., & Sadati, S. (2014). Recycled Concrete Aggregate: Field Implementation at the Stan Musial Veterans Memorial Bridge. National University Transportation Center (NUTC), Missouri University of Science and Technology, Rolla, MO, USA, (NUTC-R332).

Khayat, K. H., & Sadati, S. (2016). High-Volume Recycled Materials for Sustainable Pavement Construction. Final Report Prepared for Missouri Department of Transportation, (Report Number cmr 17-006).

Khayat, K. H., Yahia, A., & Sayed, M. (2008). Effect of supplementary cementitious materials on rheological properties, bleeding, and strength of structural grout. ACI Materials Journal, 105(6), 585-593.

Khelifi, H., Perrot, A., Lecompte, T., & Ausias, G. (2013). Design of clay/cement mixtures for extruded building products. Materials and structures, 46(6), 999-1010.

Khokhar, M. I. A., Rozière, E., Turcry, P., Grondin, F., & Loukili, A. (2010). Mix design of concrete with high content of mineral additions: optimization to improve early age strength. Cement and Concrete Composites, 32(5), 377-385.

Kim H., and Bentz D., (2008), Internal curing with crushed returned concrete aggregates for high performance concrete. NRMCA concrete technology forum: Focus on sustainable development, Denver, United States, 1-12.

Kim, J., Park, J., & Kyonggi, S. (2003). Experimental measurement of concrete thermal expansion. Journal of the Eastern Asia Society for Transportation Studies, Vol. 5, No. 13, 1035–1048.

Kim, S. W., Yun, H. D. (2013). Influence of recycled coarse aggregates on the bond behavior of deformed bars in concrete. Engineering Structures, 48, 133-143.

Kim. K., Shin. M., and Soowon Cha, (2013), Combined effects of recycled aggregate and fly ash towards concrete sustainability, Construction and Building Materials, Volume 48, Pages 499–507.

Knaack, A. M., & Kurama, Y. C. (2014). Behavior of reinforced concrete beams with recycled concrete coarse aggregates. Journal of Structural Engineering, 141(3), B4014009.

Kou SC, Poon, C.S., and Chan, D., (2007), Influence of fly ash as cement replacement on the properties of recycled aggregate concrete, Journal of Materials in Civil Engineering, 19(9), 709-717.

Kou, S. C., & Poon, C. S. (2013). Long-term mechanical and durability properties of recycled aggregate concrete prepared with the incorporation of fly ash. Cement and Concrete Composites, 37, 12-19.

Kou, S. C., Poon, C. S., & Chan, D. (2008). Influence of fly ash as a cement addition on the hardened properties of recycled aggregate concrete. Materials and Structures, 41(7), 1191-1201.

Kou, S. C., Poon, C. S., & Wan, H. W. (2012). Properties of concrete prepared with low-grade recycled aggregates. Construction and Building Materials, 36, 881-889.

Kou, S. C., Poon, C. S., Agrela, F. (2011). Comparisons of natural and recycled aggregate concretes prepared with the addition of different mineral admixtures. Cement and Concrete Composites, 33(8), 788-795.

Kou. S.C., and Poon. C.S., (2012), Enhancing the durability properties of concrete prepared with coarse recycled aggregate, Construction and Building Materials, Volume 35, 69-76.

Koulouris, A., Limbachiya, M. C., Fried, A. N., & Roberts, J. J. (2004, September). Use of recycled aggregate in concrete application: case studies. In Proceedings of the International Conference on Sustainable Waste Management and Recycling: Challenges and Opportunities. London: Thomas Telford (pp. 245-257).

Kulakowski, M. P., Pereira, F. M., & Dal Molin, D. C. (2009). Carbonation-induced reinforcement corrosion in silica fume concrete. Construction and Building Materials, 23(3), 1189-1195.

Laserna, S., & Montero, J. (2016). Influence of natural aggregates typology on recycled concrete strength properties. Construction and Building Materials, 115, 78-86.

Limbachiya M. C., Marrocchino E., and Koulouris A., (2007), Chemical–mineralogical characterization of coarse recycled concrete aggregate, Waste Management, 27, 201–208.

Limbachiya. M., Seddik. M., and Ouchangur, Y., (2012), Performance of Portland/silica fume cement concrete produced with recycled concrete aggregate, ACI Materials Journal, 109 (1), 91-100.

Liu, K., Yan, J., Hu, Q., Sun, Y., Zou, C. (2016). Effects of parent concrete and mixing method on the resistance to freezing and thawing of air-entrained recycled aggregate concrete. Construction and Building Materials, 106, 264-273.

Loser, R., Leemann, A. (2009). Shrinkage and restrained shrinkage cracking of self-compacting concrete compared to conventionally vibrated concrete. Materials and structures, 42(1), 71-82.

Mahaut, F., Mokeddem, S., Chateau, X., Roussel, N., & Ovarlez, G. (2008). Effect of coarse particle volume fraction on the yield stress and thixotropy of cementitious materials. Cement and concrete research, 38(11), 1276-1285.

Matos, A. M., & Sousa-Coutinho, J. (2012). Durability of mortar using waste glass powder as cement replacement. Construction and Building Materials,36, 205-215.

Mc Neil K., Kang T., (2012), Recycled concrete aggregate: a review, International Journal of

Mclntyre. J., Spatari. S., and MacLean. H.L., (2009), Energy and greenhouse gas emissions trade-offs of recycled concrete aggregate use in nonstructural concrete: A north American case study, Journal of Infrastructure Systems, 15, 361-370.

Medina, C., Zhu, W., Howind, T., de Rojas, M. I. S., Frías, M. (2014). Influence of mixed recycled aggregate on the physical–mechanical properties of recycled concrete. Journal of Cleaner Production, 68, 216-225.

Mellmann G. Processed concrete rubble for the reuse as aggregate. In: Proceedings of the international seminar on exploiting waste in concrete, Dundee, Scotland; 1999. p. 171–8.

Mirzahosseini, M., & Riding, K. A. (2014). Effect of curing temperature and glass type on the pozzolanic reactivity of glass powder. Cement and Concrete Research, 58, 103-111.

Missouri Standard Specifications for Highway Construction. Missouri Highways and Transportation Commission, Jefferson City, Missouri, 1999, 581-585.

Monteiro, P. (2006). Concrete: microstructure, properties, and materials. McGraw-Hill Publishing.

Montgomery, D. C. (2008), Design and analysis of experiments. John Wiley & Sons Inc., New York.

Moradpour, S., Wu, S., & Leu, M. C. (2015). Use of traffic simulators to determine driver response to work zone configurations. In Proceedings of the International Annual Conference of the American Society for Engineering Management (ASEM), Indianapolis, IN, USA.

Movassaghi R., (2006), Durability of reinforced concrete incorporating recycled concrete aggregate (RCA), A thesis presented to the University of waterloo in fulfilment of the requirements for Master of Applied Science in mechanical engineering, University of Waterloo, Canada, 115-119.

Nagataki S., Gokce A., and Saeki T., (2000), Effects of recycled aggregate characteristics on performance parameters of recycled aggregate concrete, Proceedings of Fifth CANMET/ACI International Conference on Durability of Concrete, Barcelona, Spain, 51-71.

Naik, T. R., Ramme, B. W., & Tews, J. H. (1995). Pavement construction with high-volume class C and class F fly ash concrete. ACI Materials Journal, 92(2).

Nassar, R. U. D., and Soroushian, P., (2012), Use of milled waste glass in recycled aggregate concrete, Proceeding of the ICE Construction materials, 165(5), 304-315.

Nassar, R., Soroushian, P., & Ghebrab, T. (2013). Field investigation of high-volume fly ash pavement concrete. Resources, Conservation and Recycling, 73, 78-85.

NCHRP synthesis 435, (2013), Recycled materials and by-products in highway applications, volume 6, reclaimed asphalt pavement, recycled concrete aggregate, and construction demolition waste, Transportation research Board.

Neithalath, N., Persun, J., & Hossain, A. (2009). Hydration in high-performance cementitious systems containing vitreous calcium aluminosilicate or silica fume. Cement and Concrete Research, 39(6), 473-481.

Nixon. P. J., (1978), Recycled concrete as an aggregate for concrete-a review, Materials and Structures, 11(5), 371–8.

Obla, K., Kim, H., & Lobo, C. L. (2007). Crushed returned concrete as aggregates for new concrete. National Ready Mixed Concrete Association.

Olivier, J. G. J., Janssens-Maenhout, G., Muntean, M., Peters J. A. (2015), Trends in global CO2 emissions; 2015 Report, The Hague: PBL Netherlands Environmental Assessment Agency; Ispra: European Commission, Joint Research Centre.

Omary, S., Ghorbel, E., & Wardeh, G. (2016). Relationships between recycled concrete aggregates characteristics and recycled aggregates concretes properties. Construction and Building Materials, 108, 163-174.

Otsuki. N., Miyazato. S., and Yodsudjai. W., Influence of recycled aggregate on interfacial transition zone, strength, chloride penetration and carbonation of concrete, Journal of Materials in Civil Engineering. 2003.15:443-451.

Padmini. A.K., Ramamurthy.K. , Mathews. M.S., (2009), Influence of parent concrete on the properties of recycled aggregate concrete, Construction and Building Materials, Volume 23, Issue 2, 829–836.

Papadakis, V. G. (2000). Effect of supplementary cementing materials on concrete resistance against carbonation and chloride ingress. Cement and concrete research, 30(2), 291-299.

Pedro, D., De Brito, J., & Evangelista, L. (2014). Influence of the use of recycled concrete aggregates from different sources on structural concrete. Construction and Building Materials, 71, 141-151.

Pedro, D., De Brito, J., & Evangelista, L. (2015). Performance of concrete made with aggregates recycled from precasting industry waste: influence of the crushing process. Materials and Structures, 48(12), 3965-3978.

Piepel, G. F., & Cornell, J. A. (1994). Mixture experiment approaches: examples, discussion, and recommendations. Journal of Quality Technology, 26(3), 177-196.

Rahal, K. (2007). Mechanical properties of concrete with recycled coarse aggregate. Building and environment, 42(1), 407-415.

Rao, M. C., Bhattacharyya, S. K., & Barai, S. V. (2011). Influence of field recycled coarse aggregate on properties of concrete. Materials and Structures, 44(1), 205-220.

Rashidian-Dezfouli, H., & Rangaraju, P. R. (2017). Role of ground glass fiber as a supplementary cementitious material in improving selected properties of portland cement concrete, (No. 17-04237), Transportation Research Record, DOI: 10.3141/2629-03

Ravindrarajah S. R., and Tam C.T., (1985), Properties of concrete made with crushed concrete as coarse aggregate. Magazine of Concrete Research, 37(130), 29–38.

Folino, P., & Xargay, H. (2014). Recycled aggregate concrete–mechanical behavior under uniaxial and triaxial compression. Construction and Building Materials, 56, 21-31.

Reiner, M. (1949). Deformation and flow. An elementary introduction to theoretical rheology. H.K. Lewis & Co, Limited, Great Britain

Richardson. A., Coventry. K., and Bacon. J., (2011), Freeze/thaw durability of concrete with recycled demolition aggregate compared to virgin aggregate concrete, Journal of Cleaner Production, Volume 19, Issues 2–3, Pages 272–277.

RILEM Committee CPC-18 (1988). Measurement of Hardened Concrete Carbonation Depth, TC14-CPC.

Roussel, N., Stefani, C., & Leroy, R. (2005). From mini-cone test to Abrams cone test: measurement of cement-based materials yield stress using slump tests. Cement and Concrete Research, 35(5), 817-822.

Rubio-Hernandez, F. J., Velazquez-Navarro, J. F., & Ordonez-Belloc, L. M. (2013). Rheology of concrete: a study case based upon the use of the concrete equivalent mortar. Materials and structures, 46(4), 587-605.

Rudy, A., Olek, J., Nantung, T., & Newell, R. M. (2009). Statistical optimization of low slump ternary concrete mixtures with ground granulated blast furnace slag (GGBS) and high calcium fly ash for pavement applications. Proceeding of the 9th international symposium on Brittle Matrix Composites, 149-159, Warsaw, Poland.

Sadati, S., and Khayat, K. H. (2016). Field performance of concrete pavement incorporating recycled concrete aggregate. Construction and Building Materials, 126, 691-700.

Sagoe-Crentsil k., Brown T., and Taylor A. H., (2001), Performance of concrete made with commercially produced coarse recycled concrete aggregate, Cement and Concrete Research, 31, 707-712.

Salas A., Lange D., Roesler J., (2010), Batching effects on properties of recycled aggregate concrete for airfield rigid pavements, FAA Technology Transfer Conference and Exposition, Atlantic city, NJ, USA.

Salem, R. M., Burdette, E. G., & Jackson, N. M. (2003). Resistance to freezing and thawing of recycled aggregate concrete. Materials Journal, 100(3), 216-221.

Schubert, S., Hoffmann, C., Leemann, A., Moser, K., & Motavalli, M. (2012). Recycled aggregate concrete: experimental shear resistance of slabs without shear reinforcement. Engineering Structures, 41, 490-497.

Seara-Paz, S., González-Fonteboa, B., Martínez-Abella, F., & González-Taboada, I. (2016). Time-dependent behaviour of structural concrete made with recycled coarse aggregates. Creep and shrinkage. Construction and Building Materials, 122, 95-109.

See, H. T., Attiogbe, E. K., Miltenberger, M. A. (2003). Shrinkage cracking characteristics of concrete using ring specimens. ACI Materials Journal, 100(3).

Shah, H. R., Weiss, J. (2006). Quantifying shrinkage cracking in fiber reinforced concrete using the ring test. Materials and structures, 39(9), 887-899.

Shaikh, F. U., & Supit, S. W. (2015). Compressive strength and durability properties of high volume fly ash (HVFA) concretes containing ultrafine fly ash (UFFA). Construction and Building Materials, 82, 192-205.

Shayan, A., & Xu, A. (2006). Performance of glass powder as a pozzolanic material in concrete: a field trial on concrete slabs. Cement and Concrete Research, 36(3), 457-468.

Shayan. A., and Xu. A., (2003), Performance and properties of structural concrete made with recycled concrete aggregate, ACI Materials Journal, V. 100, No. 5, 371-380.

Siddique, R. (2004). Performance characteristics of high-volume Class F fly ash concrete. Cement and Concrete Research, 34(3), 487-493.

Silva, R. V., De Brito, J., & Dhir, R. K. (2014). Properties and composition of recycled aggregates from construction and demolition waste suitable for concrete production. Construction and Building Materials, 65, 201-217.

Silva, R. V., De Brito, J., & Dhir, R. K. (2015). Prediction of the shrinkage behavior of recycled aggregate concrete: a review. Construction and Building Materials, 77, 327-339.

Silva, R. V., de Brito, J., & Dhir, R. K. (2016). Establishing a relationship between modulus of elasticity and compressive strength of recycled aggregate concrete. Journal of Cleaner Production, 112, 2171-2186.

Sim J. and Park C., (2011), Compressive strength and resistance to chloride ion penetration and carbonation of recycled aggregate concrete with varying amount of fly ash and fine recycled aggregate, Waste Management 31, 2352–2360.

Snyder M. B. and Cavalline, T. (2016), Webinar on Concrete Pavement Recycling, National Concrete Pavement Technology Center, Iowa State University, (http://www.cptechcenter.org/webinars/documents/RCA%20Webinar%20presentations.pdf)

Sonebi, M. (2004). Medium strength self-compacting concrete containing fly ash: modelling using factorial experimental plans. Cement and Concrete research, 34(7), 1199-1208.

Soudki, K. A., El-Salakawy, E. F., & Elkum, N. B. (2001). Full factorial optimization of concrete mix design for hot climates. Journal of Materials in Civil Engineering, 13(6), 427-433.

Speare, P. R., & Ben-Othman, B. (1993). Recycled concrete coarse aggregates and their influence on durability. In Concrete 2000; Economic and durable construction through excellence: Proceedings of the international conference held at the University of Dundee, Scotland, UK (pp. 419-432).

Sulapha, P., Wong, S. F., Wee, T. H., & Swaddiwudhipong, S. (2003). Carbonation of concrete containing mineral admixtures. Journal of materials in civil engineering, 15(2), 134-143.

Surya M., Rao K. V., and Lakshmy P., (2013). Recycled aggregate concrete for transportation infrastructure. Procedia - Social and Behavioral Sciences, V. 104, 1158–1167.

Tabsh S. W., and Abdelfatah A. S., (2009), “Influence of recycled concrete aggregates on strength properties of concrete”, Construction and Building Materials 23, 1163–1167.

Tam V. W. Y., Gao X.F., and Tam C.M., (2005), “Microstructural analysis of recycled aggregate concrete produced from two-stage mixing approach”, Cement and Concrete Research, 35, 1195– 1203.

Tam V. W. Y., Tam C.M., and Wang Y., (2007), “Optimization on proportion for recycled aggregate in concrete using two-stage mixing approach”, Construction and Building Materials 21, 1928–1939.

Tashima, M. M., Soriano, L., Borrachero, M. V., Monzó, J., & Payá, J. (2013). Effect of curing time on microstructure and mechanical strength development of alkali activated binders based on vitreous calcium aluminosilicate (VCAS). Bulletin of Materials Science, 36(2), 245-249.

Tashima, M. M., Soriano, L., Borrachero, M. V., Monzó, J., Cheeseman, C. R., & Payá, J. (2012). Alkali activation of vitreous calcium aluminosilicate derived from glass fiber waste. Journal of Sustainable Cement-Based Materials, 1(3), 83-93.

Tashima, M. M., Soriano, L., Monzo, J., Borrachero, M. V., & Paya, J. (2013). Novel geopolymeric material cured at room temperature. Advances in Applied Ceramics, 112(4), 179-183.

Tashima, M. M., Soriano, L., Payá, J., Monzó, J., & Borrachero, M. V. (2016). Assessment of pozzolanic/hydraulic reactivity of vitreous calcium aluminosilicate (VCAS). Materials & Design, 96, 424-430.

Thomas, C., Setién, J., Polanco, J., Alaejos, P., & De Juan, M. S. (2013). Durability of recycled aggregate concrete. Construction and Building Materials, 40, 1054-1065.

Topçu IB, and Sengel S. (2004), Properties of concretes produced with waste concrete aggregate, Cement and Concrete Research, 34(8), 1307–1312.

Turk, K., Karatas, M., & Gonen, T. (2013). Effect of fly ash and silica fume on compressive strength, sorptivity and carbonation of SCC. KSCE Journal of Civil Engineering, 17(1), 202-209.

United Nations General Assembly (1987) Report of the World Commission on Environment and Development: Our Common Future. Transmitted to the General Assembly as an Annex to document A/42/427 - Development and International Co-operation: Environment. Retrieved on: 2009-02-15.

United States Environmental Protection Agency (2004), RCRA in focus: construction, demolition, and renovation, https://www.epa.gov/hwgenerators/resource-conservation-and-recovery-act-rcra-focus-hazardous-waste-generator-guidance

United States Environmental Protection Agency (2015), Advancing sustainable materials management: 2013 fact sheet, https://www.epa.gov/sites/production/files/2015-09/documents/2013_advncng_smm_fs.pdf

United States Environmental Protection Agency (2016), Advancing sustainable materials management: 2014 fact sheet, https://www.epa.gov/sites/production/files/2016-11/documents/2014_smmfactsheet_508.pdf

Van Dam, T. J., Harvey, J. T., Muench, S. T., Smith, K. D., Snyder, M. B., Al-Qadi, I. L., ... & Kendall, A. (2015). Towards sustainable pavement systems: a reference document. Urbana, 51, 61801.

Vázquez, E., Hendriks, C., Janssen, G.M.T. (Eds.), (2004). Fsccs, Draft of Spanish regulations for the use of recycled aggregate in the production of structural concrete (Task Force of the Standing Committee of Concrete of Spain), International RILEM conference on the use of recycled materials in building and structures, RILEM Publications SARL, Barcelona, Spain T. pp. 511–525.

Vieira, J. P. B., Correia, J. R., & De Brito, J. (2011). Post-fire residual mechanical properties of concrete made with recycled concrete coarse aggregates. Cement and Concrete Research, 41(5), 533-541.

Volz, J. S., SE, P., Khayat, K. H., Arezoumandi, M., Drury, J., Sadati, S., Smith, A., & Steele, A. (2014). Recycled Concrete Aggregate (RCA) for Infrastructure Elements. National University Transportation Center (NUTC), Missouri University of Science and Technology, Rolla, MO, USA, (NUTC R312).

Wade, M. J., Cuttell, G. D., Vandenbossche, J. M., Yu, H. T., Smith, K. D., and Snyder, M. B. (1997). Performance of concrete pavements containing recycled concrete aggregate (No. FHWA-RD-96-164).

Wang, W. L., Kou, S. C., & Xing, F. (2013). Deformation properties and direct shear of medium strength concrete prepared with 100% recycled coarse aggregates. Construction and Building Materials, 48, 187-193.

Weiss, W. J., Shah, S. P. (2002). Restrained shrinkage cracking: the role of shrinkage reducing admixtures and specimen geometry. Materials and Structures, 35(2), 85-91.

Wongkeo, W., Thongsanitgarn, P., & Chaipanich, A. (2012). Compressive strength and drying shrinkage of fly ash-bottom ash-silica fume multi-blended cement mortars. Materials & Design, 36, 655-662.

World Business Council for Sustainable Development (WBCSD) Report, 2012. Recycling concrete, http://www.wbcsdcement.org/index.php/key-issues/sustainability-with-concrete/54, (accessed date: August 21, 2014).

Worrell, E., Price, L., Martin, N., Hendriks, C., & Meida, L. O. (2001). Carbon dioxide emissions from the global cement industry 1. Annual Review of Energy and the Environment, 26(1), 303-329.

Xiao JZ, and Li JB. (2005), Study on relationships between strength indexes of recycled concrete. Chinese Journal of Building Materials, 9(2):197–201 [only available in Chinese].

Xiao, J. Z., Li, J. B., & Zhang, C. (2006). On relationships between the mechanical properties of recycled aggregate concrete: an overview. Materials and structures, 39(6), 655-664.

Xiao, J., Li, J., & Zhang, C. (2005). Mechanical properties of recycled aggregate concrete under uniaxial loading. Cement and concrete research, 35(6), 1187-1194.

Xiao, J., Li, W., Fan, Y., & Huang, X. (2012). An overview of study on recycled aggregate concrete in China (1996–2011). Construction and Building Materials, 31, 364-383.

Xiao, J., Lu, D., & Ying, J. (2013). Durability of recycled aggregate concrete: An overview. Journal of Advanced Concrete Technology, 11(12), 347-359.

Yang KH, Chung H.S., Ashour AF (2008) Influence of Type and Replacement Level of Recycled Aggregates on Concrete Properties. ACI Materials Journal, 105 (3): 289-296.

Yeau, K. Y., & Kim, E. K. (2005). An experimental study on corrosion resistance of concrete with ground granulate blast-furnace slag. Cement and Concrete Research, 35(7), 1391-1399.

Yildirim, S. T., Meyer, C., Herfellner, S. (2015). Effects of internal curing on the strength, drying shrinkage and freeze–thaw resistance of concrete containing recycled concrete aggregates. Construction and Building Materials, 91, 288-296.

Yong, P. C. and Teo, D.C.L., (2009), Utilization of recycled aggregate as coarse aggregate in concrete, UNIMAS E-Journal of Civil Engineering, 1(1), 1-6.

Zaharieva, R., Buyle-Bodin, F., Wirquin, E. (2004). Frost resistance of recycled aggregate concrete. Cement and Concrete Research, 34(10), 1927-1932.

Zega, C. J., & Di Maio, A. A. (2010). Recycled concretes made with waste ready-mix concrete as coarse aggregate. Journal of Materials in Civil Engineering, 23(3), 281-286.

Zhao, H., Sun, W., Wu, X., & Gao, B. (2015). The properties of the self-compacting concrete with fly ash and ground granulated blast furnace slag mineral admixtures. Journal of Cleaner Production, 95, 66-74.

Zilch K, Roos F. An equation to estimate the modulus of elasticity of concrete with recycled aggregates. Civil Eng 2001; 76(4):187–91 (only available in German).

VITA

Seyedhamed Sadati was born in 1983 in Iran. He earned his Bachelor's degree in Civil Engineering from Iran University of Science and Technology (IUST), Tehran, Iran, in 2006. In 2007, Hamed started his studies as a Master's student of Civil Engineering under the supervision of Dr. Mohamed Shekarchi, at University of Tehran, Tehran, Iran, and graduated at 2010.

In August 2012, Hamed started his PhD program at Department of Civil, Architectural, and Environmental Engineering at Missouri University of Science and Technology, Rolla, Missouri, under the supervision of Dr. Kamal H. Khayat. His research was devoted to development of sustainable concrete mixtures for transportation infrastructure, with a main focus on using recycled concrete aggregate in concrete production. He received a PhD in Civil Engineering from Missouri University of Science and Technology in July 2017. Results of his research were published in several technical reports, journal papers, conference proceedings and presentations, as well as the current dissertation.

Hamed was a member of several professional and student organizations, including the American Concrete Institute (ACI), American Society of Civil Engineers (ASCE), American Society of Non-Destructive Testing (ASNT), American Society of Engineering Education (ASEE), Precast/Prestressed Concrete Institute (PCI), American Civil Engineers Honor Society (Chi Epsilon), and Engineering Honor Society (Tau Beta Pi).